

早稲田大学 博士論文

Effectiveness of Hybrid Air Conditioning
System in a Residential House

住宅におけるハイブリッド空調システムの
有効性に関する評価研究

2003 年 3 月

許 雷

Lei, XU

©2003 Lei XU

早稲田大学 博士論文

Effectiveness of Hybrid Air Conditioning
System in a Residential House

住宅におけるハイブリッド空調システムの
有効性に関する評価研究

2003年3月

早稲田大学大学院理工学研究科
建設工学専攻 都市環境研究

許 雷

Lei, XU

Effectiveness of Hybrid Air Conditioning System in a Residential House

DISSERTATION

SUBMITTED IN PARTIAL FULFILLMENT OF THE REQUIREMENTS
FOR THE DEGREE OF DOCTOR OF ENGINEERING
IN THE GRADUATE SCHOOL OF SCIENCE AND ENGINEERING OF
WASEDA UNIVERSITY

BY

LEI XU

Dr. TOSHIO OJIMA, ADVISOR

March 2003

ACKNOWLEDGEMENTS

I would like to thank my advisor, Prof. Toshio Ojima of Waseda University for acceptance of my entrance to the doctoral course, for his kindly instruction and inspiration throughout my graduate study. He gives me a lot of chance to do my study in practical projects, especially the field experiment in the Steel Perfect Recycle House (SPRH) in 2001. Without his guidance, the quality of this thesis would not have been achieved. I am also grateful for his introduction of the Japanese traditions and culture.

I would like to thank Prof. Yuji Hasemi, and Prof. Shin-ichi Tanabe of Waseda University, and Visiting Prof. Yasutaka Nakajima of Advanced Research Institute for Science and Engineering of Waseda University, for their careful reviewing and advice on my thesis.

I would like to thank Associate Prof. Weijun Gao of Kitakyushu University for his help therefore I could enter Ojima Laboratory. I sincerely appreciate his introduction not only on my study but also on my daily life, which makes my research and life go smoothly.

I am very grateful to Prof. Nobuyuki Takahashi of Advanced Research Institute for Science and Engineering of Waseda University for his care and instruction. I also thank Ms. Chikako Kobayashi, secretary of Ojima Lab, especially for her help in correcting my abstract in Japanese.

I would like to thank Mr. Kazutaro Oyabu of Indoor Climate Engineering Institute for giving me a lot of advice and instruction on the displacement ventilation system and thermal storage system since the designing period. He also gave me many advices on the field experiment and my thesis.

I am grateful to Lecturer Yusuke Nakajima of Advanced Research Institute for Science and Engineering of Waseda University for his help in the SPRH project, especially during the field experiment in Kitakyushu last year. I also thank the members of Ojima Laboratory, especially Haifeng Li, Eiji Hara, Yuki Kanemori for their help during my study. I am grateful to Takashi Yagi (of Kajima Co. now) for designing of the air conditioning system in the experimental house, Katsuhisa Yoshida (of Obayashi Co. now), Koji Sugihara for their help in the field experiment. I thank Yoshida for spending long time on experiment in Kitakyushu.

I would like to thank Associate Prof. Hirotohi Yoda of Kinki University, Assistant Nan Zhou of Kyushu Sangyo University, for their help in the field experiment. I also give my thanks to Prof. Noriyasu Sagara of Kitakyushu University for his advice on the displacement

ventilation experiment in Kitakyushu. I especially thank Associate Prof. Tatsuo Nobe of Kogakuin University for his reference book of displacement ventilation, and constant care of my study and life.

I thank Keisuke Teshima, Takeshi Nagasue, Yuji Gotoh (of Kinki University in 2001), and Imati Satoshi (of Kyushu Sangyo University in 2001) for their help and time on the field experiment. I would thank all those participated in the Steel Prefect Recycle House (SPRH) project, especially Mr. Hiroshi Nakatani of Nippon Steel Co., Mr. Kiyotaki Tamon of Kimura Kohki Co., Mr. Yuan Chen and Mr. Hajime Tanaka of Nippon Fläkt Co. I am grateful to Mr. Toshio Murata of Nippon Fläkt K.K., Mr. Daisuke Sadamitsu, and Mr. Takashi Minabe of Fluent Asia Pacific Co. for their instructions on CFD simulation with Airpak. And I also express my thanks to Japan Society for the Promotion of Science to support the SPRH project.

I am much obliged to Yoshida Scholarship Foundation for giving me constant financial support, therefore I am able to be concentrated on my study, and finish my thesis smoothly in three years. She also provides many chances of visiting, traveling and concert, which make my life colorful.

I would like to thank Prof. Cunyang Fan of Tongji University for his constant support, providing chances to continue my study, and giving me constant advice and instruction on my study. I thank Prof. Weilong Wu of Tongji University for his constant support.

Last but not least, I am indebted to my parents who constantly support my every pursuit. I thank Wenting for her care, help and lasting support during my study.

March 2003

A handwritten signature in cursive script, appearing to read 'Insei'.

ABSTRACT

The energy consumption in residential and commercial sector accounts for 1/4 of the total in Japan. With the information technology (IT) revolution and the improving requirement for indoor air environment, the energy consumption for household air conditioning has increased. On the other hand, the air conditioning systems turn to be more sophisticated and difficult for operation in order to make a good environment and to be energy saving. In this research, a hybrid air conditioning system, which is an integration of double skin system, displacement air conditioning and thermal storage system, has been proposed for energy conservation and thermal comfort in a residential house. The effectiveness of this hybrid system is appraised by CFD simulation and field measurement.

In Chapter 1 *Introduction*, the reasons for the increase of energy consumption, especially for air conditioning in residential houses are explained, and the conventional research on energy conservation and indoor environment is overviewed. For the sake of energy conservation, occupancy health and easy operation, the importance of the proposition of a new air conditioning system for residential houses is illustrated. The passive system, such as the double skin system and efficient air conditioning system, such as displacement system and thermal storage will be good solutions.

In Chapter 2 *Concept of Hybrid Air Conditioning System and its Plan for Residential House*, the definition and targets of hybrid air-conditioning system are presented. By the integration of passive air conditioning system and improvement on active air conditioning system, hybrid air conditioning system will be a good solution for energy conservation and occupant healthy in residential houses. According to the current technology, the double skin system, which is one example of the passive system, and the displacement ventilation system, together with the thermal storage system, which is the improvement of active air conditioning system, are designed for an experimental house in Kitakyshu. The details of the experimental house and its hybrid air conditioning system are also introduced.

In Chapter 3 *Simulation on Natural Energy Utilization in a Residential House with Double Skin System*, compared with the conventional house without double skin system, the

double skin system is expected to be more effective in residential house. Considering the weather conditions of Kitakyushu, because of the effects of sun shadings and stack effect, natural ventilation is promoted by the double skin, about 10% solar radiation from the south direction can be cut down in the summer, which leads to about 15% energy conservation for cooling load. In winter as more solar radiation enters the house, indoor temperature is able to become 10-15°C higher than the outside air. At daytime about 20-30% heating load can be cut down because the double skin space acts as a buffer between outside and inside environment.

In Chapter 4 *Field Experiment of Double Skin System in the Experimental House*, experimental results of the double skin system are detailed. In summer, the stack effect is verified in the double skin space with the temperature gradient of 0.5-1°C/m in the vertical direction. About 10-25% solar radiation is exhausted by natural ventilation, and this will lead to 15-20% energy saving in cooling. In winter, air temperature in double skin becomes 5-10°C higher than outside air temperature. 20-30% heating load can be cut down because of the green house effect in the double skin space. The results of simulation and experimental measurements keep a good coincidence with each other. In the intermediate seasons, the indoor environment can be greatly improved by suitable controlling on the double skin system without active air conditioning.

In Chapter 5 *Evaluation of Displacement Ventilation System in a Residential Room by CFD Simulation*, the improvement on active air conditioning system is proposed, and the effectiveness of the displacement system is predicted. Simulations of different air change rates, different inlet/outlet positions and diffuser characters are carried out in a residential room. And the energy consumption for cooling and the thermal comfort in the occupied zone are analyzed. According to the simulation results, although the air temperature is stratified in the vertical direction, this may not have an effect on thermal comfort in the occupied zone with enough air supply. Compared with the mixing system, the displacement ventilation may cut down 12-26% of the cooling load, and the outlet of return air set at a lower position may lead to more energy saving. And the displacement ventilation system has a better air change efficiency, which is 30% higher than the mixing system. In addition, the swinging diffusers will be helpful for air distribution, especially when there are some partitions in rooms.

In Chapter 6 *Field Experiment of Displacement Ventilation in a Residential Room*, the

availability of displacement air conditioning system is verified. Air temperature is stratified in the vertical direction, and it is 26-28°C in the occupied zone (below 1.8m), about 2°C smaller than that above 1.8m. The temperature gradient is about 2-2.5°C/m, which is smaller than the recommendation of ISO7730. PMV is in the range of -0.5 to 0.5 under 1.4m, which means comfortable environment is realized. The average CO₂ concentration is 600ppm in the occupied zone, while it is 200ppm greater near the ceiling, which shows the air exchange effectiveness of the displacement system is better. When return outlet is set at 1.8m high, the exhaust outlet is set on the ceiling, and the cooling load is about 50-60W/m², which is 20-30% smaller than that of conventional mixing system. In addition, the simulation results in Chapter 5 have a good accordance with the measured values, and the correlation coefficient for temperature is 0.95, 0.82 for air velocity.

In Chapter 7 *Effectiveness of Thermal Storage System in a Residential House*, the improvement on heating and cooling system is proposed. With the introduction of displacement air conditioning system, in order to make use of midnight electricity and supply air with great temperature difference, effectiveness of thermal storage system is studied. The proposed system uses heat pump to produce ice during the nighttime, store it for air conditioning in the next day, and the waste heat will be used for hot water supply. The direct heat exchange between air and ice is adopted in the thermal storage system in the experimental house. The performance of this system is analyzed by simulation. From the results, electricity consumption of proposed system is 23% lower than that of the conventional system. About 40% energy cost can be saved and 25% CO₂ emission can be cut down because of the nighttime operation and heat recovery. Suppose the life of the equipment as 20 years, the sum of initial cost and running cost of these two systems is almost the same. The experimental results in summer show that the direct heat change is successful, and the performance of the thermal storage system will go up with the predictions if the heat loss is small.

In Chapter 8 *Conclusions*, the whole summary of this thesis is presented.

TABLE OF CONTENTS

ACKNOWLEDGEMENTS.....	i
ABSTRACT	iii
TABLE OF CONTENTS.....	vii
LIST OF FIGURES.....	xiii
LIST OF TABLES.....	xix
NOMENCLATURE.....	xxi
CHAPTER 1 INTRODUCTION.....	1
1.1. Lifestyle variation and household energy consumption.....	1
1.2. Healthy requirement and ventilation.....	4
1.3. Conventional research.....	5
1.3.1. Double skin system.....	5
1.3.2. Displacement ventilation	9
1.3.3. Thermal storage.....	11
1.4. Objective of this research.....	13
CHAPTER 2 CONCEPT OF HYBRID AIR CONDITIONING SYSTEM AND ITS PLAN FOR RESIDENTIAL HOUSE.....	17
2.1. Concepts of hybrid air conditioning system.....	17
2.1.1. Definition and targets of hybrid air conditioning	17
2.1.2. Available technologies for hybrid air conditioning in residential house	22
2.2. Design strategies of hybrid air conditioning	28
2.2.1. Double skin and residential house	28
2.2.2. Plan of the hybrid air conditioning system.....	31
2.2.3. Outline of the experimental house	31
2.2.4. Outline of Air conditioning system.....	34
2.3. Research method.....	36
2.3.1. Building models.....	36
2.3.2. Generating meshes.....	37

2.3.3.	Calculating process.....	38
2.3.4.	Examining results	39
2.3.5.	Model used in this research.....	40
CHAPTER 3 SIMULATION ON NATURAL ENERGY UTILIZATION IN A RESIDENTIAL HOUSE WITH DOUBLE SKIN SYSTEM.....		41
3.1.	Climate conditions in Kitakyushu	41
3.1.1.	Outside air temperature and humidity	41
3.1.2.	Wind.....	42
3.1.3.	Solar radiation	43
3.2.	Outline of the double skin system in residential house.....	44
3.2.1.	Proposed model and reference model.....	44
3.2.2.	Components of the double skin system.....	45
3.2.3.	Property of Materials	47
3.2.4.	Setting of cases.....	50
3.3.	Description of the simulation model.....	51
3.3.1.	Macro model.....	51
3.3.2.	Air flow around buildings	59
3.3.3.	Initial conditions for simulation	60
3.3.4.	Micro model.....	64
3.4.	Simulation results.....	67
3.4.1.	Air flow around the house	67
3.4.2.	Simulation results in summer.....	68
3.4.3.	Simulation results in winter	72
3.5.	Summary and Conclusion.....	77
CHAPTER 4 FIELD EXPERIMENT OF DOUBLE SKIN SYSTEM IN THE EXPERIMENTAL HOUSE.....		79
4.1.	Details of the Double Skin System.....	79
4.2.	Outline of field experiment.....	81
4.2.1.	Testing points and instruments	81
4.2.2.	Mode of double skin	82
4.3.	Experiment results	85
4.3.1.	Field experiments in summer	85
4.3.2.	Field experiments in autumn	93

4.3.3.	Field experiments in winter	99
4.4.	Subjective experiments.....	104
4.4.1.	Outline of subjective experiment.....	104
4.4.2.	Results of subjective experiment.....	104
4.5.	Summary and Conclusion.....	108
CHAPTER 5 EVALUATION OF DISPLACEMENT VENTILATION SYSTEM IN A RESIDENTIAL ROOM BY CFD SIMULATION.....		111
5.1.	Outline of displacement ventilation and mixing ventilation system.....	111
5.1.1.	Sketch of these two systems.....	111
5.1.2.	Difference in design.....	113
5.2.	Description of the simulation model.....	113
5.2.1.	Micro-model.....	113
5.2.2.	Calculation for energy consumption	115
5.3.	Evaluation of thermal comfort in the occupied zone	116
5.3.1.	Evaluation Parameters.....	116
5.3.2.	Case study.....	118
5.4.	Simulation result.....	126
5.4.1.	Time to temperature balance.....	126
5.4.2.	Effect of air change rate.....	127
5.4.3.	Effect of position of air inlet and outlet.....	137
5.4.4.	Effect of swinging louver	141
5.5.	Summary and Conclusion.....	144
CHAPTER 6 FIELD EXPERIMENT OF DISPLACEMENT VENTILATION IN A RESIDENTIAL ROOM.....		147
6.1.	Details of the Displacement System.....	147
6.1.1.	Outline of the Displacement System.....	147
6.1.2.	System design.....	149
6.1.3.	Control system.....	149
6.2.	Outline of Field Experiment.....	151
6.2.1.	Site conditions	152
6.2.2.	Test points and instruments.....	152
6.2.3.	Scene on site.....	154

6.3. Results of experiment and simulation.....	154
6.3.1. Climate conditions	154
6.3.2. Conditions of Supply air	155
6.3.3. Temperature distribution.....	156
6.3.4. Air humidity	163
6.3.5. Velocity distribution	163
6.3.6. Draft.....	165
6.3.7. PMV	165
6.3.8. CO ₂ concentration.....	166
6.3.9. Energy consumption of cooling.....	167
6.4. Summary and Conclusion.....	168
CHAPTER 7 EFFECTIVENESS OF THERMAL STORAGE SYSTEM IN A RESIDENTIAL HOUSE.....	171
7.1. Proposition of thermal storage system for residential house.....	171
7.1.1. Thermal storage air-handling unit	171
7.1.2. Hot water tank.....	173
7.1.3. Characteristics of the proposed system.....	174
7.2. Case study.....	175
7.2.1. Air conditioning load	175
7.2.2. Hot water load.....	177
7.2.3. Setting of thermal storage air conditioning system.....	177
7.2.4. Setting of conventional system.....	179
7.3. Evaluation by simulation.....	180
7.3.1. Simulation model.....	180
7.3.2. Simulation results	183
7.4. Prospect evaluation for thermal storage system in residential house.....	189
7.4.1. Comparison of electricity consumption.....	189
7.4.2. Electricity cost.....	189
7.4.3. Comparison of annual cost	191
7.4.4. Impact on environment.....	192
7.5. Field experiment.....	193
7.5.1. Test points	193
7.5.2. Test results	194
7.5.3. Existing problems and prospect analysis	199

7.6. Summary and Conclusion.....	201
CHAPTER 8 CONCLUSIONS.....	203
REFERENCE.....	209
APPENDIX 1. ABSTRACT (IN JAPANESE).....	213
APPENDIX 2. RESUME (IN JAPANESE).....	217
APPENDIX 3. RESEARCH EXPERIENCE (IN JAPANESE)	219
APPENDIX 4. COMMITTEE REPORT ON EXAMINATION OF CANDIDATE FOR THE DEGREE OF DOCTOR OF ENGINEERING (IN JAPANESE).....	223

LIST OF FIGURES

Fig. 1-1.	Household energy consumption and numbers of household	2
Fig. 1-2.	Popularity rate of room air conditioner and computer in Japan.....	2
Fig. 1-3.	Detail household energy consumption in 2000	3
Fig. 1-4.	Ratio of energy consumption for cooling in recent decades.....	3
Fig. 1-5.	Survey of indoor pollution by National Consumer Affairs Center of Japan.....	4
Fig. 1-6.	Development of indirect solar house to double skin house	6
Fig. 1-7.	Multi-story type double skin system in the building of Obayashigumi Technology Research Institute, Tokyo, Japan (1982)	7
Fig. 1-8.	Single-story type double skin system in RWE Tower, Essen, Germany (1997)	8
Fig. 1-9.	Sketch of the SEA house and its performance in summer	9
Fig. 1-10.	Sketches of mixed ventilation and displacement ventilation system	10
Fig. 1-11.	Ratios of household appliances in the SOHO rooms	12
Fig. 1-12.	Electricity Power Demand for common use in a house with a SOHO room	12
Fig. 1-13.	Main parts of the Eco-ice Storage System.....	14
Fig. 1-14.	Features of future residential houses.....	15
Fig. 2-1.	Consideration of creating indoor environment.....	18
Fig. 2-2.	Outdoor air of Yahata in the typical meteorological year.....	19
Fig. 2-3.	Considerations of hybrid air conditioning system.....	20
Fig. 2-4.	Outdoor temperature difference between Fukuoka and Copenhagen.....	20
Fig. 2-5.	Illustration of an add-on green house.....	23
Fig. 2-6.	Double skin system in residential house	24
Fig. 2-7.	Sketch of water roof spray cooling system.....	24
Fig. 2-8.	Sketch of roof planting.....	25
Fig. 2-9.	Sketch of cool tube system	26
Fig. 2-10.	Sketch of displacement ventilation, task and ambient air conditioning	27
Fig. 2-11.	Example of Japanese Folk House	29
Fig. 2-12.	Development from exterior corridor to double skin space	29
Fig. 2-13.	Surface pressure on the roof with different slope	30
Fig. 2-14.	Plan of hybrid air conditioning system for an experimental house.....	31
Fig. 2-15.	Exterior appearance of the experimental house.....	32
Fig. 2-16.	Section of experimental house.....	32
Fig. 2-17.	Plan of the experimental house.....	33
Fig. 2-18.	Sketch of the ventilation system.....	34
Fig. 2-19.	Sketch of the energy system in the experimental house	35

Fig. 2-20.	Program structure of Airpak.....	36
Fig. 2-21.	Interface of Airpak2.0.....	37
Fig. 2-22.	Solution procedure for Airpak.....	39
Fig.3-1.	Outside air temperature at Yahata of Kitakyushu in TMY	42
Fig.3-2.	Prevailing wind direction in summer and intermediate seasons	42
Fig.3-3.	Wind speed in the whole year	43
Fig.3-4.	Average solar radiation and sunshine hours.....	43
Fig.3-5.	Sections of the house with and without double skin system.....	44
Fig.3-6.	Illustration of multi-layer structure of fenestration.....	47
Fig.3-7.	Heat transfer model for the house with double skin system.....	53
Fig.3-8.	Heat transfer process for the windows in the conventional model.....	57
Fig.3-9.	Simulation model of air flow around house.....	65
Fig.3-10.	Layout of double skin space and mesh profile	66
Fig.3-11.	Air flow and pressure around the model house.....	67
Fig.3-12.	Natural room temperature distribution for Cases 3-1 and 3-2	68
Fig.3-13.	Natural ventilation by stack effect.....	69
Fig.3-14.	Temperature stratification in vertical direction (at Y=0.6m)	70
Fig.3-15.	Velocity distribution at the section of openings	71
Fig.3-16.	Comparison of Cooling load between house with double skin and conventional house in summer	73
Fig.3-17.	Natural temperature distribution in winter for Cases 3-3 and 3-4.....	74
Fig.3-18.	Comparison of heating for Cases 3-3 and 3-4.....	76
Fig. 4-1.	Section of the double skin system in the experimental house (with test points).....	80
Fig. 4-2.	Scenery of the double skin system in the experimental house.....	80
Fig. 4-3.	Basic operation modes of the double skin system.....	83
Fig. 4-4.	Diversity operation modes of the double skin system.....	84
Fig. 4-5.	Outside air temperature and solar radiation in the summer experiment.....	85
Fig. 4-6.	Relative humidity of outside air and wind speed in the summer experiment	86
Fig. 4-7.	Wind rose in the summer experiment.....	86
Fig. 4-8.	Temperature distribution in the double skin and rooms	87
Fig. 4-9.	Variation of air velocity with temperature difference between average temperature in double skin and temperature under floor	88
Fig. 4-10.	Airflow by natural ventilation and mechanical ventilation, and the temperature difference between double skin and under floor (on Aug. 5)	89
Fig. 4-11.	Ratio of heat exhaust by ventilation in the double skin	91
Fig. 4-12.	Energy conservation in 1F SOHO Room.....	92
Fig. 4-13.	Energy conservation in 2F Living Room.....	92

Fig. 4-14.	Outside air temperature and solar radiation from Oct.10 to 15 in autumn	93
Fig. 4-15.	Outside air humidity and wind speed from Oct.10 to 15 in autumn	94
Fig. 4-16.	Wind rose from Oct.10 to 15 in autumn	94
Fig. 4-17.	Comparison of temperature distribution with different operation modes in the double skin in the middle of October 2001	95
Fig. 4-18.	Climate conditions on Nov. 8 (closed mode) and Nov.9 (mechanical ventilation mode).....	95
Fig. 4-19.	PMV improvement by ventilation.....	96
Fig. 4-20.	Sketch of the measurement of VOC.....	96
Fig. 4-21.	Outside air temperature and solar radiation in winter	99
Fig. 4-22.	Outside air humidity and wind speed in winter	99
Fig. 4-23.	Wind rose in winter (Feb.3 to Feb.10).....	100
Fig. 4-24.	Temperature distribution on Feb. 6 and 7 by Mode 2	100
Fig. 4-25.	The ratio of Energy conservation for heating in 1F SOHO room in the daytime ..	102
Fig. 4-26.	The ratio of energy conservation for heating in 2F Living room in the evening ...	102
Fig. 4-27.	Free heating hours in 2F Living room from 9:00 to 18:00 in winter	103
Fig. 4-28.	Temperature variation at different places in an hour	104
Fig. 4-29.	Temperature distribution and climate conditions in the subjective experiment in November 6 to 22.....	105
Fig. 4-30.	PMV in the middle of Living room in the subjective experiment (Nov. 6 to 22) ..	105
Fig. 4-31.	Results of subjective vote on the controlling in the double skin	107
Fig.5-1.	Sketch of the displacement ventilation system.....	112
Fig.5-2.	Sketch of the mixing ventilation system	112
Fig.5-3.	Layout of the SOHO with displacement ventilation system.....	119
Fig.5-4.	Illustration of the swinging louvers at the diffuser of air inlet.....	121
Fig.5-5.	Profile of mesh in the room without partitions.....	125
Fig.5-6.	Temperature vary with time for displacement ventilation at Cord 5 X=2.7m, Y=1.8m (Case 5).....	126
Fig.5-7.	Temperature vary with time for mixing ventilation at Cord 5 X=2.7m, Y=1.8m (Case 10).....	126
Fig.5-8.	Temperature distribution in displacement ventilation and mixing ventilation system (Cases 1 to 5, and 10)	128
Fig.5-9.	Temperature distribution at different heights for Case 3.....	129
Fig.5-10.	The relationship of temperature deviation at different heights gradient with air change rate (Cases 1 to 5).....	130
Fig.5-11.	The temperature gradient for Case 3.....	131
Fig.5-12.	Temperature distribution with air change rate for displacement ventilation.....	131

Fig.5-13.	Recommended air change rate from temperature gradient	132
Fig.5-14.	Velocity distribution in Cases 1 to 5 and Case 10	133
Fig.5-15.	Turbulence intensity and draft rating in Cases 1 to 5.....	134
Fig.5-16.	PMV distribution in Case 3.....	135
Fig.5-17.	PMV distribution with air change rate	135
Fig.5-18.	Distribution of local age of air in Case 3.....	136
Fig.5-19.	Air conditioning load with air change rate	137
Fig.5-20.	Comparison of temperature distribution for the displacement ventilation systems (Cases 3 and 6) and the mixing ventilation system (Case 10).....	138
Fig.5-21.	Comparison of PMV distribution for the displacement ventilation systems (Cases 3 and 6) and the mixing ventilation system (Case 10)	138
Fig.5-22.	Temperature difference between displacement ventilation and mixing system near the floor and ceiling in X direction	140
Fig.5-23.	Temperature difference between displacement ventilation and mixing system near the south glass in Z direction.....	140
Fig.5-24.	Detail composition of cooling load for displacement ventilation (Case 3, Case 6) and mixing system (Case 10)	141
Fig.5-25.	Temperature profile at Y=1.8m for Cases 3, 7-10	142
Fig.5-26.	Temperature distribution for Cases 8 and 9.....	142
Fig.5-27.	Velocity distribution at 0.1m for Cases 8 and 9.....	143
Fig. 6-1.	Air conditioning system in the experimental house.....	148
Fig. 6-2.	Construction of the fan unit	150
Fig. 6-3.	Sketch of the control system for air conditioning in the experimental house	151
Fig. 6-4.	Points distribution in the SOHO (plan view and section view)	153
Fig. 6-5.	Scene of the displacement ventilation test in Aug. 2001	155
Fig. 6-6.	Outside temperature and solar radiation on August 2, 2001.....	155
Fig. 6-7.	Supply air temperature and airflow rate from the AHU	156
Fig. 6-8.	Temperatures of interior surfaces during 9:00 to 19:00	157
Fig. 6-9.	Air temperature at different heights in the middle of the room (Cord 5 X=2.7m, Y=1.8m, Z=0m from 9:00 to 19:00)	158
Fig. 6-10.	Air temperature at different heights in the middle of the room (at the section of Y=1.8m, at 12:00)	158
Fig. 6-11.	Correlation coefficient of the simulation result and measurement	159
Fig. 6-12.	Temperature distribution at different heights at 12:00 on August 2.....	160
Fig. 6-13.	Indoor temperature gradient.....	162
Fig. 6-14.	Comparison of temperature gradient between experiment and simulation.....	162
Fig. 6-15.	Dissatisfaction rate casued by temperature stratification.....	163

Fig. 6-16.	Distribution of relative humidity in the middle of the room (at Y=1.8m)	164
Fig. 6-17.	Velocity at 1.1m in the middle of the room from 9:30 to 11:00	164
Fig. 6-18.	Comparison of velocity distribution between field experiment and simulation (at the height of 0.1m at 12:00)	165
Fig. 6-19.	PMV distribution at Y=1.8m in the middle of the room at 12:00	166
Fig. 6-20.	CO ₂ concentration distribution at the section	167
Fig. 6-21.	Calculated cooling load in the experiment room	167
Fig.7-1.	Energy system in the experimental house.....	171
Fig.7-2.	Heat exchange of the conventional system.....	172
Fig.7-3.	Heat exchange of the proposed system.....	172
Fig.7-4.	Plan view and elevation of the proposed thermal storage air handling unit	173
Fig.7-5.	Daily schedule in the experimental house	175
Fig.7-6.	Comparison of air conditioning load between the experimental house and other houses	176
Fig.7-7.	Hourly cooling load on August 4 in the experimental house	177
Fig.7-8.	Layout of proposed direct heat exchange tubes in the air conditioning unit	180
Fig.7-9.	Illustration of the coil layout in the thermal tank	181
Fig.7-10.	Profile of mesh around the tubes	182
Fig.7-11.	Temperature variation at different air velocity when the tubes are at 0°C and 7°C	184
Fig.7-12.	Temperature distribution at different air velocity when the direct heat exchange tubes are at 0°C.....	184
Fig.7-13.	Distribution of air velocity around tubes in the heat exchanger when the velocity at air inlet is 2m/s	185
Fig.7-14.	Relationship of maximum velocity and average velocity with inlet velocity.....	186
Fig.7-15.	Pressure distribution around the tubes when the air velocity at the inlet is 2m/s...	186
Fig.7-16.	Pressure drop between columns in Case 7-2 and Case 7-6.....	187
Fig.7-17.	Pressure drop at different velocity through direct heat exchange tubes.....	187
Fig.7-18.	Heat transfer coefficient on the surface of tubes.....	188
Fig.7-19.	Comparison of electricity consumption between the proposed system and the conventional system.....	190
Fig.7-20.	Comparison of Annual CO ₂ Emission between the proposed system and the conventional system.....	193
Fig.7-21.	Illustration of test points in thermal storage system	194
Fig.7-22.	Scene after charge and in discharging in the thermal storage tank.....	194
Fig.7-23.	Temperature variation in a charge-discharge process	195
Fig.7-24.	Temperature variation at different airflow rates.....	196

Fig.7-25.	Energy utility analysis on August 1,2001	198
Fig.7-26.	Coefficient of performance of the whole system.....	199
Fig.7-27.	Energy conservation of the proposed system (in one day)	200
Fig.7-28.	Energy cost saving of the proposed system (in one day).....	200

LIST OF TABLES

Table 1-1.	Specification of the Eco-ice Storage Unit	13
Table 2-1.	COP of room air conditioner for houses in the summer of 2002	28
Table 3-1.	Thermal properties of surface materials	48
Table 3-2.	Optical properties of glass, indoor shading and wall	50
Table 3-3.	Cases description for double skin system.....	51
Table 3-4.	Convection heat transfer coefficients for simulation.....	60
Table 3-5.	Outside climates of summer for natural temperature and cooling load calculation .	61
Table 3-6.	Outside climates of winter for natural temperature and heating load calculation ...	62
Table 3-7.	Coefficients of conduction transfer functions	63
Table 3-8.	Boundary conditions of atmosphere velocity.....	65
Table 3-9.	Boundary conditions (temperature).....	66
Table 3-10.	Solar heat gain exhausted in the double skin system	72
Table 4-1.	Detail constitution of the double skin in the experimental house.....	81
Table 4-2.	Testing points and instruments in the double skin	82
Table 4-3.	Energy flow in double skin in Mode 1	90
Table 4-4.	Cases setting for energy consumption with/without double skin	91
Table 4-5.	Testing of air change rate by natural ventilation.....	97
Table 4-6.	Pollutant emissions tested in the experimental house	98
Table 4-7.	Comparison of VOC emissions between Sept. and Mar. 2001.....	98
Table 5-1.	Comparison of difference in design between the displacement ventilation system and the mixing ventilation system	113
Table 5-2.	Description of cases for simulation	120
Table 5-3.	Calculation of the turbulent intensity I_{tur} in a cycle	122
Table 5-4.	Details of boundary conditions	123
Table 5-5.	Under-relaxation factors for equations	125
Table 6-1.	Detail construction and overall heat transfer coefficient U of materials	148
Table 6-2.	Site conditions in the experiment room.....	152
Table 6-3.	Test points and instruments in displacement ventilation system in summer.....	154
Table 6-4.	Comparison of simulation and measurement at Y=1.8m (12:00)	159
Table 6-5.	Temperature deviation at difference heights (12:00).....	161
Table 7-1.	Set values and calculation of air conditioning load in the experimental house.....	176
Table 7-2.	Thermal storage capacity and electricity consumption of the proposed system....	179
Table 7-3.	Composition of the conventional system.....	179
Table 7-4.	Cases of direct heat exchange.....	181

Table 7-5. Under-relaxation factors for equations	183
Table 7-6. Electricity charge with different contract plans	190
Table 7-7. Electricity cost for two systems.....	191
Table 7-8. Comparison of cost effectiveness between the proposed system and the conventional system.....	192
Table 7-9. Test points of thermal storage air conditioning unit	193
Table 7-10. Energy flow on August 1	200

NOMENCLATURE

A	Area, m ²
<i>a</i>	Absorptance
C	CO ₂ concentration, ppm; or Constant
CW	Cold water
C _D	Discharge coefficient for opening, dimensionless
C _p	Specific heat at constant pressure, J/kg.°C
C _v	Effectiveness of openings, dimensionless
C _n	Ventilation effectiveness
F	View factor, dimensionless
G _k	Generation of turbulent kinetic energy due to mean velocity gradient
G _b	Generation of turbulent kinetic energy due to buoyancy
g	Accelerate of gravity, 9.8m/s ²
h	High, m; or enthalpy, J/kg
H	High, m
I	Solar Radiation (direct and diffused), W/m ²
K	Conductive coefficient, W/m ² .K
<i>k</i>	Molecular conductivity, W/m.K
<i>k_t</i>	Conductivity due to turbulent transport, W/m.K
<i>m</i>	Air flow rate, m ³ /s
N	Air change rate, per hour
P	Air pressure, Pa
Pr	Prandtl number
T	Temperature, K
t	Temperature, °C; or time (s)
t _e	Solar temperature, °C
Q	Heating/cooling load, W; or heat rate
q	Heat rate, W
q _k	Heat conductive rate, W
R	Thermal resistant, m ² .K/W
U	Wind speed, m/s; or overall heat transfer coefficient, W/m ² .K
u	Air speed, m/s
<i>V</i>	Air flow rate, m ³ /s

X	Outside conductive transfer functions; or radiation constant
x	Coordinate direction
Y	Cross conductive transfer functions
Z	Inside conductive transfer functions

Greek Symbols

α	Overall heat transfer coefficient, W/m^2 ; or absorptance
α_c	Convective heat coefficient, W/m^2
β	Thermal expansion coefficient of air, K^{-1}
δ	Time step, s; or thickness, mm
ΔP	Pressure difference, Pa
ΔR	Difference between long-wave radiation incident on surface from sky and surroundings and radiation emitted by blackbody at outdoor air temperature, W/m^2
ε	Emittance
ϕ	Flux conductive transfer functions
λ	Conductivity, $W/m.K$
μ	Viscosity, $N.s/m^2$
θ	Time
ρ	Air density, kg/m^3 ; or reflectance
σ	Stefan-Boltzmann Constant, i.e. 5.67×10^{-8} ($W/m^2.k^4$)
τ	Transmittance; or time (s)
Γ	Diffusive coefficient

Subscripts

ac	Air conditioning
asol	Absorbed direct and diffuse solar radiation
CE	Convective parts of the internal part
cl	Cooling
conv	Convective heat exchange
ds?	Double skin
eff	Effective

ex	Exhaust air
ew	East wall
fl	Floor
g	Exterior window (glass)
g'	Interior window (glass)
gl	Exterior glass
i	Inside; or interior surface; or <i>i</i> term; or inlet
IV	Infiltration and ventilation
j	<i>j</i> term
LWR	Net long-wave radiation between air and surroundings
LWX	Net long-wave radiation between interior surfaces
m	Middle air between shading and exterior glass
n	Nominal
NPL	Neutral pressure level
o	Outside air; or outside surface; or out
OA (oa)	Outside air
rad	Radiation
RA (ra)	Return air
rf	Roof
rm	Room
s	Surface
SA (sa)	Supply air
sd	Sun shading
si	Interior surface
so	Exterior (outside) surface
t	Turbulent
w	Exterior wall
w'	Interior wall
ww	West wall
sw	Short-wave radiation from lights and equipment

CHAPTER 1

INTRODUCTION

The energy consumption in residential and commercial sector accounts for 1/4 of the total, and the energy consumption in residential houses accounts for 14% of the total in 1999 in Japan with the annual increase of about 2%. In order to fulfill the targets of Kyoto Protocol, the energy conservation for residential houses should be paid more attention. With the information technology (IT) revolution, SOHO (Small Office and Home Office) applications are popularized to realize working in homes. At the same time, the human requirement for living has also been improved, especially for indoor air environment. All these lead to the increase of energy consumption for household air conditioning.

On the other hand, the air conditioning systems seems to be more sophisticated and difficult for operation in order to make a good environment and to be energy saving. It is known that many of the existing buildings consume more energy than they were designed without good commissioning or maintenance.

Therefore, the residential houses should be designed for the sake of energy conservation, occupancy health and convenience of operation.

1.1.Lifestyle variation and household energy consumption

Japan has become an aging society with fewer children, and the ratio of population over age of 65 will increase from 14.6% in 1995 to 32.3% in 2050, while the total fertility rate decreases from 1.75 in 1980 to 1.39 in 1997, according to the statistics of Ministry of Public Management, Home Affairs, Posts and Telecommunications (Statistics Bureau of Japan, 2001). The variation of household structure is shown in Fig.1-1, and the average number of persons per household declines from 3.28 in 1975 to 2.67 in 2000. On the other hand, the living conditions have been greatly changed, as well as their lifestyle. For example, Fig.1-2 shows that the popularity rate of room air conditioner increases from 2% in 1965 to 86.2% in 2000, while computer increases from 11.7% in 1986 to 50.1% in 2000 (IEEJ, 2002).

Correspondingly, the household energy consumption has increased in recent decades. The household energy consumption reaches 53219×10^{10} kcal in 2000, which is 2.2 times as much as that in 1973 (IEEJ, 2002), and the detail structures are shown in Fig.1-3.

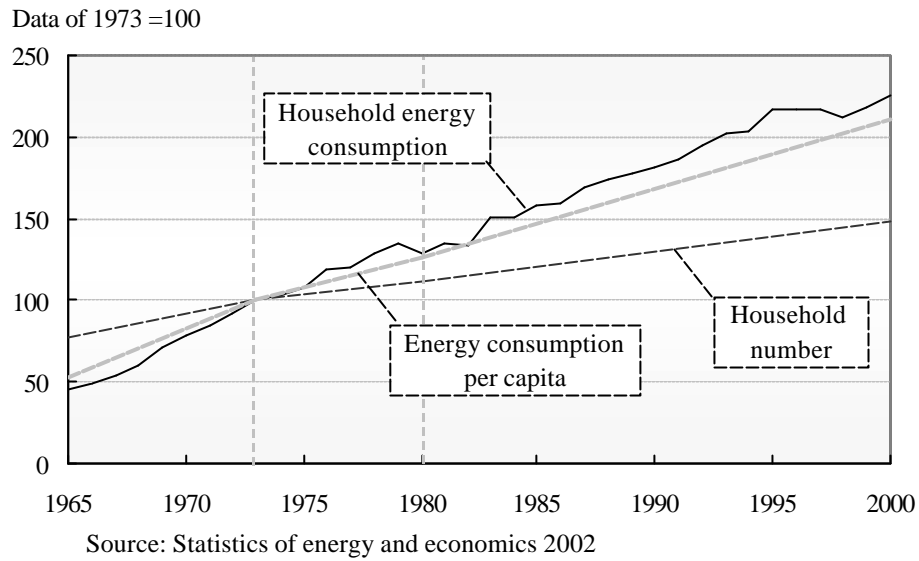


Fig. 1-1. Household energy consumption and numbers of household

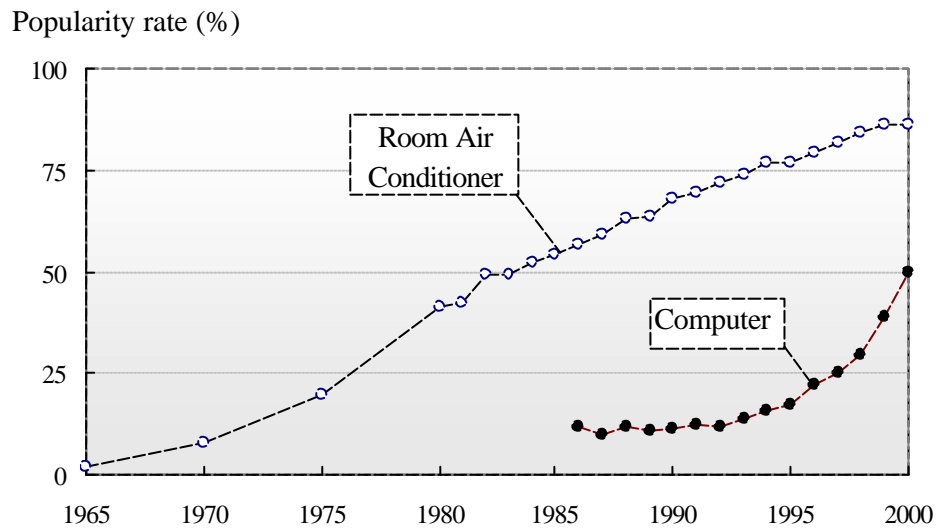


Fig. 1-2. Popularity rate of room air conditioner and computer in Japan

Energy consumption for heating accounts for 27.6%, hot water for 28.3%, and other appliances for 35.2%. Although the ratio of cooling is the smallest, it has increased fastest in recent decades. Fig.1-4 shows that the ratio increases from 0.4% in 1965 to 2.2 % in 2000 (IEEJ, 2002).

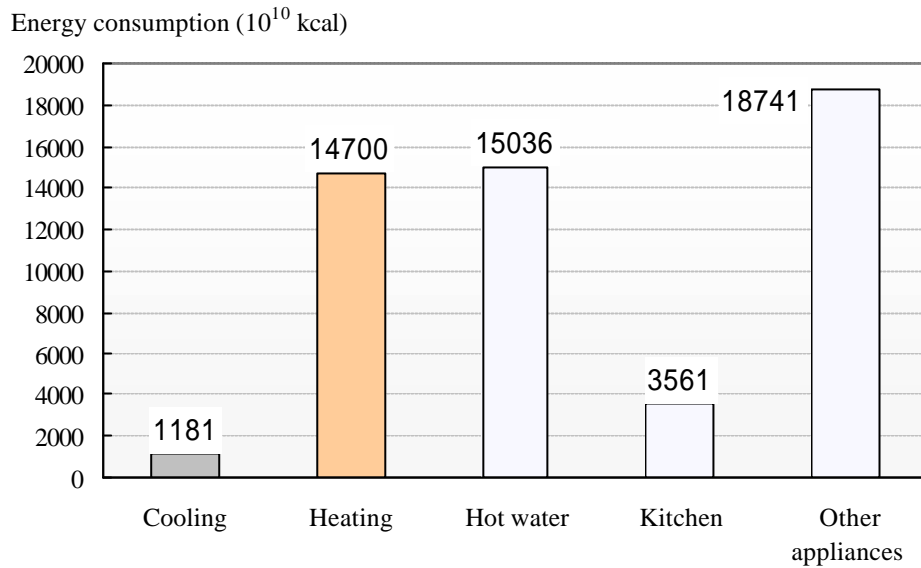


Fig. 1-3. Detail household energy consumption in 2000

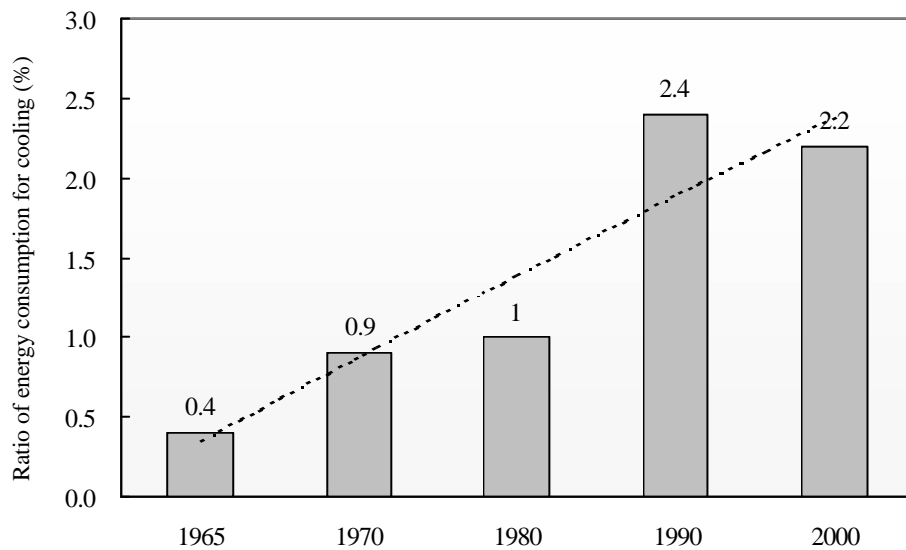


Fig. 1-4. Ratio of energy consumption for cooling in recent decades

The reason why the cooling part has increases so fast lies in that the living conditions have been improved, as well as the variation of lifestyle and occupant requirements.

According to *National Time Use Survey 1995* of NHK Broadcasting Culture Research Institute, about 60% people stay up until 11:00 in the night, while only 25% in 1995.

With the information technology (IT) development, small office & home office (SOHO) applications have been popularized in recent years. People work at their homes by means of computers and information technology.

All these lead to the increase of cooling load in houses, therefore energy saving for air conditioning should be paid more attention.

1.2. Healthy requirement and ventilation

So far people spend about 90% of their time indoors. With the popularization of SOHO applications, people will spend more time in their homes and the health risks associated with indoor environment may be greater.

The houses become more airtight for energy saving and thermal comfort in these days with the synthetic and mineral insulation materials, but most of them may emit volatile organic compounds (VOCs). Furthermore, hazardous chemicals such as paints for furniture, cleaning materials, polishes and other interior decorations exist in many houses. All these could lead to the sick house problems.

According to the survey on indoor pollution by National Consumer Affairs Center of Japan (NCAC, 1998), sick house problems occurred in 13.1% newly built mansions (Fig.1-5a), among which 50% accounts for formaldehyde, 15.4% for xylene and toluene, 5.8% for pesticide, unknown sources 19.2%, and the others 9.6% (Fig.1-5b).

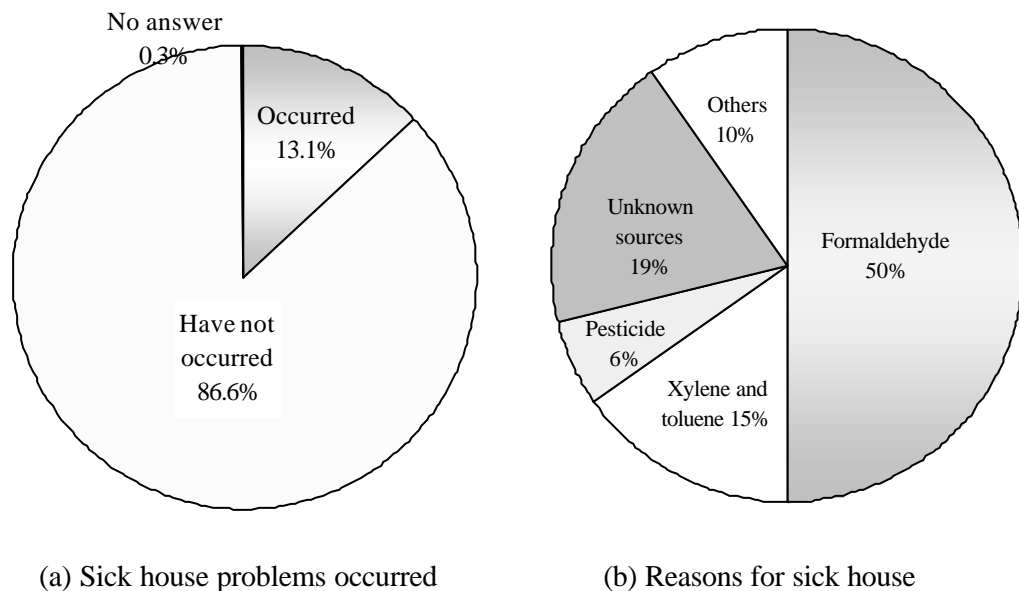


Fig. 1-5. Survey of indoor pollution by National Consumer Affairs Center of Japan

On the other hand, the tight structures separates people from the outside atmosphere, occupancy is very difficult to communicate with the outside world. While the conventional room air conditioners only cool the room air and make air circulation within rooms, the inadequate fresh air supply contributes to poor indoor air quality.

According to the survey of the National Association of Home Builders, among 60963 single and multifamily homes built by 2282 different American building companies in 1995, only 3.3% are equipped with fresh air exchanger (Schoenwetter, W. F. 1997).

Ventilation plays an active role in exhausting contaminants, diluting potentially contaminated indoor air, as well as controlling the indoor humidity and temperature. According to ASHRAE *Standard 62*, the minimum outside air ventilation for one person is 8L/s, i.e. 28.8m³/h.

There are two ways for realize ventilation in houses, one is mechanical ventilation, which is independent from the building shell, and the other is natural ventilation, which relies on leakages or openings, such as windows and doors.

Samet et al. note, "Control of ventilation in residences is particularly difficult. Natural ventilation varies with weather conditions, construction, and occupant activities, and air exchange can be readily altered only if the house is equipped with a central heating and cooling system designed to control fresh air intake. Equipping a home with a heat exchanger, either a window unit or a central system, provides a modest increase in air volume exchange" (Samet, J.M. 1988).

If the mechanical ventilation operates constantly and consistently, it will be good for indoor environment. Of course, this will lead to more energy consumption.

1.3. Conventional research

As for the energy conservation and the indoor air quality in buildings, a lot of researches have been carried out. Many technologies, which are often used in office buildings with large floor area, may be possible for residential houses.

1.3.1. Double skin system

Nowadays the fully glazed façade systems become very popular, which satisfy human needs for visual communication with the outside world, and admit more solar radiation for lighting and heating. The exterior and interior appearance of a building has been greatly

improved.

And the indirect gain solar houses use the south-facing wall surface or the roof of the structure to absorb solar radiation, which causes a rise in temperature. With using the glass instead of masonry wall, the glazing reduces the loss of heat from the wall back to the atmosphere (ASHRAE, 1995). Openings in the walls, near the floor, and near the ceiling allow convection to transfer heat to the room, the air in the room warmed by solar radiation rises and can be exhausted to the outside. Cool air flows through the lower openings. This system is illustrated in Fig.1-6 (a), which is the prototype of the double skin system (IBEC, 1985). The disadvantage of this system is that the natural ventilation will be not possible when the outdoor temperature is high or too low. Recent development is the double skin system shown in Fig.1-6 (b). At the outside of the south wall, one more exterior glass wall is built, and this space between the two walls is called double skin space. The main components are glass windows, sun shading and ventilation devices.

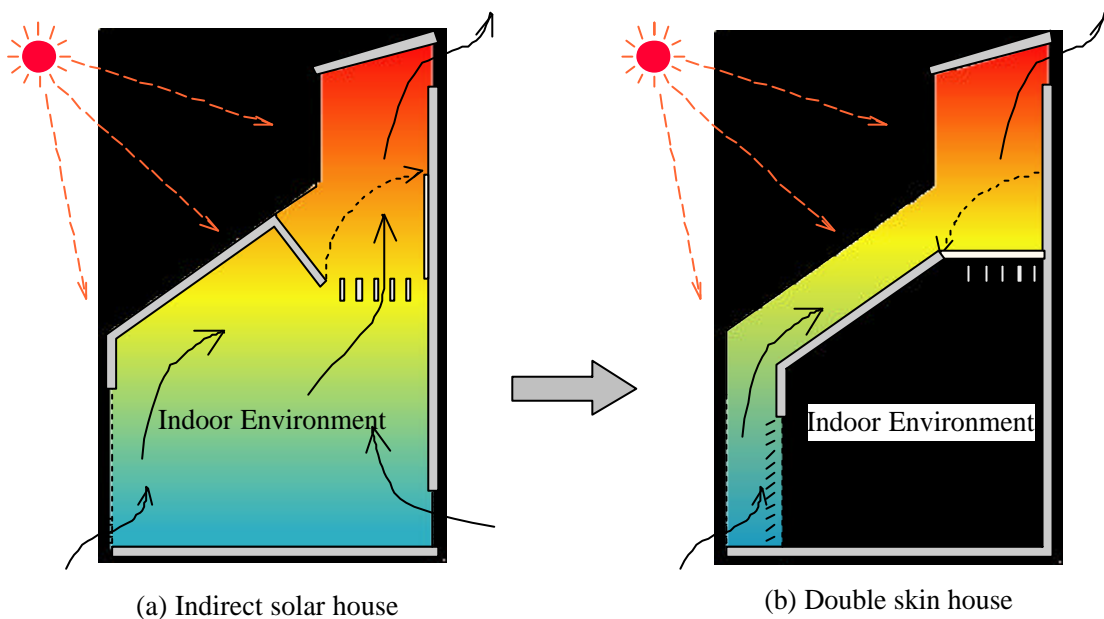


Fig. 1-6. Development of indirect solar house to double skin house

There are basically two kinds of double skin systems, one is the multi-story type and the other is the single-story type.

The example of the multi-story type double skin system is illustrated in Fig.1-7, which was adopted in the main building of Obayashigumi technology research institute completed in 1982. This building has a floor area of 3775m² with four stories (three stories above the ground,

one story under the ground). The exterior glass is reflective coated type with the thickness of 8mm, while the interior glass is ordinary flat glass with the thickness of 5mm. The exterior wall has a slope of 5° to reflect the solar radiation in the summer. The width of the double skin is 1.2m at the bottom floor, while it is 2.4m at the top. The double skin space is divided into four stories by grills, which can also act as shadings. In addition, the ventilation devices are also equipped.

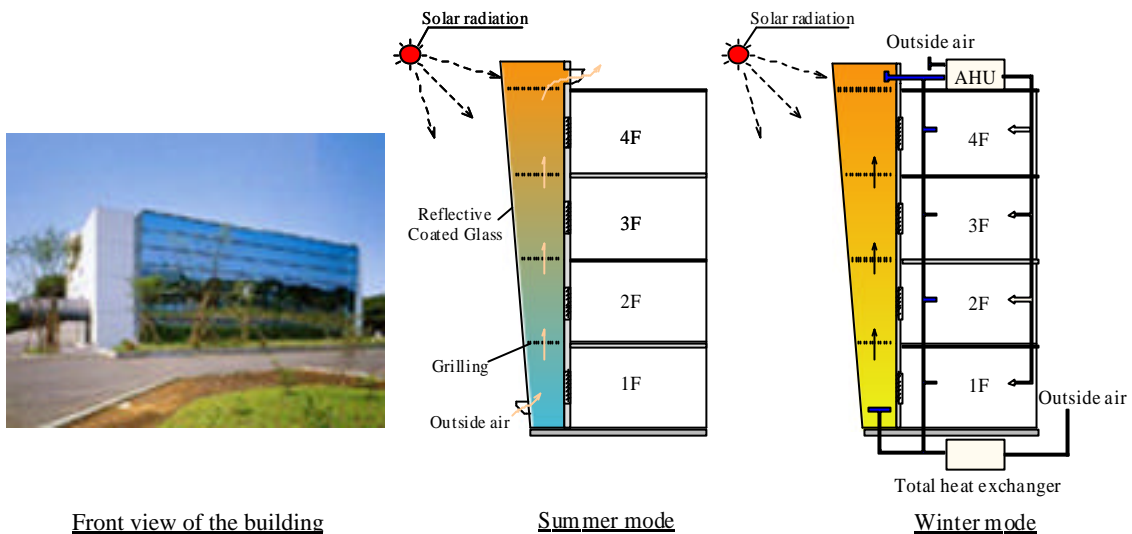


Fig. 1-7. Multi-story type double skin system in the building of Obayashigumi Technology Research Institute, Tokyo, Japan (1982)

In the summer, the upside and lower openings are opened, although the temperature in the double skin space will be increased, natural ventilation caused by thermal forces can exhaust heat, which is called stack effect. While in the winter, the openings are closed, the double skin space act as a greenhouse, which can be used for pre-heating the outside air of the whole air conditioning system. Oka, T. (1984) did some measurements in this building. The air change rate caused by natural ventilation reaches 50-100 per hour in the cloud days in summer with the temperature in double skin of 3-4°C higher than the outside, and 22% energy consumption can be cut down by stack effect when the rate of south window area is 50%; while the air in this space can absorb 16% solar radiation with the temperature of 27-32°C, and 24% energy consumption can be reduced in winter.

The example of the single-story type double skin system is illustrated in Fig.1-8, which was adopted in RWE tower in Essen, Germany in 1997. The building has a floor area of 36000m² with twenty-nine stories and three basements, and it has a cylindrical shape with a

double skin system around the entire façade. The exterior glass is 10 mm thick strengthening glass, while the interior glass is multi-type or Low-E glass (6mm+air 14mm+6mm), which is 0.5m away from the exterior glass. And the louver sun shadings are also installed. About 30-35% of the energy for air conditioning can be saved in one year (Ohga, H. 2001).

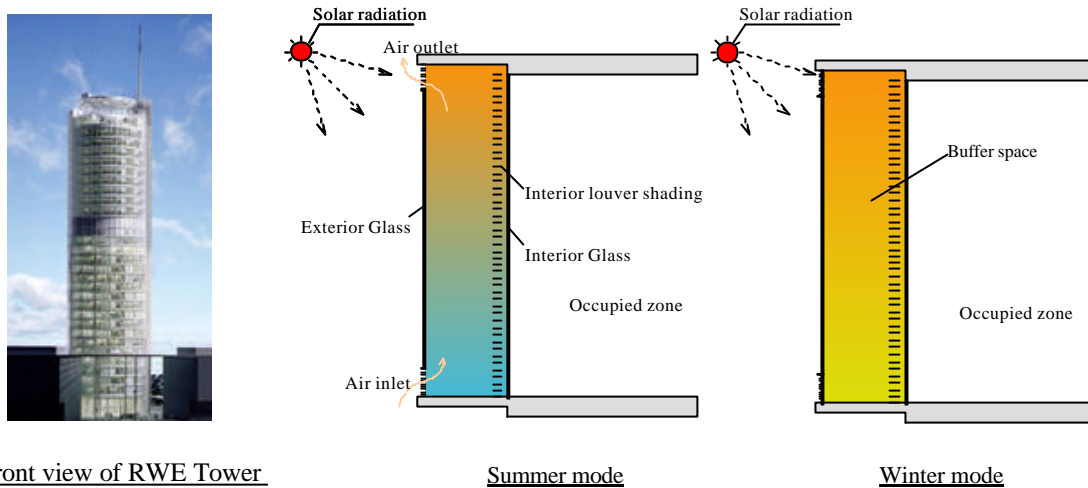


Fig. 1-8. Single-story type double skin system in RWE Tower, Essen, Germany (1997)

Recent studies about the double skin system can also be found in Sendai Mediatheque completed in 2001 in Japan, according to the measurement in winter, even with less solar radiation, the air in the second story is 5°C higher than the outside air, while it is 8-10°C above the third story, and 30-50% heating load can be cut down (Furubayashi, T. et al. 2001.). Henson (2002) made a study on the energy conservation performance of double skin and confirmed that 15-17% cooling load from 2nd floor to 8th floor in summer can be cut down. The lower stories would have more significant energy savings.

The similar system is also proposed by Zhang and Ishihara (1997) in a new type of residence with solar heating, earth cooling, and air circulation, which is called the SEA house. Thermal insulation, heat storage and air circulation are used to maintain the room temperature at a comfortable level and reduce the temperature difference between the south side and the north side of the house. In summer, the opening in the lower floor is opened so that the air can be led to the ventilating layers through the earth tubes. After cooling the solar collection storage wall on the south and the heat storage wall on the north side, the air is exhausted to the outdoors by a fan, as shown in Fig.1-9. While in winter, the cap of earth tube is closed, solar radiation is absorbed by the solar collection wall and southern storage wall, then the air temperature in the

south ventilation layer is raised, and the air temperature in the north ventilation layer drops because of the northern storage wall, therefore the air circulates in the room. Simulation results show that the room temperature can be maintained at less than 28°C in summer and more than 18°C in winter without air conditioning. This SEA house is a fully passive house and almost free of nonrenewable energy for cooling and heating in mild regions, such as Tokyo. The function of ventilation layer in this study is similar to that of the double skin space.

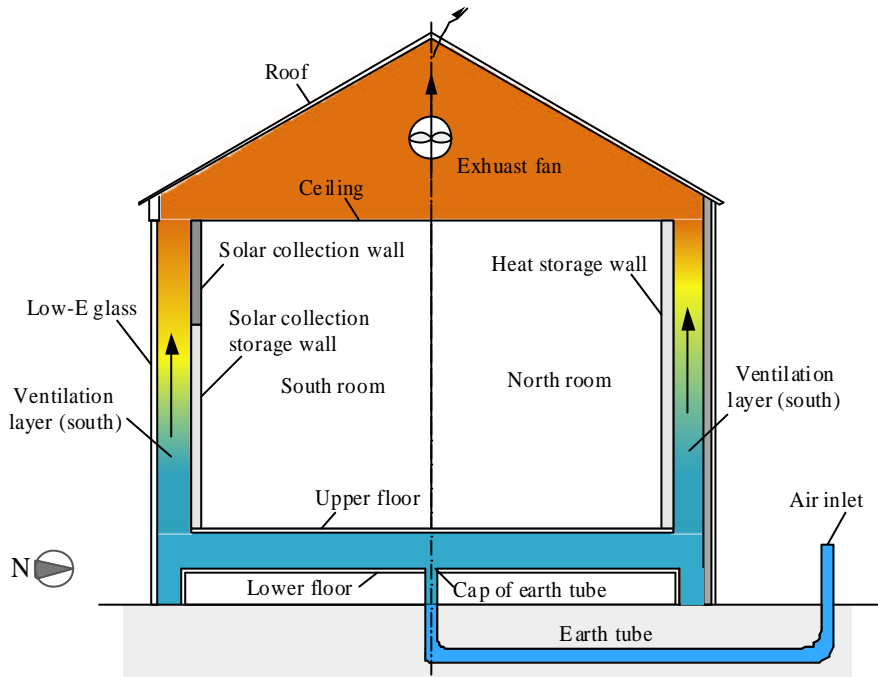


Fig. 1-9. Sketch of the SEA house and its performance in summer

1.3.2. Displacement ventilation

If people work in the SOHO, they will need a longer time air conditioning and a better indoor environment. As for the conventional mixed ventilation system (Fig.1-10a), it supplies air from near the ceiling, and the outlet is set near the floor, and the whole room will be kept to a uniform temperature, even those places near the ceiling, where air conditioning is unnecessary in fact. But for the displacement ventilation (Fig.1-10b), it supplies air from near the floor, and the return air outlet is set at the high part of the room, while the exhaust outlet is on the ceiling. Only the occupied zone is conditioned. And the convection heat from the ceiling, as well as the heat from lights, would be discharged with the exhaust air. Furthermore, the contaminant occurs from the occupant will also be exhausted at the higher places, and they would have little effect on the occupied zone, thus the ventilation effectiveness of displacement system is good.

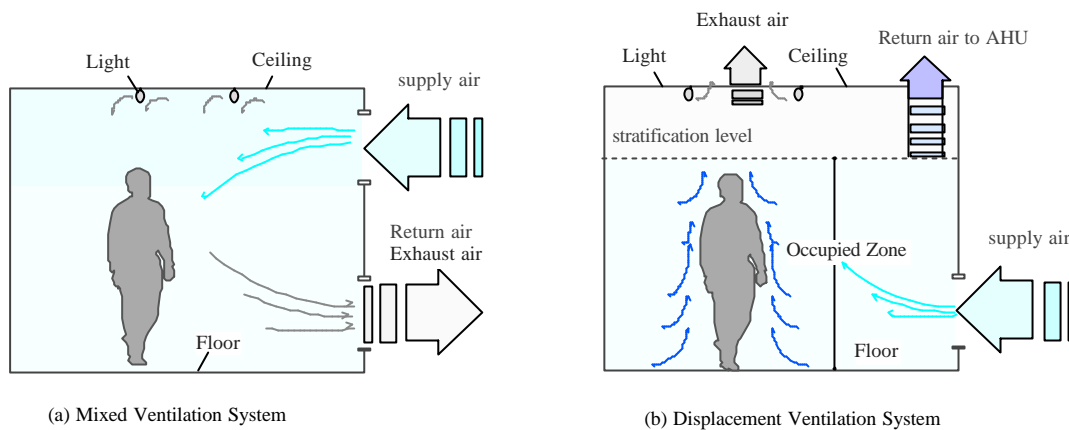


Fig. 1-10. Sketches of mixed ventilation and displacement ventilation system

The displacement ventilation system has been widely used in office buildings in the North Europe. As the conditioned air is directly supplied into the occupied zone at a low velocity, and the temperature stratification occurs in the vertical direction by the buoyancy force. Skistad, H. (2002) stated that the displacement ventilation had more potential for free cooling, and needed less cooling energy than mixing ventilation. This is very obvious in high rooms. And the air change efficiency of displacement ventilation would be 20-40% higher than that of mixing ventilation (Mundt, 1994). Svensson, A. G. L. (1989) stated that the convection heat from the ceiling, as well as the heat from lights, would be discharged with the exhaust air. And the contaminant occurs from the occupant can also be exhausted at the higher places, and they have little effect on the occupant area, thus the ventilation effectiveness is good.

Tanabe, S. and Kimura, K. (1996) measured the age of air in an office room with three different ventilation systems, they concluded that a wall-mounted displacement system provides better air quality than a floor-mounted displacement, and the floor-mounted system is better than a ceiling-mounted mixing system. Murata, T. (1998) investigated the displacement ventilation system in a concert hall, and the PMV in the occupied zone is below 0.5, and the energy consumption of air conditioning was about 70W/m^2 in the summer.

The air exchange effectiveness of the completely mixed air conditioning system is 1, while it is 2 for an ideal piston type displacement ventilation system (Matsumoto, H. 2002). Therefore the practical air exchange effectiveness is usually between 1 and 2.

Ikeda, K. (1996) pointed out that the temperature difference between supply air and room air was $4\text{-}5^\circ\text{C}$, while it was about $8\text{-}15^\circ\text{C}$ for the mixed system, but the airflow rate would be larger.

He compared the thermal comfort in the indoor environment between the displacement ventilation system and the conventional system, and stated that the displacement system had a low dissatisfactory and was expected to have a low air conditioning load.

As the supply air temperature of displacement ventilation can be higher, the availability for free cooling natural ventilation may be enlarged.

Jackman, P. J. (1991) stated that a way of increasing the cooling capacity of displacement ventilation systems is to recirculate some of the room air in the occupied zone through an induction circuit, i.e. the room air is induced into the supply air and is mixed with it before being discharged through the low-velocity air terminal device into the room. This reduces the room air temperature gradient for a given cooling load, thus allowing a cooling load limit of up to 50W/m^2 .

But it should be pointed out that as temperature stratification occurs in the occupied zone, according to the standard of ISO7730, the recommended temperature gradient should be smaller than 3°C/m . And for an occupant, the air velocity in the occupied zone should not be larger than 0.3m/s .

In addition, if the displacement system is adopted, air-handling unit, which supplies conditioned air, is necessary. Therefore there should be a heating and cooling machine, and the energy saving for machine is also important.

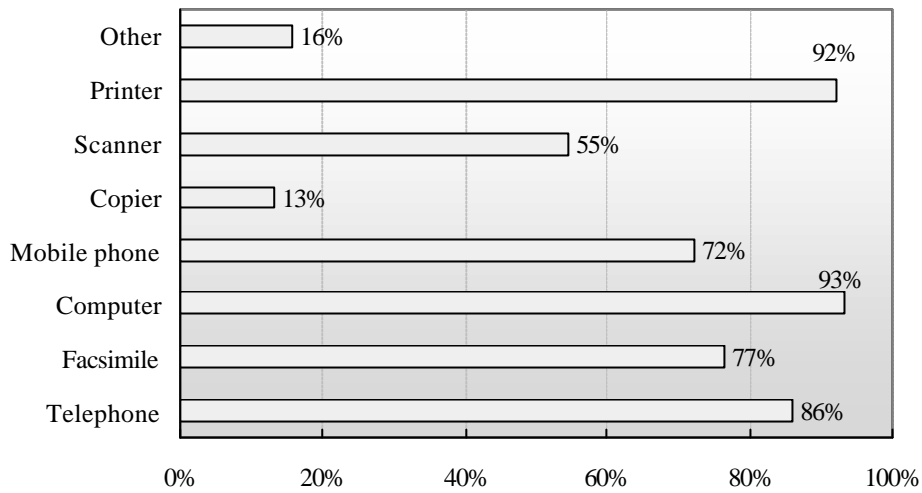
1.3.3. Thermal storage

As SOHO applications have been popularized fast, the electricity consumption will be increased with the popularization of the household appliances. According to the survey conducted by SOHO Think Tank (2001), the popularity of computer accounts for the biggest of 93%, then the printer for 92%, and telephone for 86%, as shown in Fig.1-11.

The electricity consumption in a house with SOHO application with floor area of 180m^2 , among which 25m^2 is for SOHO, is shown in Fig.1-12. The electricity demand of SOHO can be calculated by the unit of intelligent office, while the demand of conventional room is calculated by the unit of a suburb residential house (Ojima, T. 1995).

Because the electricity demand increases in the daytime, the air conditioning load will increase correspondingly, while it is small in the evening. The difference between peak load and off-peak is also increases.

Therefore it is necessary to use the thermal storage system in the residential house, and it has the following benefits:



Source: SOHO White Book (2001)

Fig. 1-11. Ratios of household appliances in the SOHO rooms

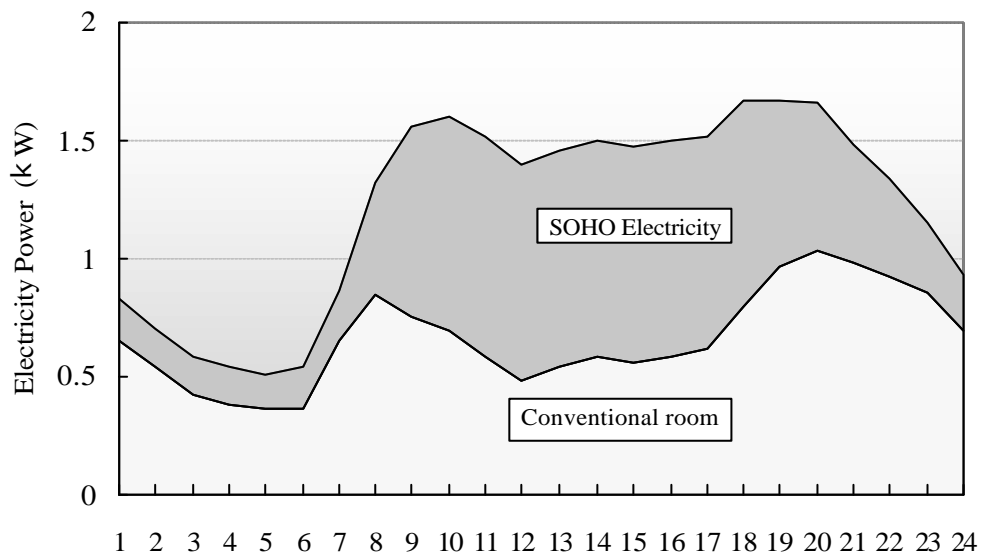


Fig. 1-12. Electricity Power Demand for common use in a house with a SOHO room

- Reducing equipment size: it can be used to meet a portion of peak loads, equipment size will also be reduced, as well as the capital cost;
- Energy cost savings: because the nighttime price of electricity is only 1/4 to 1/3 of the daytime, more electricity used in the night will lead to more energy cost saving;

- Energy savings and environmental benefits: thermal storage permits the operation of equipment under full-load conditions, avoiding inefficient part-load performance. Fiorino (1994) stated that it reduce annual energy consumption for air conditioning by up to 12%. And the energy savings will decrease the emissions of CO₂, NO_x.

The research and development of small size thermal storage system has been done for a long time. Ten electricity power companies of Japan (Tokyo Electricity Power Co. and others), together with four air conditioner manufactures developed an Eco-ice storage unit in 1999, which aims to the small shops, and office with floor area of 100-200m². The detail specification of this unit is shown in Table 1-1.

Table 1-1. Specification of the Eco-ice Storage Unit

Item	Cooling	Heating
Output	12.5-19.1kW	11.2-19.4 kW
Power (Input)	3.2-4.7 kW	3.39-5.12 kW
Thermal storage capacity	95MJ	
Charging time	5 hour	
Discharging time	8.1 hour	
Thermal storage method	Static mode	Defrost mode
Dimension	L1000×W620×H1455 (Thermal storage unit)	
	L880×W345×H1345 (Outdoor unit)	

Source: http://www.daikinaircon.com/catalog/d-catalog/ice/ekoaisu/f_set1.html

As the Eco-ice storage system is not designed for residential houses, whose cooling load is smaller, the size is very difficult for a common house (Fig.1-13). Therefore a smaller system is needed for a residential house with SOHO applications.

1.4.Objective of this research

In modern society, with the quick development in economic s, lots of buildings have been constructed, while a great number of wastes have been left. In order to reduce their impacts on global environment, the technology of recycle is a good solution. The energy conservation should be paid enough attention in the periods of construction, operation and dismantling. Nakajima, Y. (2000) provided a residential system for low environment impacts and resources

circulation in the recycling of building material especially in the period of construction and dismantling. And the proposition was verified in the experimental house in Kitakyushu with the ratio of recycle of 0.87 and reuse ratio of 0.97 (Kanemori, Y. 2002). In this research the energy conservation is studied in the design and operation period from the point of building equipment in the future houses.

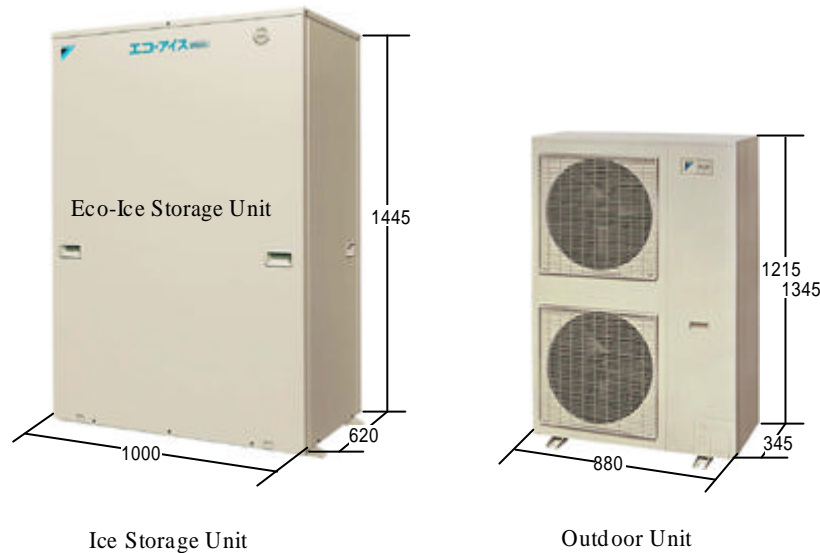


Fig. 1-13. Main parts of the Eco-ice Storage System

The features of future residential houses are shown in Fig.1-14. The electricity demand and air conditioning demand will be increased, because of the popularization of SOHO applications and healthy demand from occupancy.

As for energy conservation in residential houses, using natural energy will be the best choice, and people will have more chance to access the outside world, communicate with it, and enjoy it.

Solar energy is a basic kind of natural energy, and it is well known that solar radiation can be used for heating for a long time, but it can be used for cooling in summer.

As the double skin system works effectively in both summer and winter, it can not only exhaust solar heat by the stack effect in the summer, but also introduce more sunlight and acquire heat by greenhouse effect in the winter. During the intermediate seasons, natural ventilation can be easily promoted by opening the windows, and this will give people chance to access the outside world. Therefore, this system would be available for residential houses, and it can be called passive air conditioning system.

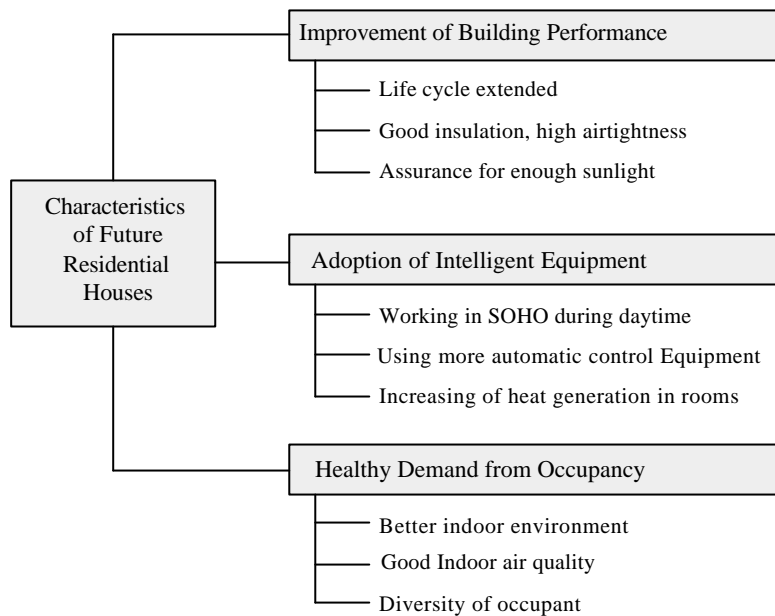


Fig. 1-14. Features of future residential houses

But the biggest shortcoming of passive system is that the uncertainty and variation of climates, i.e. it is not available in hot and humid days or in cold days without enough solar radiation. Mostly, It can only act as an auxiliary for the mechanical air conditioning. Therefore, something should be also considered for the mechanical air conditioning system, i.e. active air conditioning system.

As it is well known there is not necessary to supply conditioned air to the whole room, supplying conditioned air only to those occupied zone will lead to more energy saving. The displacement ventilation system can be available to supply air directly to the occupied zone. Because the supply air can be a little higher, the outside air can be used a little widely. Moreover, the displacement ventilation has good air change effectiveness, and this will meet the occupant healthy requirement.

In addition, with the introduction of displacement system, air-handling unit (AHU) is necessary. If AHU can not only supply air for the displacement ventilation, but also use for thermal storage, this will leads to saving more space for equipment, as well as energy cost and energy consumption.

From the above discussions, the best means of air conditioning is the integration of the passive air conditioning system and the active system, i.e. the hybrid air conditioning system.

In this research, first the author describes the basic concepts of hybrid air conditioning

system, and then proposes a hybrid system plan for a residential house based on the consideration of architecture design and equipment system design with the integration of passive system and active air conditioning system, finally appraises the effectiveness of the proposed hybrid air conditioning system in a residential house by simulation and field experiment.

CHAPTER 2

CONCEPT OF HYBRID AIR CONDITIONING SYSTEM AND ITS PLAN FOR RESIDENTIAL HOUSE

In Chapter 1, it is noted that the hybrid air conditioning system is the integration of passive air conditioning system and active air conditioning system. In the following part, firstly, the targets and concepts of hybrid air conditioning system are described, and then the possibility and availability of the hybrid air conditioning system is discussed, finally a hybrid air conditioning plan is proposed for a residential house.

2.1. Concepts of hybrid air conditioning system

Under the natural climate conditions, the worst indoor environment may occur because of poor insulation and air tightness of building envelopes, lack of sun shadings, or too much heat release from appliances, which lead to low temperature in winter and high temperature in summer. The basic consideration for indoor environment is by the architecture design, such as good insulation, consideration of solar radiation, and natural ventilation. By the introduction of solar radiation and outside air, the indoor environment can be improved greatly, which is called natural energy utility. But according to the real situations, when it is impossible to make comfort environment, the further improvement depends on the mechanical means, exhausting heat or acquiring heat by refrigerator or boilers, which is called active air conditioning. Of course, this consumes energy, such as fuels or electricity.

The similar situation in Fig.2-1 occurs in every day, which means the natural energy utility can be combined with the mechanical air conditioning even in summer or in winter by making the best of the outside climate.

2.1.1. Definition and targets of hybrid air conditioning

The acceptable indoor environment for residential houses is dry-bulb temperature of 17-28°C with the relative humidity of 40-70% (Inoue, U. 1996). The design of indoor environment can be divided into two aspects, one is architecture means, and the other is mechanical means (Fig.2-1). Although the passive systems can realize thermal comfort with less energy consumption by the way of natural ventilation and solar radiation, they are mainly depended on the outside climate conditions. Accounting for the limits of application for the

passive system, the mechanical system is designed for the insurance of indoor environment, especially in the peak time of summer and winter. The heating and cooling devices are often used for air conditioning, with the consumption of electricity, gas or oil.

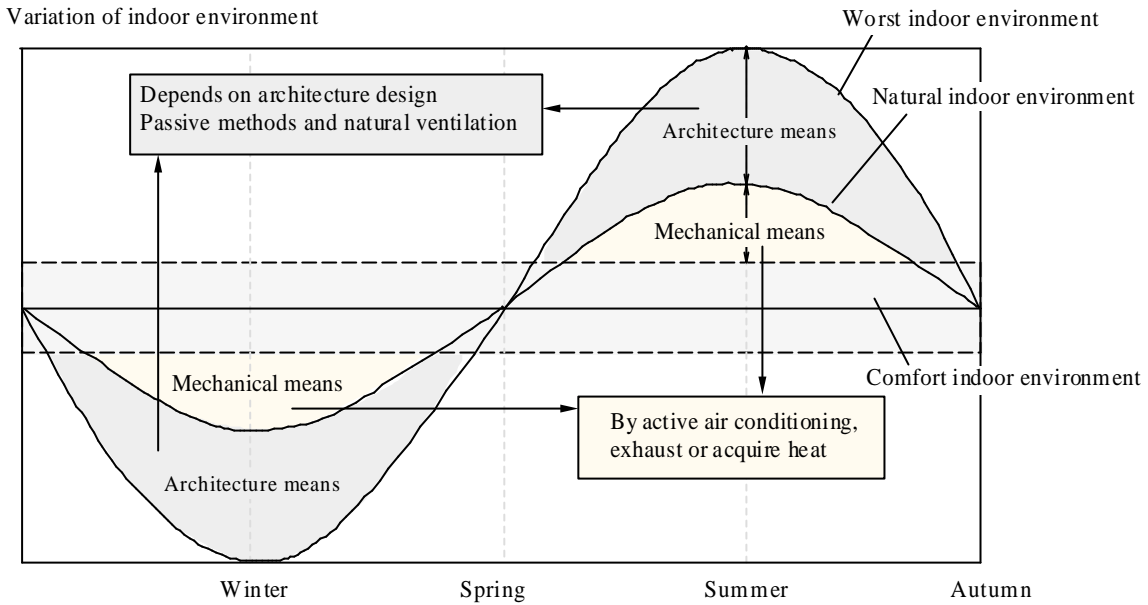


Fig. 2-1. Consideration of creating indoor environment

According to the outdoor climate of Yahata (Kitakyushu) in the typical meteorological year, the time when the outdoor climate is in the acceptable range is 11% of 8760 hours in a year (Fig.2-2), which means free cooling maybe available only by introducing the outside air into the houses, if the indoor heat release is not so large.

When the outside air is higher than 28°C, it is not available for free cooling by ventilation. People have to use mechanical air conditioning for cooling to ensure indoor thermal comfort. With the application of specially designed passive system, the energy consumption for the mechanical cooling will be also reduced even in the peak summer.

Therefore using both passive (natural) air conditioning and active (mechanical) air conditioning, i.e. the hybrid air conditioning system maybe the good solution for a residential building.

The target of hybrid air conditioning system aims to using more natural energy, such as solar radiation, natural ventilation and less mechanical air conditioning to control the indoor environment within the acceptable range, thus to reduce the overall energy consumption in buildings, as well as occupant healthy.

In the past, most air conditioning systems just create an indoor environment that will

remain at a relatively constant temperature and humidity, regardless of the outdoor conditions. The basic consideration of the hybrid system is to actively use the outdoor environment climate to control the indoor environment. Since the indoor environment will be greatly affected by this application, there needs an integration designing of architecture and equipment.

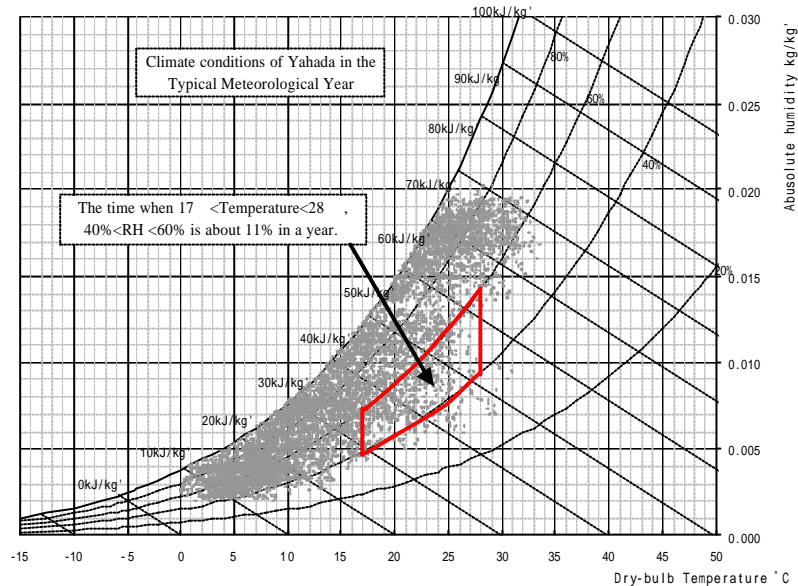


Fig. 2-2. Outdoor air of Yahata in the typical meteorological year

Furthermore, with using the outdoor conditions occupants play an active role in controlling the indoor environment. They can open the windows to make natural ventilation, draw up/put down the blinds to control solar radiation or lights according to own will, therefore they may have more chances to communicate with the outside world for visual enjoying, healthy requirement, and thermal demand.

In general, the basic considerations of hybrid air conditioning system are illustrated in Fig.2-3. The integration of the passive air conditioning system and the active air conditioning aims to energy conservation, occupant healthy. In addition it should be easy to operate.

Hybrid ventilation is very popular in Europe, and there are many successful applications in Norway, Netherlands and Denmark. The main reason may lie in that the outdoor temperature is lower even in the summer, which can be used for free cooling.

According to the program of Weather data for Energy Analysis and Design of Air conditioning system (WEADAC) made by Akasaka Hiroshi (1998), the comparison of average temperature in summer between Fukuoka of Japan (August) and Copenhagen of Denmark (July) is shown in Fig.2-4. The maximum temperature of Copenhagen is about 20°C, which is in the

acceptable range shown in Fig.2-2, and only ventilation may be available for cooling in buildings there. But the temperature in Fukuoka is much higher than that in Denmark, with the maximum of 32°C. Only ventilation will be not available for thermal comfort, therefore the active cooling system is necessary in Fukuoka in summer.

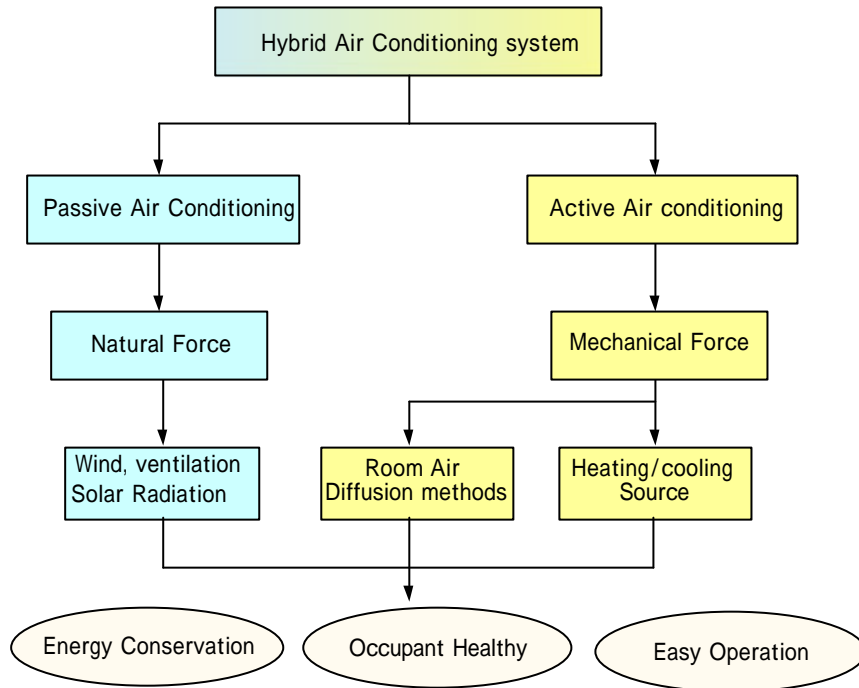


Fig. 2-3. Considerations of hybrid air conditioning system

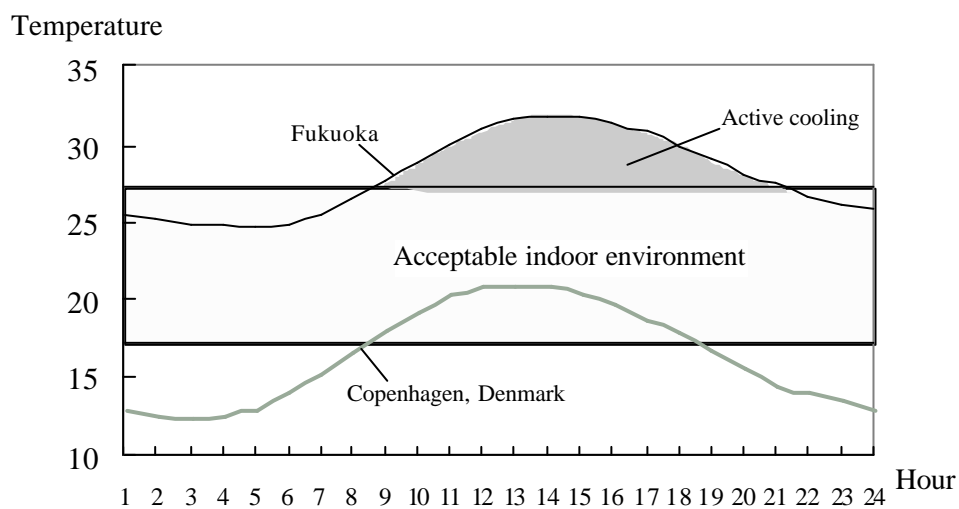


Fig. 2-4. Outdoor temperature difference between Fukuoka and Copenhagen

The main difference between hybrid ventilation and hybrid air conditioning lies in that the later is emphasis on taking advantages of outdoor climate, even when it is difficult to use passive air conditioning system directly. Because ventilation depends on the temperature difference between outdoor and indoor environment, hybrid air conditioning have a more widely application.

The targets of hybrid air conditioning can be expressed as follows.

2.1.1.1. Energy conservation and Global pollution reduction

By using more passive air conditioning and less active air conditioning, the hybrid air conditioning system aims to reduce the household energy consumption. Studies show that compared with buildings with a conventional cooling and ventilation system, buildings using natural and hybrid ventilation systems have a 25-50% reduction in energy use (CIBSE, 1997). Because the air conditioner consumes about 30% of the final energy consumption in residential house in Japan, the hybrid system will bring about significant energy consumption. Also, from the point of global environment protection, this will have an active impact on the decrease of emissions of CO₂, NO_x, SO_x and so on.

2.1.1.2. Occupant healthy and higher satisfaction

As the outdoor climate will be actively introduced into the room by hybrid systems. Brager, G. S. et al. (2000) conducted a research on adaptation in buildings. They collected 21,000 sets of raw data compiled from previous thermal comfort field experiments in 160 office buildings in four continents covering a wide range of climate conditions. This research shows that:

- People adapt their behavior to become more active participants in the control of their environment, when they can open/close windows.
- People prefer a wider range of indoor temperatures, and they have tolerance to temperature deviations in an open space, while they have less tolerance in a sealed, air-conditioning space.

This confirms that when the outdoor climate is available for free cooling or natural ventilation, occupants should be given enough chances to have access to the environmental control, which will be good to eliminate the pollutant in rooms, and introduce more outside air for refreshing. According to the climate situations in the intermediate seasons, natural ventilation is possible for the many places in Japan. But during the summer, only a few time is

available for free cooling, the active air conditioning should be adopted to realize the healthy requirement.

According to different room air diffusion systems, the displacement ventilation system, which has a better air change effectiveness, can remove contaminants in the occupied zone and will be good to the occupant healthy.

In addition, as the displacement system supplies air directly to occupied zone, the convection heat from the ceiling, as well as the heat release from lights, would be discharged with the exhaust air. Therefore, the cooling load from the high places will be decrease, and this can lead to energy conservation in residential houses.

2.1.1.3. Easy operation and maintenance

Hybrid air conditioning system is the integral of passive system and active system, but it does not mean its comprehensive operation. These days, the commissioning and maintenance of an installation seems to be difficult, which needs qualified technical personnel. As for the equipment in the residential houses, considering the age of occupants, the operation and maintenance for the hybrid system should be simple, and easy to be manipulated. It needs comprehensive design of architecture and equipment system.

2.1.2. Available technologies for hybrid air conditioning in residential house

Technologies for hybrid air conditioning can be divided into two types, one is passive air conditioning and the other is active air conditioning. The former pays more attention on natural energy utilization and less nonrenewable energy, while the later emphasizes on the efficient use of nonrenewable energy.

2.1.2.1. Passive air conditioning system

The passive systems make the most of the outdoor conditions to improve the indoor environment, such as solar radiation, therefore little nonrenewable energy is required for heating, cooling and lighting. By adjusting the opening area of windows or other equipment, the outdoor air temperature, humidity, wind or geothermal energy can be used to control the indoor environment. The active use of solar radiation system for heating has been widely used, such as the solar collection, storage and distribution system for domestic hot water and space heating. The passive solar systems can be divided into two categories, one is the direct gain passive system, such as the green house, and the other is the indirect gain passive system, such as the double skin system.

- Green house

The green house uses a large south-facing glass to take in solar radiation, and the direct solar gain can not only warm the room in the daytime, but also can be stored for the nighttime heating. The add-on greenhouse (Fig.2-5) can be used as solar attachments in suitable orientation, which provide a buffer between the indoor environment and the outside conditions (IBEC, 1985). During the daytime the warm air from the greenhouse can be introduced into the occupied area in winter. Of course, sun shadings, ventilation in the green house and insulation of the roof should be paid enough attention to avoid overheating in summer.

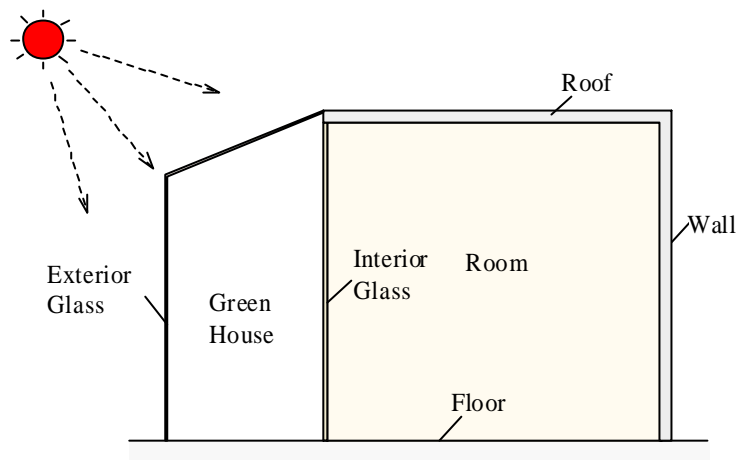


Fig. 2-5. Illustration of an add-on green house

- Double skin system

The double skin system also uses the south-facing wall/windows to absorb solar radiation, which is shown in Fig.2-6. Compared with the green house, the width of the double skin space is smaller, and the ventilation equipment and shadings are equipped too. This double skin space acts as a buffer between the indoor environment and outdoor climate. Solar radiation can be reduced by the interior shadings, and some can be exhausted by the natural ventilation because of the stack effect in summer, therefore the solar heat gain can be greatly reduced.

While in the winter openings are all closed, more solar radiation can be introduced into the rooms from the south windows, and the air in the double skin space can also be warmed up to prevent heat loss from the house. During the intermediate seasons, the outdoor air/wind can be easily introduced into the rooms through the exterior windows. In these passive systems, the indoor environment can be controlled by operating the window shades or openings manually. It is the most simplest and reliable control method, which has been widely used so far.

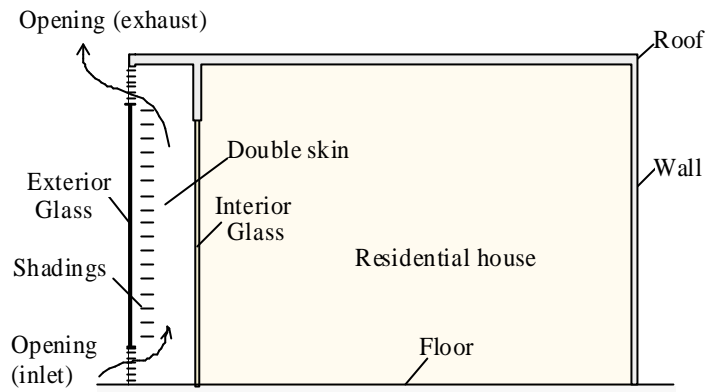


Fig. 2-6. Double skin system in residential house

- Evaporative cooling

As for the roof, the cooling effect from water evaporative can be used in the cooling seasons, which depends on the outside air temperature, humidity and wind. The example is the roof spray cooling system, which is shown in Fig.2-7. Water is sprayed over the roof surface, and it will evaporate with the help of wind, at the same time absorbing heat from the roof. This can reduce the roof surface temperature by 4-15°C (ASHRAE, 1997). If there is solar radiation, the increase of roof temperature will make the water evaporation faster. On the contrary, the evaporation can protect the roof from temperature increase.

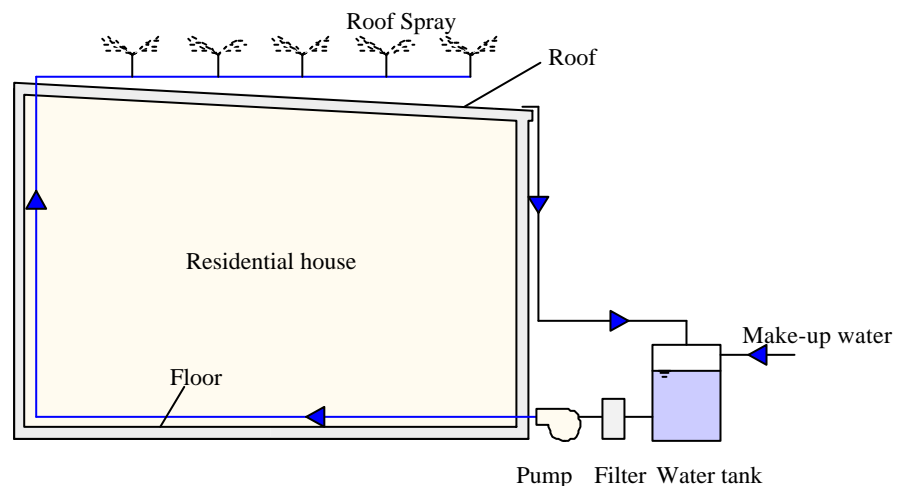


Fig. 2-7. Sketch of water roof spray cooling system

- Roof planting

Another consideration for the roof is planting, i.e. covering the roof by trees or lawns (Fig.2-8). The plants and the soil (with the thickness of about 200mm) provide shading from the direct solar radiation, and they also provide good insulation. They can keep the surface temperature of roof to be relatively constant both in summer and in winter. During the summer, the evaporate effect of plant is expected to reduce the air conditioning load. In addition, it also provides the occupants more chances to have access to the outside environment, which will be helpful to improve occupant health.

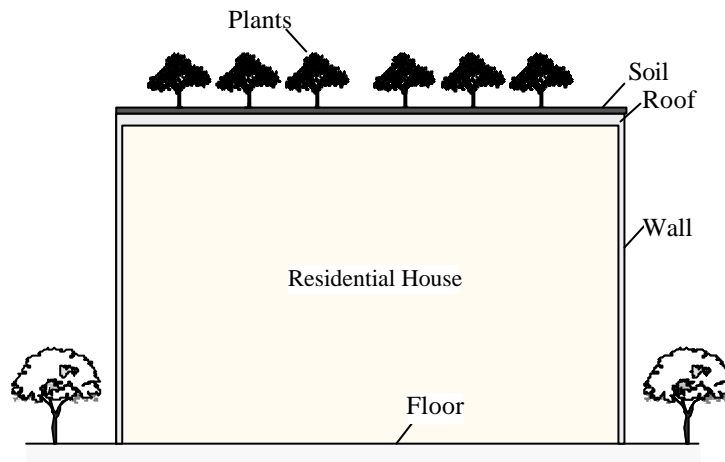


Fig. 2-8. Sketch of roof planting

- Cool tube system

The variation of temperature in the ground is very small, it is about 20°C at the depth of 2m from the surface of the earth even in summer, and it can be available for cooling. The outdoor air runs through the tube buried in the ground with the help of a small fan (Fig.2-9), and it can be cooled the room for air conditioning.

Other technologies are also available for passive cooling. For example, the solar chimney system, which absorbs heat from solar radiation, makes the indoor air move by stack effect, and this will lead to natural ventilation in buildings.

Accounting for the comparison in cost and maintenance, the double skin system is proposed in a residential house in the next section.

2.1.2.2. Active air conditioning system

As for the active air conditioning system, it can be considered from two aspects: one is the air diffusion method, and the other is heating/cooling source.

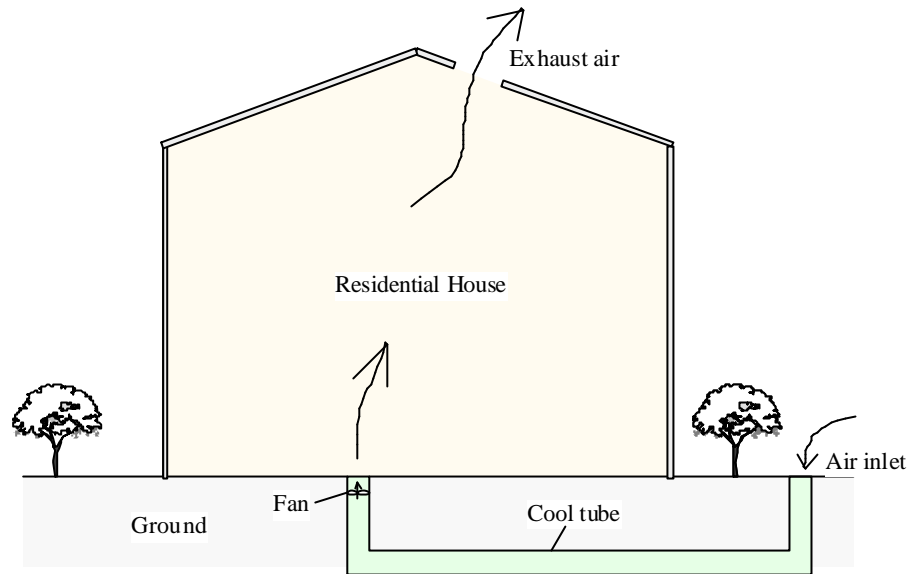


Fig. 2-9. Sketch of cool tube system

According to the air diffusion methods, systems can be divided into mixed type, displacement ventilation and local type. As the mixed type has been widely used, it creates relatively uniform air velocity, temperature, humidity and air quality in the occupied zone. But considering occupant healthy, the indoor contaminants cannot be discharged effectively, and the places where air conditioning is not needed are also conditioned. Therefore the mixed system can be regarded as a good air diffusion method.

Displacement ventilation and local systems, such as task and ambient air conditioning, are better in the point view of healthy and energy saving.

- Displacement ventilation

As is mentioned in Chapter 1, the air (from air handling unit) with temperature slightly lower than the room air is supplied directly from the diffuser near the floor, and then goes directly to the occupied zone with an average velocity of about 0.5m/s. The exhaust outlet is located near the ceiling, which can exhaust the warm and polluted air (Fig.2-10a), therefore the energy will be used more efficiently.

- Task and ambient air conditioning

The task and ambient system is developed from the displacement ventilation, and conditioned air is supplied locally for occupied area, such as desks, seats. Conditioned air is supplied to the breathing zone of the occupants to create comfortable conditions and discharge the contaminants at the same time (Fig.2-10b). As the area of air conditioning becomes smaller,

the energy efficiency can be further improved.

Compared with displacement system, the task and ambient system is a new field and it is being studied in laboratory, while the displacement system is easy to be realized.

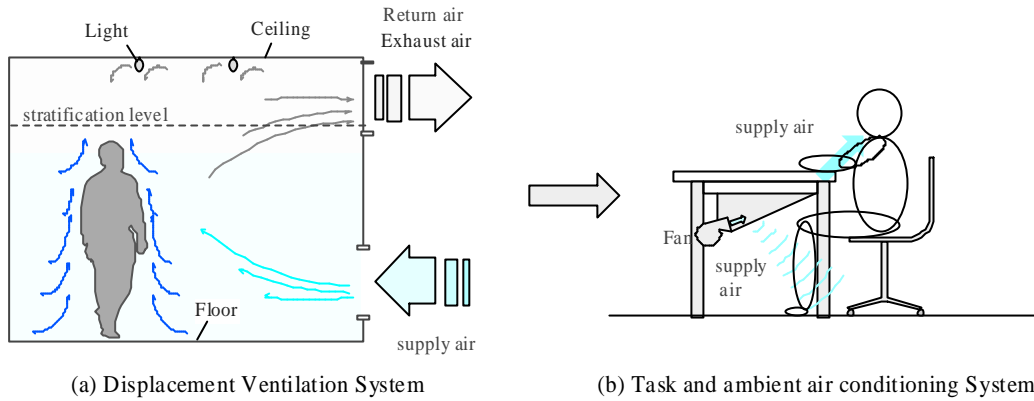


Fig. 2-10. Sketch of displacement ventilation, task and ambient air conditioning

- Thermal storage system

As for the heating/cooling system, it is very important to improve the performance of machines and operation of machines. The thermal storage system can be regarded as a solution to energy saving for the machines.

With the development of technology, the coefficient of performance (COP) of machines at the load rate of 100% has been increased, such as room air conditioner, heat pumps, and chillers. According to the data from the Energy Conservation Center (ECCJ, 2002), the COP of room air conditioner is shown in Table 2-1, and the average value is in the range of 3 to 4.5. Accounting for the real situations and part load rate, COP is a little smaller. Therefore, it is more effective to improve the operation conditions. As for a heat pump with waste heat recovery, it can generate 55-60°C warmer water even under the cooling conditions (ASHRAE, 1996), which can meet the hot water demand thus to increase the whole COP.

In Chapter 1, the Eco-ice Thermal Storage Unit developed by ten main electricity companies and other manufactures, makes thermal storage possible for small offices. But for the domestic use, the dimensions of the equipment should be smaller. As the Eco-ice Thermal Storage Unit has not used the heat recovery, the efficiency of the whole system can be further improved if the hot water is made by heat recovery. Furthermore, accounting for the requirement from occupant health, the Eco-ice system has paid much attention on the outside air conditioning and occupant health requirement.

Table 2-1. COP of room air conditioner for houses in the summer of 2002

COP \ Output*	Maximum	Minimum	Average
2.2 kW	6.01	2.76	4.46
2.5 kW	5.71	2.55	4.39
2.8 kW	5.95	2.67	4.52
3.2 kW	3.35	2.76	3.07
3.6 kW	5.01	2.98	4.25
4.0 kW	4.71	2.54	3.91

Note: Output* refers to the output for cooling.

2.2. Design strategies of hybrid air conditioning

2.2.1. Double skin and residential house

As to the traditional corridor space of Japanese Folk House shown in Fig.2-11, the corridor is used as a buffer space between the indoor environment and the outside atmosphere. During the summer, the exterior shading device can prevent from intensive solar radiation. While it can introduce more sunlight into the house during the winter, and during the intermediate seasons, natural ventilation can be introduced into the rooms. The function of these corridors is similar to the consideration of double skin system.

If the ventilation openings are designed on the floor and on the ceiling, the corridor will turn to be a double skin space (Fig.2-12). The exterior glass/shadings absorbed solar radiation can warm the air in the double skin, according to the stack effect or by wind, the air under the floor will be introduced and the warm air will be exhausted to the outside. Of course, corresponding modifications with architecture are necessary. Air under the floor will be introduced and the warm air will be exhausted to the outside. Of course, corresponding modifications with architecture are necessary.

The driven force of airflow in the double skin can be divided into two types, one is caused by wind, and the other is caused by thermal forces (ASHRAE, 2001). The former can be decided by Equation (2-1):

$$\dot{m}_{wind} = C_v AU \quad (2-1)$$

where \dot{m}_{wind} is the airflow caused by wind (m^3/s), C_v is effectiveness of openings, A is free area of inlet openings (m^2), U is wind speed (m/s).

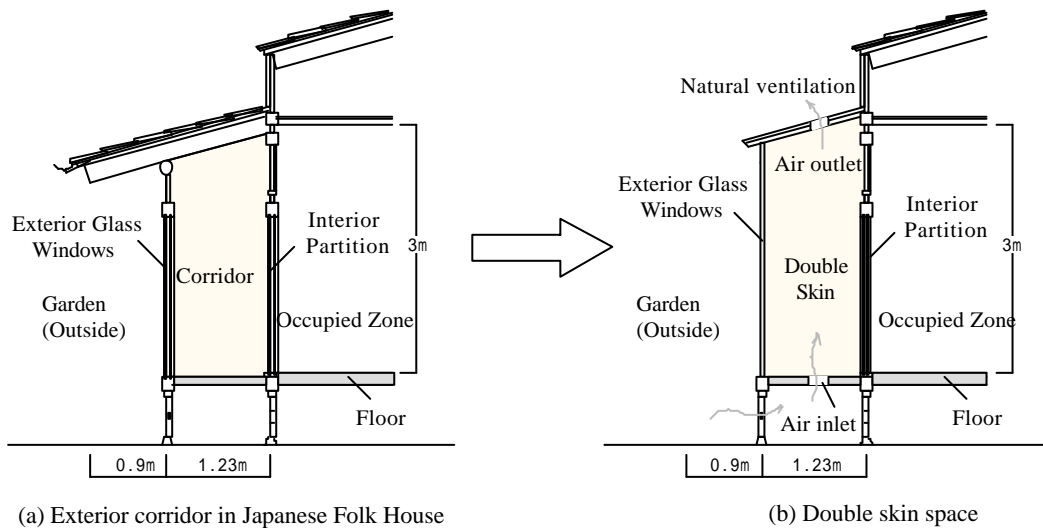


(a) Outside view of a Japanese Folk House



(b) Inside view of a Japanese Folk House

Fig. 2-11. Example of Japanese Folk House



(a) Exterior corridor in Japanese Folk House

(b) Double skin space

Fig. 2-12. Development from exterior corridor to double skin space

C_v is assumed to be 0.5 to 0.6 for perpendicular winds and 0.25-0.35 for diagonal winds. Inlets in the direction of prevailing wind will be helpful for airflow, while the outlet should be located in the exterior low-pressure regions, which depends on the slope of the roof (Fig.2-13). If the roof slope is very small, the pressure is negative over the whole surface. If it becomes steeper, the pressure is weakly positive on the windward slope and negative within on the leeward. Considering the variation of wind, the roof slope should be smaller than 20°

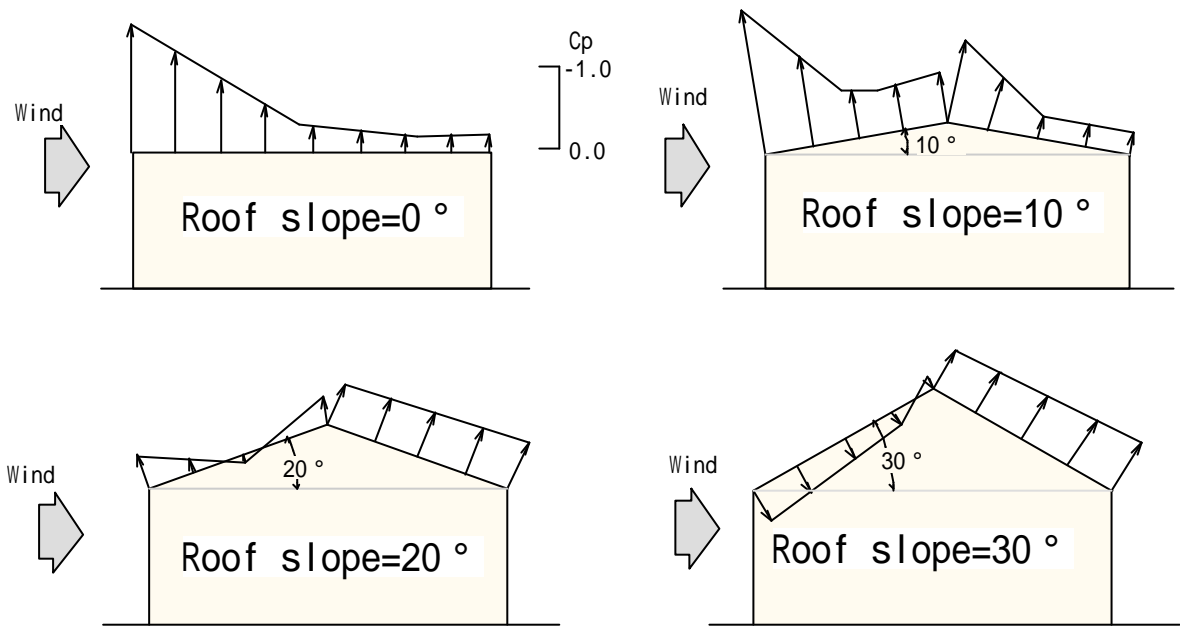


Fig. 2-13. Surface pressure on the roof with different slope

The flow caused by thermal forces can be expressed by Equation (2-2):

$$\dot{m}_{thermal} = C_D A \sqrt{2g\Delta H_{NPL} (T_i - T_o) / T_i} \quad (2-2)$$

where $\dot{m}_{thermal}$ is airflow caused by thermal forces (m^3/s); C_D is discharge coefficient for opening; ΔH_{NPL} is the height from midpoint of lower opening to neutral pressure level (NPL); T_i is the average temperature in double skin (K); T_o is outdoor temperature (K).

ΔH_{NPL} is assumed to be the half of the height of the double skin. The discharge coefficient of C_D is in the range of 0.4-0.65. When $T_i < T_o$, replace T_i in the denominator with T_o , and replace $(T_i - T_o)$ in the numerator with $(T_o - T_i)$, which means the flow direction is changed

(ASHRAE, 2001).

It should be pointed out that the greatest flow rate per unit area of openings is obtained when inlet and outlet areas are equal, which is the basic condition for Equation (2-1)-(2-2). Otherwise, there should be some correction.

The exhaust heat Q_{ex} in the double skin can be expressed by Equation (2-3):

$$Q_{ex} = r\dot{m}C_p(T_i - T_o) \quad (2-3)$$

where C_p is the specific heat (kJ/kg); \dot{m} is the airflow rate by wind and thermal effect (m³/s); r is air density (kg/m³).

2.2.2. Plan of the hybrid air conditioning system

Accounting for the above analysis, the double skin system is easy to be adapted by the Japanese Folk House. Considering the better air change effectiveness, displacement ventilation can be introduced, and it can provide mechanical ventilation in the intermediate seasons. Thermal storage system is also proposed, with the expectation for cost saving and global environmental protection.

The plan of hybrid air conditioning system proposed for an experimental house is shown in Fig.2-14.

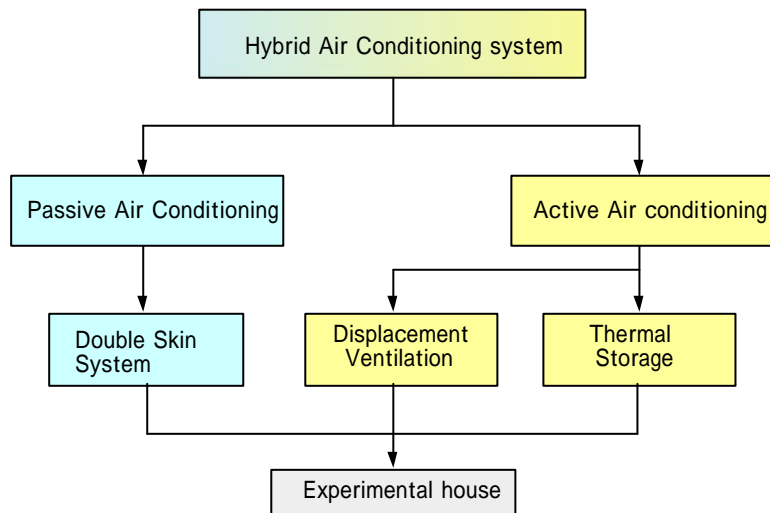


Fig. 2-14. Plan of hybrid air conditioning system for an experimental house

2.2.3. Outline of the experimental house

The experimental house is located in Kitakyushu Science and Research Park, Fukuoka, and the exterior appearance is shown in Fig.2-15.



Fig. 2-15. Exterior appearance of the experimental house

The two-story residential house with floor area of 174.6m^2 is designed for a two-person family. The first floor is designed for future residential houses, including a SOHO room, a reception room and a machine room, and the second floor is conventional living space, including a living room, a bedroom and a bathroom. The section and plan are shown in Fig.2-16 and Fig.2-17.

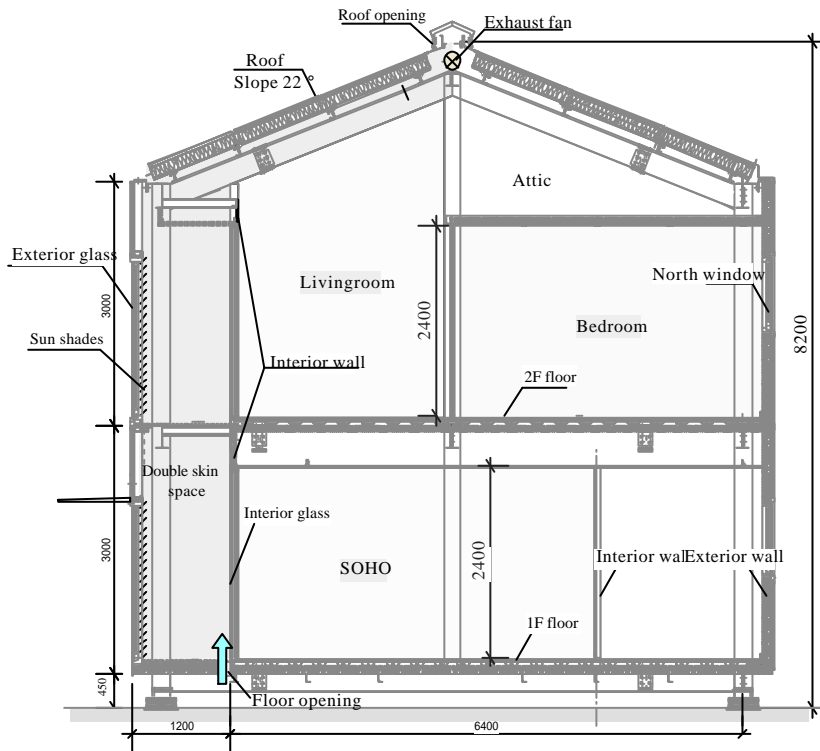
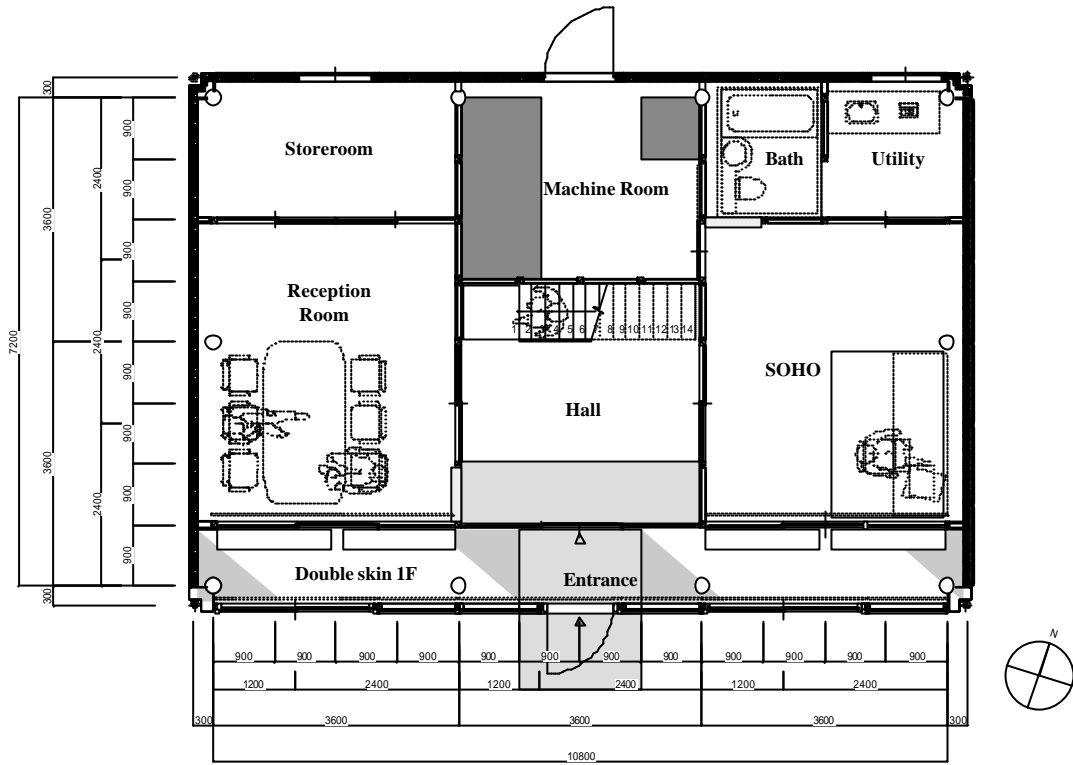
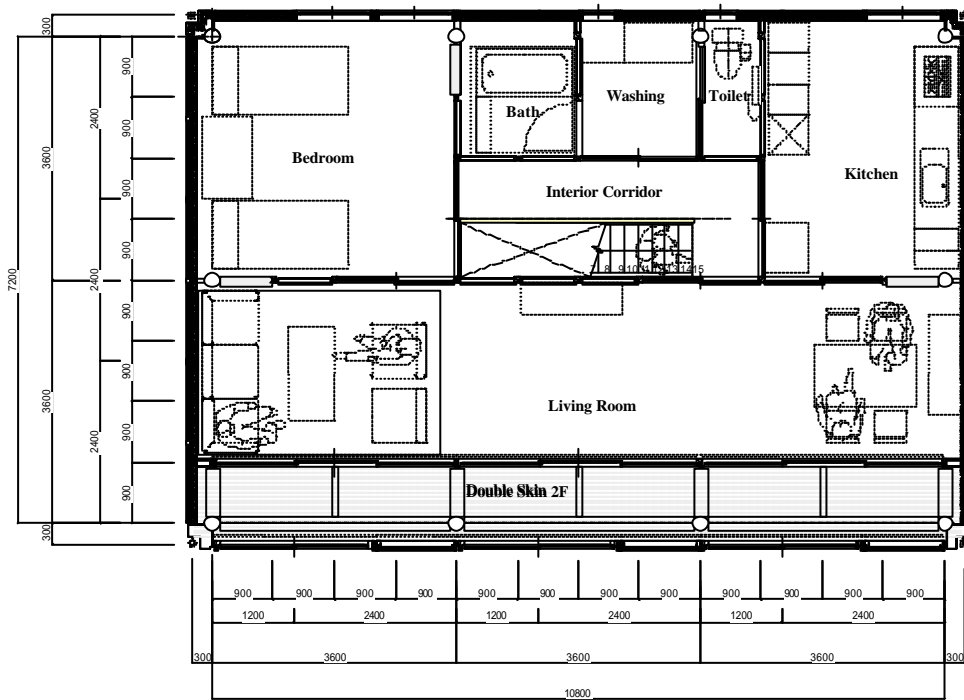


Fig. 2-16. Section of experimental house



(a) 1F Plan in the experimental house



(b) 2F Plan in the experimental house

Fig. 2-17. Plan of the experimental house

It can be seen that the double skin space is 6m high and 1.2m wide, and located in the south side of the house. The south façade is made of glass, which aims for material recycle and good appearance. Four openings on the floor have a total area of about 0.6m², which is equal to the area of the roof openings. Auxiliary fans are also installed on the roof. In addition, the roof slope is 22°.

The details of the proposed double skin system will be introduced in Chapter 4.

2.2.4. Outline of Air conditioning system

- Displacement Ventilation system

The sketch of the proposed displacement ventilation air conditioning system is shown in Fig.2-18.

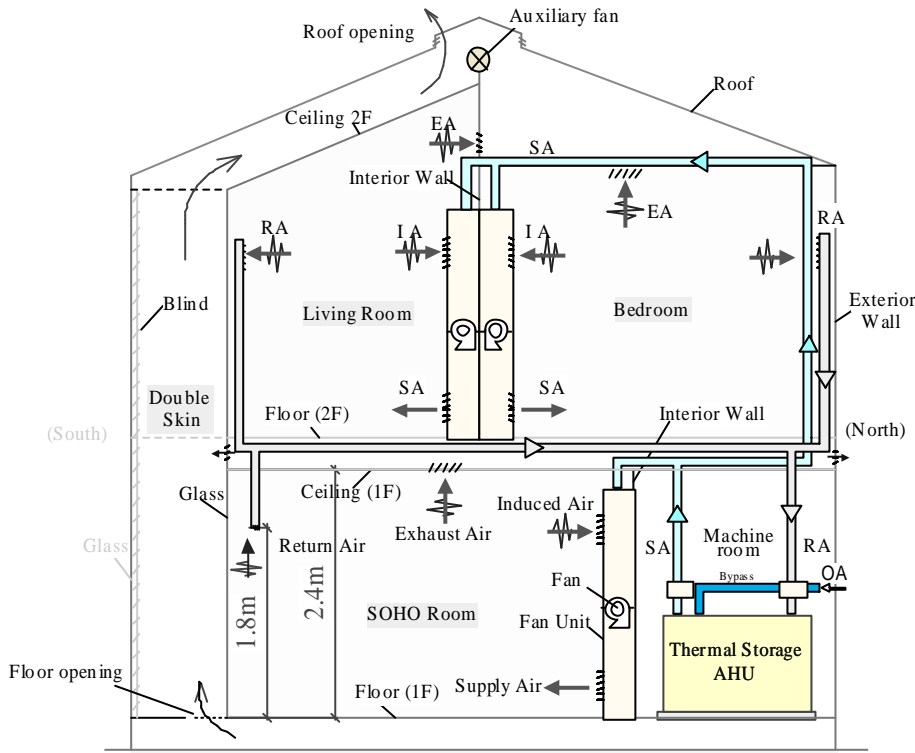


Fig. 2-18. Sketch of the ventilation system

In summer, the conditioned air from air conditioning unit (AHU) is supplied to the fan units in rooms. After mixing with the induced room air, it is supplied from the opening near floor. The return air comes back from the outlets at 1.8m, and the exhaust outlet is on the ceiling. And the outside air is set to meet the requirement of about 30m³/h for each person. The details of the displacement are discussed in Chapters 5 and 6.

In the intermediate seasons, outside air bypasses the coils in AHU, and is supplied directly into rooms, thus to realize mechanical ventilation.

In winter, when the thermal storage unit is charged with hot water, it can also supply warm air as an auxiliary means for heating.

- Energy system

Heat pump is the energy center in this system, which can produce ice for storage during summer, and the waste heat can be charged in hot water tank at the same time (Fig.2-19). While it can produce hot water for storage in the winter.

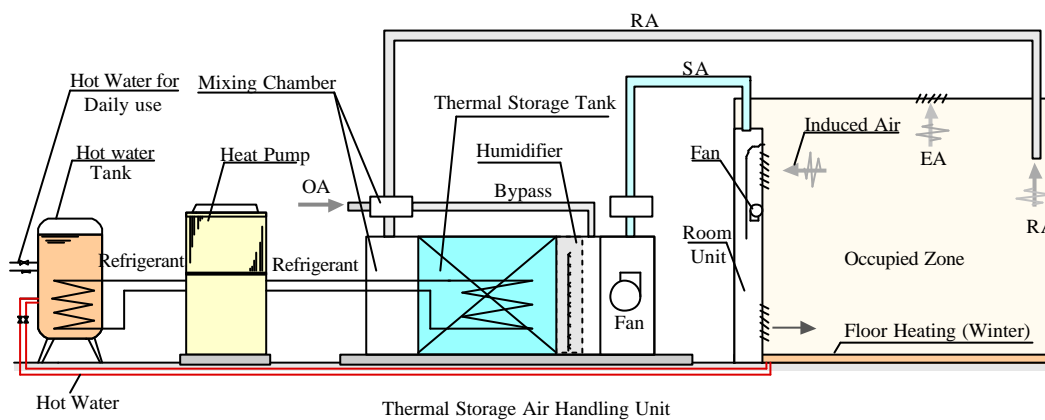


Fig. 2-19. Sketch of the energy system in the experimental house

The thermal storage tank is also used as an air-handling unit, in which ice storage happens during summer and hot water storage happens during winter.

Accounting for the residential conditions, direct heat exchange, which is detailed in Chapter 7, happens between air (the mixing of fresh air and return air) and storage pipes inside the tank, then the conditioned air is supplied into rooms by a fan. As the temperature difference between supply air and room air is relatively high, induced air currents are created through a small fan inside the room unit.

Hot water is mainly stored in the water tank, which can not only meets the need for kitchen, bathroom all the year, but also for the floor heating system.

2.3. Research method

The effectiveness of the proposed hybrid air conditioning system is predicted by computational fluid dynamics (CFD) simulation, and then the predictions will be checked according to the field experiment in the experimental house.

The CFD simulation code used in this research is Airpak 2.0, which is developed by Fluent Inc. and ICEM-CFD Engineering. The basic program structure of Airpak is shown in Fig.2-20, and it uses a finite-volume solver to deal with problems for ventilation systems, such as airflow, heat transfer, contaminant transport, and even the external building flows, and it is helpful to evaluate the indoor air quality, thermal comfort, (Fluent Inc. 2001). There are four steps to solve the problems, building models, generating meshes, calculating, and examining the results.

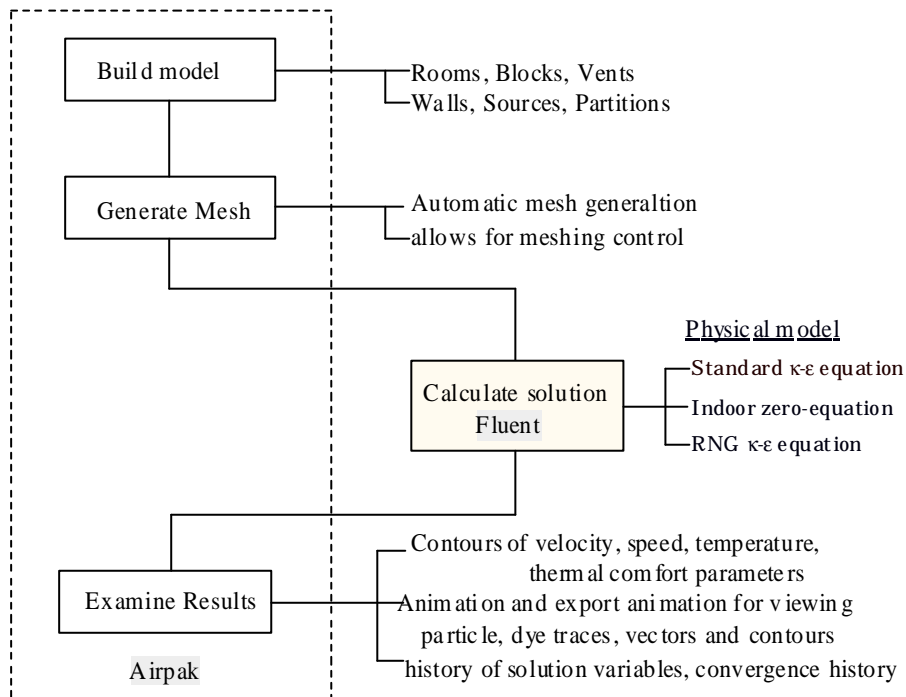


Fig. 2-20. Program structure of Airpak

2.3.1. Building models

Airpak provides predefined 2D object shapes, and complex 3D objects, such as rooms, blocks, fans, person, openings, partitions, walls, sources, and so on. And the rectangular, circular, inclined, or polygon 2D shapes can be created easily, as well as the prisms, cylinders, ellipsoids, or elliptical and concentric cylinders 3D shapes. Therefore the furniture, electrical appliances,

walls and other elements in a room can be modeled using the predefined objects, and new objects can also be defined.

The interface of Airpak2.0 is shown in Fig.2-21. There are three primary components: the main menu bar is on the top, the options menu is on the upper right, and the middle display window is at the below. In the example model, there are a prism pillar block, a prism bookshelf block, a person, several openings (air inlet), vents (exhaust air outlet), heat source of computers and lights in a room.

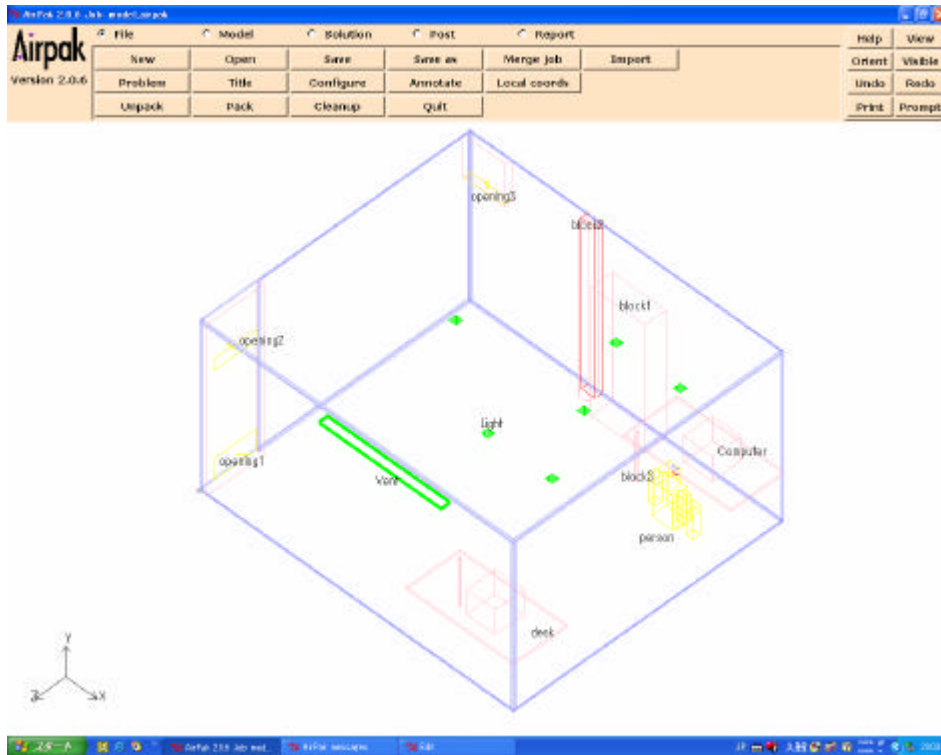


Fig. 2-21. Interface of Airpak2.0

As to the boundary conditions of different objects, wall and surfaces can be specified with heat flux, temperature, species, convective heat transfer coefficient, radiation, and symmetry conditions are also available. Openings and vents can be specified with inlet/exit velocity, exit static pressure, inlet total pressure, inlet temperature, and species. Fans can be specified with mass flow rate, fan performance curve, and angular specification of velocity direction. And recirculating boundary conditions for external heat exchanger simulation or species filters, time-dependent sources or ambient temperature are also available.

2.3.2. Generating meshes

Airpak automates the mesh generation procedure, but allows people to customize the

meshing parameters, in order to refine the mesh and optimize trade-offs between computation cost and solution accuracy. There are two types of meshes available in Airpak: hexahedral and tetrahedral. The hexahedral mesher (the default) is appropriate for most applications. The tetrahedral mesher produces a better mesh than the hexahedral mesher for geometrically complicated models that include, such as, spherical or ellipsoidal objects.

Coarse mesh generation option can be used for preliminary analysis, and then they can be refined globally or locally, finally the mesh quality can be viewed and checked. For a hexahedral element, the aspect ratio of an element is defined as the ratio of its shortest edge length to its longest edge length. The best elements are those with an aspect ratio close to 1. An aspect ratio less than 0.15 would indicate a distorted element. And the extremely small elements are recommended to be larger than the order of 10^{-12} .

The meshes number effects on the computational time and capacity, usually the computer with random access memory (RAM) of 100MB can deal with 10,000 meshes.

2.3.3. Calculating process

Airpak uses FLUENT, Fluent Inc.'s finite-volume solver to deal with the Navier-Stokes equations for turbulent flow problems by solving the transient transport equations of mass, momentum, energy, turbulent kinetic energy and turbulent dissipation rate. There are three choices for the basic model equations, as follows:

- Standard k - ϵ equation

This model is recommended for the fully developed turbulence problems, and the detail equations are shown in Chapter 5. It is a semi-empirical model, and the derivation of the model equations relies on phenomenological considerations and empiricism

As the turbulent kinetic energy, and its rate of dissipation are obtained from the additional differential equations, which will cost more time for calculation.

- RNG k - ϵ equation

This model is derived from the instantaneous Navier-Stokes equations, using a mathematical technique called “renormalization group” (RNG) methods. The analytical derivation results in a model with constants different from those in the k - ϵ equation, and additional terms and functions in the transport equations for k and ϵ .

The standard k - ϵ model is valid for a high-Reynolds-number turbulence, but the RNG theory provides an analytically derived differential formula for effective viscosity that accounts for low-Reynolds-number effects. Therefore, the RNG k - ϵ model is more accurate and reliable

for a wider class of flows than the standard $k-\epsilon$ model, but it tends to take 10-15% more CPU time.

- Indoor HVAC zero-equation

As the above two models have to solve one or more additional differential equations, which will lead to larger computing cost, and it limits their implication in the practical designing. Indoor zero-equation model is proposed by Chen (1998), by using the concept of eddy-viscosity, turbulent viscosity is approximated by a length scale and mean velocity. The main difference between zero-equation model and the $k-\epsilon$ model is that the former does not solve the equations for turbulent energy and dissipation rate. Therefore, the convergence speed of the zero-equation model is 10 times faster, and this model is ideally suited for predicting indoor air flows that consider natural convection, forced convection, mixed convection, and displacement ventilation.

After one choosing the physical model, according to the outline of the solution procedure is shown in Fig.2-22, the calculation begins.

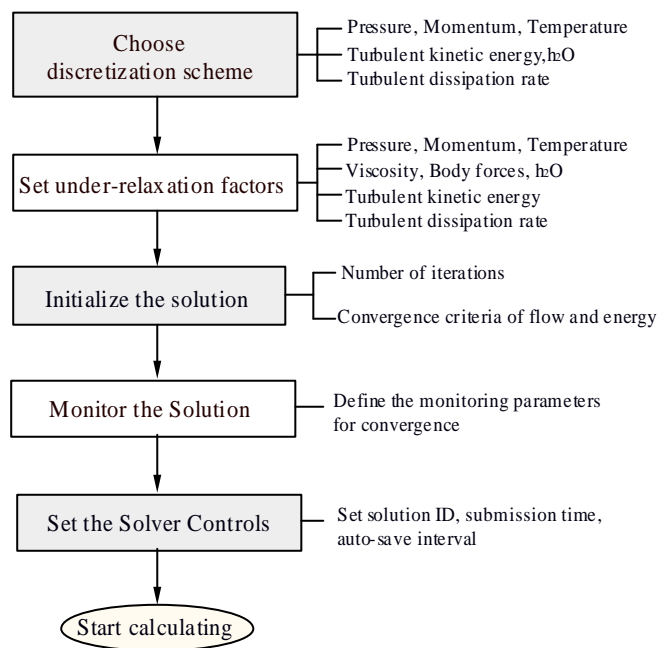


Fig. 2-22. Solution procedure for Airpak

2.3.4. Examining results

Airpak provides a number of different methods for examining the results of simulation, such as 3D modeling, dynamic viewing features. The following visualizations are available:

- Velocity vectors, contours, particle traces, grid, cut planes, and iso-surfaces, point

probes and XY plotting for data reporting;

- Contours of velocity components, speed, temperature, species mass fractions, relative humidity, pressure, heat flux, heat transfer coefficient, flow rate, turbulence parameters, vorticity, thermal comfort parameters, and many more quantities;
- Velocity vectors color-coded by temperature, velocity magnitude, pressure, or other solved/derived quantities;
- Animation for viewing particle and dye traces;
- Animation of vectors and contours in transient analyses;
- Export of animations in AVI, MPEG, FLI, and animated GIF formats.

2.3.5. Model used in this research

Airpak has been used for prediction of air temperature, velocity distribution, and air change efficiency to assess the effectiveness of the hybrid air conditioning system.

According to the above comparison of the different models, the RNG $k-\epsilon$ model is used for the simulation of airflow around the house, considering the ambient conditions and a large simulation scale. The zero-equation model is used for the natural ventilation in the double skin, considering the natural convection is predominated in this system. While the standard $k-\epsilon$ model is used for the displacement ventilation in the room and the heat transfer in the thermal storage tank.

The simulation results are also compared with the field experimental results respectively.

CHAPTER 3

SIMULATION ON NATURAL ENERGY UTILIZATION IN A RESIDENTIAL HOUSE WITH DOUBLE SKIN SYSTEM

As double skin systems have often been used in office buildings, in this chapter, the double skin system is proposed in a two-story house in Kitakyushu.

Firstly, the climate conditions in Kitakyushu have been analyzed for study on the possibility of natural energy utility. Secondly, the components of the proposed double skin system are detailed, as well as the reference house, which has not double skin system. Then the macro-simulation model for the two houses is made, according to the heat balance. Finally, the stack effects in summer, and the green house effect in winter are studied to analyze the characteristics of thermal transfer of the double skin systems. By comparing with the reference case, the energy conservation and natural energy utilization have been evaluated.

3.1. Climate conditions in Kitakyushu

According to AMeDAS climate data in the typical meteorological year from 1981 to 1995 of Kitakyushu (Akasaka, H. et al. 2000), the natural climate conditions are studied.

3.1.1. Outside air temperature and humidity

The outside air temperature is in the range of 0-32°C in the whole year (Fig.3-1), and the variation of the maximum and minimum temperature is approximately to be the function of time t , which is the hour number, i.e. 1 is for 1:00 on Jan. 1, and 8760 is for 24:00 on Dec. 31.

$$t_o = 16 \sin\left(\frac{2\pi t}{8760} - \frac{5620\pi}{8760}\right) \quad (3-1)$$

And the ratio of time when the outside temperature is between 17-28°C accounts for about 39% in the whole year, which shows the possibility of natural energy utility. Although in the whole summer this ratio reaches 78%, it is possible for feel cooling with the outside air if there is enough openings or windows.

While in winter as the outside temperature is quite cold, the infiltration and leakage of the outside air should be prevented.

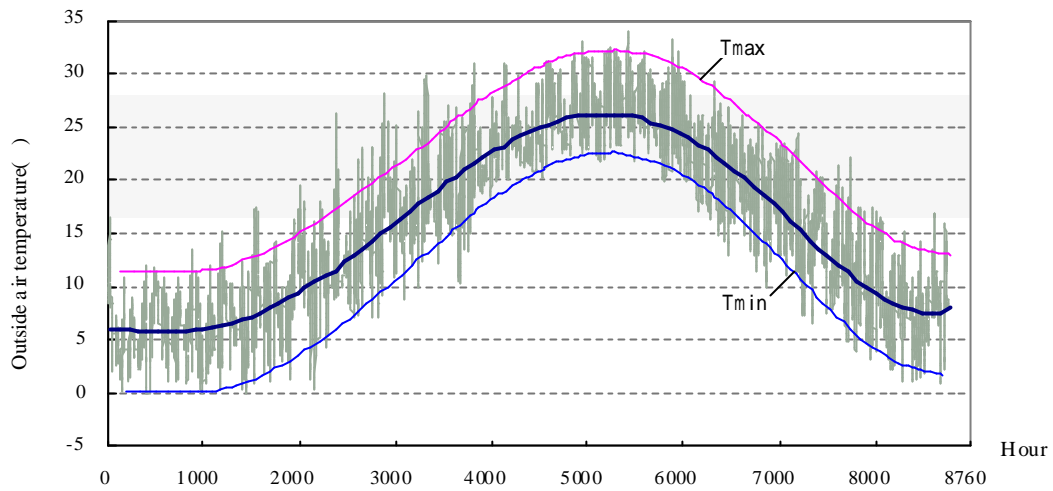


Fig.3-1. Outside air temperature at Yahata of Kitakyushu in TMY

3.1.2. Wind

The prevailing wind direction is about 22.5° west from the south in the summer (July and August), while it is mainly south in the intermediate seasons (April and November).

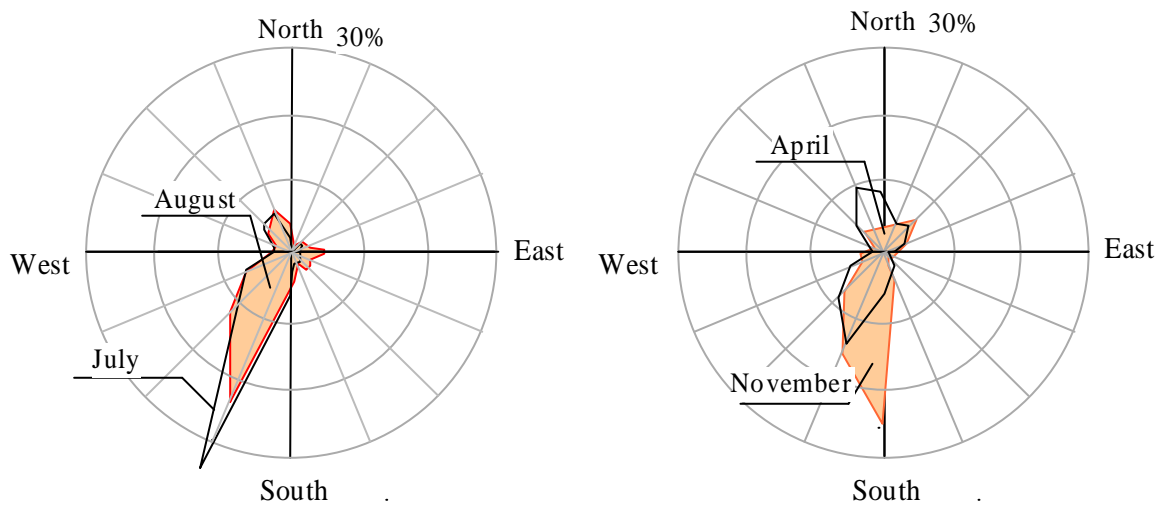


Fig.3-2. Prevailing wind direction in summer and intermediate seasons

The wind speed is in the range of 0-9m/s with an average of 2m/s (Fig.3-3). And the average wind speed is 2.1m/s in summer, 1.9m/s in the intermediate seasons, and 2.2m/s in winter.

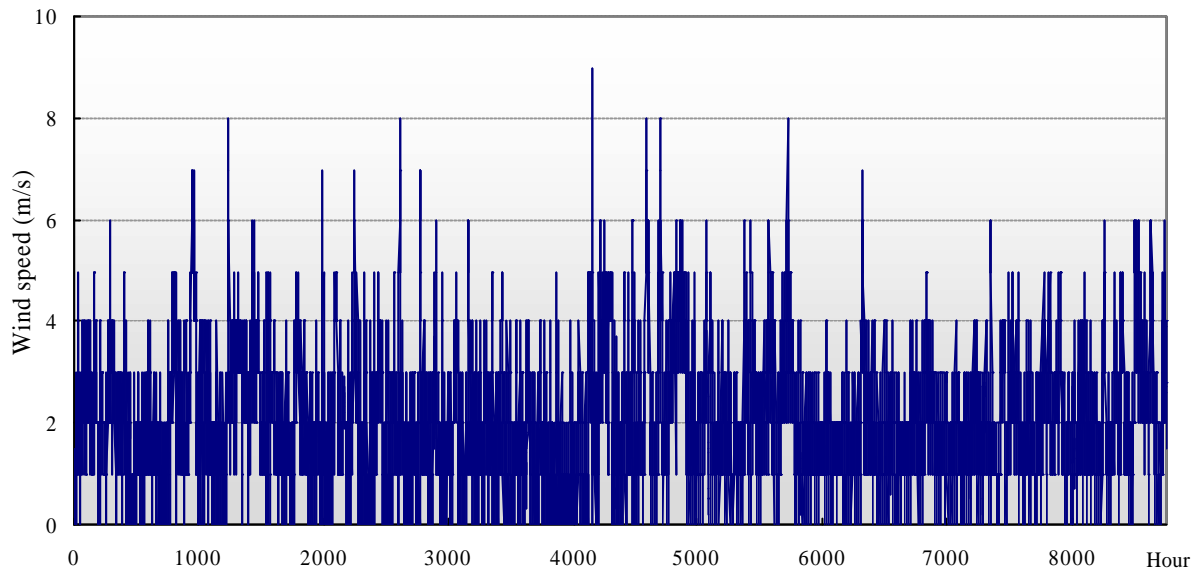


Fig.3-3. Wind speed in the whole year

3.1.3. Solar radiation

The average solar radiation is about 280W/m^2 in the daytime all the year round, and the average value in winter is the lowest of 200W/m^2 . The maximum value of radiation on the horizontal surface is 750W/m^2 in winter, and 900W/m^2 in summer. And the number of solar radiation hour reaches 506 hours in summer, 975 hours in spring and autumn, and 306 hours in winter.

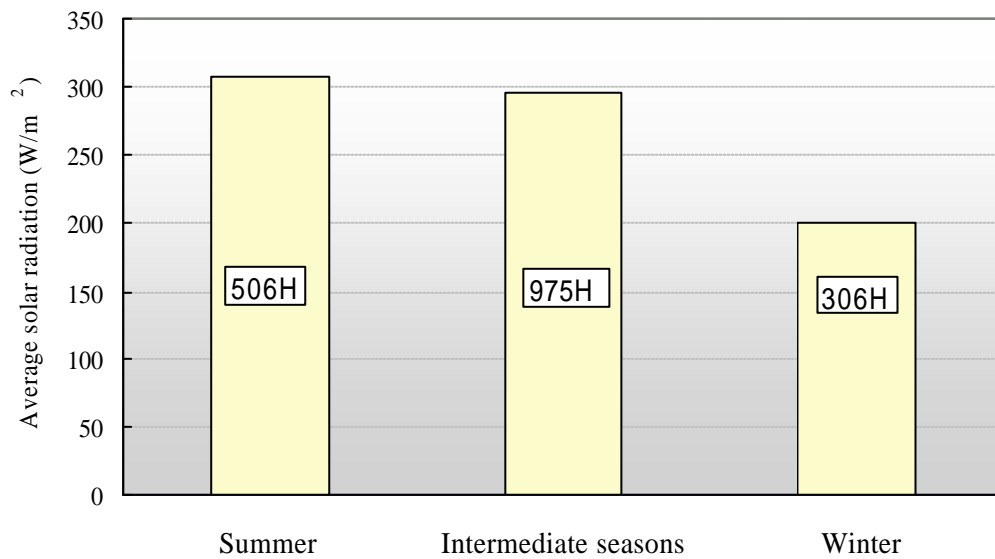


Fig.3-4. Average solar radiation and sunshine hours

3.2.Outline of the double skin system in residential house

The double skin system has been proposed in a residential house, not only to satisfy the occupant needs for visual communication with the outside world, but also to realize the energy conservation and thermal comfort. The model house for simulation has a flat roof surface, which is a little difference from the real model.

3.2.1. Proposed model and reference model

A conventional south-facing two-story house, which is illustrated in Fig.3-5 (a), is 10m long from East to West, 4.5m wide from South to North. The 1F floor is 0.5m above the ground, the ceiling height is 3m for each floor, and the total height is 6m, here the thickness of walls and floors are neglected.

In Fig.3-5 (b), an additional glass wall is designed at the outside of the south wall, thus to create an air space, which is called the double skin space.

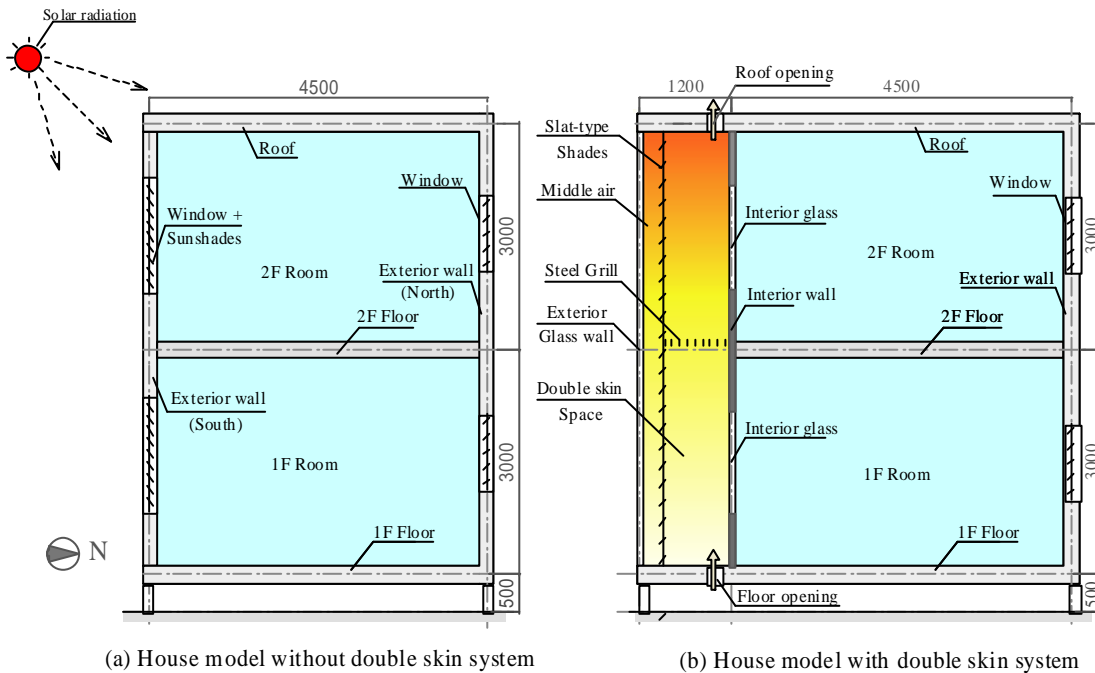


Fig.3-5. Sections of the house with and without double skin system

These two houses have the same orientation, and same material construction. The azimuth of the exterior walls (east, south, west and north) is -90° , 0° , 90° and 180° respectively.

The convective house without double skin system serves as a reference model, and the

proposed model is a house with double skin system. The main components of the double skin system are detailed in the following part.

3.2.2. Components of the double skin system

3.2.2.1. Exterior wall/windows

The sun radiation transmits through the exterior wall or windows, some will also be reflected to the outside ground and atmosphere. According the visual effect, it is required to be clear and transparent.

In summer, the exterior wall/windows are required to be able to reflect more solar radiation, and have less transmittance, but in winter they are required to have more transmittance.

So far there is not such a material to meet the two different requirements. Here the clear flat glass is used in the proposed model.

The exterior windows absorb some of the solar radiation and reflect some to the ground and sky, at the same time exchange heat with the outside air and surroundings.

In addition, the exterior windows can be opened, thus to make good ventilation and even cool down the house, according to the occupants' operation, especially in the intermediate seasons.

3.2.2.2. Sunshades

As the clear flat glass is used for the exterior wall, it probably leads to too much direct radiation into the room, when the sunlight or skylight is too bright or glaring, especially in the summer. Here the slat-type sunshades, integrated in the double skin space, are adopted to intercept the direct solar radiation. Although its shading effect is smaller than that of the exterior shading devices, it can be protected from effect of weather and air pollution.

During the summer, the heat absorbed by the interior shades causes the air temperature on both sides to rise, and they can also emit the long-wave radiant flux to the other surfaces, and they act as the energy source in the double skin system.

During the winter, the sunshades will be drawn up to let enough solar radiation transmit into the room for heating.

3.2.2.3. Middle air

The middle air refers to those between the exterior glass wall and the interior shading,

which exchange heat with the exterior wall and the shades by the means of convection.

3.2.2.4. Double skin space

The proposed double skin space is 1.2m wide, which is separated into two parts by the steel grill at the height of 3m. This space can be used in various ways, such as for planting, drying washings, which serves as a semi-outdoor space. It should be noted that the width of the double skin space should not be larger, or the air velocity will be too small to exhaust heat effectively. According to the existing double skin system in office buildings, the width of such spaces is smaller than 1.5m.

In the summer, the air in this space exchange heat with the interior shades and the interior walls. As the temperature in the higher places is higher, the stack effect will occur in the double skin space, thus the hot air can rise to the top by the buoyancy force. Furthermore, if some plants are placed on the grill, evaporate effect would be expected to take away an extra part of solar radiation.

In the winter, the air can also be heated by the solar radiation, which acts as a buffer between the outdoor environment and the indoor environment. Lower air speed and a higher temperature in this space will lead to the decrease of heat losses. And the heated air even can be transported to the other room as per-heated fresh air, if the air inlets are opened.

All the year round, occupants may have access to this semi-outdoor environment easily.

3.2.2.5. Ventilation devices

The ventilation devices include air inlets and outlets on the floor and ceiling of the double skin space. In the proposed model, there are two openings on the floor each with an area of 0.3m^2 , while there is an opening on the ceiling with an area of 0.6m^2 .

During the summer, the inlets and outlets are often opened, when the inside air is higher than the outside air, the air in the double skin will rise with the buoyancy, then it will be expelled to the atmosphere, as well as the heat got from the slatted shadings.

While in the winter, the openings will be closed to store heat.

As an additional means to help the air movement in the double skin space, low power axial-flow fan can be used when the stack effect is not enough to drive the flow.

3.2.2.6. Interior walls/windows

The interior walls or windows may accept the heat from the exterior walls or the shadings, they also exchange heat with the air in the double skin and the indoor air. Together with the

operable exterior windows, the interior windows can make good ventilation by the natural forces or mechanical forces, especially in the intermediate seasons or at nights.

These days the ratio of interior window has increased for the need of more natural daylight, and the exterior and interior appearance.

3.2.2.7. Other items

Pebbles paved on the floor of the double skin, not only can enhance the interior appearance, but also can help for thermal storage especially during winter. And the steel grills for access in the second floor of the double skin can also absorb solar radiation, which can be regarded as a heating source for air, especially when there are no sun shadings.

3.2.3. Property of Materials

All the thermal properties of materials, structure of exterior envelopes and interior walls are described in Table 3-1. The absorptance for solar radiation for glass is 0.9, 0.4 for the pebble floor (light color), and 0.75 for the steel grills in the second floor (ASHRAE, 2001). As for the walls the absorptance is approximate to be $0.026a_o$, where a_o is the coefficient of heat transfer at the outside of wall (ASHRAE, 2001).

As to the multi-layer structure of fenestration device shown in Fig.3-6, reflection, absorption and transmission occur between different layers, and the total reflectance, absorptance, and transmittance for the conventional window with shading and the double skin system are calculated by Equations (3-2)-(3-11) (Kimura, K. 1997).

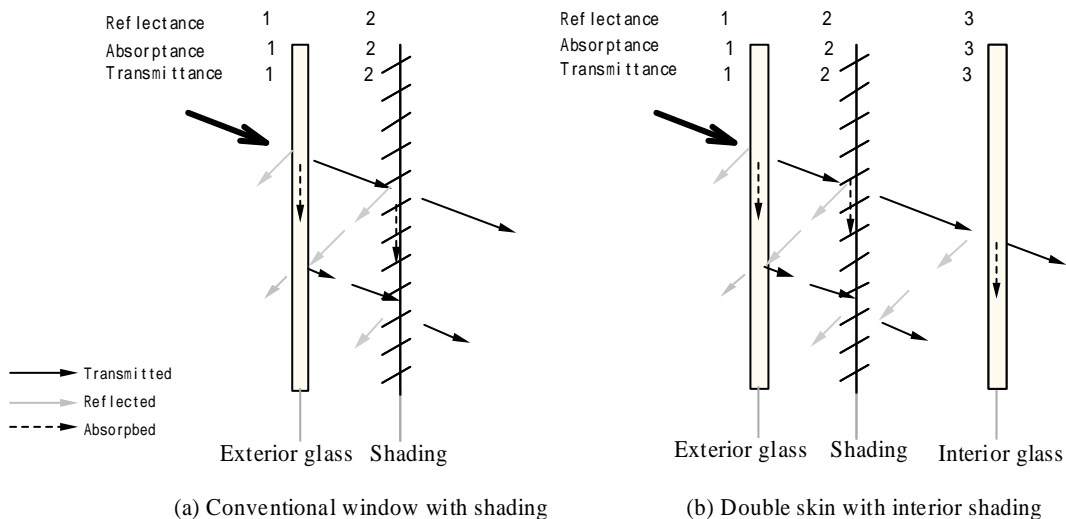


Fig.3-6. Illustration of multi-layer structure of fenestration

Table 3-1. Thermal properties of surface materials

Composition	Material	δ	λ	ρ	C_p	R	U
		mm	W/m.K	Kg/m ³	J/kg.K	m ² .K/W	W/m ² .K
Exterior glass	Glass	8	0.780	2500	840		97.5
Interior glass	Glass	6	0.780	2500	840		130
Roof	Glass	8	0.780	2500	840		
	Insulation	140	0.050	20	1470		
	Aluminum board	1.5	200	2702	0.903		
	Airspace	20	0	0	0	0.17	
	Recycled pet board	20	0.033	41	1720		
							0.282
Exterior wall	Glass	8	0.780	2500	840		
	Airspace	10		0	0	0.17	
	Insulation	90	0.050	20	1470		
	Recycled pet board	20	0.033	41	1720		
							0.388
Interior wall	Insulation	70	0.050	20	1470		
	Recycled pet board	10	0.033	41	1720		
							0.587
Floor (1F)							
	Insulation	125	0.050	20	1470		
	Airspace	50		0	0	0.17	
	Recycled pet board	12	0.033	41	1720		
							0.331
Floor (2F)	Insulation	80	0.050	20	1470		
	Airspace	50		0	0	0.17	
	Recycled pet board	12	0.033	41	1720		
							0.470

Note: δ refers to thickness; λ , Conductivity; ρ , Density; C_p , Specific heat; R, Resistance; U, Overall heat transfer coefficient. Considering the thickness and overall heat transfer coefficient of the glass, the temperature difference between the interior side and exterior side is neglected during simulation.

The total transmittance of the conventional window with interior shading t_{12} is calculated by the following equation:

$$t_{12} = \frac{t_1 t_2}{1 - r_1 r_2} \quad (3-2)$$

where t_1 is transmittance of exterior glass, t_2 is transmittance of shading; r_1 is reflectance of exterior glass; r_2 is reflectance of shading.

The total absorption of exterior glass a_{12} and interior shading a_{12} are calculated by

$$a_{12} = a_1 \left(1 + \frac{t_1 r_2}{1 - r_1 r_2} \right) \quad (3-3)$$

$$a_{12} = \frac{t_1 a_2}{1 - r_1 r_2} \quad (3-4)$$

where a_1 is absorptance of exterior glass; a_2 is absorptance of exterior glass.

The total transmittance of double skin system t_{123} is calculated by

$$t_{123} = \frac{t_{12} t_3}{1 - r_{21} r_3} \quad (3-5)$$

where t_3 is transmittance of interior glass, r_3 is reflectance of interior glass, r_{21} is sub-total reflection on the shading surface, i.e.

$$r_{21} = r_2 + \frac{t_2^2 r_1}{1 - r_1 r_2} \quad (3-6)$$

The total absorption of exterior glass a_{123} , interior shading a_{123} , and interior glass a_{123} are calculated by

$$a_{123} = a_1 \left(1 + \frac{t_1 r_{23}}{1 - r_1 r_{23}} \right) \quad (3-7)$$

$$a_{123} = \frac{t_{12} r_3}{1 - r_{21} r_3} \quad (3-8)$$

$$a_{123} = 1 - t_{123} - r_{123} - a_{123} - a_{123} \quad (3-9)$$

where r_{23} is the sub-total reflectance of shading and interior glass, r_{123} is the total reflectance, which are expressed by

$$r_{23} = r_2 + \frac{t_2^2 r_3}{1 - r_2 r_3} \quad (3-10)$$

$$r_{123} = r_2 + \frac{t_{12} r_3}{1 - r_{21} r_3} \quad (3-11)$$

Therefore the optical properties of the fenestration are shown in Table 3-2. The absorption of the conventional shading is 0.32, while it is 0.3 for the interior shading in the double skin system. And the transmittance of the convectional type is 0.04, while it is 0.03 for the double skin type.

Table 3-2. Optical properties of glass, indoor shading and wall

Material \ Performance	Reflectance ρ	Absorptance α	Transmittance τ	Emissivity ratio ϵ
Exterior glass 1	0.1	0.15	0.75	0.9
Slat type shading 2*	0.55	0.4	0.05	0.9
Exterior glass 3	0.1	0.15	0.75	0.9
Conventional fenestration				
Exterior glass		0.22		0.9
Slat type shading		0.32		0.9
Total	0.43		0.04	
Double skin fenestration				
Exterior glass		0.216		0.9
Slat type shading		0.303		0.9
Interior glass		0.017		0.9
Total	0.434		0.03	
Wall		0.44		0.9

Note: * ASHRAE Fundamentals 1997, Chapter 29, Table28, other data of exterior/interior glass are from catalog of Nippon Glass Co.

3.2.4. Setting of cases

In the following part, cases will be studied according to the different window ratio and

materials. Accounting for the initial cost of Low-E glass, only the flat glass is used here. According to the model type with/without double skin system and interior ratio of windows, the following cases are set as shown in Table 33, while the ratio of north-facing windows is supposed as 20% in each case. Other conditions, such as the exterior envelopes are the same.

Table 3-3. Cases description for double skin system

Case No.	Double skin	Interior window ratio
Summer		
3-1	Yes+sun shading	100%
3-2	No	100%+sunshading
Winter		
3-3	Yes+ no shading	100%
3-4	No	100%+no shading

3.3.Description of the simulation model

Simulation is conducted on two models to understand the effect of double skin space on indoor environment. Surface temperatures of double skin and average air temperature can be calculated through solving heat balance equations, which is called macro-model here, and the detail distribution of air flow and temperature in the double skin can be predicted by the CFD simulation, which is called micro-model.

3.3.1. Macro model

For different surfaces, the heat balance model has different expressions. According to the Handbook of ASHRAE (2001), they can be expressed as follows:

3.3.1.1. Heat balance

- Exterior surface heat balance

The heat balance on the exterior surface can be expressed by Equation (3-12)

$$q_{asol} + q_{LWR} + q_{conv} - q_{ko} = 0 \quad (3-12)$$

where q_{asol} is the absorbed direct and diffuse solar radiation (W); and q_{LWR} is the net long-wave radiation exchange with air and surrounds (W); q_{conv} is the convective heat exchange with the outside air (W); q_{ko} is the conductive heat to from the outside to the inside (W).

The heat absorbed by the surface is taken to be positive, while the heat released is negative.

- Interior surface heat balance

The heat balance on the interior surface can be expressed by Equation (3-13)

$$q_{LWX} + q_{sw} + q_{LWS} + q_{ki} + q_{sol} + q_{conv} = 0 \quad (3-13)$$

where q_{LWX} is the net long-wave radiant between interior surfaces (W); and q_{sw} is the net short-wave radiation from lights; q_{LWS} is the long-wave radiation from equipment in zone (W); q_{ki} is the conductive heat through the wall (W); q_{sol} is the transmitted solar radiation at the interior surface; q_{conv} is the convective heat to inside air (W).

- Wall conduction Process

Wall conduction process is formulated using the conduction transfer functions (CTFs), in which the conductive heat fluxes are calculated according to the current and past surface temperatures and the past fluxes, and the heat fluxes on the exterior and interior surfaces at time \mathbf{q} (q_{ko} and q_{ki}) in Equations (3-12) and (3-13) can be expressed

$$q_{ko}(\mathbf{q}) = -Y_0 T_{si,\mathbf{q}} - \sum_{j=1}^{nz} Y_j T_{si,\mathbf{q}-j\delta} + X_0 T_{so,\mathbf{q}} + \sum_{j=1}^{nz} X_j T_{so,\mathbf{q}-j\delta} + \sum_{j=1}^{nq} \Phi_j q_{ko,\mathbf{q}-j\delta} \quad (3-14)$$

While the q_{ki} in Equation (3-13) at time \mathbf{q} can be expressed as

$$q_{ki}(\mathbf{q}) = -Z_0 T_{si,\mathbf{q}} - \sum_{j=1}^{nz} Z_j T_{si,\mathbf{q}-j\delta} + Y_0 T_{so,\mathbf{q}} + \sum_{j=1}^{nz} Y_j T_{so,\mathbf{q}-j\delta} + \sum_{j=1}^{nq} \Phi_j q_{ki,\mathbf{q}-j\delta} \quad (3-15)$$

where X_j is outside CTF; Y_j is cross CTF; Z_j is inside CTF; f_j is flux CTF; \mathbf{q} is time; δ is time; step; T_{si} is the interior surface temperature; T_{so} is the exterior surface temperature.

- Air heat balance

As the heat balance for the indoor air can be expressed as

$$q_{conv} + q_{CE} + q_{IV} + q_{ac} = 0 \quad (3-16)$$

where q_{conv} is the convective heat transfer from surfaces (W); q_{CE} is the convective parts of the internal loads (W); q_{IV} is the sensible load due to infiltration and ventilation (W); and q_{ac} is the

heat transfer to/from the air conditioning system (W).

3.3.1.2. Heat balance in the double skin in summer

Fig.3-7 illustrates the heat transfer process in the proposed double skin house. For each surface, the equation of heat balance can be got.

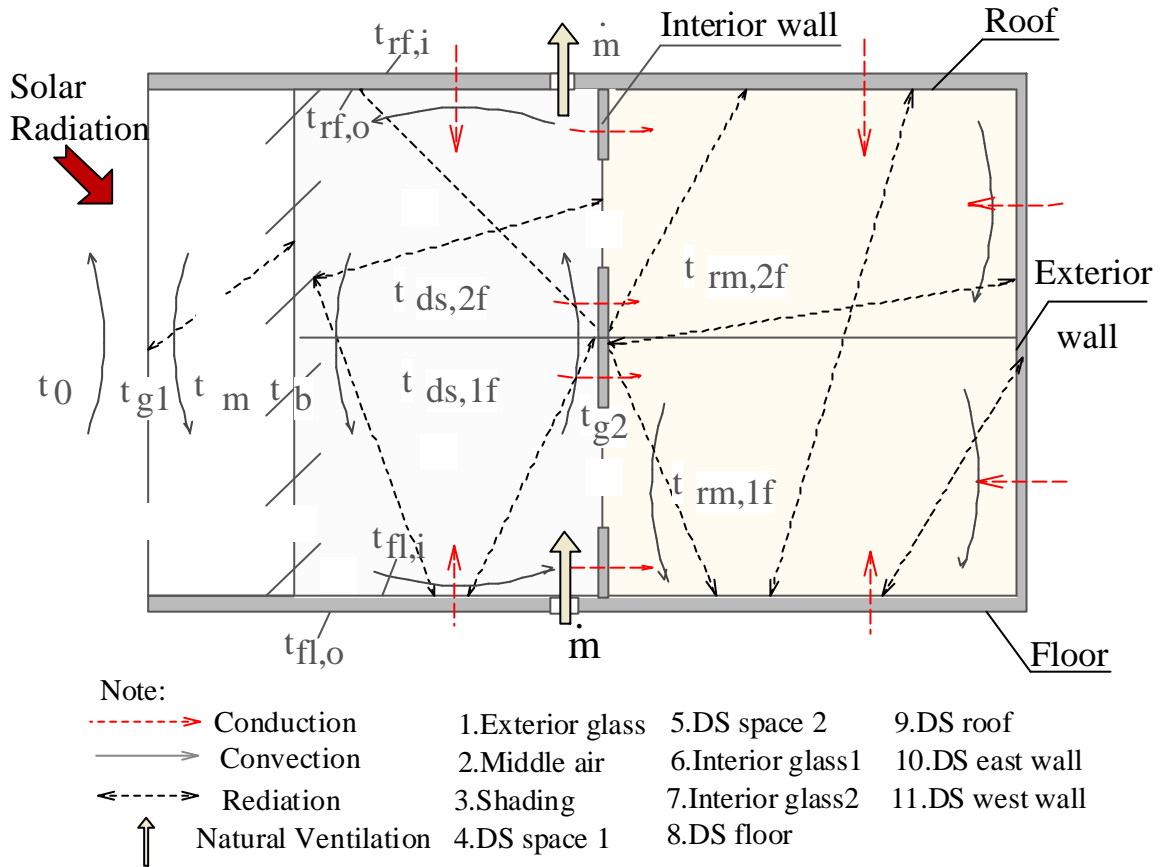


Fig.3-7. Heat transfer model for the house with double skin system

The air in the double skin space is divided into two parts (DS1f and DS2f); while the air between the shading and the exterior glass is taken as one block.

The glass and slatted shadings are assumed to have no effective thermal mass; hence the CTF is zero order, i.e. no flux history term. Furthermore, Because of the small thickness, the temperature difference between outside and inside is neglected here. The equations of the double skin/room can be expressed as follows:

- Exterior glass wall (t_{g1})

$$\mathbf{s} \mathbf{e}_g \mathbf{e}_{sd} A_{g1} F_{g1, sd} (T_{sd}^4 - T_{g1}^4) + \mathbf{a}_{c,m} A_{g1} (t_m - t_{g1}) - \mathbf{a}_o A_{g1} (t_{g1} - t_0) + a_g I_{south} A_{g1} = 0 \quad (3-17)$$

where \mathbf{s} is the Boltzmann constant, i.e. 5.67×10^{-8} (W/m².k⁴); and $\mathbf{e}_g, \mathbf{e}_{sd}$ is hemispherical emittance of glass and slat-type shading; a_g is absorptance of glass; I_{south} is solar radiation in south direction; $\alpha_{c,m}$ is convective heat coefficient in the middle space; α_o is convective heat coefficient at outside; A is area.

- Middle air (between glass and shading) (t_m)

$$\mathbf{a}_{c,m} A_{g1} (t_{sd} - t_m) - \mathbf{a}_{c,m} A_{g1} (t_m - t_{g1}) = 0 \quad (3-18)$$

- Slat-type sunshades (t_{sd})

$$\sum_{i=1}^n \mathbf{s} \mathbf{e}_i \mathbf{e}_{sd} A_i F_{i, sd} (T_{i,o}^4 - T_{sd}^4) + \mathbf{a}_{c,m} A_{sd} (t_m - t_{sd}) + \mathbf{a}_{c, sd} A_{sd} [(t_{ds1} + t_{ds2}) / 2 - t_{sd}] + a_{sd} I_{sol} A_{g1} = 0 \quad (3-19)$$

where i is number of surfaces which exchange radiation with the sunshades, a_{sd} is absorption for sunshades.

- Air in the double skin

As there is no heat of equipment in the double skin,

$$\sum_{j=1}^n \sum_{k=1}^2 \mathbf{a}_{c,j} A_j (t_j - t_{ds,k}) + \dot{m} C_p (t_0 - t_{ds}) = 0 \quad (3-20)$$

where \dot{m} is the airflow rate by natural ventilation, which can be expressed by Equation (3-21) if the flow from wind is neglected,, and j refers to the surface which has conductive heat with the double skin air.

$$\dot{m} = C_D A_{eff} \sqrt{2g \Delta H_{NPL} (\bar{T}_i - T_o) / \bar{T}_i} \quad (3-21)$$

where C_D is discharge coefficient for opening; \bar{T}_i is the average temperature in the double skin, ΔH_{NPL} is height from midpoint of lower opening to neutral pressure level (NPL), A_{eff} is the effective area of opening, and it can be assumed by

$$\Delta H_{NPL} = 0.5h \quad (3-22)$$

where h is the height of double skin. And if the flow is caused by wind forces:

$$\dot{m}_w = C_v A_{eff} U \quad (3-23)$$

where C_v is effectiveness of opening, and U is wind speed.

- Outside surface of exterior wall (t_{w_o})

$$\mathbf{a}_{c,0} A_w (t_0 - t_w) + a_w I_{south} A_w - q_{w_o} = 0 \quad (3-24)$$

where q_{w_o} is calculated by the CTF method.

- Inside surface of exterior wall (t_{w_i})

$$\mathbf{a}_{c,0} A_w (t_{site} - t_{w_i}) + a_w I_{south} A_w + q_{w_i} + \sum_{k=1}^m \mathbf{se}_w \mathbf{e}_{w,k} F_{wk,w} A_{wk} (T_{wk}^4 - T_{w_i}^4) = 0 \quad (3-25)$$

where $site$ refers to room or double skin, q_{w_i} is calculated by the CTF method according to Equation (3-15).

- Interior window g' in the double skin

$$\begin{aligned} \sum_{j=1}^n \mathbf{se}_{g'} \mathbf{e}_{ids} A_{g'} F_{ids,g'} (T_{w_i,j}^4 - T_{g'}^4) + \mathbf{a}_{c,ds} A_{g'} (t_{ds} - t_{g'}) \\ + \sum_{k=1}^m \mathbf{se}_{g'} \mathbf{e}_{irm} A_{g'} F_{irm,g'} (T_{w_i,k}^4 - T_{g'}^4) + a_{g'} I_{south} A_{g'} = 0 \end{aligned} \quad (3-26)$$

where j refers to the number of surfaces in the double skin space; while k refers to the number of surfaces in the room.

- Interior wall w' in the double skin ($t_{w'o}$)

$$\sum_{i=1}^n \mathbf{se}_w \mathbf{e}_{ids} A_{w'} F_{ids,w'} (T_{ids}^4 - T_{w'o}^4) + \mathbf{a}_{c,ds} A_{w'} (t_{ds} - t_{w'o}) + a_{w'} I_{south} A_{w'} - q_{w'o} = 0 \quad (3-27)$$

where $t_{w'o}$ refers to outside temperature of w' ; $q_{w'o}$ is calculated by the CTF method according to Equation (3-14).

- Interior wall w' in the room side ($t_{w'i}$)

$$\sum_{i=1}^n \mathbf{se}_w \mathbf{e}_{i,rm} A_{w'} F_{i,rm,w'} (T_{i,rm}^4 - T_{w'i}^4) + \mathbf{a}_{c,rm} A_{w'} (t_{rm} - t_{w'i}) + \mathbf{a}_{w'} I_{south} A_{w'} - q_{w'i} = 0 \quad (3-28)$$

where $t_{w'i}$ refers to outside temperature of w' ; $q_{w'i}$ is calculated by the CTF method according to Equation (3-15).

3.3.1.3. Heat balance in the double skin in winter

The heat transfer model for winter is similar to that in the summer, while there is no equation for sunshades.

3.3.1.4. Heat balance in conventional house

As for the conventional house, the calculation of the exterior surfaces, such as roof and floor, is also solved by the CTF method. For the south wall with windows the heat transfer process is detailed in Fig.3-8, and all equations are similar to those in the double skin, except for the heat balance on the shadings:

- Slat-type sunshades

$$\mathbf{se}_{g1} \mathbf{e}_{sd} A_{g1} F_{sd,g1} (T_{g1}^4 - T_{sd}^4) + \mathbf{a}_{c,m} A_{sd} (t_m - t_{sd}) + \mathbf{a}_{c,rm} A_{sd} (t_{rm} - t_{sd}) A_{sd} + \sum_{l=1}^q \mathbf{se}_l \mathbf{e}_{sd} A_j F_{j,sd} (T_{j,o}^4 - T_{sd}^4) + \mathbf{a}_{sd} I_{sol} A_{g1} = 0 \quad (3-29)$$

where l refers to the inside surfaces, and the total number is q . The sunshades exchange heat directly with the interior surfaces in the room.

The shadings exchange heat radiation with the interior surfaces directly, which is the difference from that in the proposed model.

3.3.1.5. Solution procedure for heat balance equations

The heat balance equations for different surfaces can be solved by iterative calculation, which consists of initial calculations for the outside climate conditions, followed by a double iteration loop, as shown in the following steps:

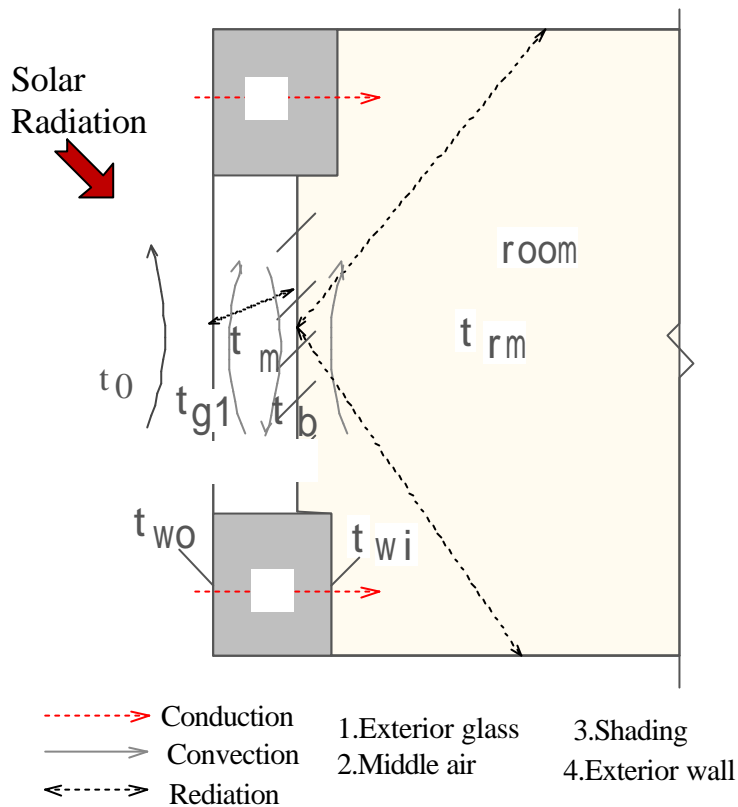


Fig.3-8. Heat transfer process for the windows in the conventional model

- Given initial conditions: site, surface areas, thermal properties (such as coefficient of CTFs, absorptance of solar radiation, convection), face temperature
- Calculate Solar radiation: included the incident and transmitted solar flux for all surfaces in 24 hours, and distributed transmitted solar energy to all the interior surfaces
- Calculate Long wave radiation and between the interior surfaces and short wave radiation from equipment and human, and a simplified approximation of long wave radiation is expressed by Equation (3-30)

$$se_i e_j A_j F_{j,i} (T_j^4 - T_i^4) \approx X_{rad} se_i e_j A_j F_{j,i} (T_j - T_i) \quad (3-30)$$

where X_{rad} is a constant, $X_{rad}=1.1$ is used in this study. And the short wave radiation from equipment is calculated according to the radiant-convective split percentage for equipment and human.

- Calculate natural ventilation volume and the infiltration, here the infiltration is described by air change rate, which is equal to the fresh air requirement according to

the number of occupant, and air change rate 1 per hour (135m³/h) is used in this study, which can meet the fresh air demand for four people in the room. The natural ventilation in double skin is calculated by Equation (3-21).

- Calculate the surface temperature $T_{so_{i,j}}$ and $T_{si_{i,j}}$ according to

$$T_{so_{i,j}} = \left(\sum_{k=1}^{nz} Y_{i,k} T_{si_{i,j-k}} - \sum_{k=1}^{nz} X_{j,k} T_{so_{i,j-k}} - \sum_{k=1}^{nq} \Phi_{i,k} q_{k_{o_{i,j-k}}} \right. \\ \left. + q_{asoli,j} + q_{LWRi,j} + Y_{i,0} T_{si_{i,j}} + T_{0j} a_{co_{i,j}} \right) / (X_{i,0} + a_{co_{i,j}}) \quad (3-31)$$

$$T_{si_{i,j}} = \left(\sum_{k=1}^{nz} Y_{i,k} T_{so_{i,j-k}} - \sum_{k=1}^{nz} Z_{i,k} T_{si_{i,j-k}} + \sum_{k=1}^{nq} \Phi_{i,k} q_{k_{i,j-k}} \right. \\ \left. + q_{sol} + q_{LWX} + q_{SW} + Y_{i,0} T_{so_{i,j}} + T_{aj} a_{ci_{i,j}} \right) / (Z_{i,0} + a_{ci_{i,j}}) \quad (3-32)$$

- Calculate the system cooling load according to

$$q_{ac,j} = \sum_{i=1}^n A_i a_{ci} (T_{si_{i,j}} - T_{aj}) + q_{CE} + q_{IV} \quad (3-33)$$

As for the calculation of natural indoor temperature, the cooling load $q_{ac,j}$ is zero.

- Iterate Equations (3-31) to (3-33) until it is converged, thus to get the system cooling load or the natural temperature.

As for the heating load, according to the conventional heating load calculation method of ASHARE (2001), the credit for solar heat gains or for internal heat gains is not included in the heating load. Considering the solar passive effect of double skin system, the heat gain in the double skin should not be neglected, i.e. the heat gains from pebble floor and 2F steel grills is used in simulation, while the transmitted solar radiation and heat gains from equipment and lights in rooms is not include.

$$q_{heat,j} = \sum_{i=1}^n A_i a_{ci} (T_{aj} - T_{si_{i,j}}) + q_{IV} \quad (3-34)$$

Iterate Equations (3-31), (3-32) and (3-34) until it is converged, thus to get the system heating load or the natural temperature when heat load is zero. The maximum room temperature in the winter will be got when the solar radiation is quite intensive, while the energy conservation is analyzed according to the average solar intensity and outdoor temperature in

January, as a “worse case” standing for the common situations.

3.3.2. Air flow around buildings

The airflow around buildings can be predicted by the RNG k - ϵ Model, which is similar to the standard k - ϵ Model. It is more responsive to the effects of rapid strain and streamline curvature than the standard k - ϵ model. And the transport Equations for the RNG k - ϵ Model are:

- The mass conservation equation

$$\frac{\partial u_i}{\partial x_i} = 0 \quad (3-35)$$

where μ_i is the velocity component in the x_i direction.

- Momentum equations

$$\frac{\partial(\mathbf{r}u_i)}{\partial t} + \frac{\partial(\mathbf{r}u_i u_j)}{\partial x_j} = -\frac{\partial p}{\partial x_i} + \frac{\partial}{\partial x_j} [\mathbf{m}_{eff} (\frac{\partial u_i}{\partial x_j} + \frac{\partial v_j}{\partial x_i})] + \mathbf{b} \mathbf{r} g_i (T_0 - T) \quad (3-36)$$

where p is the static pressure, \mathbf{r} is the air density, g_i is the gravitational body force in the i direction; \mathbf{b} is the thermal expansion coefficient of air, T_0 is the temperature at a reference point, and T is the air temperature; \mathbf{m}_{eff} is the effective viscosity; μ_t is the turbulent viscosity; μ is the laminar viscosity; C_m is a constant, i.e. 0.09, k and ϵ is given below and

$$\mathbf{m}_{eff} = \mathbf{m} + \mathbf{m}_t \quad (3-37)$$

$$\mathbf{m}_t = \mathbf{r} C_u \frac{k^2}{\epsilon} \quad (3-38)$$

- Energy conservation equation

$$\frac{\partial}{\partial t} (\mathbf{r}T) + \frac{\partial}{\partial x_j} (\mathbf{r}u_j T) = \frac{\partial}{\partial x_i} (k + k_t) \frac{\partial T}{\partial x_i} + \frac{q}{C_p} \quad (3-39)$$

where q is heat source; and k is the molecular conductivity, and k_t is the conductivity due to turbulent transport ($k_t = C_p \mathbf{m}_t / Pr_t$), Pr_t is the turbulent Prandtl number.

$$\mathbf{r} \frac{Dk}{Dt} = \frac{\partial}{\partial x_i} (\mathbf{a}_k \mathbf{m}_{eff} \frac{\partial k}{\partial x_i}) + G_k + G_b - \mathbf{r} \mathbf{e} \quad (3-40)$$

$$\mathbf{r} \frac{D\mathbf{e}}{Dt} = \frac{\partial}{\partial x_i} (\mathbf{a}_e \mathbf{m}_{eff} \frac{\partial \mathbf{e}}{\partial x_i}) + C_{1e} \frac{\mathbf{e}}{k} (G_k + C_{3e} G_b) - C_{2e}^* \mathbf{r} \frac{\mathbf{e}^2}{k} \quad (3-41)$$

where G_k represents the generation of turbulent kinetic energy due to the mean velocity gradients; G_b is the generation of turbulent kinetic energy due to buoyancy; α_k and α_e are the inverse effective Prandtl numbers for k and \mathbf{e} , respectively, and C_{2e}^* is given by

$$C_{2e}^* = C_{2e} + \frac{C_m \mathbf{r} h^3 (1 - h/h_0)}{1 + \mathbf{b} h^3} \quad (3-42)$$

3.3.3. Initial conditions for simulation

The initial conditions for simulation are listed as follows:

3.3.3.1. Heat transfer coefficients and air conditioning temperature

The convection heat transfer coefficients for surfaces in summer and winter are shown in Table 3-4.

Table 3-4. Convection heat transfer coefficients for simulation

Location	Convection heat transfer coefficient (W/m ²)	Location	Overall Convection heat transfer coefficient (W/m ²)
Middle air	$\alpha_c=4$ (S/W)	Roof	$\alpha_o=23$ (S) / $\alpha_o=35$ (W)
Double skin	$\alpha_c=8$ (S) / $\alpha_c=5$ (W)	Vertical exterior wall	$\alpha_o=17$ (S) / $\alpha_o=23$ (W)
Interior surface	$\alpha_c=5$ (S/W)		
Air conditioning Temperature	Ta=26°C (S) Ta=22°C (W)	Discharge coe. for opening C_D	$C_D=0.65$

Note: S refers to summer; W refers to winter.

3.3.3.2. Weather data

The selected weather data comes from AMeDAS climate data of Yahata in the Typical Meteorological Year, the conditions on Aug. 8 are chosen to study the highest natural temperature and cooling load of summer, while conditions on Feb. 6 are chosen for the highest natural temperature of winter, and the lowest average conditions in January are used for heating load analysis. According to the heat balance at the outside surface, the sol-air temperature t_e can be expressed by Equation (3-43).

$$t_e = t_0 + \frac{aE_t}{\mathbf{a}_0} - \frac{\mathbf{e}\Delta R}{\mathbf{a}_0} \quad (3-43)$$

where \mathbf{a} is the absorption of solar radiation; E_t is the total solar radiation incident on surface, $\text{W/m}^2\cdot\text{K}$; \mathbf{a}_0 is coefficient of heat transfer by long-wave radiation and convection at outer surfaces, which is shown in Table 3-4, $\text{W/m}^2\cdot\text{K}$; t_0 is outdoor air temperature; \mathbf{e} is hemispherical emittance of surface; ΔR is difference between long-wave radiation incident on surface from sky and surroundings and radiation emitted by blackbody at outdoor air temperature, W/m^2 .

For the horizontal surfaces the appropriate value of ΔR is 63 W/m^2 , while for the vertical surfaces, it can be assumed to be zero (ASHRAE, 2001).

Thus the heat transfer at an exterior surface can be expressed as:

$$q_o = \mathbf{a}_0 A(t_e - t_s) \quad (3-44)$$

According to AMeDAS climate data of Yahata in the Typical Meteorological Year, the conditions of Aug. 8 and Feb. 6 are chosen to represent the outside climates for summer and winter, which are shown in Tables 3-5 and 3-6.

Table 3-5. Outside climates of summer for natural temperature and cooling load calculation

Hour	Outside Temp(°C)	Total solar radiation (W/m^2)					Solar temperature (°C)				
		East	South	West	North	Horiz.	East	South	West	North	Horiz.
8/8	Winter (Light-Colored Surface, absorptance/outside convection coefficient=0.026)										
1	4.6	0.0	0.0	0.0	0.0	0.0	4.6	4.6	4.6	4.6	0.6
2	4.4	0.0	0.0	0.0	0.0	0.0	4.4	4.4	4.4	4.4	0.4
3	3.5	0.0	0.0	0.0	0.0	0.0	3.5	3.5	3.5	3.5	-0.5
4	3.2	0.0	0.0	0.0	0.0	0.0	3.2	3.2	3.2	3.2	-0.8
5	3.2	0.0	0.0	0.0	0.0	0.0	3.2	3.2	3.2	3.2	-0.8
6	2.1	0.0	0.0	0.0	0.0	0.0	2.1	2.1	2.1	2.1	-1.9
7	2	2.8	2.8	2.8	2.8	2.8	2.1	2.1	2.1	2.1	-1.9
8	2.6	50.0	38.9	30.6	30.6	55.6	3.9	3.6	3.4	3.4	0.0
9	3.9	344.4	266.7	66.7	66.7	219.4	12.9	10.8	5.6	5.6	5.6
10	7.4	350.0	375.0	97.2	97.2	361.1	16.5	17.2	9.9	9.9	12.8
11	11.5	380.6	641.7	97.2	97.2	538.9	21.4	28.2	14.0	14.0	21.5
12	11.3	200.0	672.2	100.0	100.0	602.8	16.5	28.8	13.9	13.9	23.0
13	12.9	94.4	752.8	200.0	94.4	638.9	15.4	32.5	18.1	15.4	25.5
14	13.6	91.7	627.8	361.1	91.7	544.4	16.0	29.9	23.0	16.0	23.8
15	12.3	72.2	544.4	494.4	72.2	436.1	14.2	26.5	25.2	14.2	19.6
16	12	69.4	333.3	433.3	69.4	272.2	13.8	20.7	23.3	13.8	15.1
17	10.5	30.6	47.2	63.9	30.6	58.3	11.3	11.7	12.2	11.3	8.0
18	9.8	2.8	2.8	2.8	2.8	2.8	9.9	9.9	9.9	9.9	5.9
19	9.5	0.0	0.0	0.0	0.0	0.0	9.5	9.5	9.5	9.5	5.5
20	9	0.0	0.0	0.0	0.0	0.0	9.0	9.0	9.0	9.0	5.0
21	8.8	0.0	0.0	0.0	0.0	0.0	8.8	8.8	8.8	8.8	4.8
22	8.1	0.0	0.0	0.0	0.0	0.0	8.1	8.1	8.1	8.1	4.1
23	8.2	0.0	0.0	0.0	0.0	0.0	8.2	8.2	8.2	8.2	4.2
24	7.8	0.0	0.0	0.0	0.0	0.0	7.8	7.8	7.8	7.8	3.8

Table 3-6. Outside climates of winter for natural temperature and heating load calculation

Hour	Outside Temp(°C)	Total solar radiation (W/m ²)					Solar temperature (°C)				
		East	South	West	North	Horiz.	East	South	West	North	Horiz.
2/6 Winter (Light-Colored Surface, absorptance/outside convection coefficient=0.026)											
1	4.6	0.0	0.0	0.0	0.0	0.0	4.6	4.6	4.6	4.6	0.6
2	4.4	0.0	0.0	0.0	0.0	0.0	4.4	4.4	4.4	4.4	0.4
3	3.5	0.0	0.0	0.0	0.0	0.0	3.5	3.5	3.5	3.5	-0.5
4	3.2	0.0	0.0	0.0	0.0	0.0	3.2	3.2	3.2	3.2	-0.8
5	3.2	0.0	0.0	0.0	0.0	0.0	3.2	3.2	3.2	3.2	-0.8
6	2.1	0.0	0.0	0.0	0.0	0.0	2.1	2.1	2.1	2.1	-1.9
7	2	2.8	2.8	2.8	2.8	2.8	2.1	2.1	2.1	2.1	-1.9
8	2.6	50.0	38.9	30.6	30.6	55.6	3.9	3.6	3.4	3.4	0.0
9	3.9	344.4	266.7	66.7	66.7	219.4	12.9	10.8	5.6	5.6	5.6
10	7.4	350.0	375.0	97.2	97.2	361.1	16.5	17.2	9.9	9.9	12.8
11	11.5	380.6	641.7	97.2	97.2	538.9	21.4	28.2	14.0	14.0	21.5
12	11.3	200.0	672.2	100.0	100.0	602.8	16.5	28.8	13.9	13.9	23.0
13	12.9	94.4	752.8	200.0	94.4	638.9	15.4	32.5	18.1	15.4	25.5
14	13.6	91.7	627.8	361.1	91.7	544.4	16.0	29.9	23.0	16.0	23.8
15	12.3	72.2	544.4	494.4	72.2	436.1	14.2	26.5	25.2	14.2	19.6
16	12	69.4	333.3	433.3	69.4	272.2	13.8	20.7	23.3	13.8	15.1
17	10.5	30.6	47.2	63.9	30.6	58.3	11.3	11.7	12.2	11.3	8.0
18	9.8	2.8	2.8	2.8	2.8	2.8	9.9	9.9	9.9	9.9	5.9
19	9.5	0.0	0.0	0.0	0.0	0.0	9.5	9.5	9.5	9.5	5.5
20	9	0.0	0.0	0.0	0.0	0.0	9.0	9.0	9.0	9.0	5.0
21	8.8	0.0	0.0	0.0	0.0	0.0	8.8	8.8	8.8	8.8	4.8
22	8.1	0.0	0.0	0.0	0.0	0.0	8.1	8.1	8.1	8.1	4.1
23	8.2	0.0	0.0	0.0	0.0	0.0	8.2	8.2	8.2	8.2	4.2
24	7.8	0.0	0.0	0.0	0.0	0.0	7.8	7.8	7.8	7.8	3.8
Jan. Winter (Light-Colored Surface, absorptance/outside convection coefficient =0.026)											
1	5.0	0.0	0.0	0.0	0.0	0.0	5.0	5.0	5.0	5.0	1.0
2	4.8	0.0	0.0	0.0	0.0	0.0	4.8	4.8	4.8	4.8	0.8
3	4.7	0.0	0.0	0.0	0.0	0.0	4.7	4.7	4.7	4.7	0.7
4	4.6	0.0	0.0	0.0	0.0	0.0	4.6	4.6	4.6	4.6	0.6
5	4.6	0.0	0.0	0.0	0.0	0.0	4.6	4.6	4.6	4.6	0.6
6	4.5	0.0	0.0	0.0	0.0	0.0	4.5	4.5	4.5	4.5	0.5
7	4.5	0.0	0.0	0.0	0.0	0.0	4.5	4.5	4.5	4.5	0.5
8	4.7	52.8	38.9	0.0	16.7	33.3	6.1	5.7	4.7	5.1	1.6
9	5.9	141.7	122.2	16.7	44.4	113.9	9.6	9.1	6.3	7.1	4.9
10	7.0	169.4	194.4	44.4	72.2	197.2	11.4	12.1	8.2	8.9	8.1
11	8.1	166.7	261.1	72.2	88.9	266.7	12.4	14.9	10.0	10.4	11.0
12	8.4	122.2	286.1	88.9	97.2	294.4	11.6	15.8	10.7	10.9	12.1
13	8.9	97.2	294.4	97.2	97.2	297.2	11.4	16.6	11.4	11.4	12.6
14	8.8	94.4	250.0	97.2	130.6	263.9	11.3	15.3	11.3	12.2	11.7
15	8.6	75.0	222.2	94.4	169.4	213.9	10.6	14.4	11.1	13.0	10.2
16	8.3	44.4	136.1	75.0	197.2	119.4	9.5	11.8	10.3	13.4	7.4
17	7.8	13.9	41.7	44.4	161.1	30.6	8.2	8.9	9.0	12.0	4.6
18	7.1	0.0	0.0	13.9	63.9	0.0	7.1	7.1	7.5	8.8	3.1
19	6.7	0.0	0.0	0.0	0.0	0.0	6.7	6.7	6.7	6.7	2.7
20	6.3	0.0	0.0	0.0	0.0	0.0	6.3	6.3	6.3	6.3	2.3
21	6.0	0.0	0.0	0.0	0.0	0.0	6.0	6.0	6.0	6.0	2.0
22	5.6	0.0	0.0	0.0	0.0	0.0	5.6	5.6	5.6	5.6	1.6
23	5.3	0.0	0.0	0.0	0.0	0.0	5.3	5.3	5.3	5.3	1.3
24	5.1	0.0	0.0	0.0	0.0	0.0	5.1	5.1	5.1	5.1	1.1

3.3.3.3. Coefficients of CTFs

According to the thermal properties shown in Table 3-1, the coefficients of conduction transfer functions for each surface are calculated by *Energy Plus* of *Department of Energy United State* (Crawley, D. B. et al. 2001). The results are shown in Table 3-7.

Table 3-7. Coefficients of conduction transfer functions

Time	Outside (X)	Cross (Y)	Inside (Z)	Flux (CR)
Exterior wall				
0	19.89565	1.72E-02	1.735964	
1	-27.721	0.148999	-1.86081	0.427827
2	8.304418	6.55E-02	0.365903	-1.34E-02
3	-0.24564	1.84E-03	-7.44E-03	1.33E-05
4	2.34E-04	1.86E-06	5.16E-06	-2.07E-10
5	-3.00E-09	4.52E-11	-5.81E-11	3.41E-16
Roof				
0	21.61927	3.22E-04	1.753675	
1	-42.2503	1.56E-02	-2.95473	1.033183
2	25.97598	3.72E-02	1.536273	-0.28607
3	-5.64666	1.25E-02	-0.28382	2.09E-02
4	0.371491	6.37E-04	1.49E-02	-2.05E-04
5	-3.59E-03	4.05E-06	-1.13E-04	1.72E-07
Floor (Exterior)				
0	11.74199	9.96E-05	1.62649	
1	-25.1206	6.53E-03	-3.14698	1.301037
2	17.42502	1.76E-02	1.894725	-0.42227
3	-4.19611	6.18E-03	-0.35571	2.04E-02
4	0.180967	2.97E-04	1.23E-02	-1.12E-04
5	-4.85E-04	1.61E-06	-6.18E-05	1.51E-07
Exterior glass				
0	97.5	97.5	97.5	
Floor (Interior)				
0	11.40141	2.35E-02	11.18631	
1	-13.468	0.231523	-13.2452	0.253548
2	2.459611	0.10743	2.456562	-4.44E-03
3	-2.68E-02	3.78E-03	-3.14E-02	1.54E-05
4	5.53E-05	9.41E-06	4.77E-05	-6.75E-09
Interior glass				
0	130	130	130	
Interior wall				
0	1.611857	0.207053	1.611857	
1	-1.13941	0.312663	-1.13941	0.1157
2	5.93E-02	1.20E-02	5.93E-02	-2.84E-05
3	-1.02E-05	1.37E-06	-1.02E-05	7.77E-13

3.3.4. Micro model

According to the calculated results by the macro model, the surface temperatures are taken as the boundary conditions for further study. Here the zero-equation model, recommended by Chen (1998), is used to predict the detailed situations in the double skin space.

The mass conservation equation and momentum equations are the same with Equations (3-18)-(3-19), while μ_t , the turbulent viscosity, is simplified as a function of local mean velocity V and a length scale l , as listed in Equation (3-45)

$$\mathbf{m}_t = 0.03874 \mathbf{r} V l \quad (3-45)$$

And the energy equation is expressed by Equation (3-46)

$$\frac{\partial \mathbf{r} T}{\partial t} + \frac{\partial \mathbf{r} u_i T}{\partial x_i} = \frac{\partial}{\partial x_i} \left(\Gamma_{T,eff} \frac{\partial T}{\partial x_i} \right) + \frac{q}{C_p} \quad (3-46)$$

And the effective diffusive coefficient for temperature $\mathbf{G}_{T,eff}$ is expressed by Equation (3-47)

$$\Gamma_{T,eff} = \frac{\mathbf{m}_{eff}}{\text{Pr}_{eff}} \quad (3-47)$$

where the effective Prandtl number, Pr_{eff} is 0.09.

Since the zero-equation model does not solve transport equations for turbulence energy and dissipation rate, the computation speed can be faster. It is recommended for natural ventilation, especially with buoyant forces.

3.3.4.1. Simulation for airflow around buildings

The layout of the simulation model for airflow around residential house is shown in Fig.3-9. The atmosphere boundary conditions are set at the south face of the house model, and the location terrain is a flat unobstructed area with the size of 100m×100m×60m. The height displayed in this graph is only 30m, because the top wall is set to be symmetry boundaries. While the model house is put in the middle of the simulation area with the size of 5.7m×10m×6m with the floor height of 0.5m.

The basic mesh size is 2m×2m×2m, and places near the model room are subdivided into smaller mesh with the height of 0.1m, and the total mesh number reaches nearly 200000.

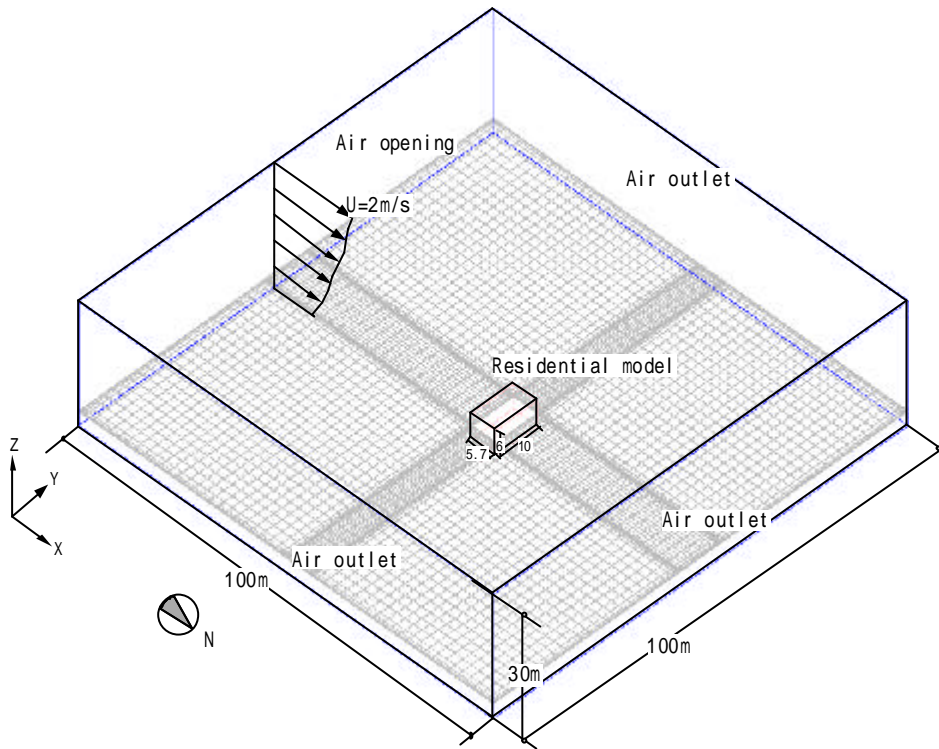


Fig.3-9. Simulation model of air flow around house

The steady turbulent RNG model is used in the simulation. The turbulent energy k is assumed to be 0.19 at $X=-50\text{m}$, others boundary conditions are shown in Table 3-8.

Table 3-8. Boundary conditions of atmosphere velocity

Y (m)	U_x (m/s)	U_y (m/s)	Turbulent dissipation
0.727308	1.800408	-9.74E-08	0.045002
1.58831	1.946671	-1.05E-07	0.020607
2.623601	2.046863	-1.11E-07	0.012475
3.89206	2.129202	-1.15E-07	0.008409
5.482456	2.203416	-1.19E-07	0.00597
7.535164	2.274617	-1.23E-07	0.004344
10.28605	2.346518	-1.27E-07	0.003182
14.16431	2.422805	-1.31E-07	0.002311
20.04157	2.508373	-1.36E-07	0.001633
30	2.611627	-1.41E-07	0.001091

3.3.4.2. Simulation in the double skin space

The layout of the simulation model for double skin space is shown in Fig.3-10, which shows the detail dimensions of the residential model in Fig.3-9.

The basic mesh size is $0.1\text{m}\times 0.1\text{m}\times 0.1\text{m}$, and places near floor openings and roof opening are strengthened, and the total mesh number is about 100000.

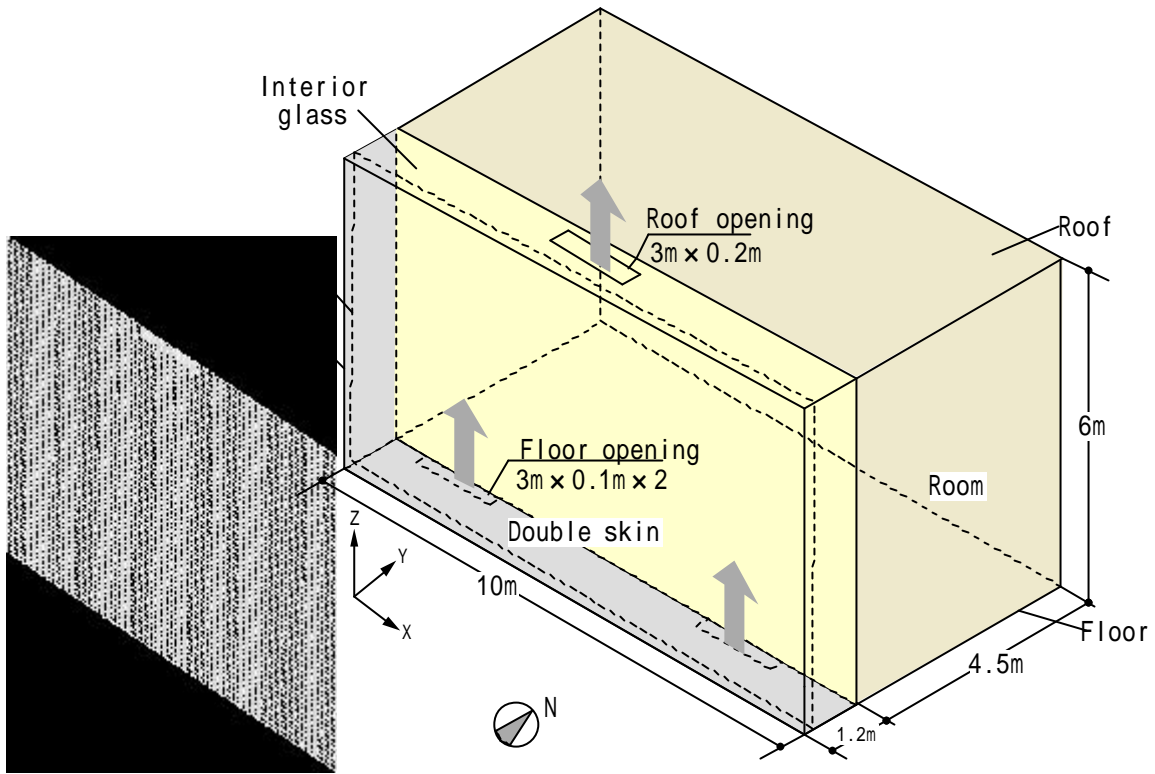


Fig.3-10. Layout of double skin space and mesh profile

The boundary conditions are set according to the surface temperatures calculated by heat balance equations, such as the temperature of roof, walls, floor and glass, and the interior sun shadings are set as a heat source with fixed temperature. The floor openings are set with fixed temperature and ambient pressure, while the same pressure is set on the roof opening. And all the openings are closed in the winter, and there is also no sun shading.

The transient turbulent zero-equation model is used in the simulation. The boundary conditions in winter and summer are detailed in Table 3-9 for the natural ventilation mode and closed mode.

Table 3-9. Boundary conditions (temperature)

Location	Temperature (°C)		Location	Temperature (°C)	
	Summer	Winter		Summer	Winter
Floor	34	-	Exterior glass	35.6	-
Roof	34.8	-	Interior glass	32.3	-
East wall	34.6	-	Sun shading	38	-
West wall	34.6	-	Outside air	31	-

3.4.Simulation results

3.4.1. Air flow around the house

According to the prevailing wind in Kitakyushu coming from the south and with the average speed of 2m/s, by using the RNG model, the static pressure around the model house (L5.7m×W10m×H6m) with a raised floor of 0.5m is shown in Fig.3-11. The front surface has a positive pressure of about 3 Pa, while the front parts of the floor and roof have negative pressure with the minimum of about -5 Pa.

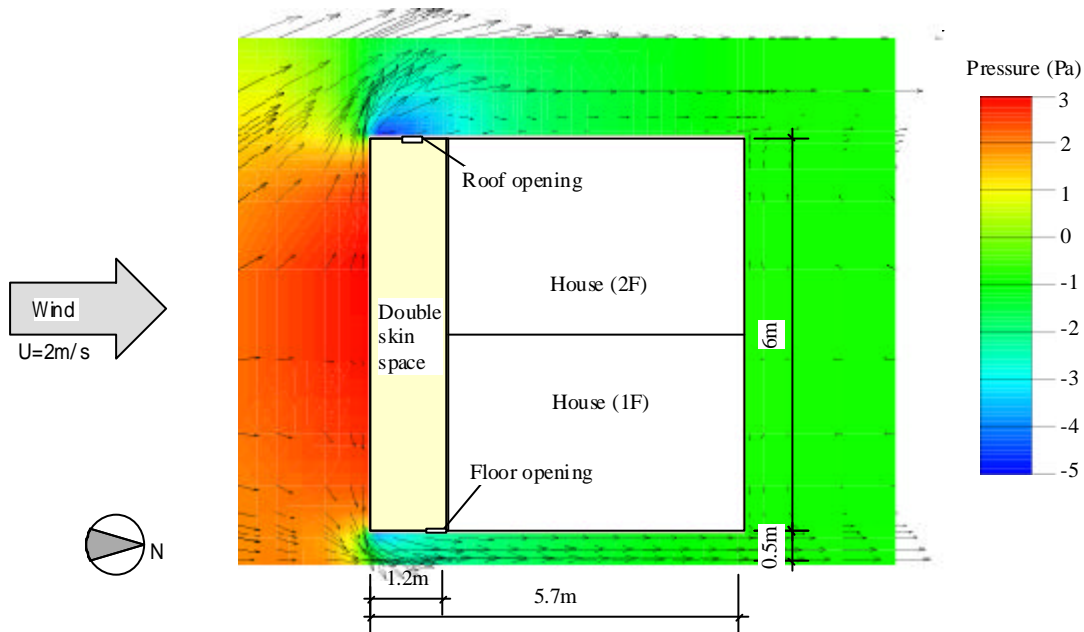


Fig.3-11. Air flow and pressure around the model house

At the floor openings there is a little negative pressure of about 0 to -2 Pa, while roof opening has a bigger negative pressure of about -4 Pa, this will help air flow in the double skin. Considering the pressure loss coefficient of opened air inlets with net filter, the resistant will be in the relative quantity with the driven force from wind. Therefore, driven force from wind is neglected in the following simulation.

And one more thing should be pointed out is that if the openings (inlets/outlets) are designed in the front surface of a building, like the TWR tower introduced in Chapter 1, although they had some special design for the outlet in the TWR tower, it is not recommended. The exhaust openings should be in the negative pressure area, just like the proposed model. Even with the variation of wind direction the exhaust openings have not a positive pressure. But relative measures for prevention from rain should be considered.

3.4.2. Simulation results in summer

According to the heat balance equations, and the outside climate on August 8 of Yahata shown in Table 3-5, the simulation results in summer are shown as follows.

3.4.2.1. Temperature distribution in double skin

The distribution of natural temperature for Case 3-1 and 3-2 is shown in Fig.3-12.

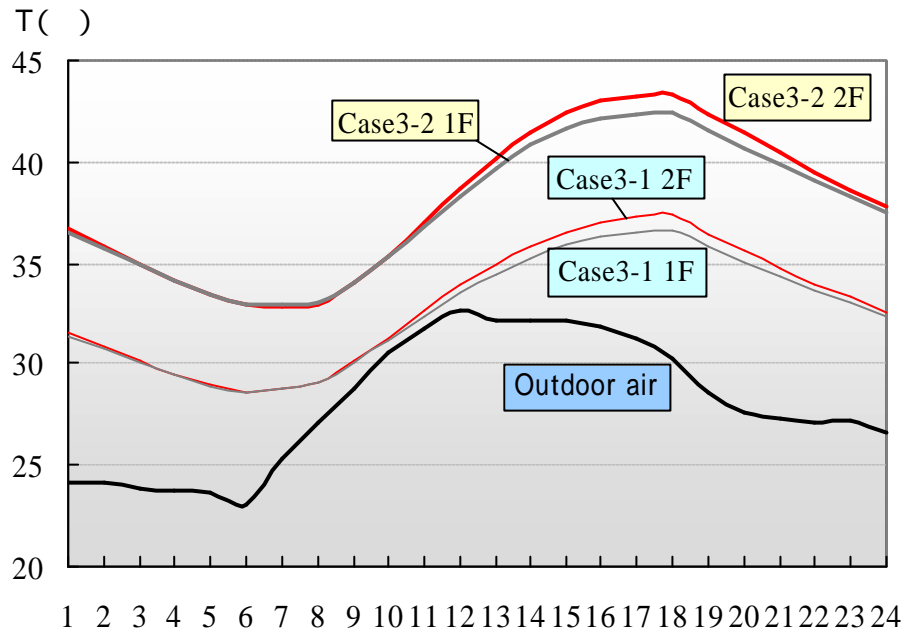


Fig.3-12. Natural room temperature distribution for Cases 3-1 and 3-2

Although the sun shadings are shut down in Case 3-2, because the conventional house is completely closed without any ventilation, the indoor temperature increases fast. The peak value reaches 41°C in the room on the second floor at 14:00 in the afternoon, while it is a little lower on the first floor at about 39°C.

As for Case 3-1, the sun shadings absorb the solar radiation, then the heated slats exchange heat with the air in the double skin. The peak temperature is about 41°C in the double skin. And the hot air rises because of the buoyancy force, at the same time the cold air under the floor will be induced into the double skin. With the help of natural ventilation, the absorbed heat can be exhausted to the outside.

Although the peak room temperature on the second floor reaches nearly 38°C during the afternoon, it is about 3°C lower than in Case 3-2. While the maximum reaches 35°C in the first floor room with about 3°C smaller than Case 3-2. Compared with the outside temperature, the maximum temperature increase reaches nearly 10°C, which refers to the temperature difference

between the air under the floor and outlet.

During the afternoon, air temperatures drop gradually, and the decrease of speed in the double skin is fastest, 1.48°C per hour from 14:00 to 18:00 in the second floor in Case 3-1, then the rooms in Case 3-2 for about 0.75°C per hour, and the lowest is the rooms in Case 3-1 for about 0.67°C per hour. The temperature in the double skin is very close to the outside air, while the indoor air remains to be about 30°C even in the midnight.

3.4.2.2. Airflow by stack effect

According to Equation (3-21), the calculated temperature difference and the airflow caused by natural ventilation is shown in Fig.3-13, here the discharge coefficient for opening is 0.65, and the resistance of ventilation devices is neglected.

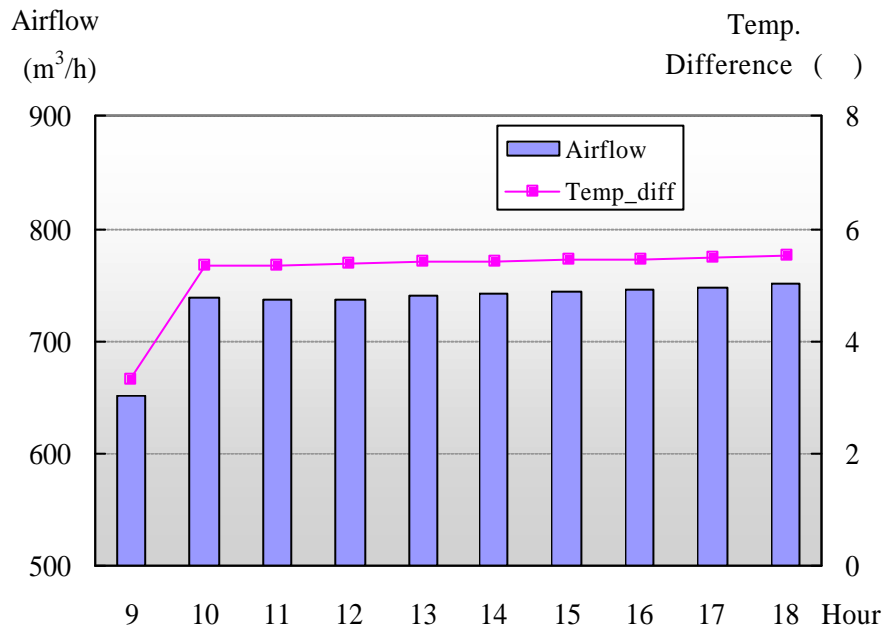


Fig.3-13. Natural ventilation by stack effect

With the increase of temperature difference the airflow rate is also increased, the maximum natural ventilation rate reaches about 750 m³/h in the afternoon when the temperature difference is about 5°C. If the temperature difference is only 2.3°C, this will lead to about 650m³/h airflow rate by natural ventilation, which is equal to the air change rate about 10 per hour for the double skin space.

The detail temperature distribution is calculated according to CFD simulation with the zero-equation model of *Airpak2.0*, and results of temperature distribution in the double skin system at 12:00 are shown in Fig.3-14, and the boundary conditionings are shown in Table 3-9.

The temperature is stratified in the vertical direction, and the temperature difference between the floor opening and the roof opening is about 4°C. While the velocity distributions at Y=0.1m (the section of floor opening) and Y=0.6m (the section of roof opening) are shown in Fig.3-15, the average velocity is about 0.3m/s at the floor opening. The airflow driven by stack effect reaches 670m³/h, which is similar to the results from the macro model of Equation (3-21).

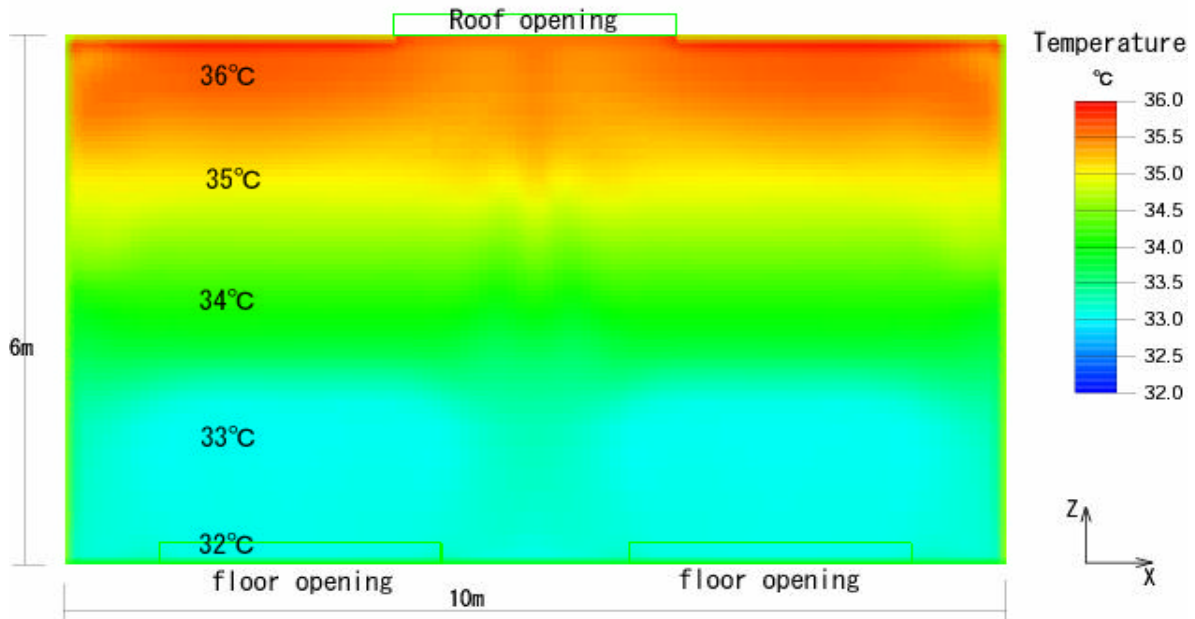


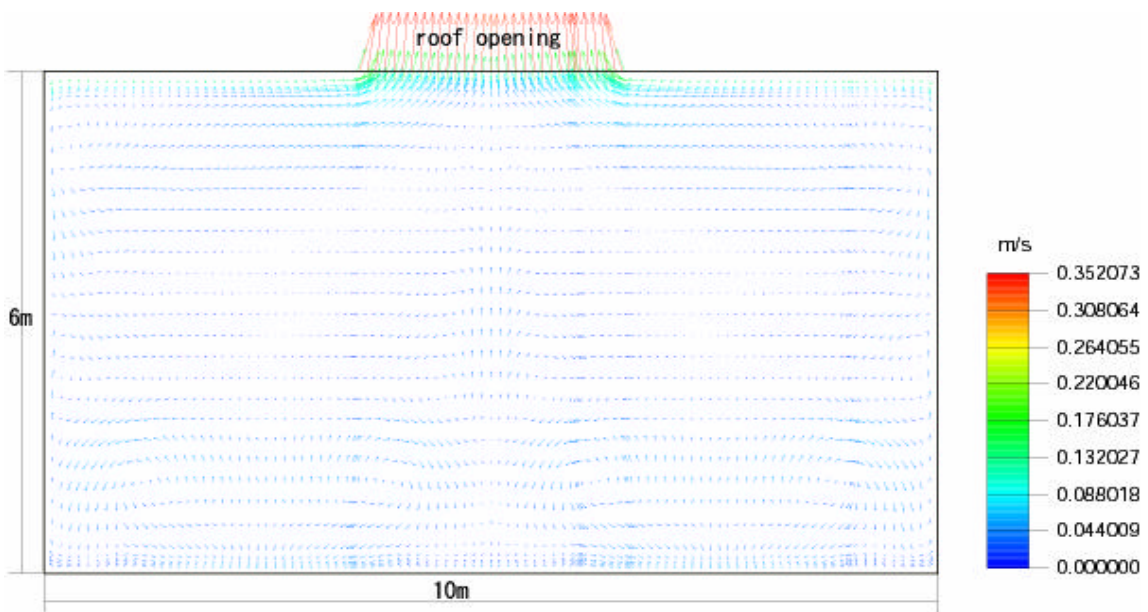
Fig.3-14. Temperature stratification in vertical direction (at Y=0.6m)

3.4.2.3. The ratio of exhaust heat

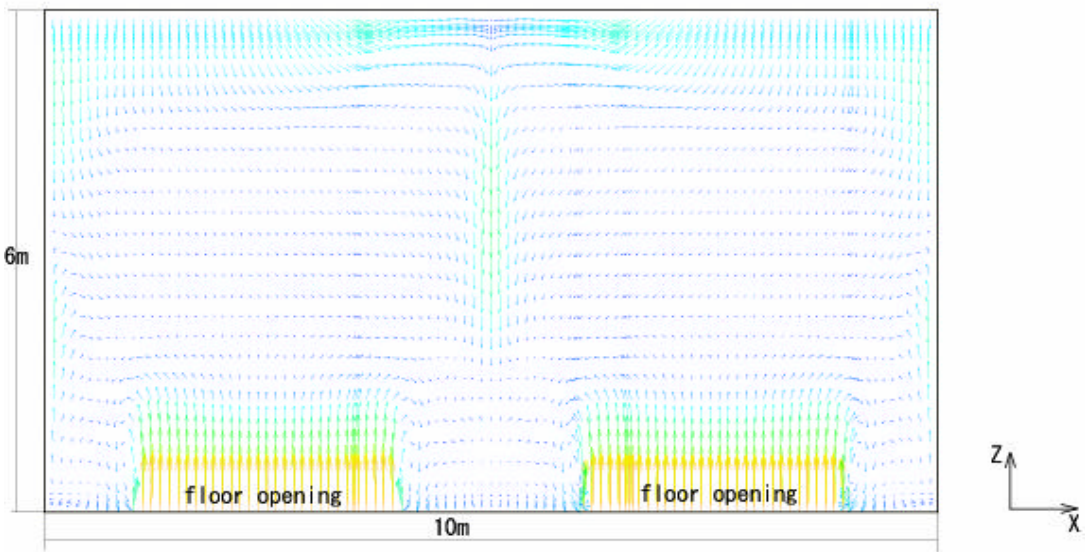
According to the calculated surface temperatures and natural airflow rate, the flow of solar radiation in the double skin system can be shown in Table 3-10.

As the heat gain mainly comes from the solar radiation from the south, while the temperature difference is small in the morning, the airflow caused by natural ventilation is smaller, which leads to a smaller exhaust ratio. With the increase of airflow rate the exhaust ratio increases fast, and the average value is nearly 10% during 11:00 to 15:00. While the ratio of exhaust heat and transmitted solar radiation from the shading is quite large, about 25%.

But after the direction radiation becomes zero, the exhaust heat still remains large, which leads to a larger ratio of heat exhaust. The reason lies in that the storage heat from the walls and room is also discharged.



(a) Velocity at section of $Y=0.6\text{m}$



(b) Velocity at section of $Y=0.05\text{m}$

Fig.3-15. Velocity distribution at the section of openings

Table 3-10. Solar heat gain exhausted in the double skin system

Hour	Solar Heat gain (W)	Shading absorbed	Airflow (m ³ /s)	Exhaust heat (W)	Exhaust ratio1(%)	Exhaust ratio2(%)
	A	B	C	D	E1=D/A	E2=D/B
9	10333	3131	0.18	727	7.0%	23.2%
10	16167	4899	0.21	1318	8.2%	26.9%
11	20167	6111	0.20	1319	6.5%	21.6%
12	21833	6615	0.20	1326	6.1%	20.0%
13	21667	6565	0.21	1341	6.2%	20.4%
14	19333	5858	0.21	1350	7.0%	23.0%
15	14833	4494	0.21	1357	9.1%	30.2%
16	8667	2626	0.21	1366		
17	3833	1161	0.21	1377		
18	2167	657	0.21	1394		
Average					7.2%	23.6%

Note: Exhaust ratio1 refers to the ratio with the solar heat gain in south direction, while exhaust ratio2 refers to the ratio with the heat absorbed by the shading. As the direct solar radiation becomes zero after 16:00, they are not included in the average value.

3.4.2.4. Cooling load

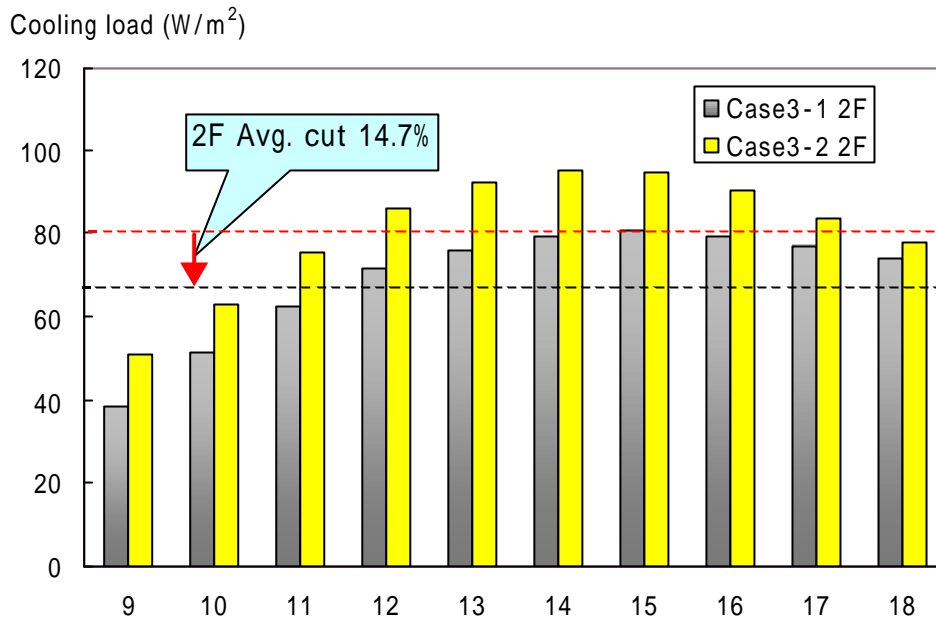
The comparison of cooling load between Case 3-1 (house with double skin) and Case3-2 (house without double skin) is shown in Fig.3-16. The average cooling load in the double skin house is 65.6 W/m² for the 1F room and 68 W/m² for the 2F room, when the set air conditioning temperature is 26°C. The cut of cooling load in the 1F room is 16%, while it is 14.7% in the 2F room, which is smaller than that in 1F. The reason lies in that there is temperature stratification in the double skin space, the higher the temperature is, the larger heat convection from the double skin space to the room is.

3.4.3. Simulation results in winter

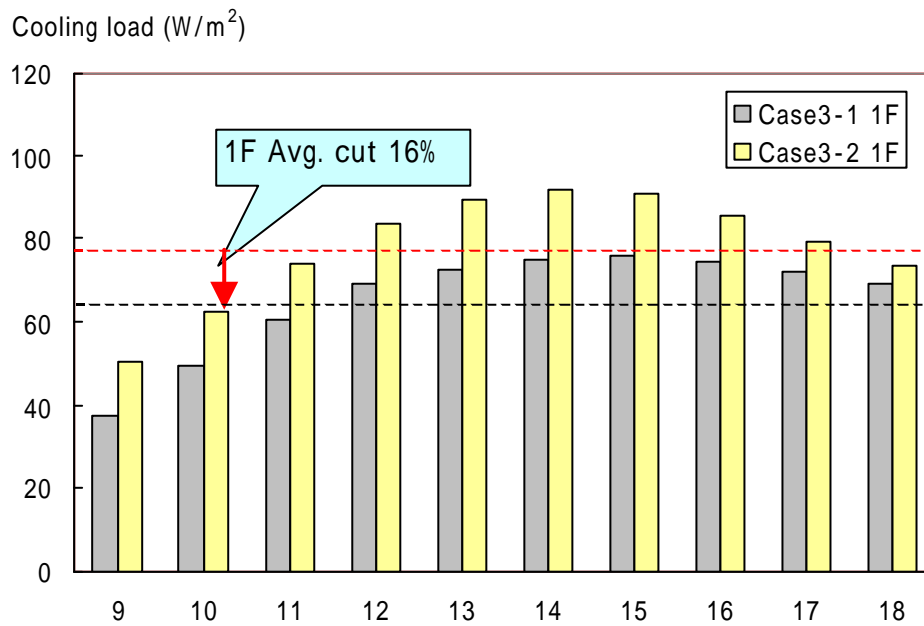
According to the heat balance equations, and the outside climate of Yahata shown in Table 3-6, the simulation results in winter are shown as follows:

3.4.3.1. Green house effect Temperature distribution in double skin

The comparison of natural temperature on Feb. 6 for Cases 33 and 34 is shown in Fig.3-17, as the average solar radiation on horizontal surface exceeds 300W/m² in the daytime, the green house effect of double skin system is very obvious.



(a) Cooling load in 2F



(b) Cooling load in 1F

Fig.3-16. Comparison of Cooling load between house with double skin and conventional house in summer

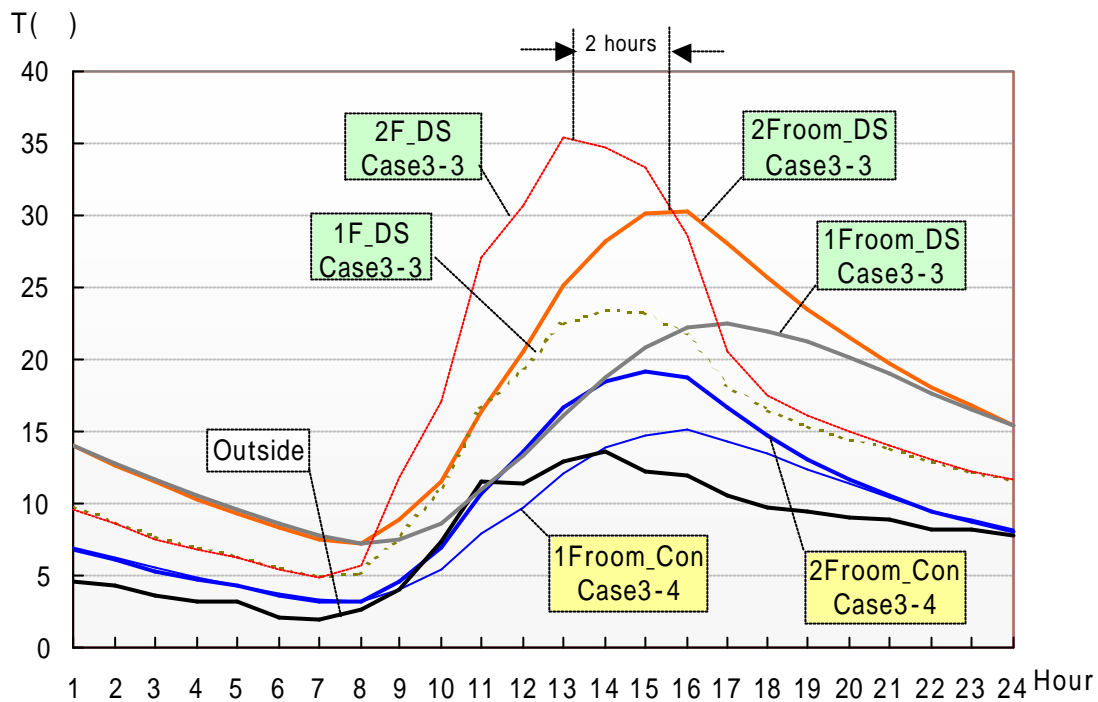


Fig.3-17. Natural temperature distribution in winter for Cases 3-3 and 3-4

In Case 3-3 the sun shadings are drawn up to let more solar radiation in, when the peak temperature in the double skin space reaches over 35°C at 13:00, which is nearly 20°C higher than the outside. While the highest temperature in 2F room reaches about 30°C during the period of 15:00 to 16:00 with 2 hour's delay compared with the peak of double skin space. The highest temperature in the 1F also exceeds 20°C.

While shadings are also drawn up in Case 3-4, the room temperature is only about 15°C, which is only 2 to 3 degrees higher than the outside air. The reason lies in that the south glass exchanges heat intensively with the outside air, and the heat cannot be stored within the houses. The room temperature difference between the double skin type and the conventional one reaches 8-10°C. The 2F room in Case 3-3 does not need air conditioning in the afternoon, while air conditioning is necessary in Case 3-4.

The double skin space acts as a buffer between the room and the outside air, which not only introduces more solar energy, but also prevents the heat from escaping, therefore the whole house is just like a green house, the room air temperature in Case 3-3 is 7°C higher than that in Case 3-4 even in the midnight. This will lead to great energy conservation. It is estimated that about 60-70% heating load can be reduced when there is enough solar radiation.

Although all the openings are closed in the double skin space, temperature difference

between the 1F and 2F is quite big. The main reason lies in that the steel grills between the 1F and 2F absorbs the solar radiation, which will be absorbed by the air. Because of the increased temperature, the buoyancy makes the high temperature air rise to the 2F space.

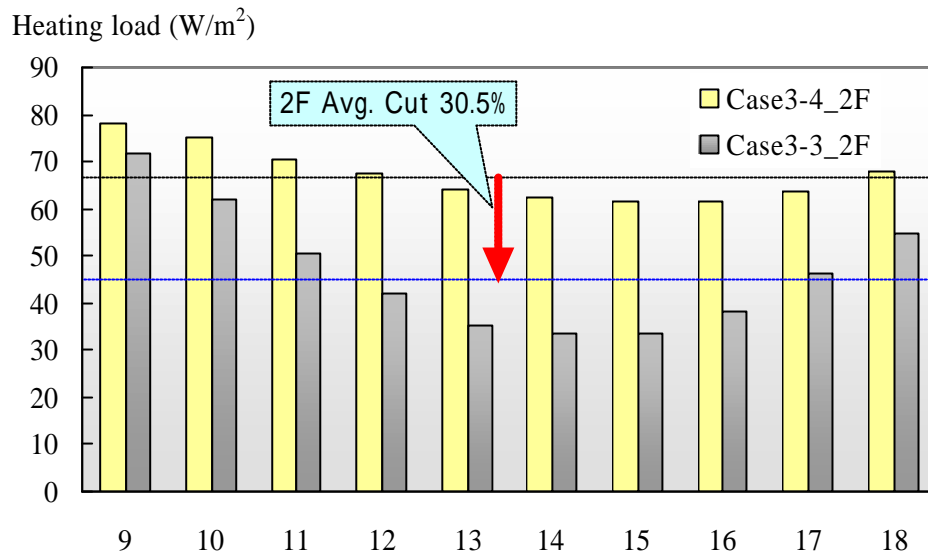
As the thermal capacity is very small in the double skin space, the speed of temperature drop is very fast. The temperature drops over 3°C per hour from 14:00 to 19:00 in the double skin space, while it is only 1°C per hour in the rooms. This means it is better to shut down the shadings when the south solar radiation becomes to drop after 15:00, and this will bring to more energy saving.

3.4.3.2. Heating load

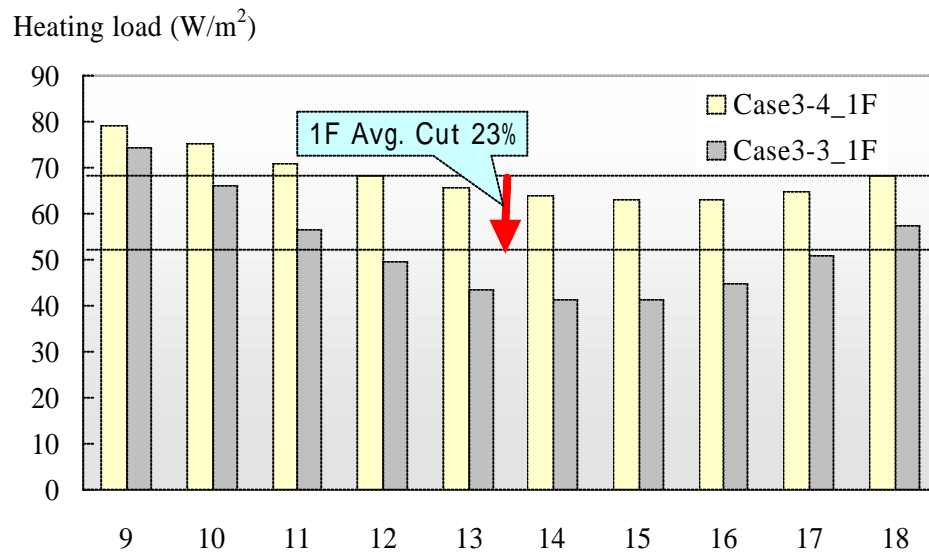
As is mentioned in last section, the comparison of heating load should be made on “worst conditions”, the average climate conditions in the coldest month shown in Table 3-6 are used for heating load comparison. The set indoor temperature for heating is 22°C, and the total airflow rate of infiltration and fresh air is taken as to be equal to air change rate of 1 per hour.

The heating load in the double skin house is smaller than that in the conventional house because of the green house effect of the double skin space, as is shown in Fig.3-18. Compared with the conventional type (Case 3-4), the average heating load in the 2F room in double skin house (Case 3-3) is about 53 W/m², with a cut of about 30%. While the heating load in the 1F room is about 47 W/m², which accounts for a cut of 23%.

Although the average solar intensity in January is only half of that on Feb. 6, i.e. about 180W/m², it will also bring about great energy saving. If the direct heat gain from solar radiation is taken into consideration, the energy conservation will become greater.



(a) Heating load in 2F



(b) Heating load in 1F

Fig.3-18. Comparison of heating for Cases 3-3 and 3-4

3.5. Summary and Conclusion

Compared with the conventional house without double skin system, the effectiveness of double skin system in residential house is evaluated by simulation. The air pressure at the floor openings caused by the wind effect is similar to that at the roof opening, therefore only the thermal effect is considered in this study. The double skin space acts as a buffer between the room and the outside air, which not only can lead to more heat exhaustion in summer, but also can prevent the heat from escaping in winter, and the detail conclusions are as follows:

During the summer when sunlight is very strong, temperature stratification occurs in the vertical direction, and the maximum temperature in the double skin can be about 5°C higher than the outside air. When all the openings are on, the natural ventilation caused by the buoyant force is promoted, which reaches 750m³/h, therefore the air change rate in the double skin space is 10 per hour. The solar radiation can be effectively exhausted with the stack effect, and nearly 10% of the total solar radiation in the south direction has been exhausted. Compared with the transmitted solar radiation, about 20-30% solar radiation can be discharged directly. During the air conditioning period, the exhausted heat and shading effect of double skin will lead to about a 15% cut in cooling load when the room air is set to be 26°C.

During the winter, when all the openings are closed, the double skin space acts as a buffer between the room and the outside air, which prevents the heat from escaping. The peak temperature in the double skin space reaches over 30°C at about 13:00, which is about 20°C higher than the outside. While the highest temperature in 2F room reaches about 25°C at 14:00 with an hour's delay, and the maximum temperature in the 1F also exceeds 20°C.

Compared with the conventional type, the average heating load in the 2F room in double skin house is about 53 W/m², with a cut of about 30%. While the heating load in the 1F room is about 47 W/m², which accounts for a cut of 23%.

If the direct heat gain from solar radiation is taken into consideration, the energy conservation will become greater.

The effectiveness of this passive system will be further studied according to the field experiments in the next chapter.

CHAPTER 4

FIELD EXPERIMENT OF DOUBLE SKIN SYSTEM IN THE EXPERIMENTAL HOUSE

According to the simulation results in Chapter 3, the double skin system has a great effect on energy saving by the stack effect in the summer and the green house effect in the winter. In order to verify its real effect, it has been designed in the experimental house in Kitakyushu. In the following part, the details of this double skin system have been illustrated, then the climate conditions, such as solar radiation, outside air velocity, the temperature distribution in the double skin and inside rooms are measured during the summer, winter and autumn, thus to analysis its utility of natural energy, appraise its effectiveness for residential house. The experiment results have also been compared with the simulation results.

4.1.Details of the Double Skin System

The details of the double skin system in the experimental house are shown in Fig.4-1, as well as the layout of the test points. The SOHO (1F) and living room (2F) have a 2.4 meter-high south window, and there is a 6 meter-high exterior window to the south of room. The space between the fenestration and the south windows/wall of SOHO/living room constitute the double skin space. The width of this space is 1.2m, and the fenestration components are 8mm flat glass with interior slat-type sunshades.

In summer the interior shades are completely shut down to cut the solar radiation, while in winter, the shadings are drawn up to introduce more solar radiation and daylight. The openings on the floor and roof can be controlled according to outside climate to make sure of indoor thermal comfort.

The scenery of the double skin in the experimental house is shown in Fig.4-2, and this space is separated from the steel grillers at the height of 3m. The materials and ventilation devices used in this experimental house are listed in Table 4-1. The thermal resistances are the same with those in Chapter 3.

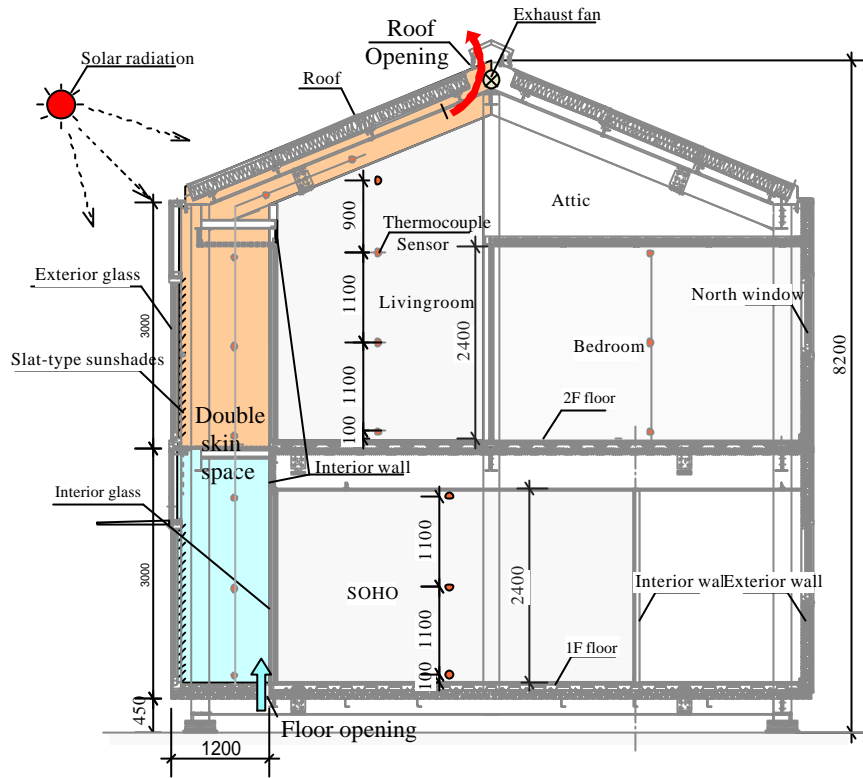


Fig. 4-1. Section of the double skin system in the experimental house (with test points)



(a) Double skin 1F



(b) Double skin 2F

Fig. 4-2. Scenery of the double skin system in the experimental house

4.2.Outline of field experiment

In order to evaluate the efficiency of natural ventilation in the double skin system, field experiments are conducted in the summer, autumn and winter of 2001.

Table 4-1. Detail constitution of the double skin in the experimental house

Composition	Structure	Overall Coe. of heat transfer (W/m ² K)	
Exterior glass	South-facing, 8mm glass	5.8	
	North-facing, 3mm glass + 6mm air layer + 3mm glass	3.4	
Interior glass	South-facing, 6mm glass	5.9	
Roof	8mm glass + 140mm insulator + 20mm air layer + 20mm recycled pet bottle	0.307	
Exterior wall	8mm glass + 90mm insulator + 10mm air layer + 20mm recycled pet bottle	0.457	
Interior wall	70mm insulator + 10mm recyc led pet bottle		
1F Floor	17mm insulator + 100mm insulator + 50mm air layer + 12mm recycled pet bottle	0.370	
2F Floor	17mm insulator + 50mm insulator + 50mm air layer + 12mm recycled pet bottle	0.553	
	Dimensions	Quantity	Memo
Opening on floor	1.4m (L)× 0.11m (W)	4	With filter
Opening on roof	3m(L) × 0.1m (W)	2	
Axial-flow fan	Airflow rate=650m ³ /h Power=56W Static pressure=60pa Current=0.56A	2	Mitsubishi JFU-65S (Low noise)

4.2.1. Testing points and instruments

Air temperature (dry-bulb) in double skin space, and each room is tested, as well as those on different surfaces. In the double skin, the temperature sensors are set in the vertical direction at the height of 0.1m, 1.2m, 2.3m, 3.4m, 4.5m and 5.6m, as well as that below the roof.

The test points in the room are set in the middle of the room with the height of 0.1m, 1.2m and 2.3m. Test points of air velocity are set on the floor opening.

At the same time, outside temperature, total solar radiation on the horizontal surface, wind speed and direction are measured. In addition, the PMV in the living room are also tested during autumn and winter.

Most of the data are recorded in a data collector, or by computer. Detail testing points and relative instruments are shown is Table 4-2.

Table 4-2. Testing points and instruments in the double skin

No.	Testing items	Points	Instruments
1	Temperature in double skin space	18	Thermocouples (T-type) T-6F 0.2
2	Temperature in double skin space	3	Thermocouples (T-type) T-6F 0.2
3	Indoor air temperature	15	Thermocouples (T-type) T-6F 0.2
	Indoor humidity	5	Electrical type
4	Air velocity	3	RION AM-097
5	Temperature and humidity in double skin space	2	Tr-72s (thermal recorder)
6	PMV	1	
7	Air flow at the opening	1	ALNOR Standard Barometer
8	Solar radiation (Second class Pyranometer)	1	MS601 (EKO INSTRUMENTS Co.) Directional response: less than $\pm 25 \text{ W}\cdot\text{m}^{-2}$
9	Wind speed direction	1	MA-110 (EKO INSTRUMENTS) Vane type Direction sensor
10	Outdoor temperature and humidity	1	Electrical type

4.2.2. Mode of double skin

As the double skin system has four floor openings, one roof opening, windows, sunshades and some ventilation devices, according to the combination of these components in different climate conditions, there are many operation modes for the double skin system, thus to make the best of natural conditions to realize thermal comfort.

The basic modes can be divided into four types illustrated in Fig.4-3, and their characteristics are as follows.

4.2.2.1. Summer mode

Mode 1 in Fig.4-3 is called the summer mode. In this mode the ventilation openings in the double skin are all opened, the interior shadings and other operable windows are completely shut down.

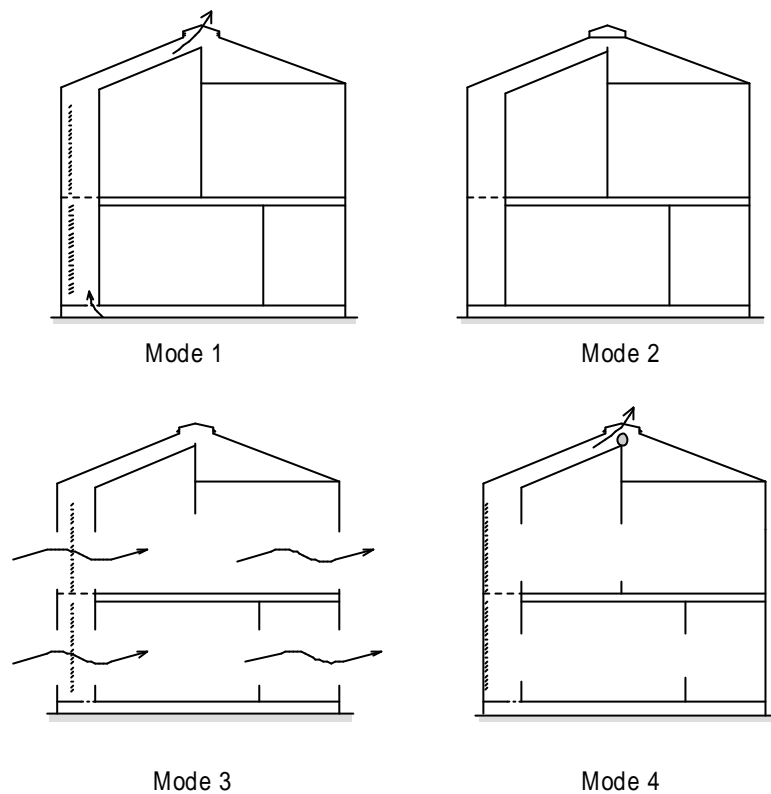


Fig. 4-3. Basic operation modes of the double skin system

This mode is suitable for summer when the sunlight and skylight is very strong during the daytime. The shadings shut down most of the solar radiation, and the air under the floor can be taken in by the stack effect, and be exhausted on the roof.

The large amount of heat is expected to be exhausted by the natural ventilation, which will lead to less cooling load.

4.2.2.2. Winter mode

Mode 2 in Fig.4-3 is called the winter mode. In this mode the ventilation openings and windows in the double skin and room are all closed, while the interior shadings are hung up during the daytime.

This mode is suitable for winter when the outside air is very cold, but the sunlight and skylight is strong. The solar radiation can be transmitted into the rooms, and the long-wave radiation can be left in the room because of the glass windows. The double skin acts as a buffer between the outside and the room.

The green house effect and heat storage by this method is expected, which will lead to less heating load.

4.2.2.3. Intermediate season mode

Mode 3 in Fig.4-3 is called the intermediate mode. In this mode the ventilation openings and windows are opened, while the interior shadings are controlled.

This mode is suitable for the time when the outside air is available for cooling or ventilation, especially during the intermediate seasons. When the sunlight and skylight is very strong, the shadings can be controlled to prevent solar radiation.

The natural ventilation for free cooling by this method is expected, when the outside air temperature is lower than the room air. And with the introduction of enough natural ventilation the occupant will feel more comfortable

4.2.2.4. Mechanical ventilation mode

Mode 4 in Fig.4-3 can be called the mechanical ventilation mode, in which the auxiliary fans on the east wall and west wall are operated.

This mode is suitable when the natural force for ventilation is not enough, especially when the wind is very small or can not easy flow into the room.

The effect of mechanical ventilation by this method is expected.

The diversity modes of double skin system are the combination of the above four mode, and the details are summed up in Fig.4-4.

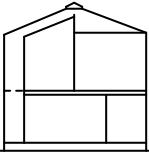
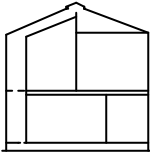
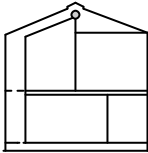
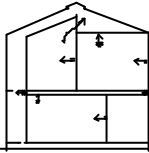
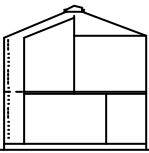
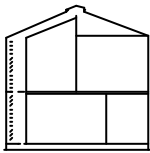
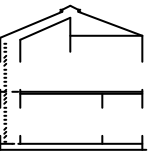
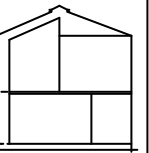
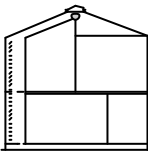
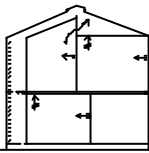
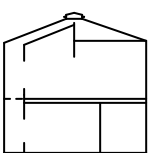
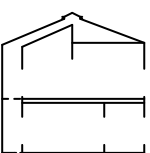
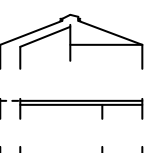
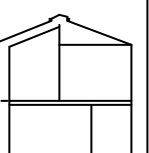
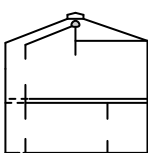
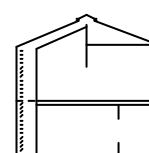
	No ventilation	Natural ventilation			Mechanical ventilation in DS	Natural ventilation in DS Mechanical ventilation in rooms
Closed type	 Mode 1	 Mode 2			 Mode 3	 Mode 4
Sunshadings	 Mode 5	 Mode 6	 Mode 7	 Mode 8	 Mode 9	 Mode 10
Partitions	 Mode 11	 Mode 12	 Mode 13	 Mode 14	 Mode 15	 Mode 16

Fig. 4-4. Diversity operation modes of the double skin system

4.3. Experiment results

The field experiments were conducted throughout the year in the experimental house in Kitakyushu in 2001. The outside conditions and the results of experiment for summer, autumn and winter are detailed in the following part according to their corresponding operation mode. The performance of the double skin system and its effect on indoor environment and energy conservation is analyzed.

4.3.1. Field experiments in summer

The field experiment in summer was conducted from Aug. 2 to Aug. 10, when it was in the peak of the summer.

4.3.1.1. Outside climate conditions

The average air temperature is 30.1°C during the experiment period, while the maximum value is 36.7°C and the minimum is 24.5°C. The average of relative humidity is about 50% in the daytime, while it is rather high at night (for about 80-90%). The peak of total solar radiation incident on surface is 3MJ/m².h (Fig.4-5). The wind speed is about 1.14m/s, with the prevailing wind direction from southwest (Fig.4-6, Fig.4-7).

The data on Aug. 5 are used to analyze the temperature distribution and effect of natural ventilation in the double skin system.

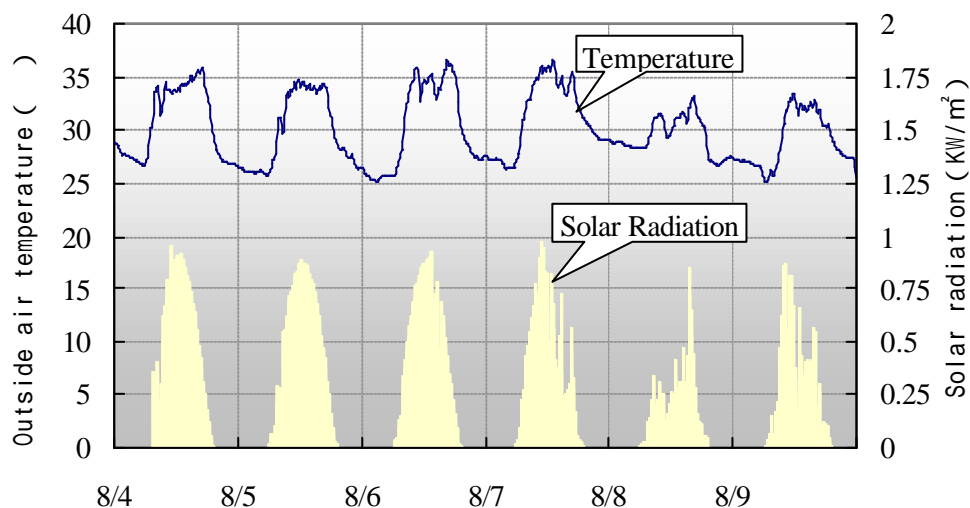


Fig. 4-5. Outside air temperature and solar radiation in the summer experiment

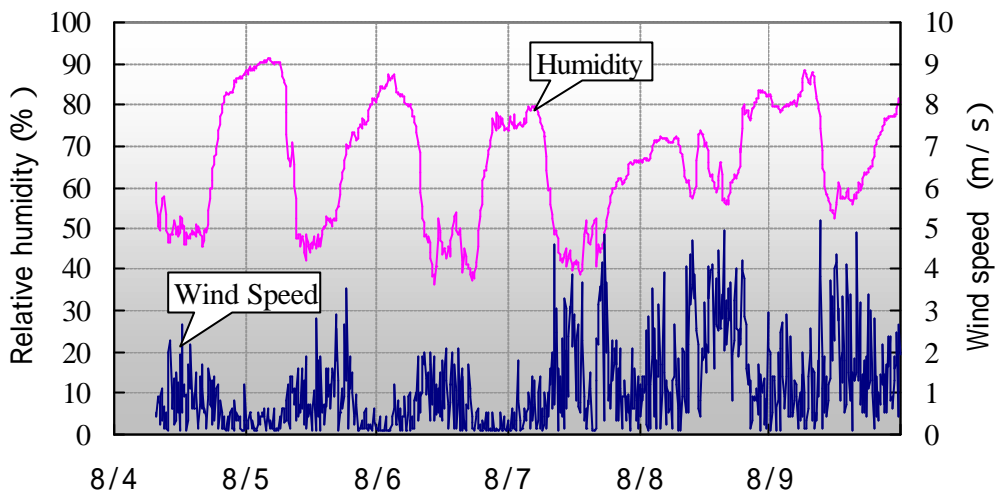


Fig. 4-6. Relative humidity of outside air and wind speed in the summer experiment

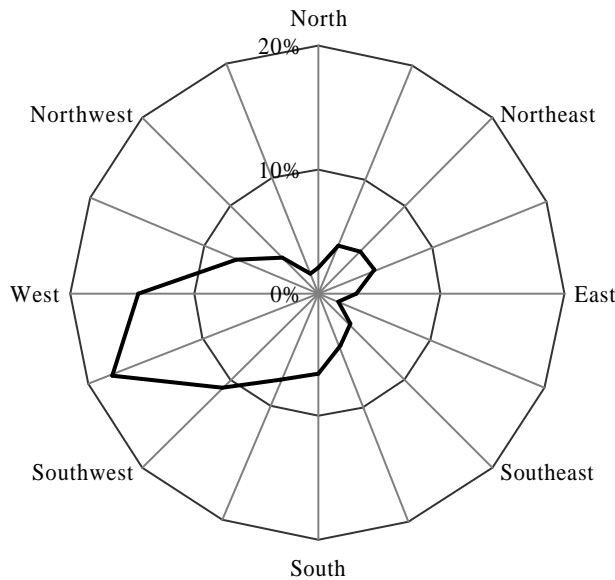


Fig. 4-7. Wind rose in the summer experiment

4.3.1.2. Temperature distribution

According to the summer mode, the variation of natural temperatures is shown in Fig.4-8. The peak temperature at the outlet reaches 42.6°C at 16:00, with the biggest temperature increase of about 12.9°C from the floor opening to the roof opening.

The natural air temperature in the living room (2F) and SOHO exceeds the outside air in the afternoon. The peak value is 37.5°C in the living room, while it is 34.4°C in the SOHO, with the biggest temperature difference of 3°C. Although the temperature increase in the double skin

is bigger than the simulation results in Chapter 3, the natural temperature in the room is very close to the simulation results.

In Fig.4-8, temperature increase in the double skin space is contributed to solar radiation, but it has a delay of 3 to 4 hours, compared with the variation of solar radiation.

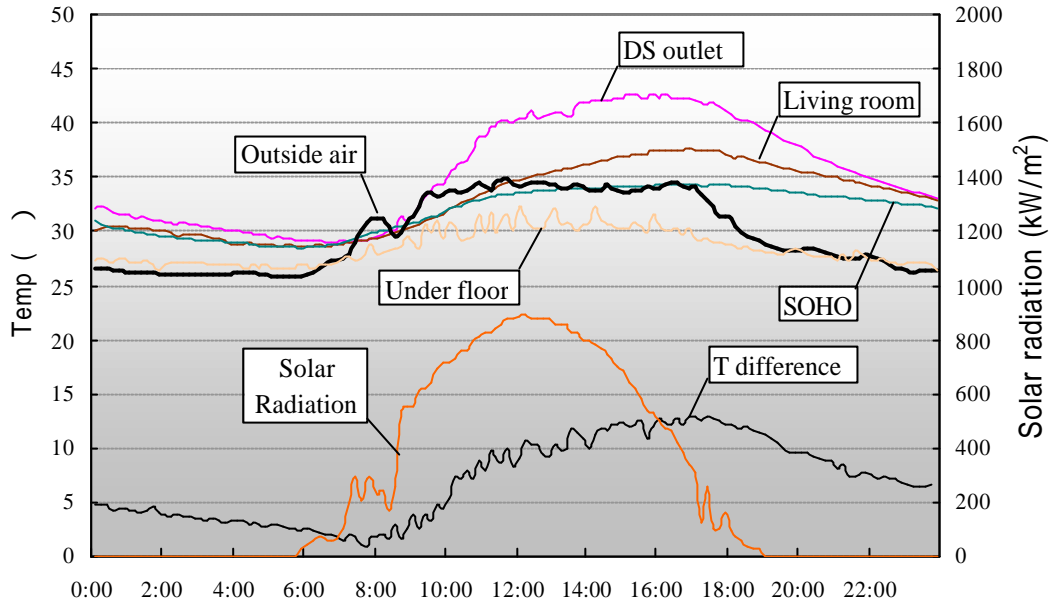


Fig. 4-8. Temperature distribution in the double skin and rooms

After 18:00 the room temperatures are still very high, while the outside air goes down to about 28°C. In this occasion, if natural ventilation or mechanical ventilation is adopted, the room will be cooled.

4.3.1.3. Airflow in the double skin space

The variation of air velocity at the inlet of the double skin is shown in Fig.4-9. The average velocity in the daytime is higher than that in the nighttime, and it reaches the maximum during the period from 11:00 to 13:00 with both natural ventilation and mechanical ventilation. It can be seen that airflow rate depends more on the temperature difference between double skin and the outside air than on the wind speed, especially in the daytime. For example, when the average temperature difference is 6.7°C from 15:00 to 16:00, the maximum air velocity is about 0.25m/s, which is corresponding to the airflow rate of 760m³/h. The experimental results are similar to the simulation results.

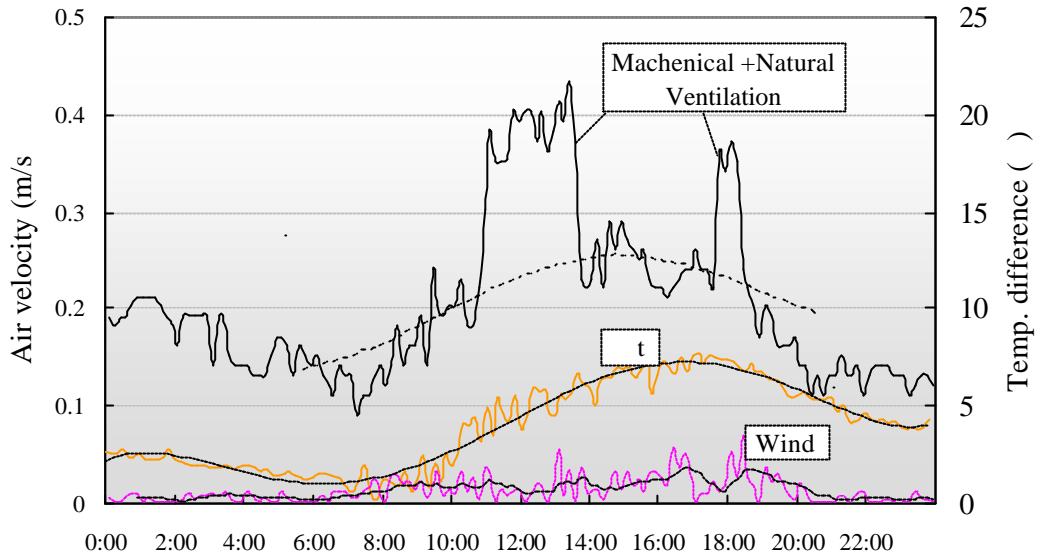


Fig. 4-9. Variation of air velocity with temperature difference between average temperature in double skin and temperature under floor

As the flow in the double skin is caused by wind and thermal forces together, the flow can be expressed by Equations (4-1)-(4-2) according to ASHRAE Fundamental Handbook 2001.

$$\dot{m}_{th} = C_D A_{eff} \sqrt{2g\Delta H_{NPL} (\bar{T}_i - T_o) / \bar{T}_i} \quad (4-1)$$

where C_D is discharge coefficient for opening, 0.65; \bar{T}_i is the average temperature in the double skin, ΔH_{NPL} is half of the height of double skin, i.e. 3.7m.

$$\dot{m}_w = C_v A_{eff} U \quad (4-2)$$

where C_v is effectiveness of opening, 0.25, U is wind speed.

The total airflow by wind and thermal forces can be expressed by Equation (4-3), according to (JBMEEA, 2000)

$$\dot{m} = \sqrt{(\dot{m}_w^2 + \dot{m}_{th}^2)} \quad (4-3)$$

Because of the mechanical ventilation during 11:40 to 12:15, and 17:40 to 18:15, the real flow rate depends on the comprehensive effect of thermal force and wind. While temperature

difference between outside and inside i.e. Δt is small, the measured flow rate is larger than that calculated by Equation (4-1). When Δt is larger than 5°C , the natural force becomes the main part, and the flow rate seems to be independent on wind force (Fig.4-10). This shows that the wind effect will be more important when the thermal effect is small. It confirms that the temperature difference is the driven force of the natural ventilation in the double skin. The total airflow can be enforced if the auxiliary fan is put into operation, as the airflow is larger than calculation during the fan operation period.

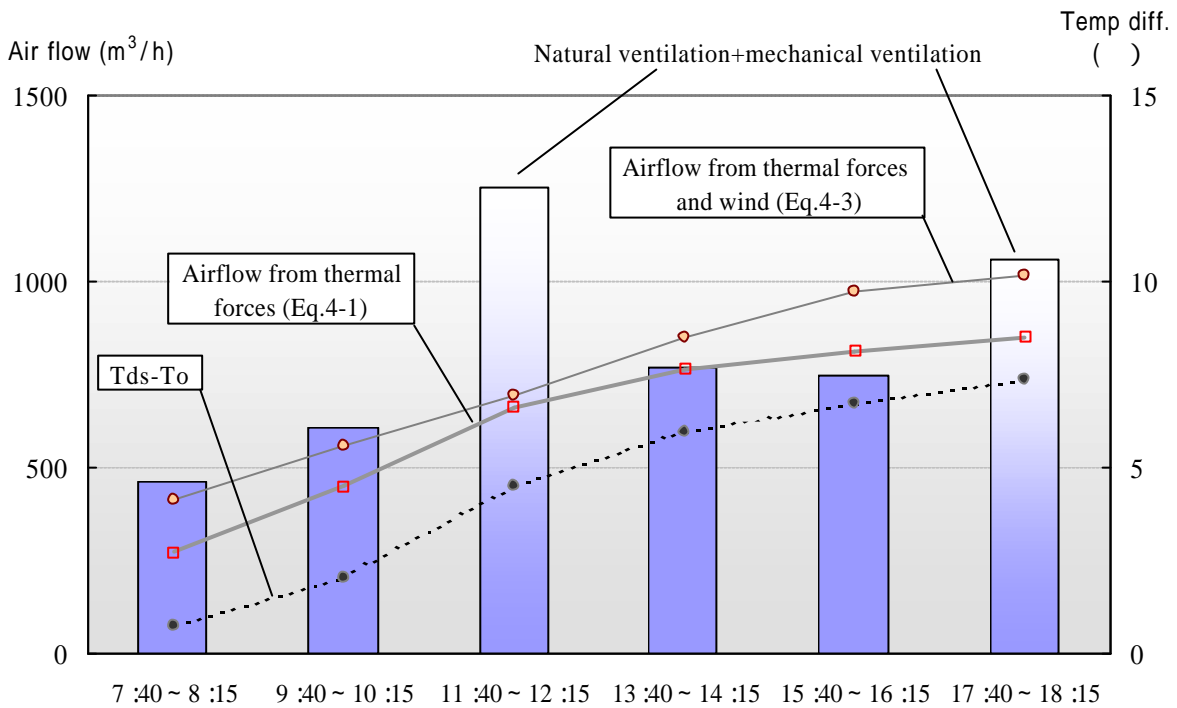


Fig. 4-10. Airflow by natural ventilation and mechanical ventilation, and the temperature difference between double skin and under floor (on Aug. 5)

4.3.1.4. Energy flow

According to the temperature distribution and air velocity at the opening in the double skin, the details of energy flow in the double skin during 9:00 to 15:00 are calculated in Table 4-3.

In Mode 1, the exhaust heat ratio from natural ventilation is about 10-15% of the solar radiation in the south direction (Fig.4-11), which is similar to the simulation result. And the exhaust ratio increases to about 30% during the period of 11:00 to 14:00 when fans are put into operation. This shows that the hybrid ventilation leads to more heat exhaust and more energy saving.

4.3.1.5. Energy conservation

According to the passive method and openings of the double skin system, the energy consumption in the experimental house is tested, and the cases and conditions are set in Table 4-4. As the outdoor climate on Aug. 2, is quite similar to that on Aug. 6 and 7, the cooling load consumption is compared in these 3 days with different modes. The exterior windows are opened in Case A, while they are closed in Case B, and floor openings and roof opening are opened for natural ventilation. Case C is assumed to be the conventional case, as the openings are closed. The cooling load is calculated by Equation (4-4)

$$Q_{cl} = \rho C_p \dot{m} (t_{ra} - t_{sa}) \quad (4-4)$$

where t_{ra} is temperature of return air; t_{sa} is temperature of supply air; C_p is specific heat of air; ρ is air density; \dot{m} is airflow rate. Here the temperature difference between return and exhaust is approximately to be zero.

Table 4-3. Energy flow in double skin in Mode 1

Time	9:00-10:00	10:00-11:00	11:00-12:00	12:00-13:00	13:00-14:00	14:00-15:00
Temperature (°C)						
DS 1F	31.21	32.36	32.48	32.68	32.94	33.59
DS2F	33.81	36.67	37.63	37.79	37.71	38.12
SOHO	31.26	32.40	33.18	33.60	33.85	34.00
Living room	31.11	32.64	34.12	35.14	35.85	36.59
DS5.6m (outlet)	34.92	38.37	39.67	39.70	39.28	39.25
DS_floor (inlet)	29.72	30.17	30.72	31.00	30.80	30.92
Air flow rate						
Opening Vel. (m/s)	0.20	0.22	0.37	0.39	0.34	0.26
Flow rate(m ³ /s)	0.11	0.12	0.21	0.22	0.19	0.15
Energy (W)						
Exhaust heat	1223.93	2180.57	4031.45	4077.97	3526.25	2633.10
Total heat gain*	9810.90	11263.53	9934.40	8280.04	8627.05	10471.28
Exhaust heat ratio						
Exhaust ratio	0.07	0.11	0.23	0.28	0.23	0.14

Note: * refers to solar heat from the south glass with the shading factor is 0.52.

Ratio of heat exhaust

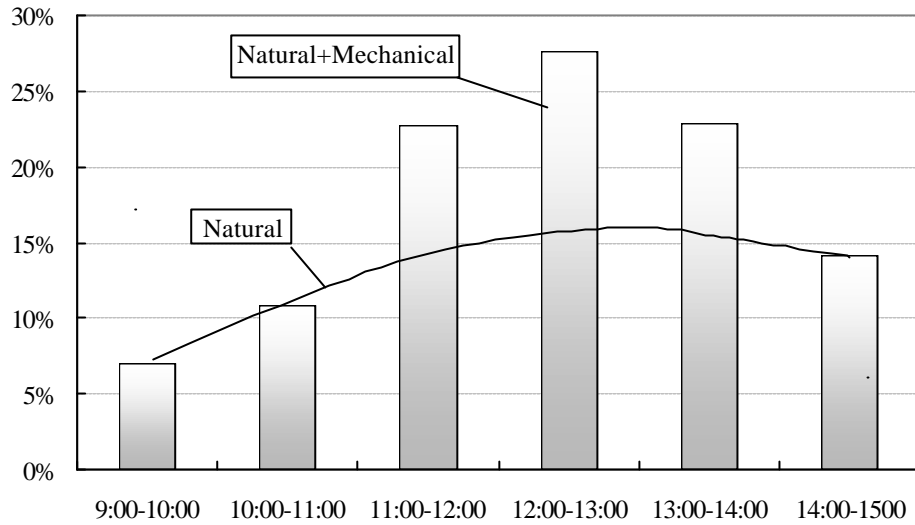


Fig. 4-11. Ratio of heat exhaust by ventilation in the double skin

Table 4-4. Cases setting for energy consumption with/without double skin

Double skin space	CASE A	CASE B	CASE C	
DATE	8/6	8/2	8/7	
Outdoor temp ()	Avg.	33.23	32.58	33.55
	Max	36.67	35.75	36.58
Solar (kW/m ²)	Avg.	0.47	0.53	0.23
	Max	0.93	0.93	0.98
Air conditioning time setting air temperature	SOHO	9:00 ~ 18:00/26		
	Living	18:00 ~ 22:00/28	-	18:00 ~ 22:00/28

The comparison of cooling load is shown in Fig.4-12 and Fig.4-13. As to the cooling load in the 1F SOHO during the daytime, Case A is the smallest about 48.5W/m², then Case B is 51.4W/m², and the largest is Case C of 60.4W/m². Compared with Case C, Case A has an

average cut of 20%, and Case B is 15%. This confirms that the double skin system can cut down about 15-20% cooling load for the 1F room.

As to the cooling load in the 2F Living room during 18:00 to 22:00, Case A is about 48.2W/m^2 , while Case C is about 52.9W/m^2 . And Case A has a cut down of about 8%. If it is in the daytime, the ratio of energy saving may increase with the larger natural ventilation.

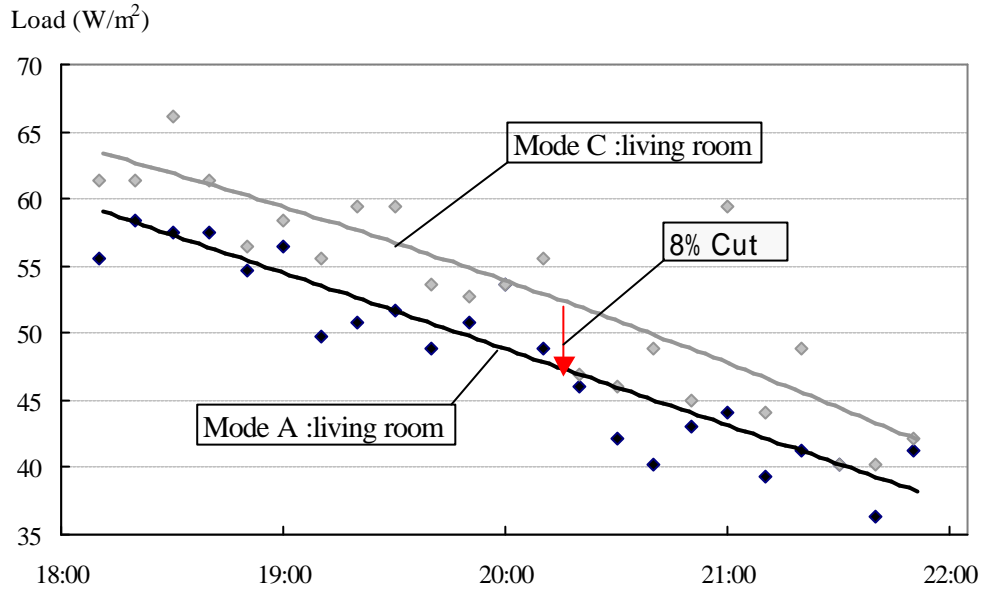


Fig. 4-12. Energy conservation in 1F SOHO Room

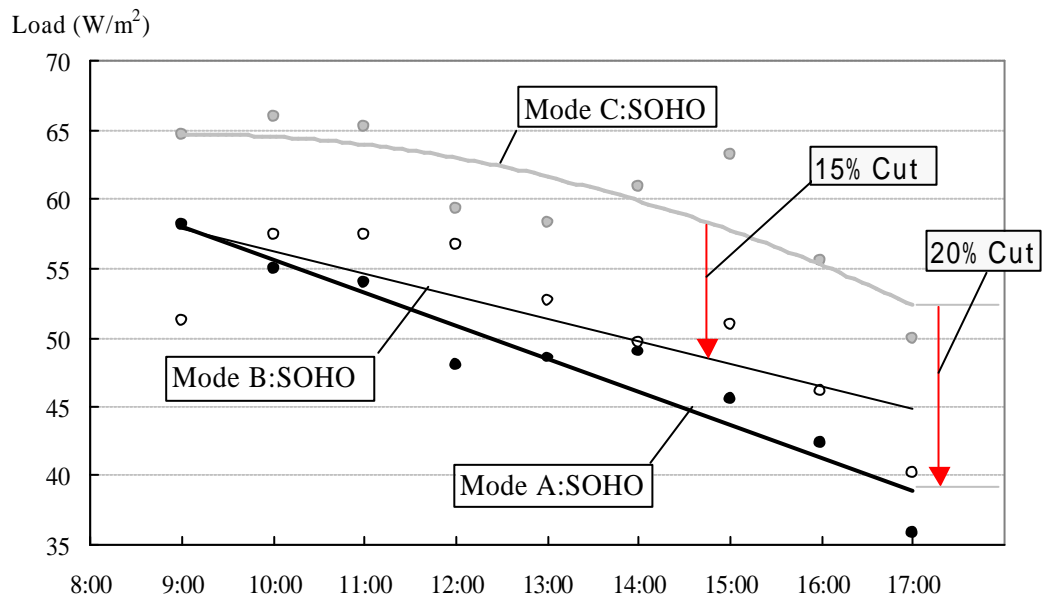


Fig. 4-13. Energy conservation in 2F Living Room

4.3.2. Field experiments in autumn

The field experiment of double skin system in the autumn was conducted from Oct. 10 to Nov. 15, both of the changes from summer to autumn and autumn to winter are observed. The air temperature in the first week was warmer, closer to the conditions in summer, while it was colder in the later, closer to the conditions in winter. Therefore the experiment results are detailed into two parts, one is from Oct. 10 to 15, and the other is from Nov.6 to 22, which pays more attention on the subjective assessment.

4.3.2.1. Climate conditions from Oct. 10 to 15

The average air temperature is 19.8°C during the experiment period, while the maximum value is 25.3°C, and the minimum is 13.5°C. But the peak of total solar radiation is still very intensive, about 0.9kW/m² (Fig.4-14). The average relative humidity remains high at night, but it is about 45% in the daytime. And the average wind speed is a little bigger (about 2m/s (Fig.4-15), with the prevailing wind in the west and east directions (Fig.4-16).

4.3.2.2. Temperature distribution with different modes

Although the solar radiation has little variation in this period, according to different operation modes, the temperature distribution is different. The comparison of temperature distribution for three modes is shown in Fig.4-17, among which one is a closed type, one is natural ventilation + shading, and the other has further mechanical ventilation in the daytime.

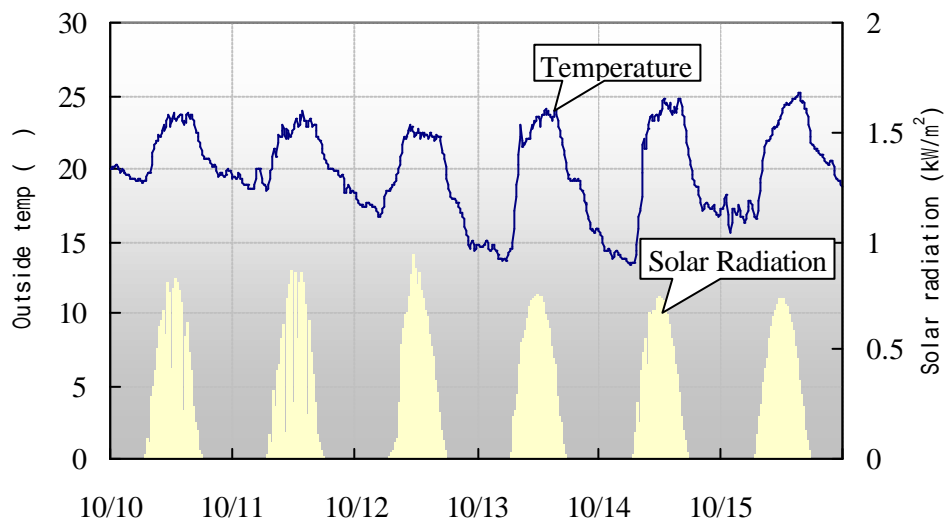


Fig. 4-14. Outside air temperature and solar radiation from Oct.10 to 15 in autumn

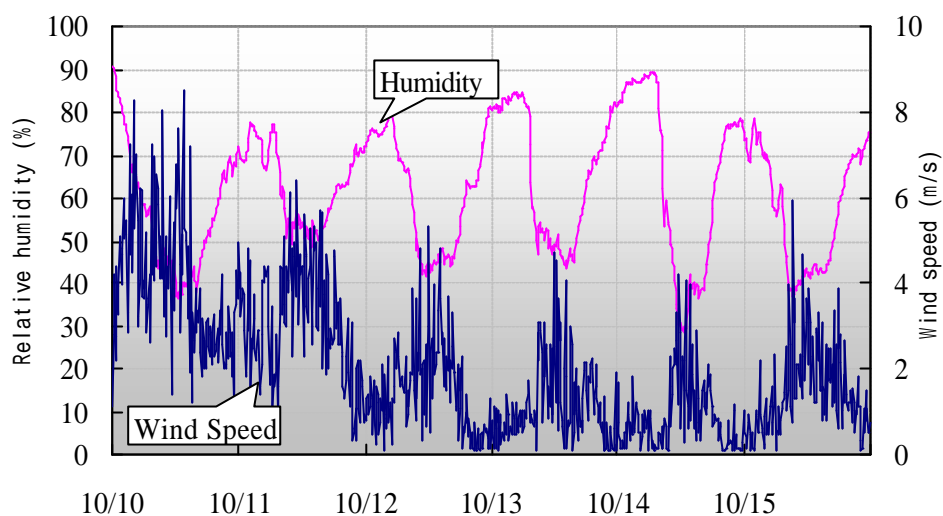


Fig. 4-15. Outside air humidity and wind speed from Oct.10 to 15 in autumn

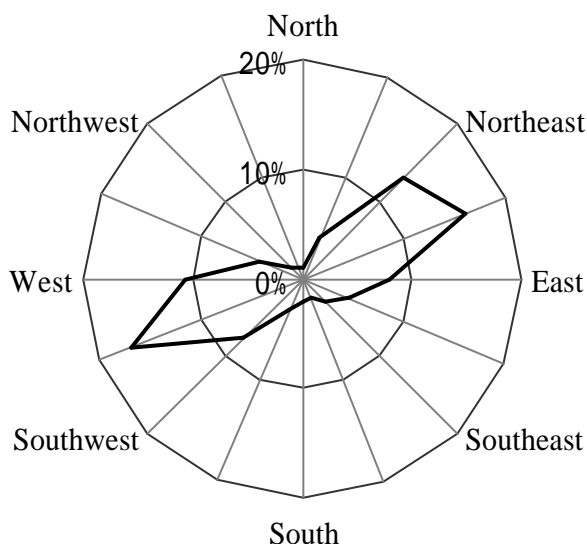


Fig. 4-16. Wind rose from Oct.10 to 15 in autumn

The outside temperatures vary in the same range from Oct. 14, 15 and 19, as well as the solar radiation. According to the different operation modes, the temperature in the living room has different variations, which shows the effect of different operation methods. The peak value reaches 37°C, which is about 12°C higher than the outside on Oct. 14 with the closed type (Mode 2). When natural ventilation and sun shading is adopted (Mode 3), it drops to 28°C, which is only 3°C higher than the outside air. Furthermore, when mechanical ventilation is put into operation on Oct.19 (Mode 3+4) with the air change rate of 2 per hour, the room air can be decreased to 25°C, which is very close to the outside air. It is confirmed that during the intermediate seasons, hybrid ventilation will be available for environmental improvement.

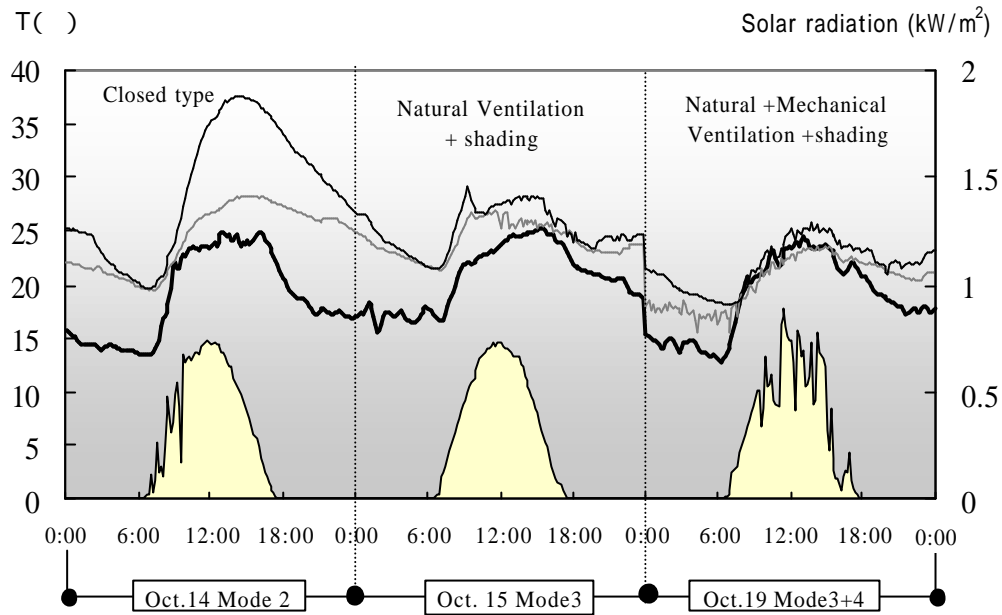


Fig. 4-17. Comparison of temperature distribution with different operation modes in the double skin in the middle of October 2001

4.3.2.3. Indoor thermal comfort

PMV in the living room is tested in November. Different modes are set on Nov. 8 and Nov. 9, although they have similar climate conditions shown in Fig.4-18. The closed mode is set for Nov. 8, and the mechanical ventilation mode is for Nov.9 with air change rate of 5 per hour. The largest temperature difference in these two days reaches 6.3°C. If the activity is set to be 1.0met, and clothing 1 clo, PMV can drop from 1.8 to 0.8 at 13:00 (Fig.4-19). This means that the indoor environment can be improved greatly only by ventilation.

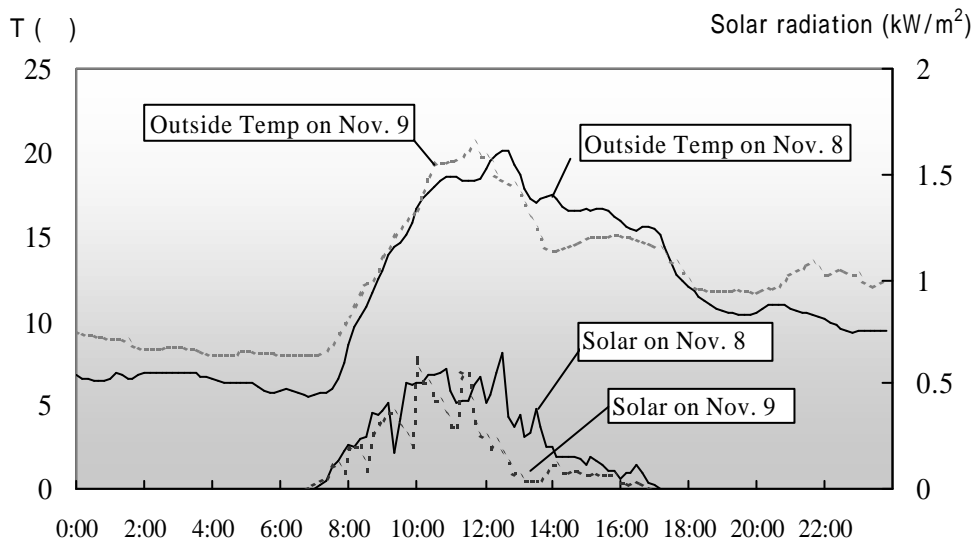


Fig. 4-18. Climate conditions on Nov. 8 (closed mode) and Nov.9 (mechanical ventilation mode)

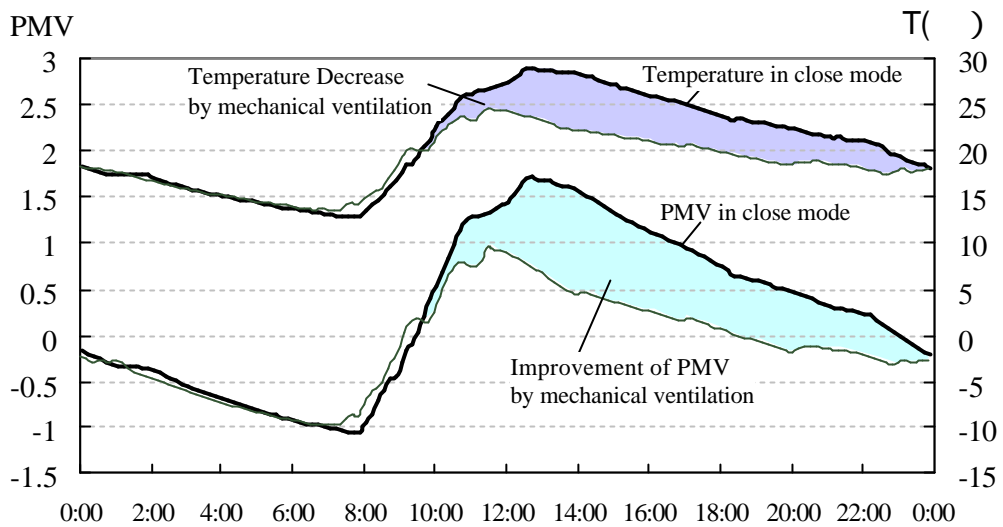


Fig. 4-19. PMV improvement by ventilation

On the contrary, when the average temperature of outside air goes down below 10°C, the indoor temperature can be increased by the closed mode, thus to realize thermal comfort without extra heating.

It can be concluded that the indoor environment can be improved by ventilation or by controlling the windows, and less energy will be consumed during the intermediate seasons.

4.3.2.4. Indoor air quality

Volatile organic compounds (VOC) in the indoor atmosphere were tested on Sept. 16, 2001 in the natural ventilation mode when all the sliding door, interior windows, and openings on the floor of double skin are opened. The sketch of the testing is illustrated in Fig.4-20.

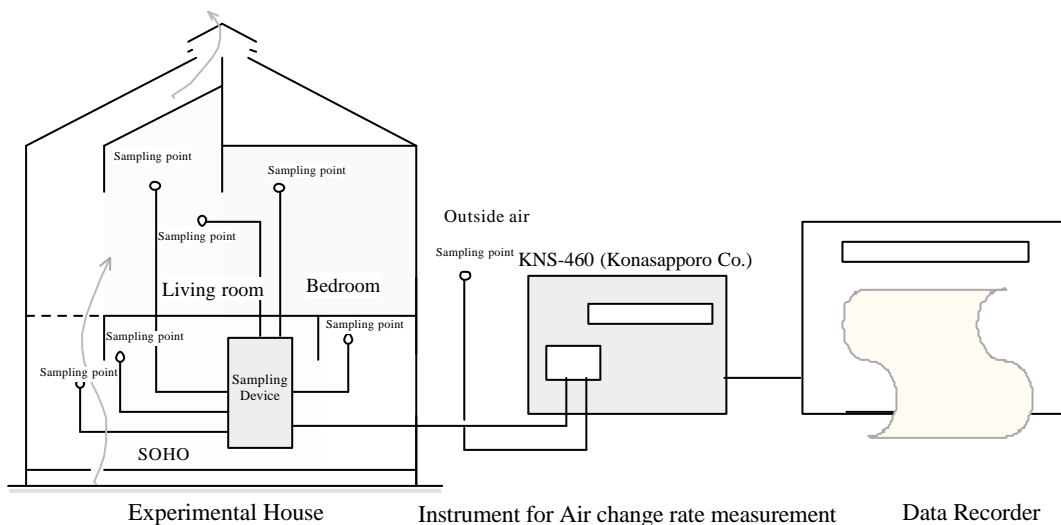


Fig. 4-20. Sketch of the measurement of VOC

- Air change rate by natural ventilation

Here the tracer gas decay method is used to test the air change rate by natural ventilation, and the tracer gas is CO₂. The air change rate can be calculated by Equation (4-5)

$$N = -2.303(\log_{10} C_1 - \log_{10} C_2) / t \quad (4-5)$$

where N is air change rate (h⁻¹); and t is sampling period of time (h); C_1 is the CO₂ concentration difference between room air and outside air at the starting time; and C_2 is the concentration difference at the ending time.

According to the field measurement, air change rate by natural ventilation reaches 1.46 per hour. The details are shown in Table 4-5.

Table 4-5. Testing of air change rate by natural ventilation

	Time	Sampling period (hour)	CO ₂ concentration (ppm)		
			Outside	Indoor	difference
Starting	15:06		500	3750	3250
Ending	16:00	54/60=0.9	600	1470	870
Air change rate by natural ventilation per hour		$N = -2.303(\log_{10} 870 - \log_{10} 3250) / 0.9 = 1.46$			

Note: The test is conducted by YKK AP Co.

- VOC emissions

The tested indoor VOC emissions are shown in Table 4-6, as well as the recommended values of Ministry of Health, Japan. It can be seen that the concentrations of contaminants are very small in the experiment house, which are much lower than the limit values of the state standard. This means that the indoor air equality is good and it has little impact on occupancy health.

The comparison of VOC emissions between September and March when it was just finished reconstruction six month ago is shown in Table 4-7. Although the VOC concentrations were quite high when the experimental house was just reconstructed, they become small after being used. Half a year later, the house can well meet the healthy requirements.

This shows that natural ventilation has exhausted the VOC emissions effectively in a quite short period.

Table 4-6. Pollutant emissions tested in the experimental house

	Outside	SOHO	Living room	Recommended*
Temperature (°C)	26.3	29.4	33.7	-
RH (%)	49.3	48.9	41	-
Emissions				
Formaldehyde (ppm)	0.002	0.010*	0.014*	0.08
Toluene ($\mu\text{g}/\text{m}^3$)	0.1	5.5	10.4	260
Xylene ($\mu\text{g}/\text{m}^3$)	0.5	2.5	4.5	-
o-xylene ($\mu\text{g}/\text{m}^3$)	0.2	1.2	1.9	870
m,p-xylene ($\mu\text{g}/\text{m}^3$)	0.3	1.3	2.6	870
Ethylbenzene ($\mu\text{g}/\text{m}^3$)	0.2	1.5	3.4	3800
Styrene ($\mu\text{g}/\text{m}^3$)	0.3	3.3	4.9	220
P-dichlorobenzene ($\mu\text{g}/\text{m}^3$)	0.7	0.6	0.7	240
DBP ($\mu\text{g}/\text{m}^3$)	0.1	0.1	0.0	220

Table 4-7. Comparison of VOC emissions between Sept. and Mar. 2001

	SOHO ($\mu\text{g}/\text{m}^3$)		Living room ($\mu\text{g}/\text{m}^3$)	
	March	September	March	September
Benzene	1.7	-	1.3	-
Toluene	821.7	5.5	1183.3	10.4
Xylene	54.3	2.5	68.4	4.5
Ethylbenzene	137.1	1.5	183.6	3.4
Styrene	-	3.3	-	4.9
P-dichlorobenzene	-	0.6	-	0.7
DBP	-	0.1	-	0

4.3.3. Field experiments in winter

The field experiment in the winter was conducted from Feb.2 to Feb. 21 in 2002, and outside temperature was rather low, especially in the nighttime.

The average outside air temperature is 7.7°C from Feb. 3 to Feb. 10, and the minimum value is -0.23°C. The peak solar radiation is 0.76W/m², which is similar to those in other seasons (Fig.4-21). The average relative humidity is 55%, while the lowest is only 16% in the daytime. And the average wind speed is 1.4m/s, with the maximum of 6.4m/s (Fig.4-22). In winter the prevailing winds comes in the southwest direction (Fig.4-23).

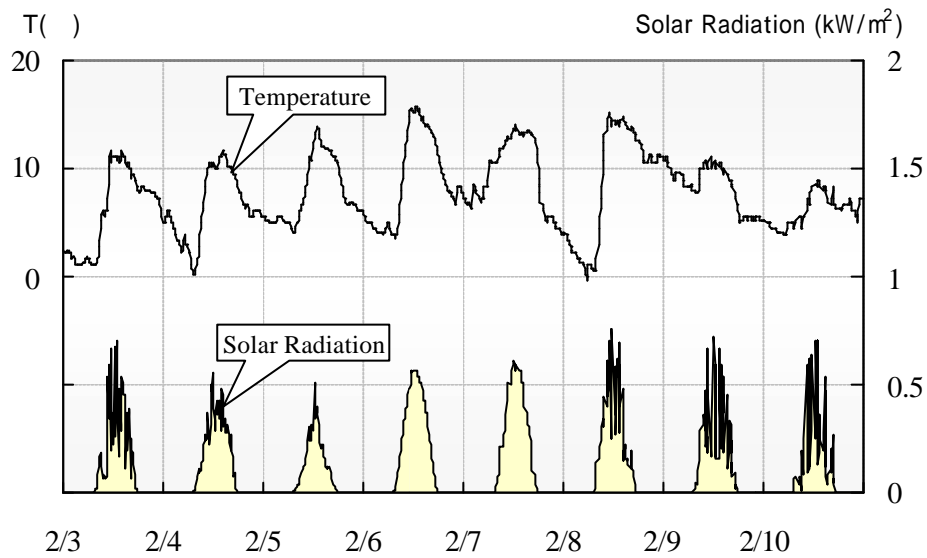


Fig. 4-21. Outside air temperature and solar radiation in winter

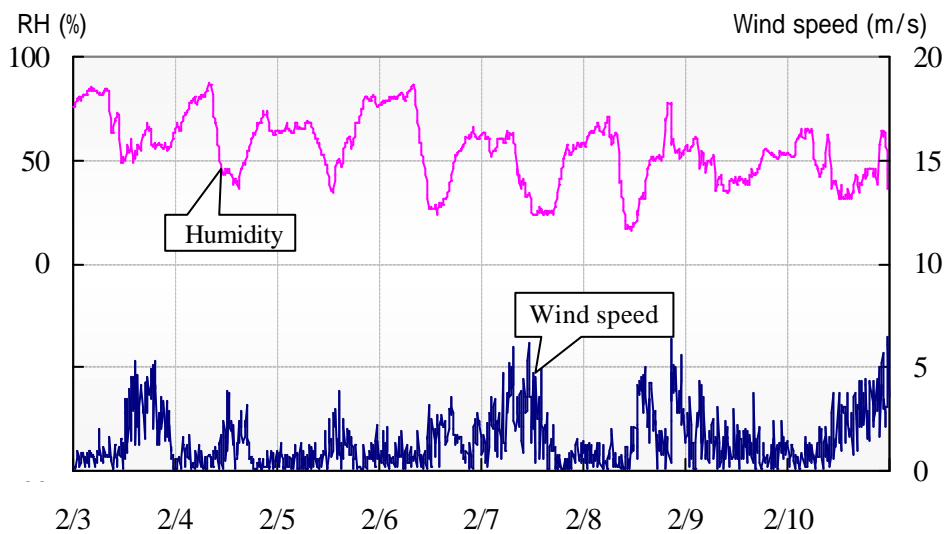


Fig. 4-22. Outside air humidity and wind speed in winter

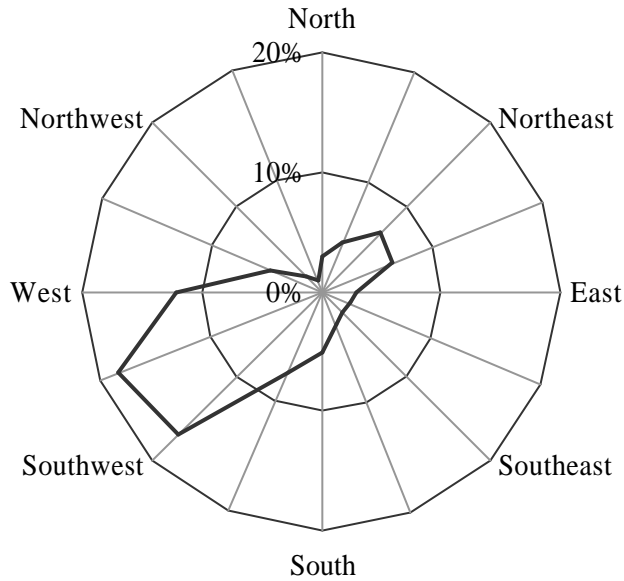


Fig. 4-23. Wind rose in winter (Feb.3 to Feb.10)

4.3.3.1. Temperature distribution by Mode 2

Because the outside air is rather cold, the closed mode (Mode 2) is often adopted in winter. Fig. 4-24 shows the temperature distributions in the experiment house on Feb. 6 and 7, when the solar radiation is still rather high with the peak of 0.57kW/m^2 .

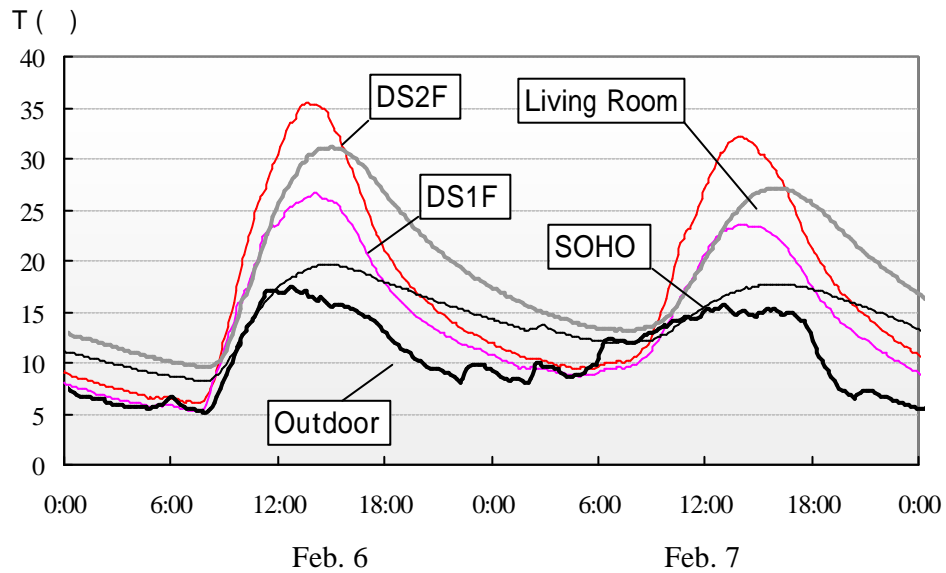


Fig. 4-24. Temperature distribution on Feb. 6 and 7 by Mode 2

Although the outside air is only 5°C during the nighttime, the peak reaches 35°C on the second floor of double skin, which is about 20°C higher than the outside air. The air in Living room (2F) also reaches nearly 30°C during 13:00 to 15:00, while it reaches nearly 20°C in

SOHO (1F). As the temperature is a little lower in the next day, the biggest temperature difference between double skin and outside air still reaches 18°C, which shows that the effect of solar radiation absorption is very significant. The other reason lies in that the equivalent leakage area is only 3.65cm²/m², which is smaller than the requirement of airtight building in Japan, i.e. 5 cm²/m² at the pressure of 9.8Pa (Committee of Speciation on New Standard for Residential Houses, 1998), and this will lead to less heat loss from the exterior envelope.

4.3.3.2. Energy conservation for heating

The heat balance of the room can be simplified as Equation (4-6):

$$Q_{heat} + Q_{gain} - W(t_{rm} - t_0) = 0 \quad (4-6)$$

where Q_{heat} is heating load from air conditioning; Q_{gain} is heat gain from solar radiation and others; t_{rm} is room air temperature; t_0 is outdoor air temperature, and W is coefficient of heat loss and according to AIJ (1980), it can be expressed by Equation (4-7):

$$W = \sum_{i=1}^N S_i K_i + rC_p \dot{m} \quad (4-7)$$

where the first item stands for heat resistance of the envelope, and the second item refers to airflow from natural ventilation. Assuming the heat loss coefficients of the rooms with and without the double skin are the same.

According to the measured natural air temperature t_{na} , i.e. when Q_{heat} is zero, according to Equation (4-6), the heat gain in the room with double skin can be expressed by Equation (4-8):

$$Q_{gain,ds} = W(t_{na} - t_0) \quad (4-8)$$

If the heat gain in room without double skin has a relationship that $Q_{gain} = n\% Q_{gain,ds}$, therefore the ratio of heating load in room with and without double skin can be expressed by Equation (4-9):

$$\frac{Q_{heat,ds}}{Q_{heat}} = \frac{W(t_{rm} - t_0) - Q_{gain,ds}}{W(t_{rm} - t_0) - Q_{gain}} = \frac{W(t_{rm} - t_{na})}{W(t_{rm} - t_0) - W(t_{na} - t_0)n\%} = \frac{t_{rm} - t_{na}}{t_{rm} - t_0 - (t_{na} - t_0)n\%} \quad (4-9)$$

Therefore the energy conservation for heating in SOHO (1F) and Living room (2F) can be calculated by Equation (4-9). Here the heat gain in rooms without double skin is set to be 50% of that with double skin, and the air conditioning temperature is set to be 22°C. The comparison results are shown in Fig.4-25 and Fig.4-26.

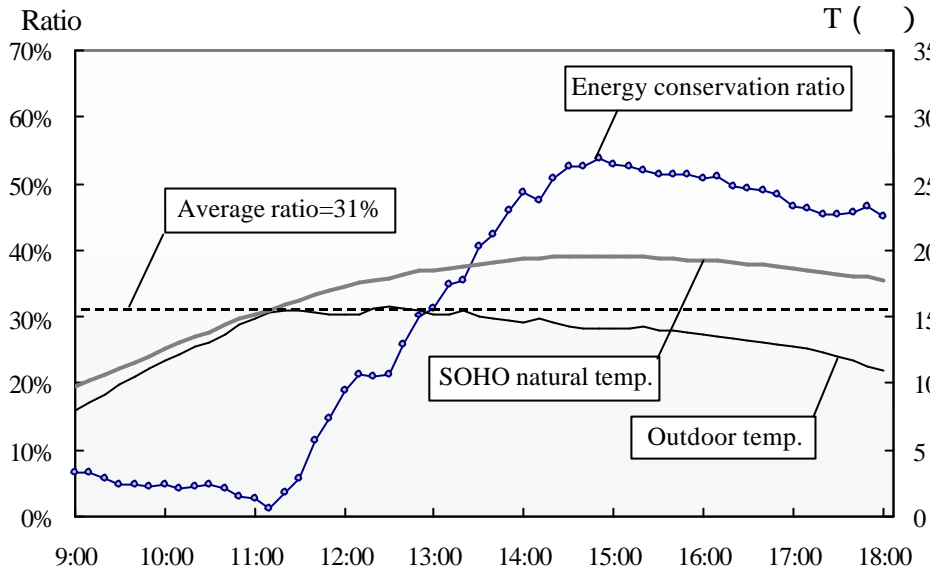


Fig. 4-25. The ratio of Energy conservation for heating in 1F SOHO room in the daytime

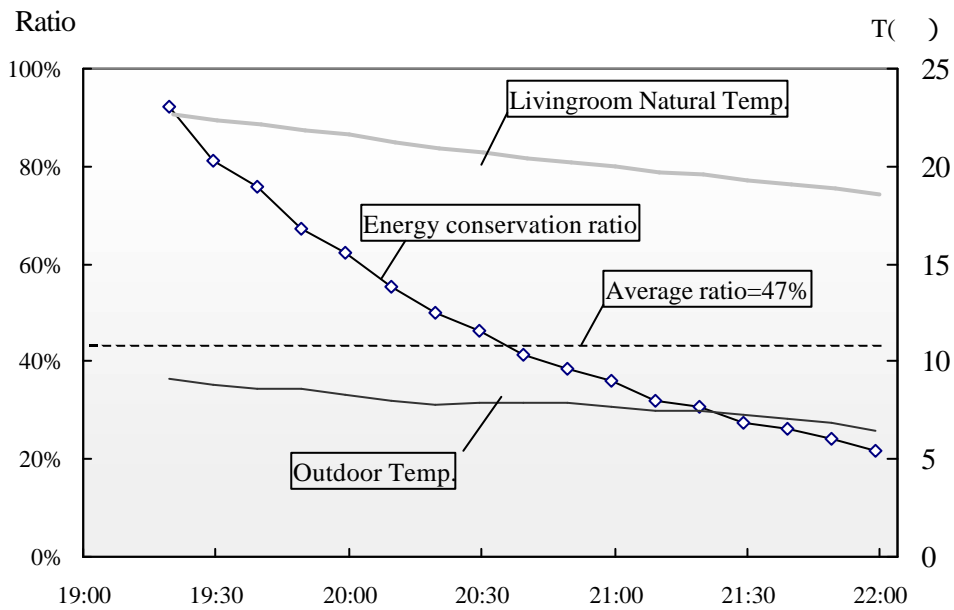


Fig. 4-26. The ratio of energy conservation for heating in 2F Living room in the evening

Compared with the conventional residential house, the SOHO room has an average cut of 31% from 9:00 to 18:00, while the Living room has a cut of about 47% during evening. As is shown in Fig.4-24, the natural temperature in the living room is over 20°C in the afternoon when it is cloudy, which means heating is not necessary. According to the measured data in Dec. 2001, and Feb. 2002, the number of hours with temperature over 20°C accounts for 29.3% of the total hours from 9:00 to 18:00 (Fig.4-27).

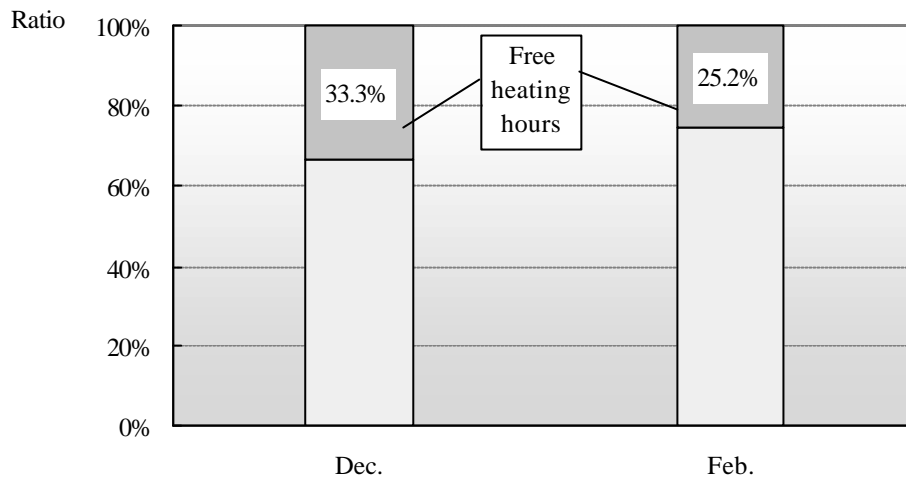


Fig. 4-27. Free heating hours in 2F Living room from 9:00 to 18:00 in winter

4.3.3.3. Thermal capacity

As is shown in Fig.4-24, all the temperatures go down gradually in the afternoon. If 14:00 on Feb. 6 is set to be the zero point, and the variation of temperatures in the later 10 hours can be illustrated in Fig.4-28 (a). According to the temperature variation calculated, the air in the double skin has the biggest decreasing speed, about 1.6 to 2.4°C in an hour, then the living room comes to the next of about 1.4°C per hour, and the smallest is in SOHO of 0.5°C per hour (Fig.4-28b). Because SOHO has more furniture and books than the other places, its thermal capacity is the largest, while the living room has less, and there is almost nothing in the double skin space. This shows that more furniture, bookcases or other things with large thermal capacity will be helpful for thermal storage, and this will leave more energy saving.

According to the experiment, if the interior curtains in the living room and SOHO are closed down after 16:00, the speed of temperature decrease in the living room can be slowed down. This shows another way for energy saving in the double skin space, the heat loss can also be cut down with the interior curtains.

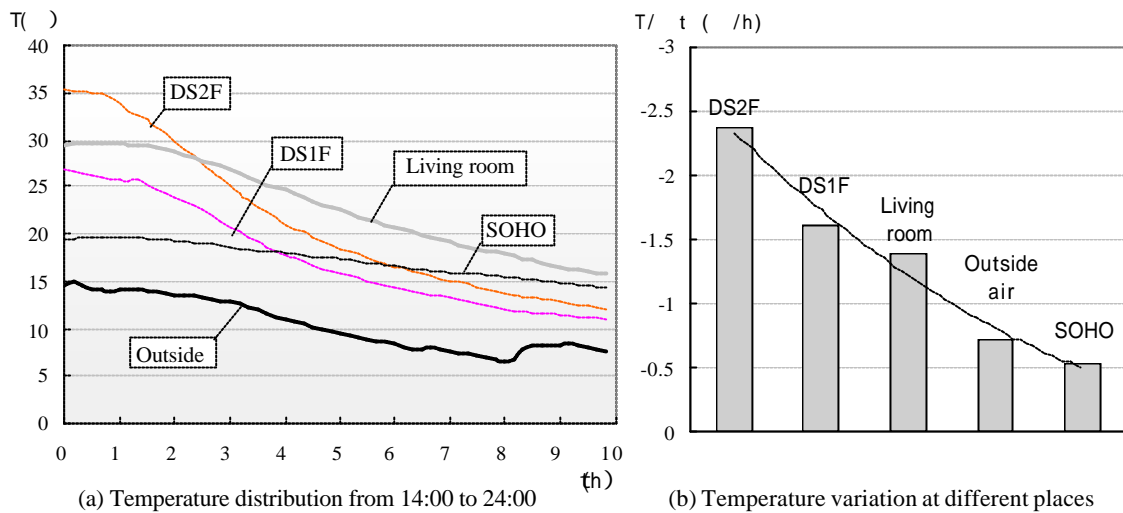


Fig. 4-28. Temperature variation at different places in an hour

4.4. Subjective experiments

4.4.1. Outline of subjective experiment

According to the above field experiments, thermal comfort can be realized in the rooms, as well as the occupancy health and energy conservation by controlling the openings of double skin space, sunshades according to the different climate conditions. As to the occupants, what would they assess the indoor environment with controlling of the double skin system? Therefore the subjective experiments are conducted in the autumn.

In this subjective experiment, subjects stay 24 hours (from 14:00 to the next 14:00) in the later autumn. A subjective questionnaire is carried out, when the subjects adjust the double skin systems, such as windows, shading and ventilation to realize thermal comfort according to their own wills. All together there are 43 subjects, and most of them are college students in the age of twenty to thirty.

4.4.2. Results of subjective experiment

4.4.2.1. Thermal comfort

The indoor temperature and climate conditions from Nov.6 to 22 are shown in Fig.4-29.

According to the adjustment of the subjects, the indoor temperatures are controlled. For example, the maximum of temperature in the living room reaches near 30°C on Nov. 8 without any controlling, but it is decreased 2-5°C after controlling the sunshades and ventilation openings in the double skin space in the other experiment time.

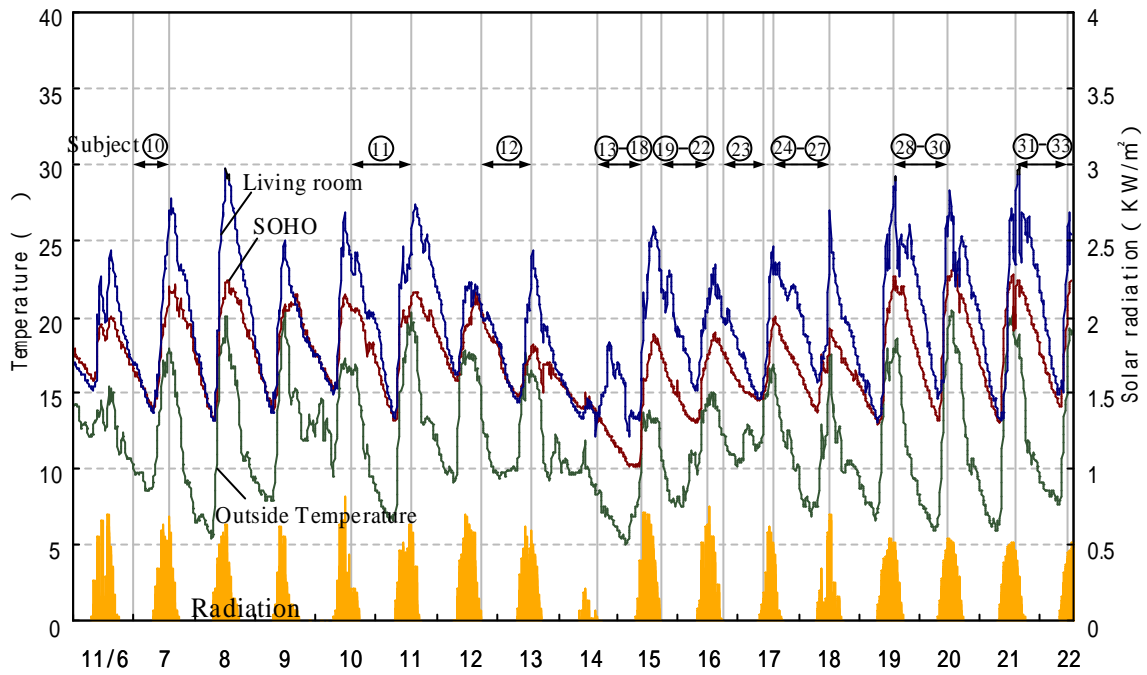


Fig. 4-29. Temperature distribution and climate conditions in the subjective experiment in November 6 to 22

From the PMV distribution in the living room, it can also be seen that the indoor thermal comfort can be improved by active controlling (Fig.4-30). It should be noted that it becomes cold at night without heating.

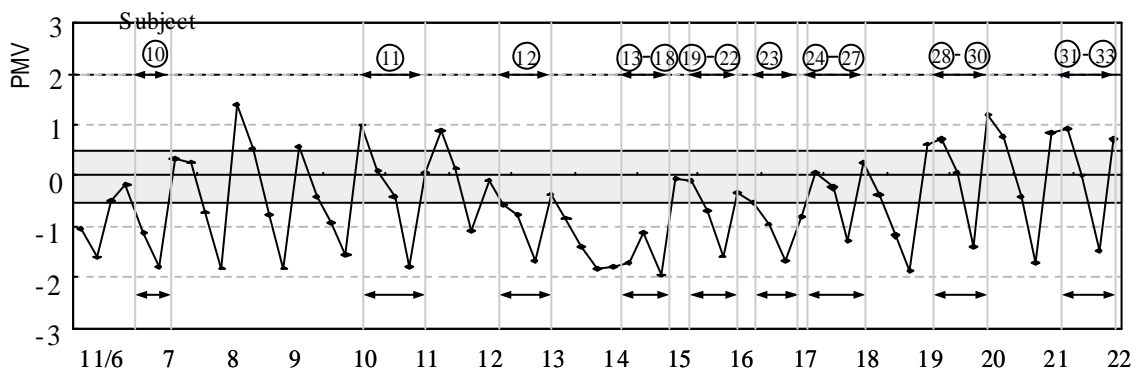


Fig. 4-30. PMV in the middle of Living room in the subjective experiment (Nov. 6 to 22)

The subjective experiment shows that with the active controlling over the double skin system, the occupants can realize thermal comfort inside the room according to their own requirements. Their assessment of controlling the double skin system is explained in the

following part.

4.4.2.2. Assessment of using double skin system

The subjective assessment of using double skin system is analyzed according to the results of vote shown in Fig.4-31. Although most of them are very young (in the early 20s), few feels it is inconvenient to control the shadings, windows or opening to achieve thermal comfort by hand.

About 48% think automatic windows are not necessary in residential houses, and they can open the windows when they needs. While 30% think automatic openings are not necessary. But 44% think automatic sun shadings are necessary, because the window ratio in the living room and SOHO is very large above 90%. In general, among the 43 subjects, 64% think the double skin system has good effect on thermal comfort and energy conservation by active ventilation and passive methods, and about 56% have new understanding for environmental control by using this system.

From the above analysis, it can be seen that most people have good assessment on environmental control. Corresponding to the new lifestyle and own requirement, people want to control the indoor environment freely. At the same time, they pay much attention on energy conservation. It shows that the occupants would be willing to use the passive systems (such as the double skin) to control the indoor environment by themselves, not by those uncontrollable air conditioners. The passive systems show good promise in future.

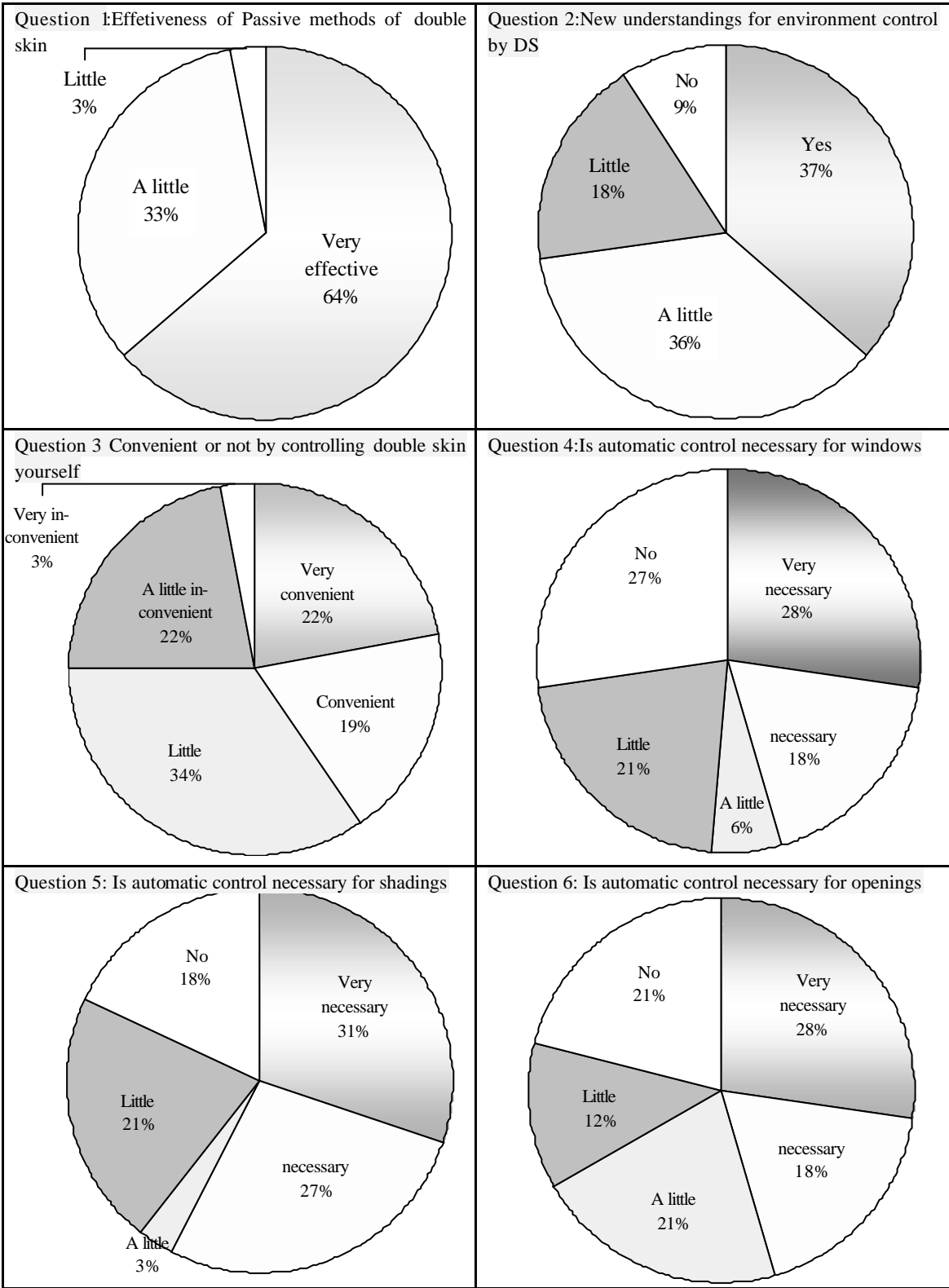


Fig. 4-31. Results of subjective vote on the controlling in the double skin

4.5. Summary and Conclusion

According to the field experiment and subjective experiment in 2001, which has good accordance with the simulation results in Chapter 3, the effectiveness of double skin system in residential house is further confirmed.

During the summer when sunlight is very strong, Mode 1, i.e. natural ventilation + sun shading is recommended; while the closed mode is not recommended. According to the temperature difference in the vertical direction, nearly 10% of the total solar radiation in the south direction can be exhausted effectively with the buoyant force. Therefore it will lead to a cut of about 15-20% in cooling load in the 1F SOHO room in the daytime, and about 8% in the 2F Living room during the nighttime.

During the autumn when sunlight is very strong, the mode of natural ventilation + sun shading is recommended, sometimes the sun shading is also needed for overheating. By opening the windows the thermal comfort will be greatly improved when the outside air is available for free cooling. On the other hand, when it turns to be cold, the completely closed mode is recommended, as the indoor temperature can be increased 5-12°C compared with the outside air. This shows that the hybrid ventilation leads to more energy saving during the intermediate seasons.

By the natural ventilation, the air change rate reaches 1.5 per hours. The concentration of VOC emissions is quite low after it has been used for half a year. And this shows that the indoor air quality is quite good.

During the winter, the completely closed mode is recommended, as the more sunlight can be introduced into the rooms, the natural room temperature can be increased greatly. In the afternoon the temperature in the 2F living exceeds 20°C when it is cloud outside, and there is no need for heating. The heating load in the 1F SOHO room has an average conservation ratio of about 31% in the daytime, while it has a conservation of about 47% in the 2F Living room from 19:00 to 22:00. The ratio of free heating hour accounts for nearly 30% from 9:00 to 18:00 in the 2F Living room.

As there is little furniture, the thermal capacity of the living room is quite small, the temperature drop is 1.4°C per hour, while it is about 0.5°C per hour in the SOHO room, because of more furniture and books. The free heating time will be extended if the thermal capacity is increased.

According to the subjective experiment on the operation of the double skin system in

autumn, although the subjects are young, few feel it is inconvenient to control the shadings, windows or opening to achieve thermal comfort by hand. About 64% people think the double skin system has good effect on thermal comfort and energy conservation by active ventilation and passive methods, and about 56% subjects have new understanding for environmental control by using this system. It shows that the occupants would be willing to use the passive systems (such as the double skin) to control the indoor environment by themselves, not by those uncontrollable air conditioners. The passive systems show good promise in future.

CHAPTER 5

EVALUATION OF DISPLACEMENT VENTILATION SYSTEM IN A RESIDENTIAL ROOM BY CFD SIMULATION

As for a residential house, it is well known that temperature stratification system for heating, such as the floor heating system, has good effect on thermal comfort for occupants. But the temperature stratification system for cooling, such as the displacement ventilation system, has few installations in residential houses so far, because the height of ceiling is lower than that in office buildings or large space buildings.

The basic consideration of displacement system is supplying conditioned air directly to the occupant zone, while those places not for occupancy, will not be specially supplied air directly, and the exhaust outlet on the ceiling will also discharge some convection heat from lights. From the point of view in energy conservation, this system is more reasonable for air diffusion in an active air conditioning system. Besides, it can provide a better indoor environment, as the pollutants from human will be discharged by the buoyancy effects. And the polluted air will not be circulated in the occupant zone.

In order to evaluate its effectiveness for residential houses, in this chapter, CFD simulations on the displacement ventilation system and the conventional mixing ventilation system are carried out, and compared their differences in the respects of thermal comfort, air change efficiency, and cooling load. The elements of displacement ventilation, such as air change rate, the position of air inlet/outlet, and diffuser characteristics are discussed. The energy consumption and thermal comfort for the displacement system and mixing system are evaluated.

5.1.Outline of displacement ventilation and mixing ventilation system

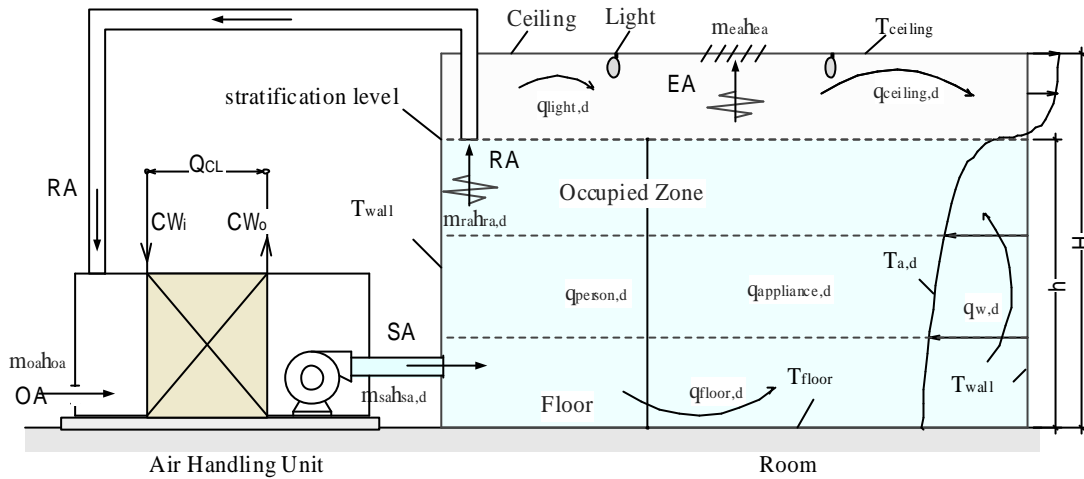
5.1.1. Sketch of these two systems

In the displacement ventilation (Fig.5-1), which intends to only cool the occupied zone, the supply diffuser is set near the floor, and the outlet of return air is at the high part of the room, while the exhaust outlet is on the ceiling. Therefore, the air temperature is expected to be stratified in the vertical direction by the force of buoyancy, while the air above the occupied zone will be kept at a rather high temperature.

But in the mixing ventilation (Fig.5-2), the cold air is supplied from near the ceiling, and

the outlet is set near the floor, which intends to cool the whole room.

Here a micro model made by CFD software is used to predict the airflow and temperature distribution for these two systems. The energy consumption for cooling is calculated according to the equations of energy balance, and the PMV distribution is also calculated to evaluate the thermal environment.



Note:
 SA: Supply Air; RA: Return Air; OA: Outside Air; EA: Exhaust Air; CWi/o: cold water in/out
 q: Heat convection ; QCL: Cooling load of Air handling unit

Fig.5-1. Sketch of the displacement ventilation system

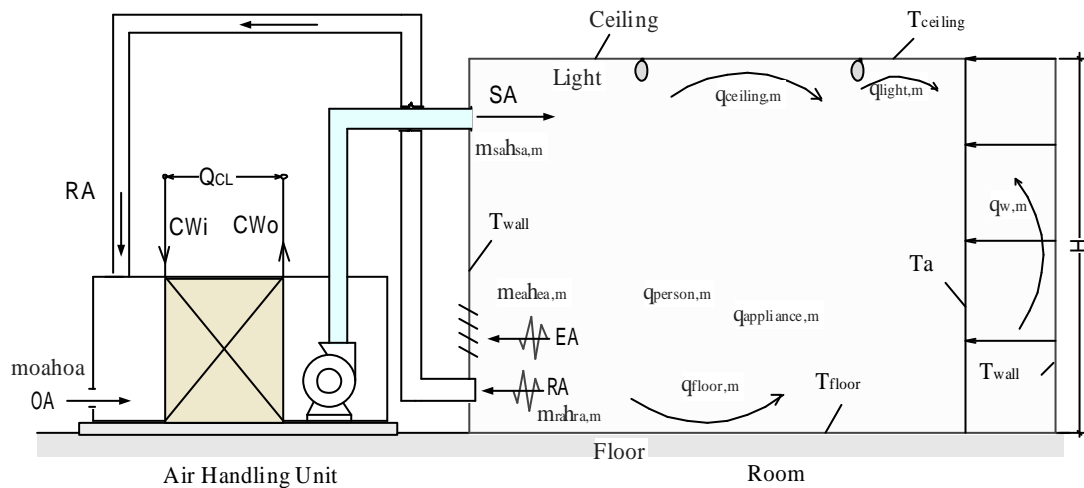


Fig.5-2. Sketch of the mixing ventilation system

5.1.2. Difference in design

Compared with the conventional system, the proposed system has the following features, as are listed in Table 5-1.

Table 5-1. Comparison of difference in design between the displacement ventilation system and the mixing ventilation system

Features \ System	Displacement Ventilation	Mixing ventilation
Air conditioning mode	All air system	All air /water -air/Refrigerant
Air conditioning area	Occupied zone only	Whole room
Temperature difference*	4-5°C	8-15°C
Position of exhaust air	Near the ceiling	Usually in the occupied zone or no exhaust
Outside Air	With outside air	With/without outside air
Others	2-3 times larger air flow rate	Possibility of refrigerant leakage for the refrigerant mode

Note: * refers to temperature difference between supply air and the air at the occupied zone, and this table is revised according the report of Ikeda, K. (1996)

If the conventional room air conditioner is used, there is no introduction of outside air. As using the displacement system, the smaller temperature difference between supply air and room air is, the larger the airflow rate is needed.

According to the design conditions, the displacement ventilation system is available for residential houses, and the effect on thermal comfort and energy consumption is discussed by CFD simulation in the following part.

5.2. Description of the simulation model

5.2.1. Micro-model

Compared with the indoor zero equation model presented by Chen (1998), an unsteady standard k - ϵ model has been adopted. By solving the transport equations of mass, momentum, energy, turbulent kinetic energy and turbulent dissipation rate, which are listed in the following part, the distribution of air temperature and airflow in the room can be predicted.

- The mass conservation equation

$$\frac{\partial u_i}{\partial x_i} = 0 \quad (5-1)$$

where μ_i is the velocity component in the x_i direction.

- Momentum equations

$$\frac{\partial(\mathbf{r}u_i)}{\partial t} + \frac{\partial(\mathbf{r}u_i u_j)}{\partial x_j} = -\frac{\partial p}{\partial x_i} + \frac{\partial}{\partial x_j}[\mathbf{m}_{eff}(\frac{\partial u_i}{\partial x_j} + \frac{\partial v_j}{\partial x_i})] + \mathbf{b}r g_i (T_o - T) \quad (5-2)$$

where p is static pressure, \mathbf{r} is air density, g_i is gravitational body force in direction i ; \mathbf{b} is thermal expansion coefficient of air, T_o is outdoor temperature (for reference), and T is air temperature; \mathbf{m}_{eff} is effective viscosity, which is given by

$$\mathbf{m}_{eff} = \mathbf{m} + \mathbf{m}_t \quad (5-3)$$

and

$$\mathbf{m}_t = \mathbf{r}C_u \frac{k^2}{\mathbf{e}} \quad (5-4)$$

where μ is viscosity; C_m is a constant, i.e. 0.09, k and \mathbf{e} are given in Equations (5-6) and (5-7).

- Energy conservation equation

$$\frac{\partial}{\partial t}(\mathbf{r}T) + \frac{\partial}{\partial x_j}(\mathbf{r}u_j T) = \frac{\partial}{\partial x_i}(k + k_t) \frac{\partial T}{\partial x_i} + \frac{q}{C_p} \quad (5-5)$$

where q is heat source; and k is the molecular conductivity, and k_t is the conductivity due to turbulent transport ($k_t = C_p \mathbf{m}_t / Pr_t$), Pr_t is the turbulent Prandtl number.

- The turbulent kinetic energy

$$\mathbf{r} \frac{Dk}{Dt} = \frac{\partial}{\partial x_i} \left[\left(\mathbf{m} + \frac{\mathbf{m}_t}{\mathbf{s}_k} \right) \frac{\partial k}{\partial x_i} \right] + G_k + G_b - \mathbf{r}\mathbf{e} \quad (5-6)$$

- The rate of dissipation

$$\mathbf{r} \frac{D\mathbf{e}}{Dt} = \frac{\partial}{\partial x_i} \left[\left(\mathbf{m} + \frac{\mathbf{m}}{\mathbf{s}_e} \right) \frac{\partial \mathbf{e}}{\partial x_i} \right] + C_{1e} \frac{\mathbf{e}}{k} (G_k + C_{3e} G_b) - C_{2e} \mathbf{r} \frac{\mathbf{e}^2}{k} \quad (5-7)$$

where C_{1e} is 1.44; C_{2e} is 1.92; C_m is 0.09 and \mathbf{s}_k is 1.0 and \mathbf{s}_e is 1.3.

5.2.2. Calculation for energy consumption

As it is known that the cooling load of an air conditioning system can be derived from the following equation:

$$Q_{cl} = \dot{m}_{ra} h_{ra} + \dot{m}_{oa} h_{oa} - \dot{m}_{sa} h_{sa} \quad (5-8)$$

where Q_{cl} is cooling load of AHU(w); \dot{m}_{sa} , \dot{m}_{ra} and \dot{m}_{oa} are air flow of SA, RA and OA respectively (kg/s); h_{sa} , h_{ra} , and h_{oa} are enthalpy of SA, RA and OA respectively (J/kg).

The energy balance of the air in the whole room, can be expressed as:

$$q_{person} + q_{appliance} + q_{light} + q_w + q_{floor} + q_{ceiling} = \dot{m}_{ra} h_{ra} + \dot{m}_{ea} h_{ea} - \dot{m}_{sa} h_{sa} \quad (5-9)$$

where q_{person} , $q_{appliance}$ and q_{light} refer to heat convection from person, appliance, and light in the room (W), and h_{ea} is the enthalpy of exhaust air; q_w , $q_{ceiling}$ and q_{floor} refer to heat convection from wall, ceiling and floor, which can be calculated by Equations (5-10)-(5-12):

$$q_{wall} = \alpha_{c_{wall}} \sum_{i=1}^n (T_{wall} - T_{a_{wall,i}}) A_{wall,i} \quad (5-10)$$

$$q_{ceiling} = \alpha_{c_{ceiling}} \sum_{i=1}^n (T_{ceiling} - T_{a_{ceiling,i}}) A_{ceiling,i} \quad (5-11)$$

$$q_{floor} = \alpha_{c_{floor}} \sum_{i=1}^n (T_{floor} - T_{a_{floor,i}}) A_{floor,i} \quad (5-12)$$

where α_c is coefficient of heat convection; $A_{wall,i}$, $A_{ceiling,i}$ and $A_{floor,i}$ refer to Area of a surface at the mesh i respectively (m^2); T_{wall} , $T_{ceiling}$ and T_{floor} refer to temperature of wall, ceiling and floor ($^{\circ}C$); $T_{aw,i}$, $T_{ac,i}$ and $T_{af,i}$ refer to air temperature near wall, ceiling and floor of mesh i ; i is mesh number near wall, ceiling or floor settled in the simulation.

From the above equations, the difference of cooling load for the displacement system and the mixing system is expressed by Equation (5-13):

$$Q_{cl,m} - Q_{cl,d} = \Delta q_{wall} + \Delta q_{ceiling} + \Delta q_{floor} + \dot{m}_{ea} \Delta h_{ea} \quad (5-13)$$

where the subscripts m and d refer to mixing system and displacement system respectively.

If the temperatures of the envelope (such as wall, ceiling) are assumed same for the two systems, the items at the right side of Equations (5-14)-(5-17) can be written as:

$$\Delta q_{wall} = a_{c_{wall}} \sum_{i=1}^n (T_{wa,d_i} - T_{wa,m_i}) A_{wall,i} \quad (5-14)$$

$$\Delta q_{ceiling} = a_{c_{ceiling}} \sum_{i=1}^n (T_{ca,d_i} - T_{ca,m_i}) A_{ceiling,i} \quad (5-15)$$

$$\Delta q_{floor} = a_{c_{floor}} \sum_{i=1}^n (T_{fa,d_i} - T_{fa,m_i}) A_{floor,i} \quad (5-16)$$

$$\dot{m}_{ea} \Delta h_{ea} = \dot{m}_{ea} (h_{ea,d} - h_{ea,m}) \quad (5-17)$$

It is obvious that the difference of cooling load for the two systems depends mainly on their air temperature distribution.

5.3. Evaluation of thermal comfort in the occupied zone

5.3.1. Evaluation Parameters

As the temperature stratification occurs in the displacement ventilation, and its effect on thermal comfort should be paid enough attention.

5.3.1.1. Stratification in temperature

The temperature in stratification at the height H is expressed by Equations (5-18)-(5-19):

$$\Delta t_{dev} = \frac{1}{\Delta t} \sqrt{\frac{1}{n-1} \sum_{i=1}^n (\Delta t_i - \overline{\Delta t})^2} \times 100\% \quad (5-18)$$

$$\Delta t_i = t_i - t_s \quad (5-19)$$

where t_i is air temperature at point i ; t_s is air temperature at the air inlet; Δt_{dev} is the deviation

of temperature difference between t_i and t_s ; n is the temperature points at a certain height.

If Δt_{dev} is smaller, it means that the temperatures at that height are more uniformly distributed. Because the ankle and the face are more sensitive to air distribution, the temperature deviation should be small.

5.3.1.2. Temperature gradient

The temperature gradient in the occupied zone is expressed by Equation (5-20)

$$\frac{\Delta T}{\Delta Z} = (T_{1.8m} - T_{0.1m}) / 1.7 \quad (5-20)$$

where $T_{1.8m}$ is the air temperature at the height of 1.8m above the floor; $T_{0.1m}$ is the air temperature at the height of 0.1m.

According to the standard of ISO7730, the temperature gradient is recommended within 3°C/m (Olesen, W. B. 2000).

5.3.1.3. Velocity distribution

According to the air velocity distribution, the turbulence intensity in the room can be given by Equation (5-21),

$$T_u = \frac{1}{\bar{v}} \sqrt{\frac{1}{n-1} \sum_{i=1}^n (v_i - \bar{v})^2} \times 100\% \quad (5-21)$$

where \bar{v} is the average air velocity; v_i is the velocity at point i ; n is the point number.

Furthermore, the air velocity can lead to draft sensation, and the draft model, which is included in ISO 7730, can be expressed as Equation (5-22):

$$DR = [(34 - t_a)(\bar{v} - 0.05)^{0.62}] (0.37\bar{v}T_u + 3.14) \quad (5-22)$$

where DR is draft rating, i.e. the percentage of people dissatisfied due to draft; t_a is local air temperature (°C).

5.3.1.4. PMV distribution

PMV in the occupied zone is calculated according to the ISO7730, which is the function of air velocity, temperature, relative humidity, radiation temperature, human metabolic rate and

clothing value. The recommended range of PMV is from -0.5 to 0.5.

5.3.1.5. Ventilation effectiveness

For an air distribution system, its ability to remove pollutants in a room can be expressed as the ventilation effectiveness C_n , which can be calculated by Equation (5-23)

$$C_n = t_n / t_{avg} \quad (5-23)$$

where t_{avg} is the average length of time that supply air has been in the room, i.e. average age of air, while t_n is the nominal time constant, which is given by Equation (5-24)

$$t_n = V_{room} / \dot{m}_{sa} \quad (5-24)$$

where V_{room} is the volume of the room, and the leakage of supply air is neglected in the above equation. In fact, Equation (5-24) is the reciprocal of air change rate.

For a totally mixing ventilation system, the average age of air is equal to the nominal time constant t_n , i.e. the average ventilation effectiveness is 1. For a piston-type displacement ventilation, which means no mixing of the room air and only occurs in an ideal displacement flow, and the average age of air is half of the nominal time constant, thus the average ventilation effectiveness is 2 (Matsumoto, H. 2002).

As air mixing occurs in a practical displacement ventilation system, the average ventilation effectiveness is in the range of 1 to 2.

5.3.2. Case study

5.3.2.1. Evaluation tool

The above parameters can be got by dissolving Equations (5-1) to (5-7), and the CFD soft *Airpak2.0* is also used in this study to predict the temperature distribution, airflow, PMV and ventilation effectiveness.

5.3.2.2. Study object

The simulation is carried out in a room (L4.41m×W3.8m×H2.4m) with the volume of 40m³, and the detail layout is shown in Fig.5-3. There are two computers, two desks, one bookcase and six lights in the room, and the situation of partitions has also been considered. As the temperature difference between the air inlet and the occupied zone is usually smaller than 4-5°C (Table 5-1), here the temperature of supply air is set to be 22°C. Considering that the

low-temperature supply air can be used in the displacement system, some of the room air is induced into the fan unit, thus to make sure of the supply air temperature.

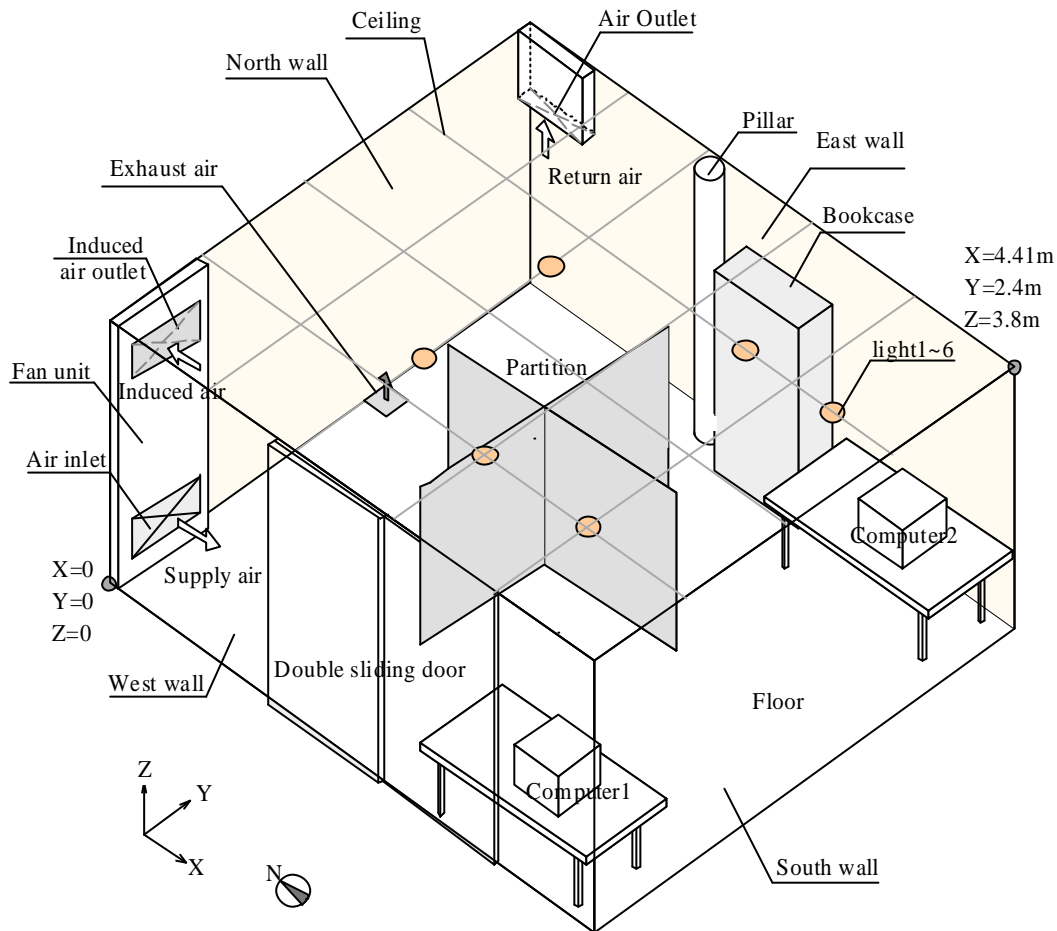


Fig.5-3. Layout of the SOHO with displacement ventilation system

For a displacement ventilation system, the air change rate, air outlet position, swinging louvers in the air inlet are the representative factors which affect the air distribution, thermal comfort in the room, as well as the energy consumption of the whole system, the following cases shown in Table 5-2 are studied by the means of CFD simulation.

- Cases with different air change rates

Cases 1 to 5 are the displacement ventilation systems all with supply air at 22°C, and the air change rate from 5 per hour to 15 per hour.

In Cases 1 to 5, the airflow rate changes from 5 per hour to 15 per hour, while the outlets are all at 1.8m. The area of air inlet is 0.18m² (length 0.6m and width 0.3m), while the outlet of return air is 0.06m² (length 0.6m and width 0.1m), and the outlet of induced air is 0.09m²

(length 0.6m and width 0.15m).

- Cases with different heights for outlet of return air and induced air

The outlet is set on the ceiling of 2.4m in Case 6, while it is at the height of 1.8m in Case 3. And the air change rate keeps the same in these two cases.

- Cases with partitions and swinging louvers

Cases 7 to 10 are studied to make sure of the function of louvers shown in Fig.5-4 in a room with partitions. The partitions are in the middle of the room with the height of 1.4m. Case 7 has swinging louvers, which can swing in the Y direction with a cycle of 40s, and it also has partitions in the room. Case 8 has neither swinging louvers nor partitions, and Case 9 has no swinging louvers but partitions.

Table 5-2. Description of cases for simulation

Case No.	Air change		Supply air			Air velocity			Height		Louvers Swing or not	With or Without Partition
	Rate	Temp.	Inlet	Outlet	Induce	Outlet	Inlet					
	N (h ⁻¹)	t _s (°C)	V _{inlet,x0}	V _{outlet,y0} (m/s)	V _{induce,x0}	Z _{outlet} (m)	Z _{inlet} (m)					
1	5	22	0.33	0.5	-0.25	1.8	0.3	Yes	No			
2	7.5	22	0.50	0.75	-0.38	1.8	0.3	Yes	No			
3	10	22	0.65	1	-0.5	1.8	0.3	Yes	No			
4	12	22	0.78	1.2	-0.78	1.8	0.3	Yes	No			
5	15	22	0.98	1.5	-0.98	1.8	0.3	Yes	No			
6	10	22	0.65	1	-0.5	2.4	0.3	Yes	No			
7	10	20	0.65	1	-0.5	1.8	0.3	No	No			
8	10	22	0.65	1	-0.5	1.8	0.3	Yes	Yes			
9	10	22	0.65	1	-0.5	1.8	0.3	No	Yes			
10	5	11	2.5	1	-	0.1	2.3	Yes	-			

Note: The height of outlet/inlet refers to the height from the floor to the center; V_{inlet,x0} is velocity in X direction at the air inlet; V_{outlet,y0} is velocity in Y direction at the outlet of return air; and V_{induce,x0} is velocity in X direction at the outlet of induced air.

In order to keep constant supply airflow at the air inlet, the velocity in the X direction is set to be constant, while the velocity in the Y direction is assumed to be the function of V_x . And the velocities can be expressed by Equation (5-25)

$$\begin{cases} V_x = V_{inlet,x0} \\ V_y = V_{inlet,x0} |\sin(t/40)| \\ V_z = 0 \end{cases} \quad (5-25)$$

where t refers to the time (s), and $V_{inlet,x0}$ is listed in Table 5-2, thus the flow direction of supply air can be changed frequently.

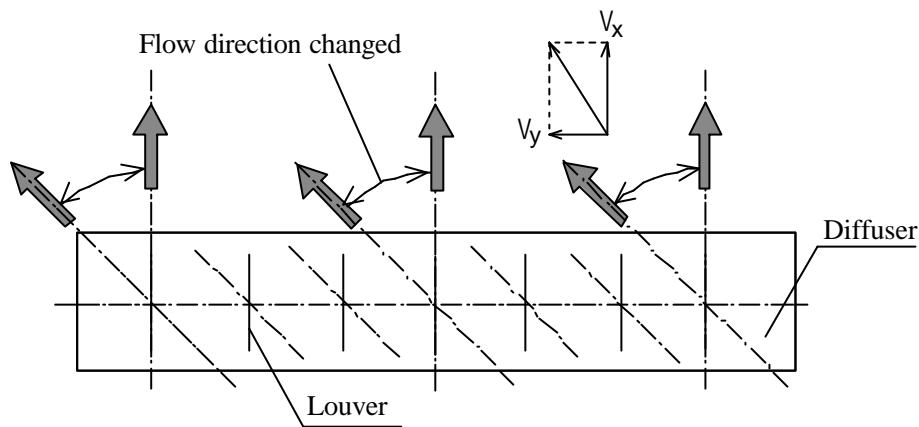


Fig.5-4. Illustration of the swinging louvers at the diffuser of air inlet

- Reference Case 10

Case 10 is the mixing ventilation system, which serves as a reference case. The cold air is supplied from near the ceiling (at the height of 2.3m), while the return air and exhaust air is discharged near the floor (at the height of 0.1m). And the supply air is at 11°C, which means that the temperature difference between supply air and room air is 15°C.

The outlets of exhaust air are set on the ceiling with area of 0.01m² (both length and width are 0.1m) in all the cases, except it is set near the floor with area of 0.03 m² in Case 10.

5.3.2.3. Boundary conditions and initial conditions

- Boundary conditions

The fixed velocity and temperature are set at the air inlet and outlets, while the static pressure at the exhaust outlet is set as the same with ambient. The fixed temperature is also set on different walls, as well as the floor and the ceiling. The computers and lights are set with fixed heat release.

As the flow at the air inlet is assumed to be fully developed, the turbulent intensity I_{tur} (Schlichting, H. 1979) at the air inlet is given by Equation (5-26)

$$I_{tur} = \frac{\sqrt{1/3(\overline{u'^2} + \overline{v'^2} + \overline{w'^2})}}{V_{avg}} \quad (5-26)$$

where V_{avg} is the average velocity, and u' , v' , w' is the fluctuation of velocity in X, Y, Z direction. And the intensity in one direction can be expressed:

$$I_{tur,i} = \frac{\sqrt{\overline{v_i'^2}}}{V_{i,avg}} \quad (5-27)$$

where the fluctuation of the velocity fluctuation is expressed by

$$\overline{v_i'} = v_i - \overline{v_i} \quad (5-28)$$

where v_i refers to the velocity in i direction, $\overline{v_i}$ is its average value.

According to Equations (5-26)-(5-28), the calculation of the turbulent intensity I_{tur} in a cycle is listed in Table 5-3, and the time step is 5s.

Table 5-3. Calculation of the turbulent intensity I_{tur} in a cycle

t (s)	V_x (m/s)	V_y (m/s)	V_z (m/s)	V (m/s)
0	1	0	0	1
5	1	0.382683	0	1.070722
10	1	0.707107	0	1.224745
15	1	0.92388	0	1.361453
20	1	1	0	1.414214
25	1	0.92388	0	1.361453
30	1	0.707107	0	1.224745
35	1	0.382683	0	1.070722
Average $\overline{v_i}$	1	0.628417	0	1.216007
Velocity fluctuation $\overline{v_i'^2}$	0	0.105092	0	-
$I_{i,tur}$	0	0.515864*	0	0.153917**
Turbulent intensity adopted	(0.515864+0.153917)/2=0.334891			

Note: during calculation V_x is taken as 1m/s, * is calculated by Equation (5-26), and ** is calculated by Equation (5-27).

Here the average of the turbulent value in Y direction and the turbulent value from velocity V is taken to be the turbulence intensity, i.e. the turbulence intensity is 0.335, which is approximated to be 0.35 in simulation.

And the turbulent length scale L_{tur} is given by Nikuradses formula (Schlichting, H. 1979)

$$L_{tur} / R = 0.14 - 0.08(1 - y / R)^2 - 0.06(1 - y / R)^4 \quad (5-29)$$

where R is the hydraulic radius, y is the distance. The maximum of L_{tur}/R is 0.14, thus an approximate relationship is

$$L_{tur} = 0.07 D_h \quad (5-30)$$

where D_h is the hydraulic diameter. In the above case, D_h of the air inlet is 0.4m, and the shortest side of the air inlet is 0.3m, thus Equation (5-24) can be written into

$$L_{tur} = 0.1 L_{width} \quad (5-31)$$

Therefore L_{tur} is 0.03, 10% of the width of the air inlet.

As the fixed temperatures for the inner surfaces of the room are set, the radiation between surfaces is neglected during computation.

The boundary conditions (temperature and heat release) are detailed in Table 5-4, in which the wall temperature variation in different cases is neglected, and the heat release is also set to be the same with all the cases.

Table 5-4. Details of boundary conditions

Item	Boundary conditions
East wall	$t=29.6^{\circ}\text{C}$
West wall	$t=28.3^{\circ}\text{C}$
North wall	$t=28.5^{\circ}\text{C}$
South glass	$t=30.8^{\circ}\text{C}$
Ceiling	$t=30.6^{\circ}\text{C}$
Floor	$t=28^{\circ}\text{C}$
Computer	Heat release= $200\text{W} \times 2$
Light	Heat release= $25\text{W} \times 6$
Person	100 W (Sensible heat of two persons)
Exhaust outlet	Static pressure=Ambient

Note: the temperature is given by the field experiment in Chapter 6.

As the temperatures of different interior surfaces are set to be constant, the heat fluxes from different surfaces are calculated by using the convective heat transfer coefficient. The heat transfer at the boundary surfaces is calculated with using a convective heat transfer coefficient (Fluent, Inc. 2001) as follows:

$$h = \frac{\mathbf{m}_{eff} C_p}{Pr_{eff} \Delta x_j} \quad (5-32)$$

where C_p is the specific heat of air, Pr_{eff} is the effective Prandtl number, and Δx_j is the grid spacing adjacent to the wall and \mathbf{m}_{eff} is the effective viscosity. Therefore the heat flux from the different surfaces can be calculated:

$$q = h(T_s - T_{x_j}) \quad (5-33)$$

where T_s is the surface temperature, T_{x_j} is the temperature at the grid x_j .

- Initial conditions

It is assumed that the air temperature in the room is uniformly distributed before air conditioning, and the initial temperature is set to be the same as the ambient air. It is set to be 30.5°C in this study.

5.3.2.4. Mesh setting

Airpak automates the mesh generation, but allows to customize the meshing parameters thus to refine the mesh.

Hexahedral mesh is used in this study. Generally, the maximum size of mesh is 0.5m×0.5m×0.5m, and the maximum size ratio is 2. The meshes near wall and objects, such as computers, desks, and so on, are refined with the element height of 0.1m, while they are refined to 0.05m in height near the air inlet or outlet.

The total number of meshes in the room reaches 106736, and the mesh section at X=1.8m, X=3.6m and Y=1.8m are shown in Fig.5-5.

5.3.2.5. Transient simulation

Transient simulation is carried out for different cases.

Time starts at 0s and ends at 2000 to 2400s, with the time increment of 5s for each step.

5.3.2.6. Under-relaxation factors

The iterations for each time step is 20, and the values of the under-relaxation factor for each of Equations (5-1)-(5-7) are detailed in Table 5-5.

As the pressure under-relaxation factor is 0.3 in the above table, this means that the change in pressure from one iteration to the next will be restricted to 30% of the difference between the initial value and the newly calculated value.

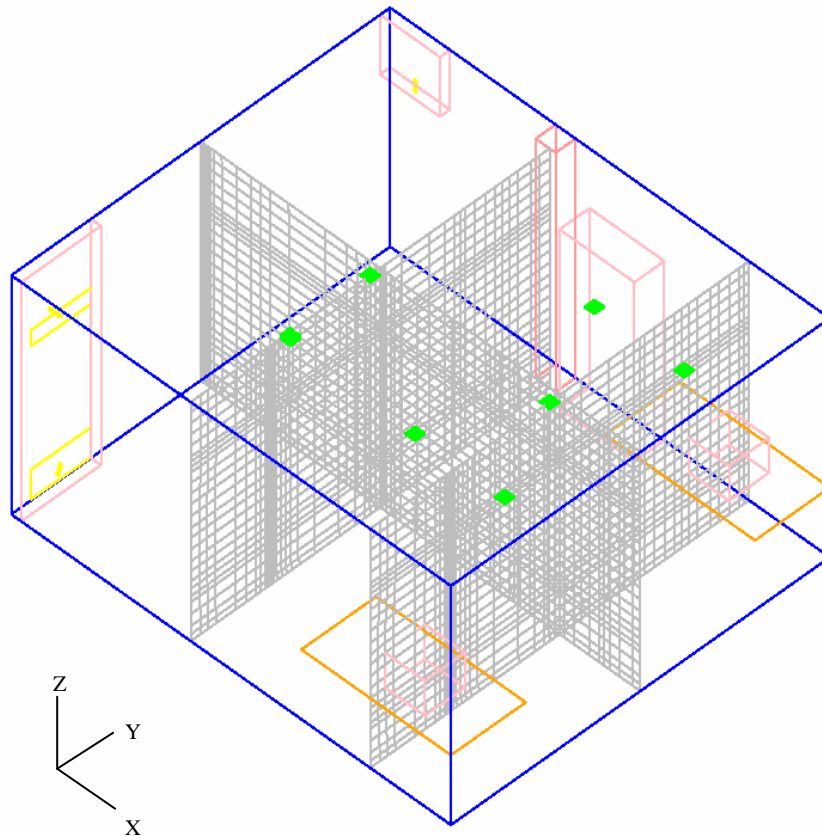


Fig.5-5. Profile of mesh in the room without partitions

Table 5-5. Under-relaxation factors for equations

Under-relaxation factor	Values
Pressure	0.3
Momentum	0.3
Temperature	0.75
Viscosity	0.75
Body forces	0.075
Turbulent kinetic energy	0.4
Turbulent dissipation rate	0.4

5.4.Simulation result

5.4.1. Time to temperature balance

Simulation results in Fig.5-6 and Fig.5-7 show that the temperature varies from the initial time until it reaches the balance state for both the displacement ventilation and mixing system.

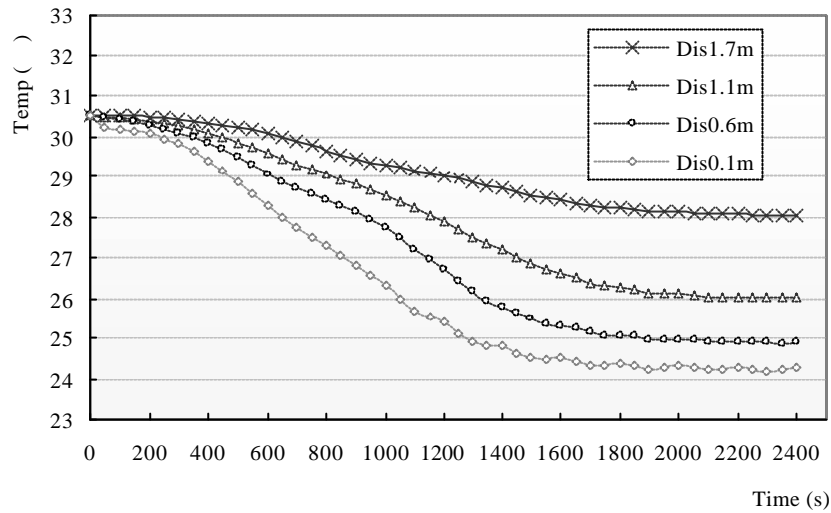


Fig.5-6. Temperature vary with time for displacement ventilation at Cord 5 X=2.7m, Y=1.8m (Case 5)

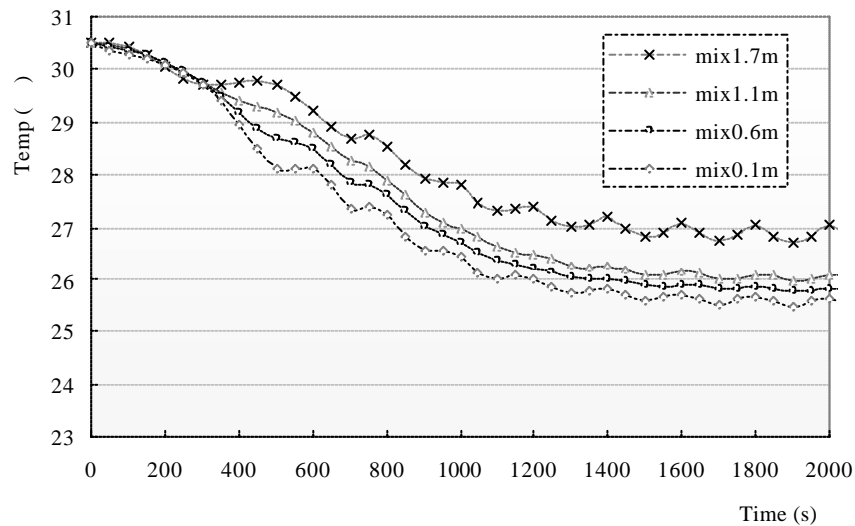


Fig.5-7. Temperature vary with time for mixing ventilation at Cord 5 X=2.7m, Y=1.8m (Case 10)

It takes about 1400 to 1600 seconds for both of the systems to reach their balance. It can be seen that the air temperature in the displacement ventilation system is stratified with height.

For example, it is about 24°C at 0.1m, 26°C at 1.1m and 28°C at 1.7m. But the air temperature is relatively uniformly distributed in the mixing ventilation system, which is in the range of 26-27°C from 0.1m to 1.7m. Furthermore, in the displacement system, the temperature balance in the higher places will take more time, while it takes almost the same time at different heights in the mixed ventilation system.

As for the other displacement cases, the figure of temperature variation with time is similar to Fig.5-6. Time to temperature balance depends on the airflow rate. The smaller the air change rate is, the longer the time to be stable. For Case 1 when the air change rate is 5 per hour, it takes about 2000s to reach the balance state, which is the longest in Cases 1 to 5.

It should be pointed out that the time to balance is affected by the under-relaxation factors listed in Table 5-5. For example, if the factor of momentum is 0.7, temperature and viscosity 1.0, body forces 0.1, and others 0.5, the time to balance will be decreased to 600 seconds. The bigger the under-relaxation factors, the shorter the time to balance, but this may lead to divergence in calculation in some cases.

5.4.2. Effect of air change rate

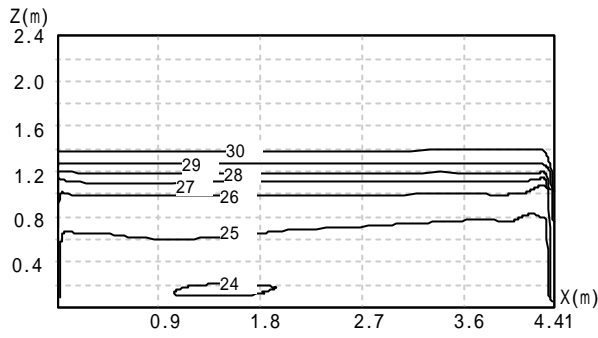
5.4.2.1. Temperature distribution and temperature gradient

- Temperature distribution

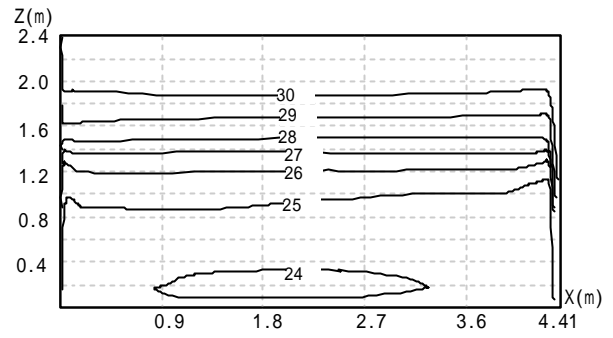
The air temperature is stratified in Z direction when the air reaches its balance state, and Fig.5-8 shows that the air temperature distribution at the middle of the room (Y=1.8m) for Cases 1 to 5, and Case 10. The temperature distribution for all the displacement systems is quite similar, the lower the height, the lower the air temperature. The temperature difference near the floor and below the ceiling reaches about 6°C, and the temperature stratification is confirmed. When the air change rate increases, the average temperature in the occupied zone goes down slowly.

On the other hand, the air temperature difference is within 1-2°C in Z direction in the mixing ventilation system (Case 10), which means that the air temperature is uniformly distributed in the mixing ventilation system.

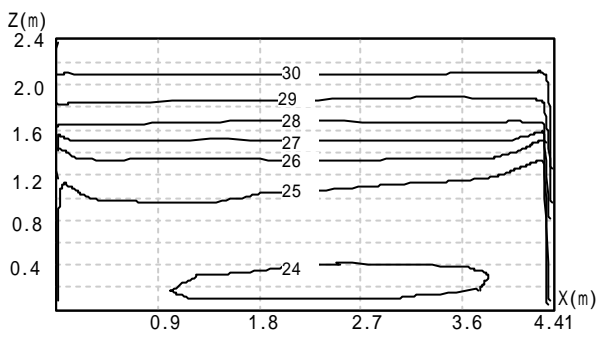
For example, the temperatures at different heights for Case 3 are shown in Fig.5-9, and the average temperature at height of 0.1m is 25.2°C, 0.6m 25.9°C, and 1.1m 26.5°C, while it is about 28.5°C at the height of 1.7m.



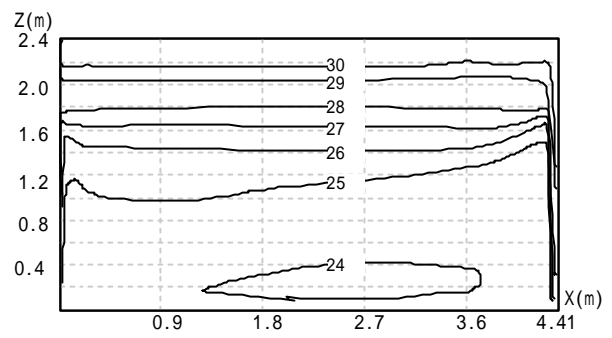
(a) Case 1 air change rate =5



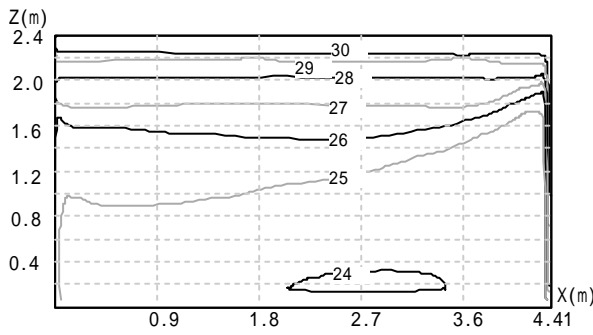
(b) Case 2 air change rate =7.5



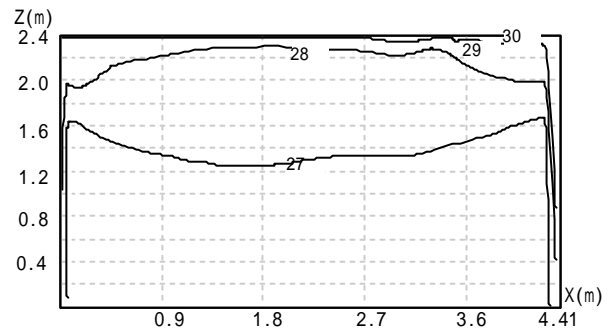
(c) Case 3 air change rate =10



(d) Case 4 air change rate =12



(e) Case 5 air change rate =15



(f) Case 10 air change rate =5 (mixing ventilation)

Fig.5-8. Temperature distribution in displacement ventilation and mixing ventilation system (Cases 1 to 5, and 10)

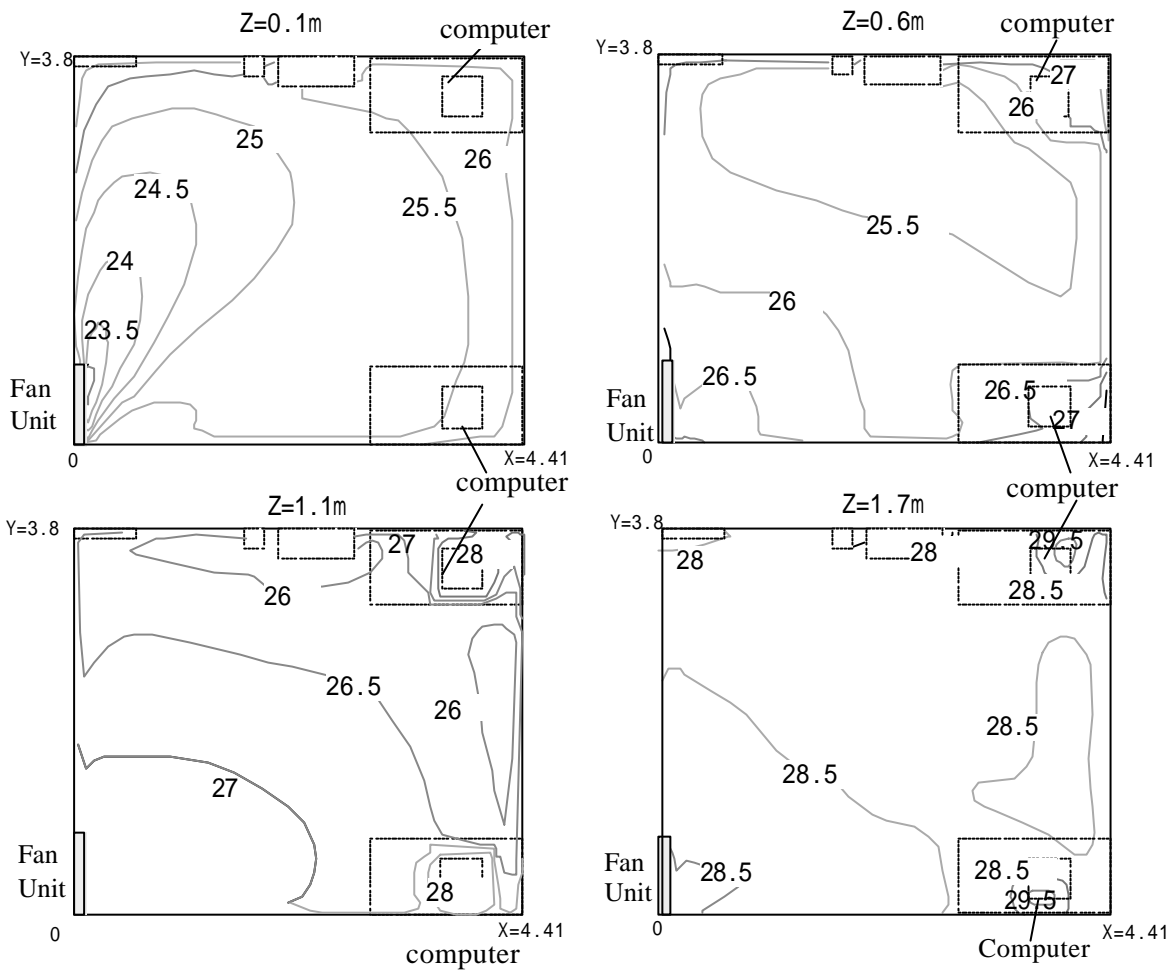


Fig.5-9. Temperature distribution at different heights for Case 3

According to the above results and Equation (5-18), the temperature difference between the supply air and the temperature deviation at different horizontal surfaces of Cases 1 to 5, is shown in Fig.5-10. Air change rate has little effect on temperature distribution for places under the height of 0.6m in the occupied zone ($0.2m < X < 4.2m$ and $1m < Y < 3m$), while it has great effect on temperature in those higher places. For example, the temperature difference goes down from 9°C to 4°C at the height of 1.7m, while the temperature deviation increases from 2% to 13%, if the air change rate increases from 5 per hour to 15 per hour. But the temperature seems to be constant at the height of 0.1m.

It should be pointed out that the temperature deviation below 0.6m is quite big, over 30%, because of the swinging louvers, and for the places near the ceiling at the height of 2.3m, the air temperature is effect by the heat release from the lighting, especially near the lights, thus the temperature deviation also becomes big.

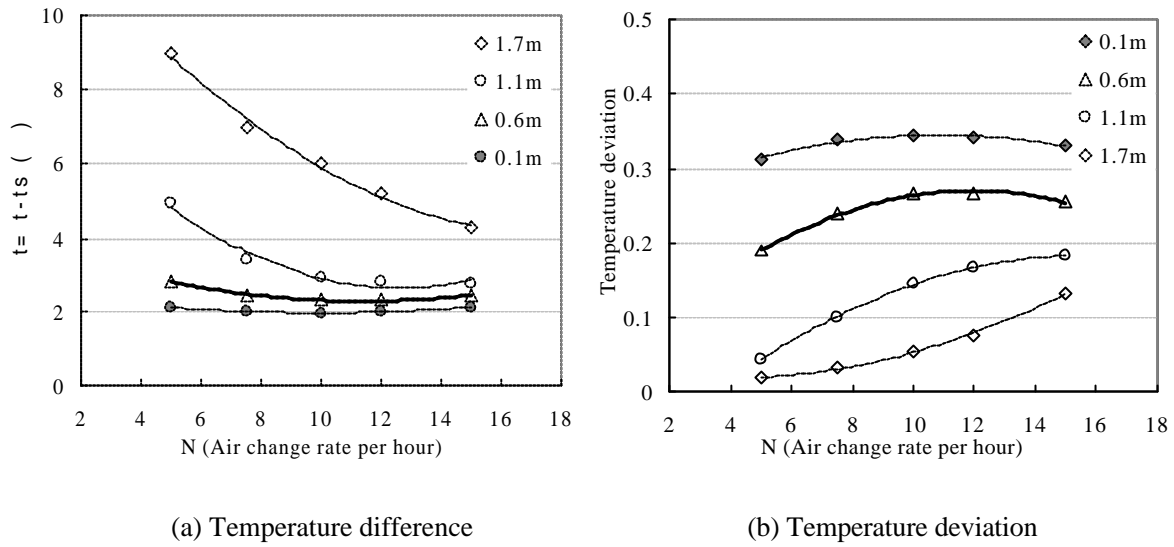


Fig.5-10. The relationship of temperature deviation at different heights gradient with air change rate (Cases 1 to 5)

- Temperature gradient

As the temperature is assumed to be uniform before air conditioning, the temperature gradient becomes greater with the time going. When the air distribution becomes stable, the comparison of the temperature gradient for displacement ventilation and mixing ventilation is shown in Fig.5-11. The temperature difference between 0.1m and 1.1m is within 2°C in most occupied zone, while it is over 3°C near the air inlet (X=0.9m and Z=0.9m) in Case 3.

On the contrary, the temperature gradient remains to be smaller than 0.3°C/m in the mixing ventilation (Case 10), which shows that the air is uniformly distributed.

As for the displacement ventilation, with the increase of air change rate, the temperature difference between the higher places and the lower places decrease, as is shown in Fig.5-12a. The average temperature gradient between 0.1m and 2m is 7.8°C for Case 2 (n=7.5), while it is 3.7°C for Case 5 (n=15).

The larger the air change rate is, the slope of the temperature profiles becomes smaller, that is, the temperature gradient is smaller. For example, at the height of 1m, it drops from 4°C/m at the air change rate of 5 per hour to 1.7°C/m at the air change rate of 15 per hour (Fig.5-12b).

According to the standard of ISO7730, the recommended temperature gradient between 0.1m and 1.1m is within 3°C/m, which means that the air change rate is necessary to be more than 8~9 per hour in this study (Fig.5-13).

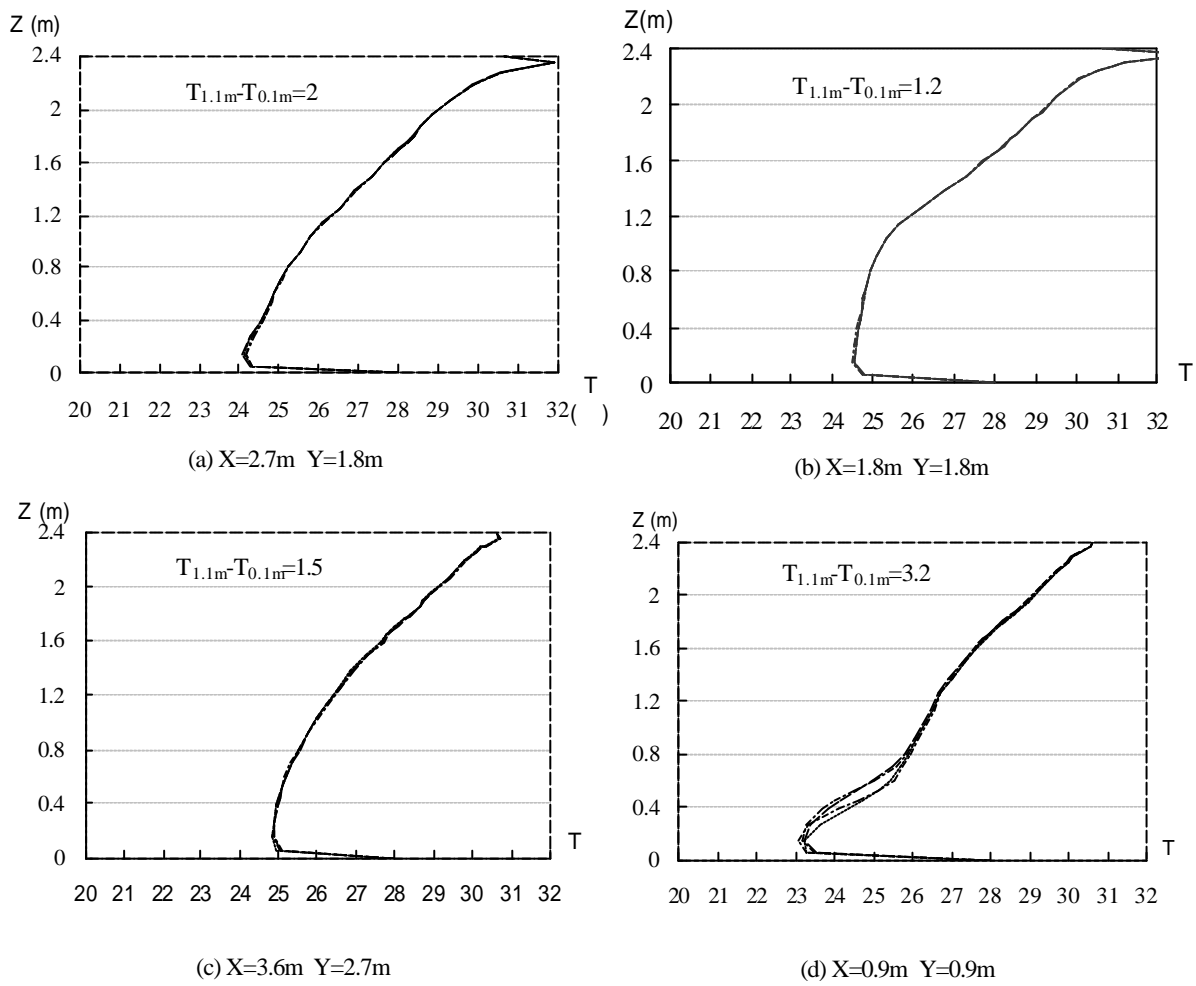


Fig.5-11. The temperature gradient for Case 3

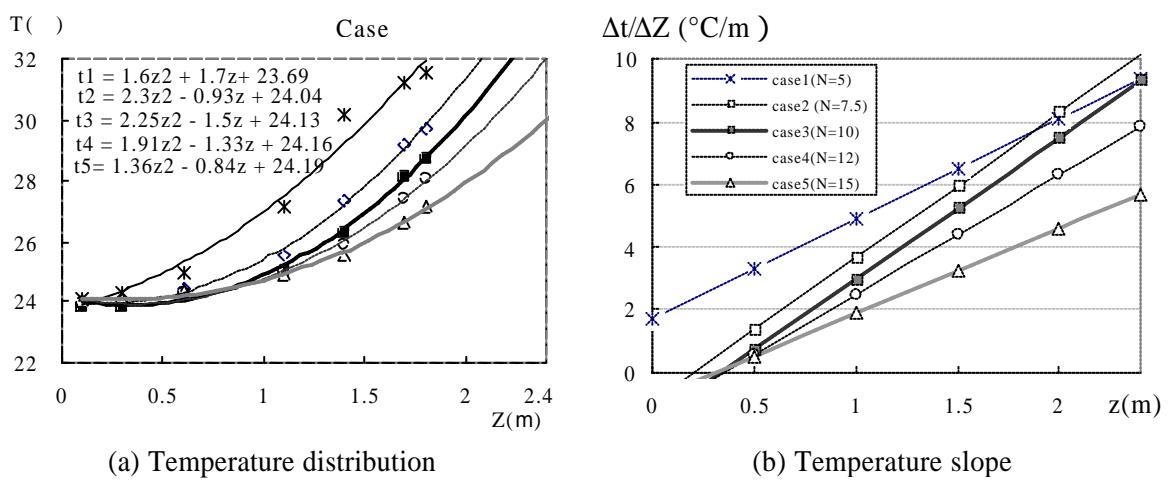


Fig.5-12. Temperature distribution with air change rate for displacement ventilation

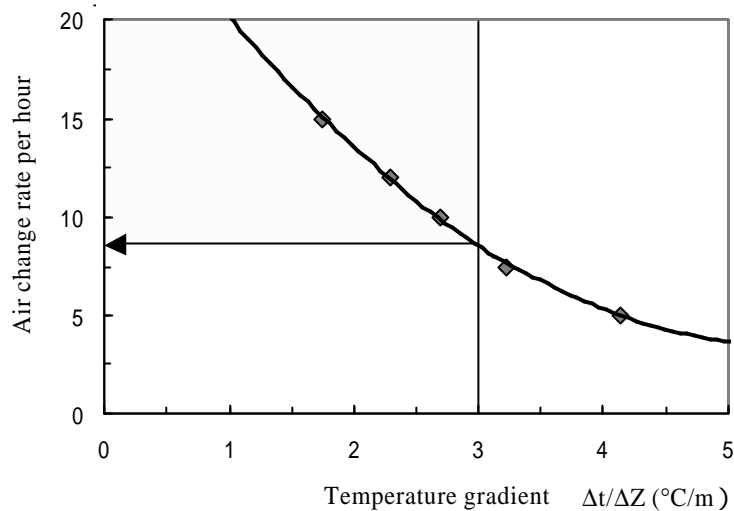


Fig.5-13. Recommended air change rate from temperature gradient

5.4.2.2. Velocity distribution

The velocity distribution at $Z=0.3\text{m}$ of Cases 1 to 5 and $Z=1.1\text{m}$ of Case 10 is shown in Fig.5-14. As for the displacement cases, the velocity increases with the distance to the air inlet, and the air in the occupied zone has smaller velocity, while it has a little bigger velocity in the occupied zone for the mixing case, especially near the desks.

From Case 1 to Case 4, the air velocity is below 0.3m/s in most occupied zone, while it is faster than 0.4m/s near the air inlet. In Case 5, when the air change rate reaches 15 per hour, the area with 0.3m/s velocity reaches up to the middle of the room, and this would bring some unsatisfactory to the occupant.

As for the mixing ventilation, the air velocity is not quite so small around the desks at the height of 1.1m .

As it is known that the occupant is more sensitive to air velocity at the height of ankle of 0.1m , the draft at this height should be paid enough attention. According to temperature and velocity distribution in the main occupied zone ($1.8\text{m}<x<4.2\text{m}$, and $0.9\text{m}<z<3\text{m}$), the turbulence intensity and draft rating at 0.1m can be got by Equations (5-21) and (5-22). Fig.5-15 shows that the turbulence intensity and draft rating increase with air change rate, and the intensity is in the range of 30-40%, while the draft rating is 10-20%. This confirms that the percentage of dissatisfied due to draft is in proportional with the air change rate.

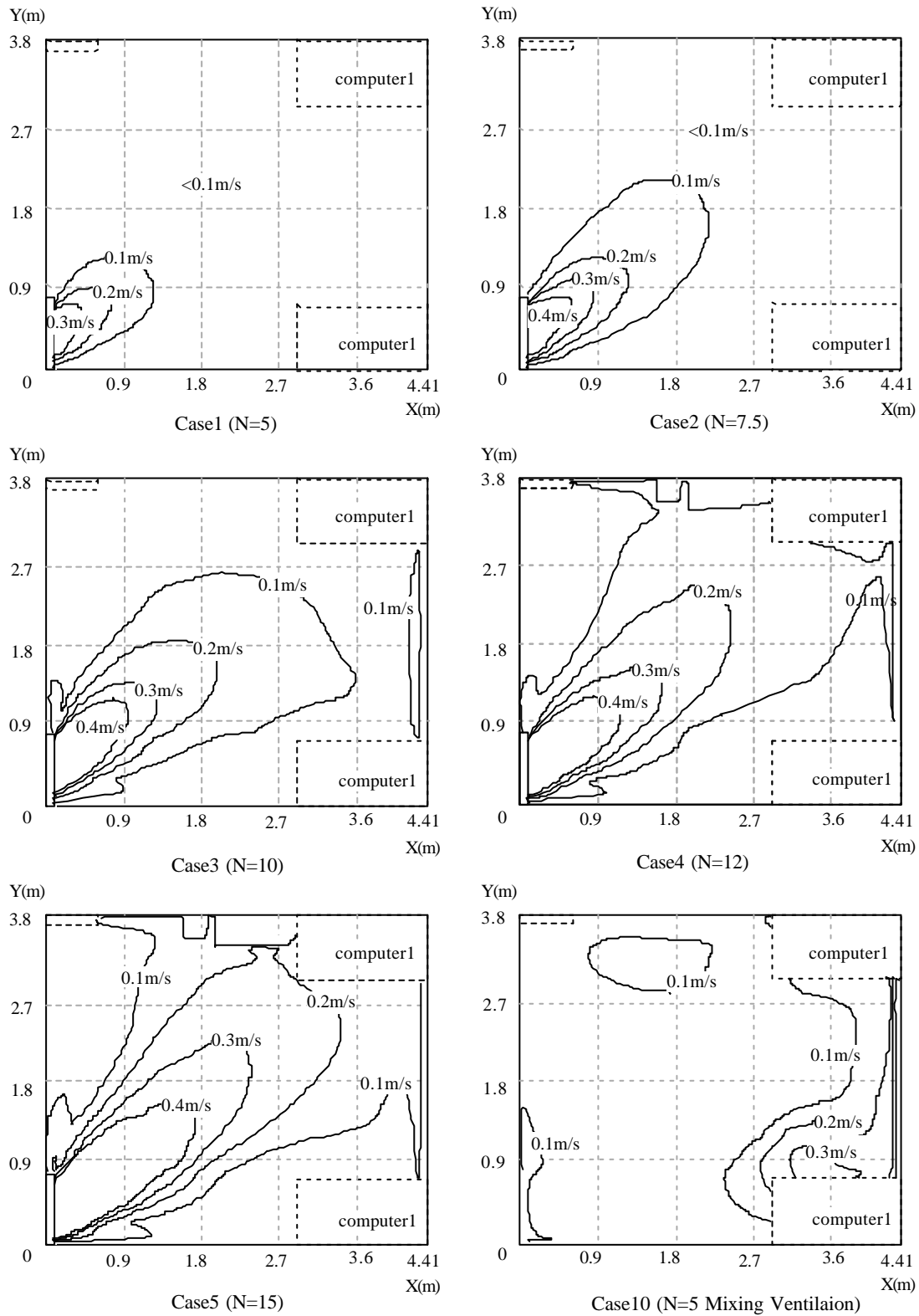


Fig.5-14. Velocity distribution in Cases 1 to 5 and Case 10

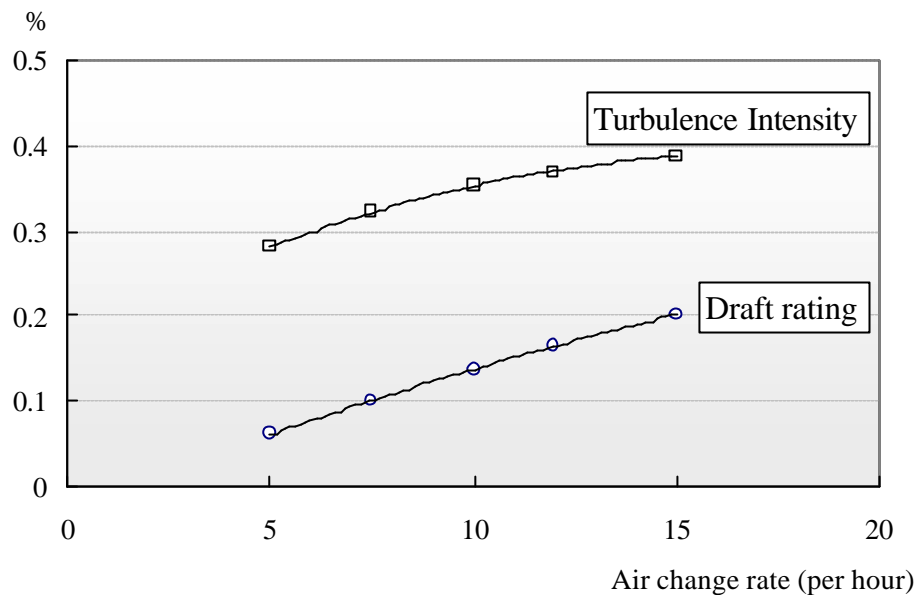


Fig.5-15. Turbulence intensity and draft rating in Cases 1 to 5

5.4.2.3. PMV distribution

According to the air temperature and velocity calculated, the PMV in the occupied zone of Case 3 is shown in Fig.5-16, where the clothing value is 0.5 clo, metabolic rate 1.2 met, and the radiation temperature is assumed to be equal to the air temperature, while the relative humidity is assumed to be 60%. Below the height of 1.5m, PMV is in the range of -0.5 to 0.5, although it is 1.0 at the height of 1.8m, it has little effect on a sitting occupant at the height of 1.1m.

Fig.5-17 shows that with the increase of the air change rate, the comfortable area will be extended. For example, PMV is smaller than 0.5 under the height of 0.9m when n is 5 per hour, but it will be extended till the height of 1.6m when n increases to 15 per hour.

It can be seen that the air change rate above 10 will lead to a better thermal environment in this study.

5.4.2.4. Age of air and air change effectiveness

Distribution of local mean age of air t_p at the section of at $Y=1.8m$ for Case 3 is shown in Fig.5-18, it is about 200-300s in the occupied zone, while it is 350s to 400s in the high places near the return area. The average age of air t in the whole room is about 272s. The nominal time constant (=room volume/supply airflow rate) is 360s when the air change rate is 10 per hour,

thus the average air change efficiency is about 1.3.

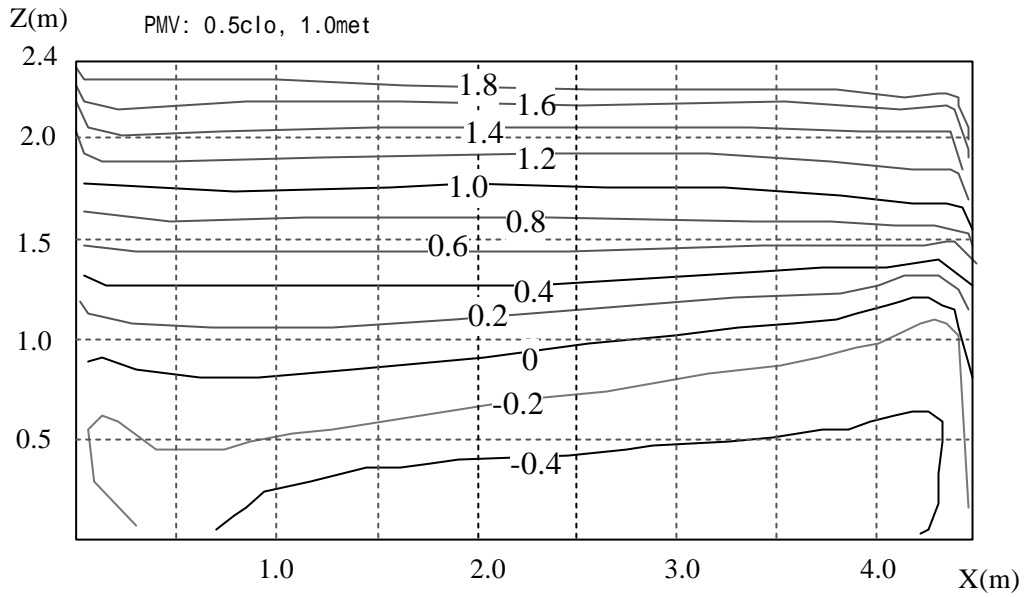


Fig.5-16. PMV distribution in Case 3

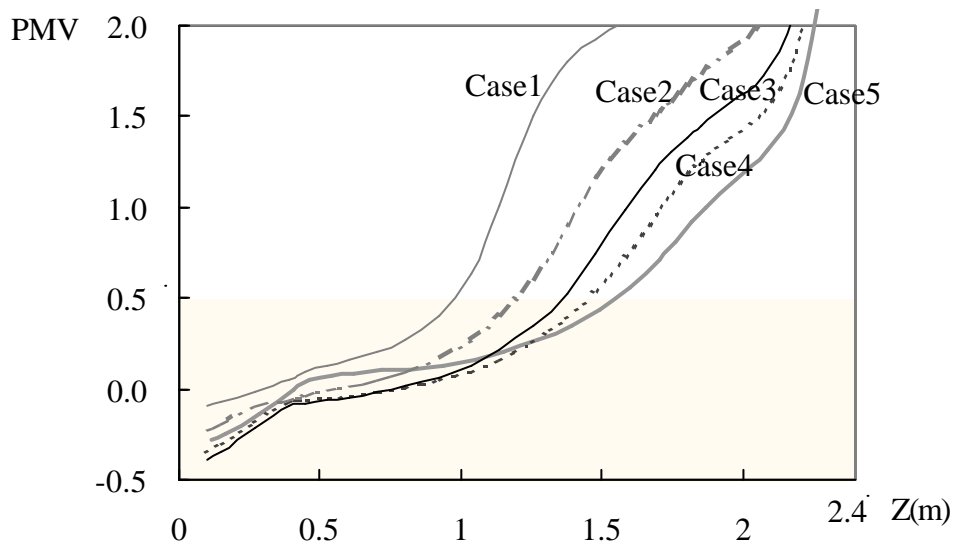


Fig.5-17. PMV distribution with air change rate

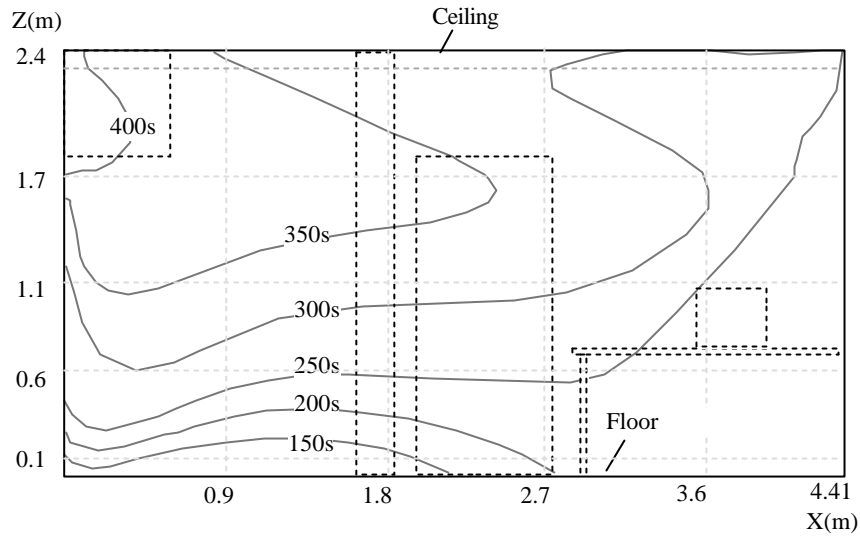


Fig.5-18. Distribution of local age of air in Case 3

Compared with the air exchange effectiveness of the mixing system, the efficiency of displacement system is about 30% higher. As for the other cases, there are similar results.

5.4.2.5. Energy consumption

According to the temperature of return air and supply air from simulation, the sensible cooling load for different cases can be got from Equation (5-34).

$$q_s = \frac{rC_p \dot{m}_{sa} (t_{rm} - t_s)}{A_{fl}} \quad (5-34)$$

where A_{fl} is the floor area.

Here the sensible heat removed by the exhaust air is neglected, as the flow rate of exhaust air is small, and the temperature of the outside air is assumed to be the same with the return air. Obviously, the energy consumption increases with the air change rate with a same temperature of supply air in Fig.5-19. When the air change rate increases 1 per hour in this study, the cooling load will increase at about $2.6\text{W}/\text{m}^2$.

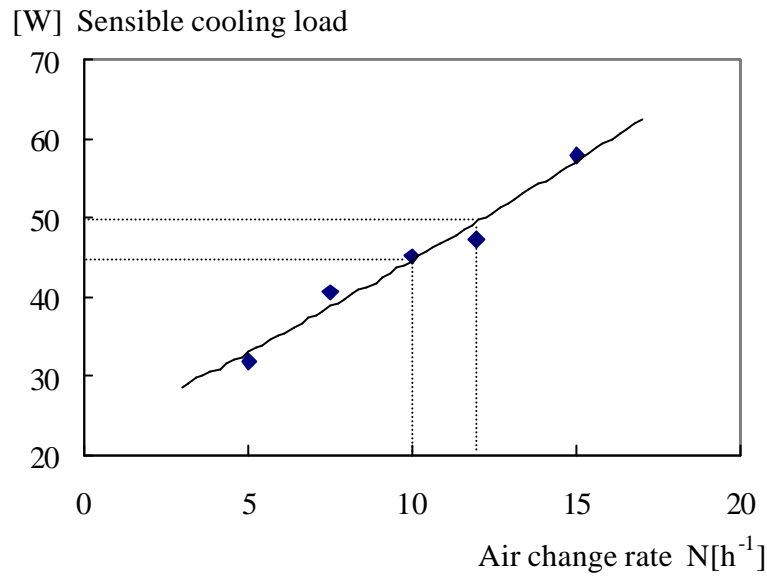


Fig.5-19. Air conditioning load with air change rate

5.4.3. Effect of position of air inlet and outlet

5.4.3.1. Temperature distribution

When the position of the outlet of return air is changed, the temperature distribution will be changed accordingly. In Case 6 the air outlet is set on the ceiling, although the stratification of air temperatures is similar to that in Case 3, it is a little higher than Case 3 under 1.4m while it is a little colder at higher places (Fig.5-20). This is because that the outlet is at the ceiling, and the cool current may reach the high places.

Compared with the displacement system, the temperature is uniformly distributed in Case 10 by the mixing ventilation. The temperature gradient in Case 10 is less than $1^{\circ}C/m$, while it is about $2.5^{\circ}C/m$ in the displacement system.

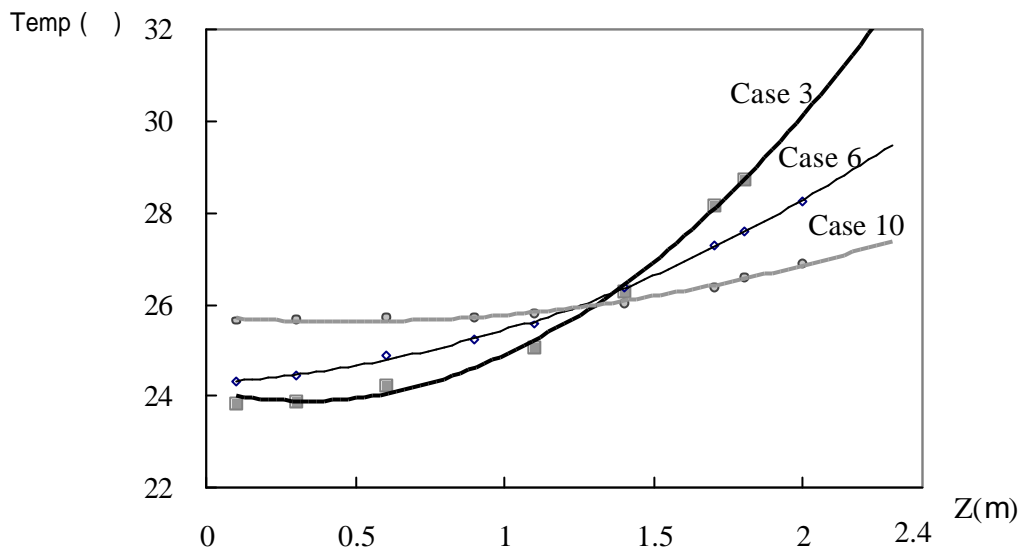


Fig.5-20. Comparison of temperature distribution for the displacement ventilation systems (Cases 3 and 6) and the mixing ventilation system (Case 10)

5.4.3.2. PMV distribution

The PMV distribution for these 3 cases is shown in Fig.5-21, and the conditions are the same with previous.

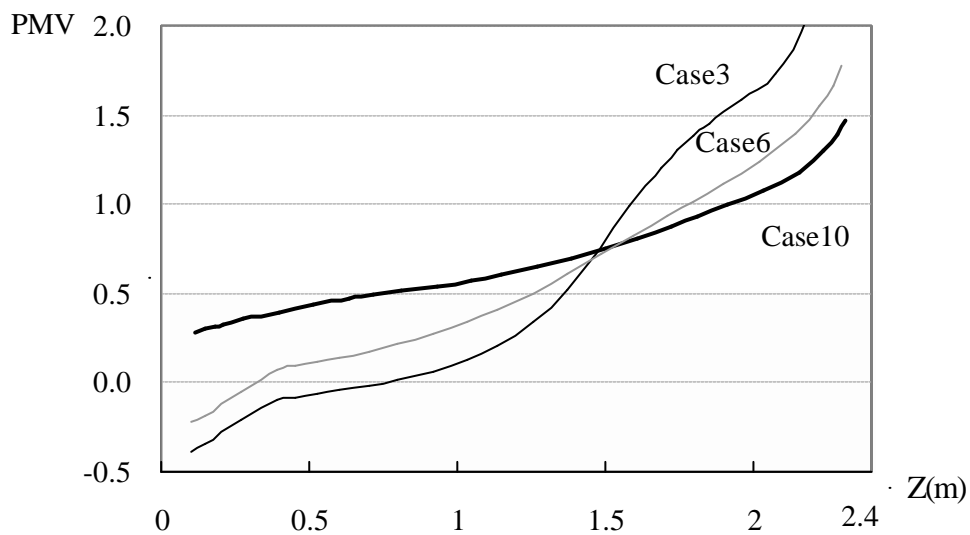


Fig.5-21. Comparison of PMV distribution for the displacement ventilation systems (Cases 3 and 6) and the mixing ventilation system (Case 10)

PMV is below 0.5 under the height of 1.5m in each case, which means they have similar thermal comfort under 1.5m. But the PMV at higher places by the displacement ventilation is a little bigger. And the position of return air for displacement system does not change the thermal comfort so greatly for a sitting person, which is similar to the temperature distribution. While PMV in the higher places will be a little smaller. For example, PMV in Case 3 is 1.6 at 2m, while it is 1.2 in Case 6.

5.4.3.3. Cooling load

On the other hand, as the air change rate increases, the temperature distribution near the surfaces of the envelope will be different and this will lead to different cooling load. Assuming the envelopes have the same temperatures in different cases, the air near floor in Case 3 is the lowest, so the heat convection from floor is the largest. But the air near the ceiling has a higher average temperature, which will lead to smaller heat convection. As for the air temperature near the walls becomes higher in the vertical direction, the heat flux of convection from the wall may change with height.

Fig.5-22 shows the temperature difference at 0.1m and 2.3m of the displacement system (Case 3) and the mixing system (Case 10) in X direction. Obviously, the temperature is higher in Case 3 than Case 10, therefore the temperature difference is plus at the ceiling, which will lead to energy saving for the displacement system. But the temperature difference is minus at the floor, which means the displacement system will cost more energy near the floor.

Fig.5-23 shows the temperature at 0.1m near south glass in Z direction, and temperature of Case 3 increases with the height, while there is only a small increase in Case 10. Therefore the temperature difference between Case 3 and Case 10 is minus in the lower places, while it is plus in the higher places.

As the total area of “plus” is larger than that of “minus”, the displacement system will cost less energy than the mixing system.

By Equations (5-10)-(5-12), the detail composition of the cooling load for Case 3, Case 6 and Case 10 are shown in Fig.5-24. The convection heat transfer coefficient a of 4 W/m^2 is used here, and the ratio of convection for the heat convection q_{light} , $q_{appliance}$ and q_{person} is 50% (Yan, 1986), and the heat sources from appliance, light and person are assumed fixed. As the different temperature distribution will lead to different cooling load for the AHU, and the temperature difference of exhaust and return is neglected because of the small flow rate of exhaust air during calculation. From Fig.5-24, it can be seen that the load from the floor in the displacement

system is about 5% to 8% greater than that in the mixing system, because of the cut-down from ceiling and other walls, the cooling load of Case 3 is 26% lower than that of the mixing system (Case 10), and Case 6 has about 12% cut-down. Among the 26% cut-down in Case 3, about 17% is attributed to the heat convection cut-down from the ceiling.

It can be concluded that if the ceiling has more cooling load, the energy saving by the displacement ventilation will increase.

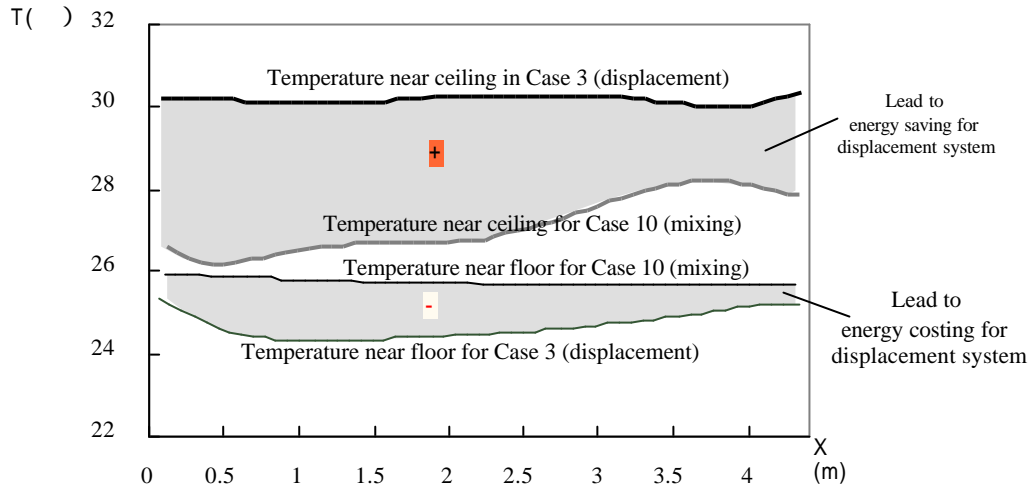


Fig.5-22. Temperature difference between displacement ventilation and mixing system near the floor and ceiling in X direction

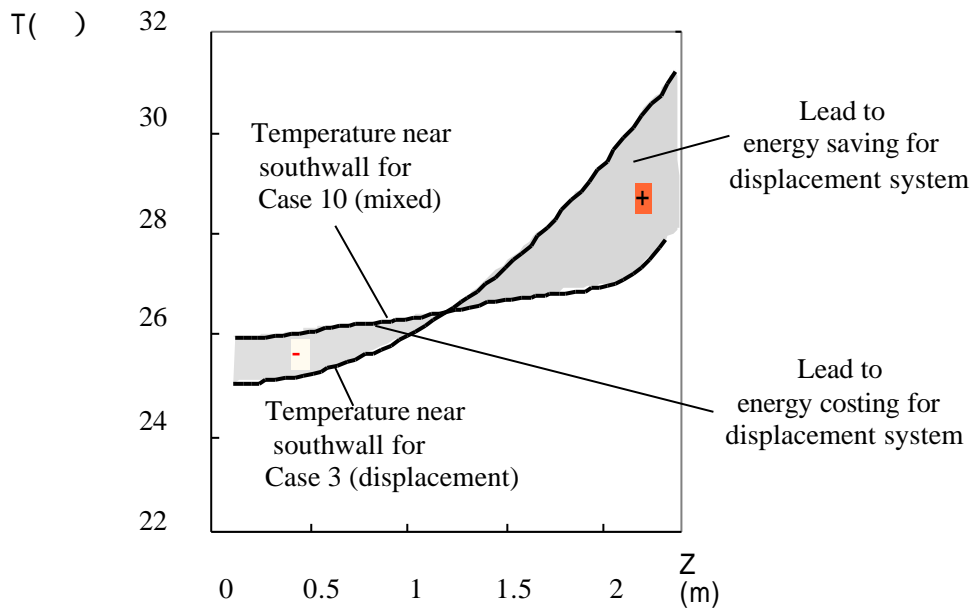


Fig.5-23. Temperature difference between displacement ventilation and mixing system near the south glass in Z direction

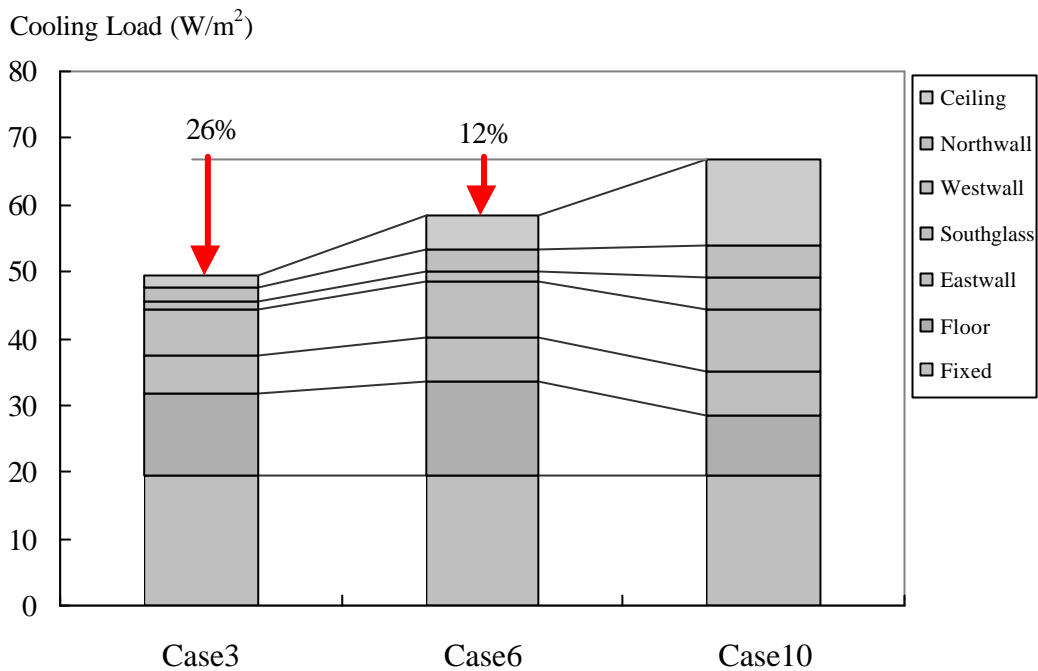


Fig.5-24. Detail composition of cooling load for displacement ventilation (Case 3, Case 6) and mixing system (Case 10)

5.4.4. Effect of swinging louver

As the louvers in the diffusers can swing in Y direction, this may also affect the air distribution, velocity and thermal comfort. In Cases 8 and 9, there are some partitions with the height of 1.4m in the middle of the room.

5.4.4.1. Temperature distribution

Fig.5-25 shows the effect of swinging louvers on temperature distribution in a room with or without partitions. Although the temperature in Case 7, which has no swing louvers, is a little higher than Case 3, which has swing louvers, their difference is only about 0.2°C, very small, which means that the louvers are helpful for air distribution but have little effect if there are no partitions or barriers for airflow in the room.

But if there are some partitions in the room, this will lead to a great effect on temperature distribution. As the temperature in Case 9, which has no swing louvers, is nearly 1°C higher than that in Case 8. And the detail temperature distribution of these two cases is shown in Fig.5-26. In Case 9, because the partitions obstruct airflow, if the airflow from the air inlet cannot change direction frequently, the temperature will be less uniformly distributed under the height of partitions, but there will be less effect for places above the partitions.

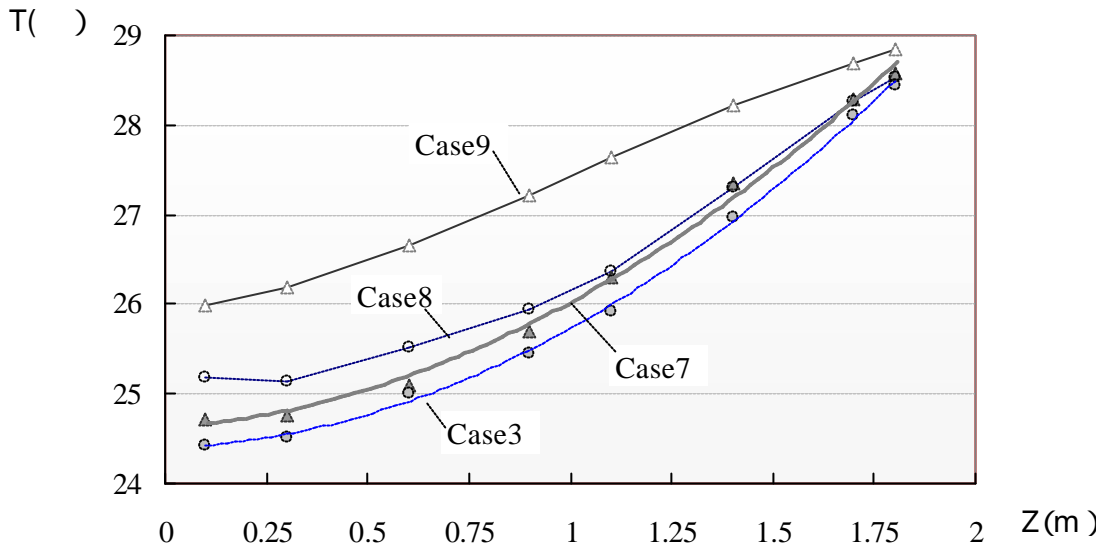


Fig.5-25. Temperature profile at Y=1.8m for Cases 3, 7-10

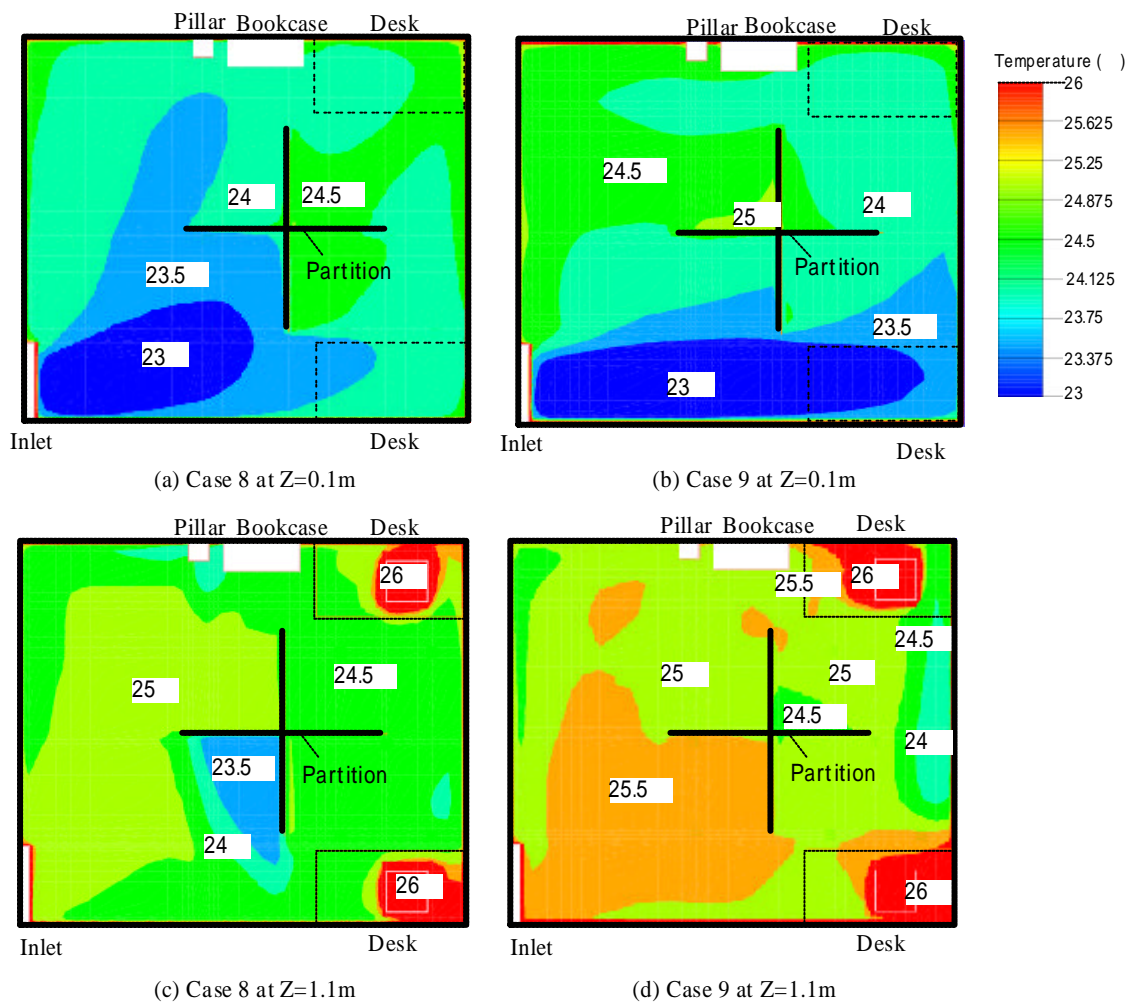


Fig.5-26. Temperature distribution for Cases 8 and 9

At places above the height of partition, the temperature distributions of Case 8 and Case 9 are similar.

5.4.4.2. Velocity distribution

From the velocity distribution in Fig.5-27, it is easy to see the effect of partition.

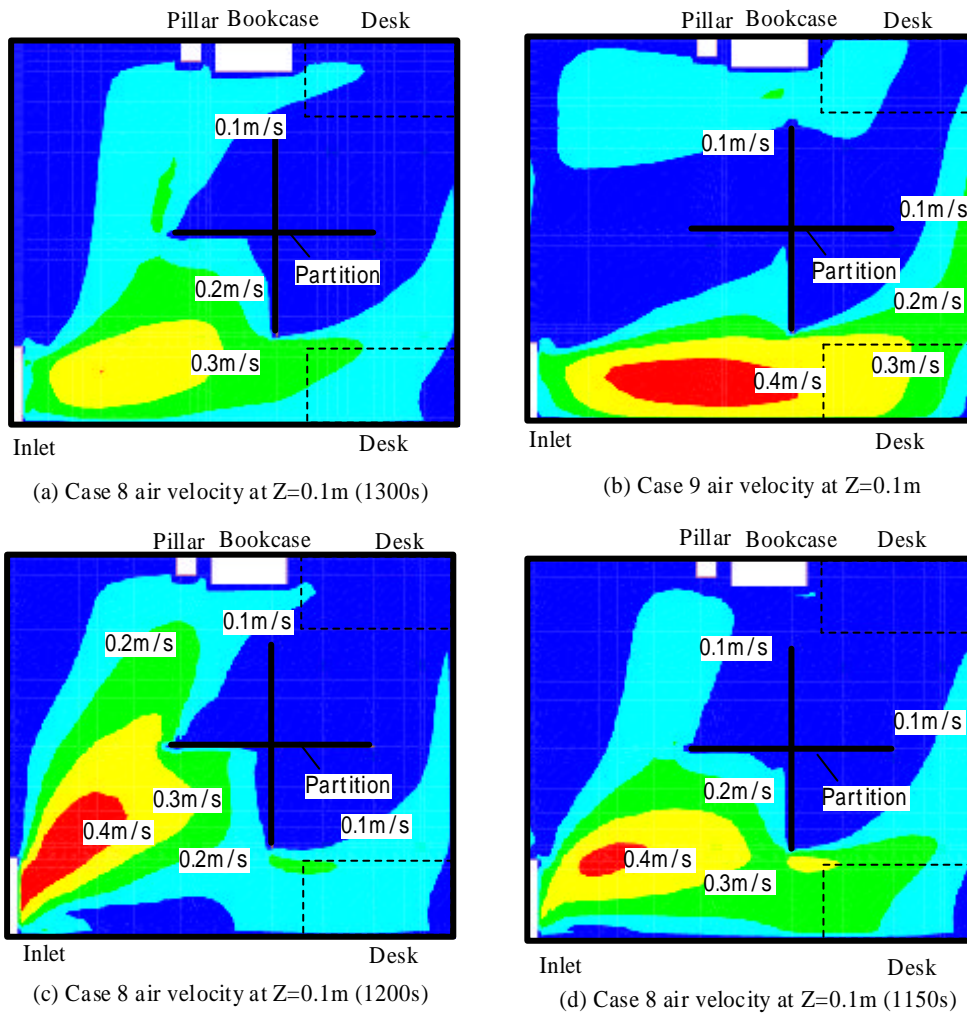


Fig.5-27. Velocity distribution at 0.1m for Cases 8 and 9

In Case 9, the velocity is very big in the vertical direction of diffuser, and the area of velocity exceeding 0.3m/s reaches the desk area. Flow direction is constant, which makes people feel discomfort.

While it is small and have little effect on working area in Case 8, and the flow direction changes frequently because of the swinging louvers. The comfort appraisalment is only a little higher than those in Case 3. This shows that if there are partitions in the room, diffuser with swinging louvers is recommended.

5.5. Summary and Conclusion

Although the height of ceiling in a residential room is lower, only 2.4m in our study, by the means of CFD simulation, the displacement ventilation system for cooling is proved to be effective for residential house. Compared with the conventional mixing system, the characteristics of thermal comfort and cooling load of displacement system are analyzed, and the effects of air change rate, height of air inlet/outlet, characteristic of diffuser, layout of room for the displacement system are studied. The conclusions are as follows:

The displacement ventilation system can realize thermal comfort and better air change effectiveness in the occupied zone, at the same time keeping the temperature gradient small, and also the small draft rating, if being carefully designed. According to simulation, the air change effectiveness of displacement ventilation is about 30% higher than the mixing system.

The air change rate has a significant effect on the thermal comfort and energy conservation in the displacement system. With the increase of air change rate, the thermal comfort will be better, but this may lead to a litter large draft rating and more energy consumption for cooling.

In this case, the air change rate of about 10-12 per hour will bring to small temperature gradient in the vertical direction, and good PMV (in the range of -0.5 to 0.5) in the occupied zone for a sitting occupant. And the sensible cooling load is about 50 W/m^2 . When the air change rate increases 1 per hour in this case, the energy consumption increases about 2.6 W/m^2 .

Compared with the cooling load of 65 W/m^2 for the mixing system in this case, the cooling load of the displacement ventilation system is about $47\text{-}56 \text{ W/m}^2$. This means that the displacement system may cut down 2-26% of the cooling load, among which about 50% comes from the decrease of heat convection from the ceiling. But it should be pointed out that the cooling load from the floor could be increased by 5-8%.

Although the position of air outlet may not change the thermal environment in the occupied zone greatly, it has an effect on the energy consumption. Compared with the mixing ventilation, the outlet at 1.8m cuts down 14% cooling load than that at the ceiling of 2.4m in this case.

As to the air diffuser with swinging louvers, they help for air distribution in the occupied zone, especially when there are some partitions in the room.

In this chapter, the basic effects of the displacement ventilation system, such as air change

rate, positions of opening and the layout of room are discussed with the help of CFD simulations. Displacement ventilation, as one type of active air conditioning method, is available for energy saving, at the same time it has a better air change effectiveness, which is suitable for occupant with high healthy requirement. The real effect for this system will be studied by field measurement in the experimental house in the next chapter.

CHAPTER 6

FIELD EXPERIMENT OF DISPLACEMENT VENTILATION IN A RESIDENTIAL ROOM

The thermal comfort and energy consumption for the displacement ventilation system has been analyzed by the means of CFD simulation in Chapter 5, in order to verify the effectiveness of the displacement ventilation system for residential house, it has been designed in the experimental house in Kitakyushu. In the following part, the details of the real system have been illustrated, then the temperature distribution, ventilation effectiveness, and energy consumption is studied according to the field experiment in the summer, and the experiment results have also been compared with the simulation result.

6.1. Details of the Displacement System

6.1.1. Outline of the Displacement System

The whole air condition system in the experimental house is shown in Fig.6-1.

The occupied zone is under 1.8m above the floor in each room. The conditioned air, which comes from the thermal storage air-handling unit (AHU) in the machine room, is mixed with the induced room air, and then the mixed air is supplied from the low part of the fan unit. The supply air goes directly to the occupant space at a quite low speed. Some of the air is induced into the fan unit, and the other goes back to the AHU as return air, while the exhaust air is discharged from the ceiling.

The detail constructions of the experiment and the thermal resistance are shown in Table 6-1. The roof, exterior wall and floor have good insulation, whose overall heat transfer coefficients are better than the recommended value in the New Energy-saving Standards. And a double skin space is set to the south of the SOHO room (1F) and the living room (2F), whose outer glazing consists of 8mm clear float with interior light blinds, while the interior glazing consists of 6mm clear float. By controlling the interior blinds, the outside solar radiation can be almost cut down, thus to cut heat gain from the south windows.

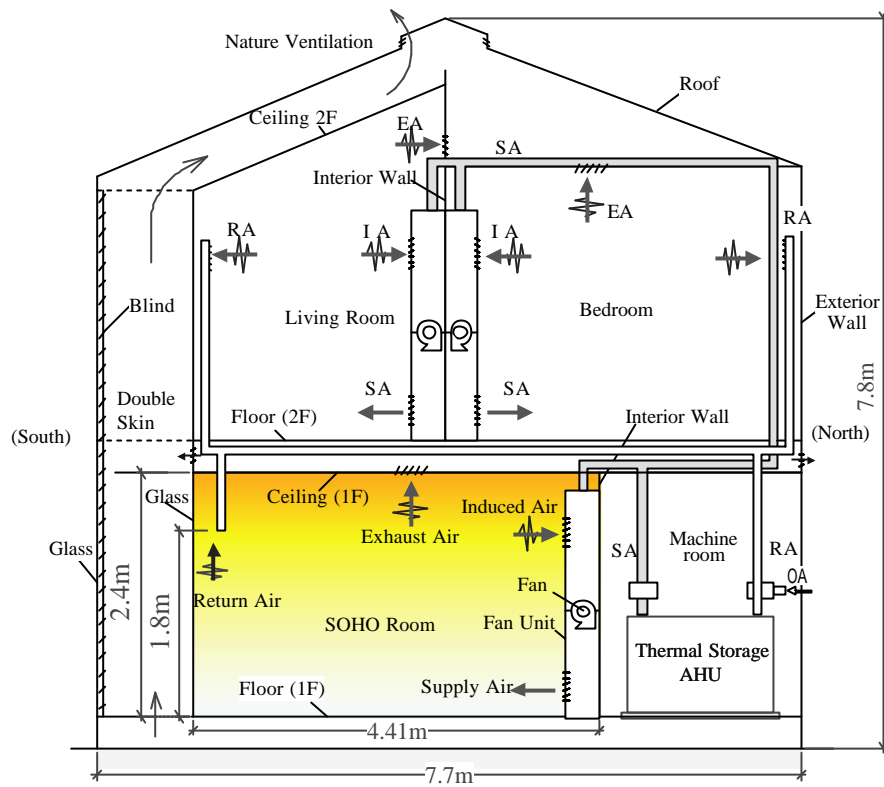


Fig. 6-1. Air conditioning system in the experimental house

Table 6-1. Detail construction and overall heat transfer coefficient U of materials

Details	Main Construction	U ($W/m^2 \cdot k$)		
		Real*	New*	Next*
Roof	8mm Glass+140mm Insulation+20mm Recycle Pet Board	0.282	0.41	0.24
Exterior Wall	8mm Glass+90mm Insulation+20mm Recycle Pet Board	0.388	0.54	0.53
Interior Wall	70mm Insulation + 10mm Recycle Pet Board	0.676		
Floor (2F)	17mm Plastic +50mm Insulation+50mm Air + 4mm Rubber+12mm Recycle Pet Board	0.47	0.62	0.48
Floor (1F)	17mm Plastic +100mm Insulation +50mm Air + 4mm Rubber+12mm Recycle Pet Board	0.33	0.43	0.34
Window	North: 3mm glass+6mm air+3mm glass	4.55	-	-
	South (double skin outside): 8mm glass	5.88		
	South (double skin inside): 6mm glass	6.67		

Note: "Real" refers to the real value in the experimental house; "New" refers to the value of the New Energy-saving Standard; and "Next" refers to the value of the Next-generation Energy-saving Standards

6.1.2. System design

6.1.2.1. Features of the Displacement System

- Induced air

As it is mentioned in Table 5-1 in Chapter 5, if the displacement system is used, the smaller temperature difference between supply air and room air would lead to a larger airflow rate. In the proposed system, some of the room air is induced into the fan unit, and then it is mixed with the cold air from the AHU before it flows into the room.

The low temperature of air from the air handling unit is designed to be 18°C, while the same amount of room air (at 26°C) is induced, the supply air from the fan unit can be mixed to be 22°C. As the VAV automatic control system have been installed, the supply air can be kept to 22±1°C.

- Low position of outlet for return air

In the summer, if there is no return air, all outside air is used for the displacement system, which will lead to a lot of energy consumption for cooling. Thus the return air outlet is set at the height of 1.8m, and the air returned to the air-handling unit can be lower than the outside air. Although the exhaust outlet is set on the ceiling, and the low amount of exhaust would not increase the cooling load so much. And there is no special consideration of air conditioning for the space over 1.8m.

6.1.2.2. Fan unit

The detail construction of the indoor fan unit is shown Fig.6-2. The vertical louvers can swing from left to right by the swing motor, and the cycle is measured to be about 40s.

The flow rate of the fan is 400m³/h at the “high volume” mode. As it is a line centrifugal fan with the power of 25W, the noise is small, and it will not affect the occupant. And the induced air outlet is also mounted with filter, which is used to clean the induced room air.

The sensors for indoor air and humidity are installed on the front side of the fan unit at the height of 1.3m.

6.1.3. Control system

The sketch of the control system for air conditioning in the experimental house is shown in Fig. 6-3.

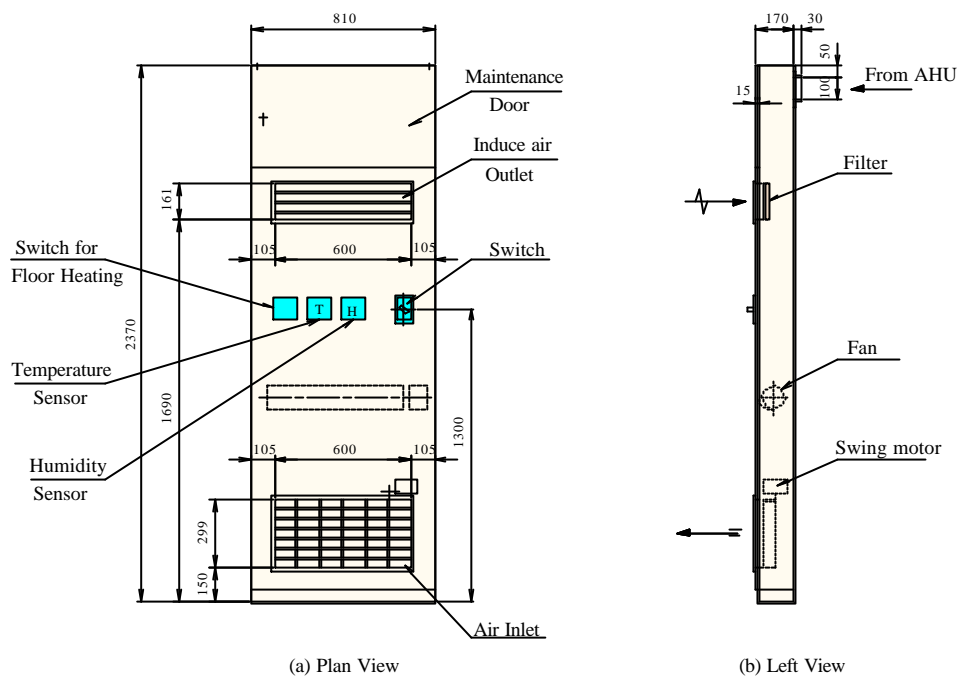


Fig. 6-2. Construction of the fan unit

The basic control method for the air conditioning system is variable air volume system (VAV). According to the temperature sensor in the return duct, automatic damper in the supply duct can be controlled. If further control is need, the inverter of the fan in the thermal storage unit also can be controlled. Here the Proportional-Integral-Derivate (PID) type of control action is adopted, which adds a derivation term to the controller, and it can reduce the risk if the controlled variables respond quickly, thus to control the system more effectively.

As there is an occupant sensor in the SOHO room, it is interlocked with the fan. If the occupant leaves the room for a period of time (setting value), the air conditioning system together with the lighting will be turned off.

The automatic control is executed by a main personal computer with the operation system of Windows NT. Through the LONWORKS net system, this main computer can communicate with the sensors and controllers. As the speed of the LONWORKS reaches 78kbps, the transfer of signals in this system is very fast. People may even revise the control program according to different requirements. The sketch of the control system is shown in Fig.6-3.

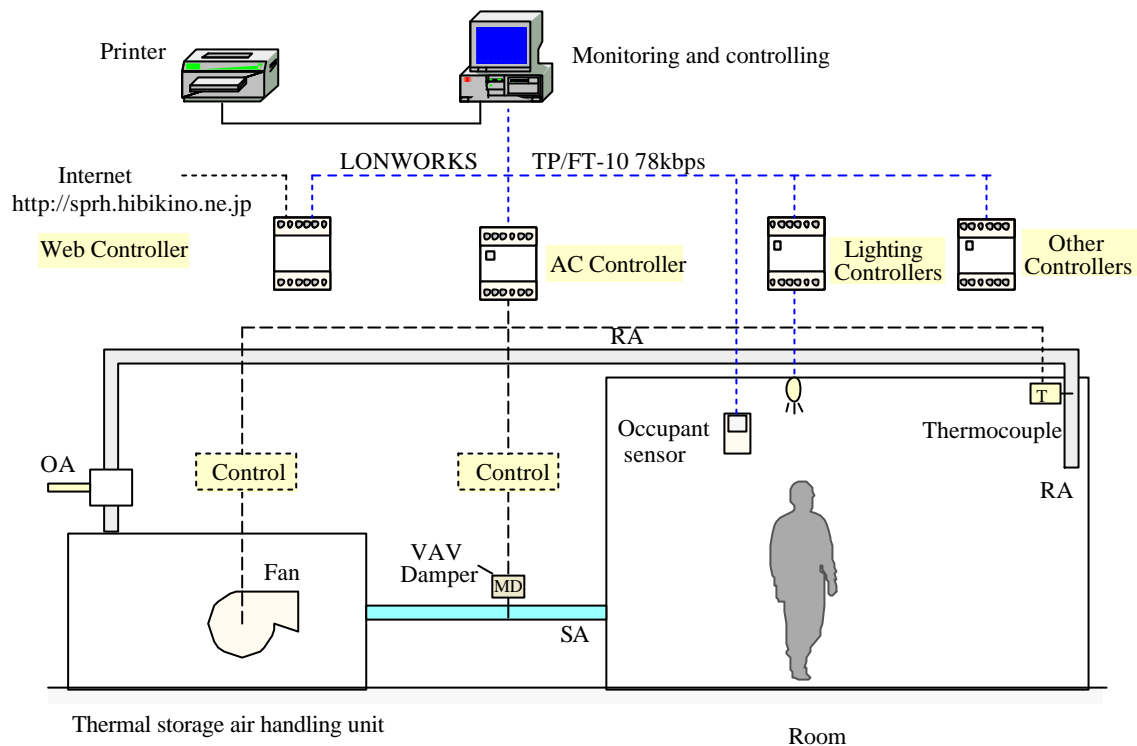


Fig. 6-3. Sketch of the control system for air conditioning in the experimental house

The other characteristic of this control system is opened to the outside world through Internet. Through the web controller, the situations of the room can be known at anywhere in the world. People may even control the system by Internet.

Accounting for the security of the Internet, the control of the experimental house by Internet is prohibited, but monitoring is available.

6.2. Outline of Field Experiment

The field experiment of displacement ventilation was carried out in the SOHO of the experimental house since July 29 to August 3 in 2001, when the outside air reached its peak during that period. During this field experiment, the blinds in the double skin were completely shut down, there were not direct solar radiation transmitted into the room.

6.2.1. Site conditions

The dimension of the SOHO room, the size of air inlet and outlet, and heat release of equipment and human are shown in Table 6-2.

Table 6-2. Site conditions in the experiment room

Item	Specification	Center Height
SOHO Room	L4.41×W3.8×H2.4=40m ³	-
Supply air inlet	L0.6×W0.3=0.18m ²	0.3 m
Induced inlet	L0.6×W0.16=0.096m ²	1.77 m
Return outlet	L0.55×W0.1=0.055m ²	1.8 m
Exhaust outlet	L0.18×W0.1=0.018m ²	2.4 m
Equipment and human heat release		
Light	25W×6=150W	2.4m
Computer	200W×2=400W	0.8m
Human (sensible)	55 W×2=110W	1.1m

Note: there were two people in the SOHO during experiment.

6.2.2. Test points and instruments

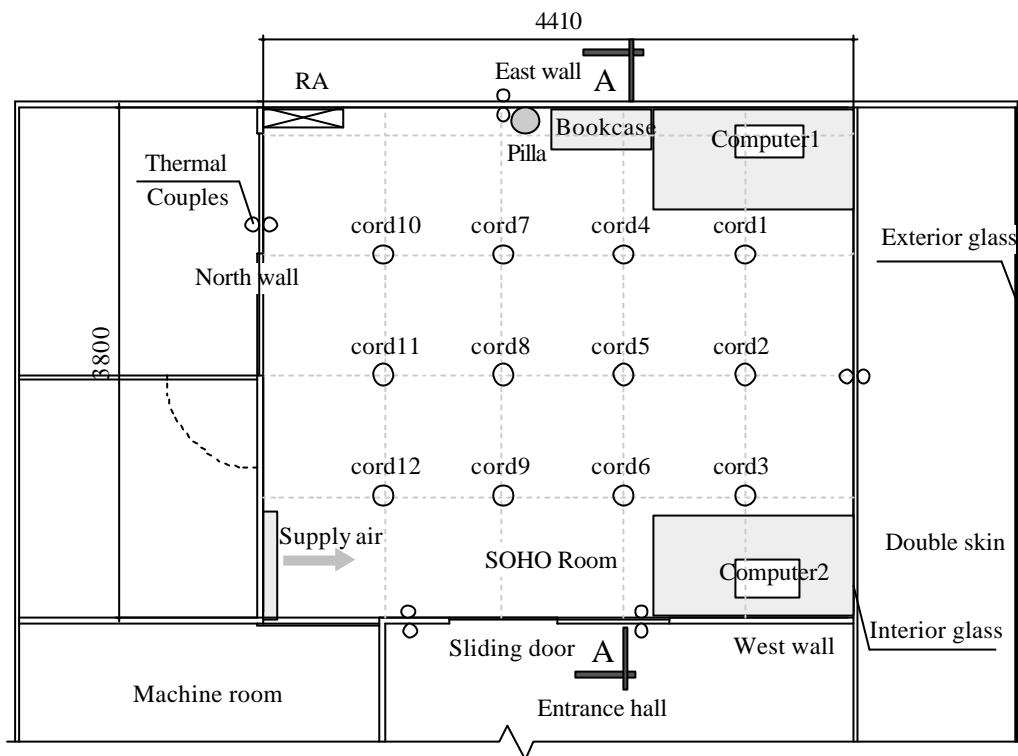
6.2.2.1. Temperature and humidity

In order to test the air temperature (dry-bulb) distribution in the occupant space, there are 12 cords in the occupied zone, and 4 sensors (T-type thermo couples) in the vertical direction with the height of 0.1m, 0.6m, 1.1m and 1.7m, all together there are 48 points to be tested, which are detailed in Fig.6-4. Here 0.1m is equal to the height of ankle, 0.6m is the height of the body for a seated people, 1.1m is the height of head for the seated people, and 1.7m is the height of a standing people.

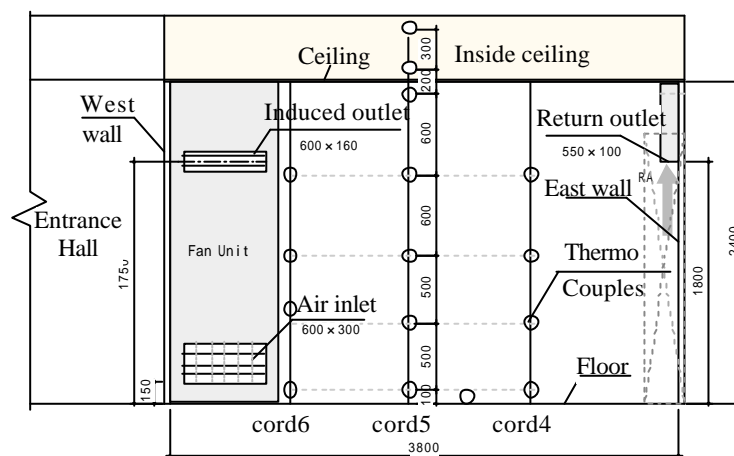
The temperature and humidity of supply air, return air and outside air are measured, as well as the interior surface temperatures, such as temperature of wall, floor and ceiling.

6.2.2.2. Air velocity distribution

Air velocity at the height of 0.1m and 1.1m is measured, and there are 8 points (Cord1-Cord6, Cord10, Cord12) in the horizontal surface. The air velocity in the high places is also tested.



(a) Plan of the test points



A-A Section

(b) Section of the test points

Fig. 6-4. Points distribution in the SOHO (plan view and section view)

6.2.2.3. CO₂ concentration

The CO₂ concentration in the occupied zone has been measured at the height of 0.1m, 1.1m, 1.7m and the places under the ceiling, as well as the CO₂ concentration of supply air and outside air.

6.2.2.4. Others

Other items such as the supply air volume, induced air volume, return air velocity, are also tested. In addition, the outside climate conditions, like solar radiation, which are detailed in Chapter 4, are recorded.

6.2.2.5. Points list and instruments

The whole test points and instruments are listed in Table 63. Most of the data are recorded in a data collector, or by computer.

Table 6-3. Test points and instruments in displacement ventilation system in summer

No.	Test points	Numbers	Instruments
1	Room air temperature	48	Thermal couples (T-6F, 0.2Φ)
2	Wall, floor, ceiling temperature	10	
3	Ceiling air temperature	3	
4	Temperature/humidity of supply air, return air, outside air	3	Thermal recorder (TR-72S)
5	Air velocity	24	RION AM-097
6	CO ₂ Concentration		ALNOR8610
7	Air flow	6	Recorded by Computer
	Air flow (for Check)	1	ALNOR Standard Balometer
8	Temperature correction	1	Assman Ventilated Psychrometer

Note: Test points for climate conditions are the same as shown in Table 4-2.

6.2.3. Scene on site

The setting of the instrument is shown in Fig.6-5 (a), and the scene of field experiment in SOHO is shown Fig.6-5 (b).

6.3. Results of experiment and simulation

6.3.1. Climate conditions

During the field experiment, the average temperature of outside air was over 30°C in the daytime, while the peak solar radiation reached 900W/m². The outside conditions on August 2, 2001 were detailed in Fig.6-6, with the peak temperature of 35.8°C at 14:00.



(a) Setting of the instruments

(b) Scene of testing

Fig. 6-5. Scene of the displacement ventilation test in Aug. 2001

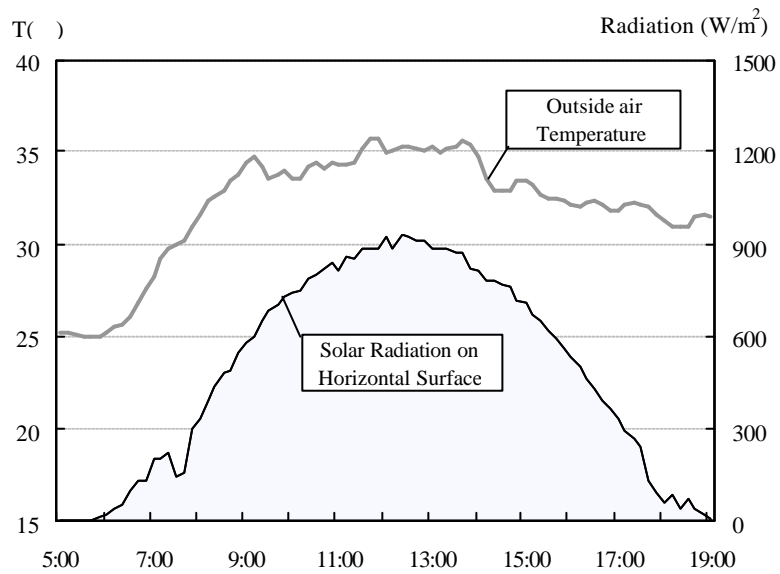


Fig. 6-6. Outside temperature and solar radiation on August 2, 2001

All the other data used for analysis were on the same day of Aug. 2 in the following discussion.

6.3.2. Conditions of Supply air

The conditions of the supply air from the AHU are detailed in Fig.6-6. The tested supply air temperature was controlled to be in the range of 18-18.5°C during most of the running time, while the airflow rate was kept to be about 280-300m³/h. And the relative humidity of the

supply air was about 80% in the duct.

The room air was kept to in the range of 26-27°C, and the temperature variation in the room was quite small, which is shown in Fig.6-7, during the testing period. At the same time, the temperatures of supply air, and airflow rate were also kept to be in balance. It should be noted that the supply air volume coming into the room is larger than that from the AHU because of the induced air. It depends on the airflow rate of the fan in the fan unit.

The flow rate was measured to be 420m³/h at the air inlet when the volume switch is at the high mode. And the temperature variation is similar to that in the above figure, while the supply air temperature was in the range of 21.5-22.5°C.

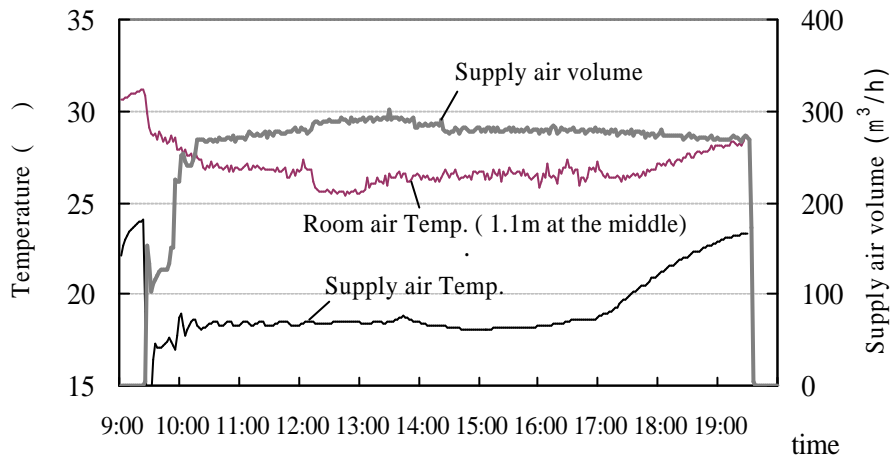


Fig. 6-7. Supply air temperature and airflow rate from the AHU

6.3.3. Temperature distribution

6.3.3.1. Temperatures of interior surfaces

As the displacement ventilation system began on 9:30, the variation of temperature on the interior surfaces in the SOHO is detailed in Fig.6-8. The surface temperature went down after the air conditioning system was turned on. For example, temperature of the east wall reached 34°C, while the others reached 30-31°C at 9:30. After the air conditioning system was put into operation, those temperatures went down slowly, and they reached the balance temperature at about 28°C.

On the other hand, temperature of the south glass reached its peak 30.8°C during 12:00 to 14:00, although the blind in the double skin space was completely shut down. And the blind temperature went down after 15:00.

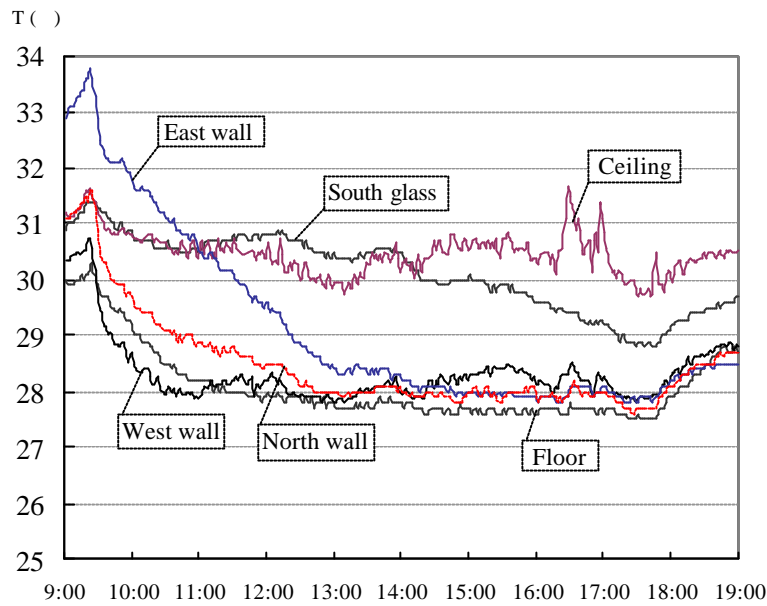


Fig. 6-8. Temperatures of interior surfaces during 9:00 to 19:00

6.3.3.2. Stratification in temperature

Fig.6-9 shows temperature variation of points at Cord 5 ($X=2.7\text{m}$, $Y=0\text{m}$, $Z=1.8\text{m}$) in the middle of the room during 9:00 to 19:00, and the other 11 cords have the similar variation.

Before air conditioning system is turned on, temperature of each point was about 30°C and vertical temperature difference is very small, which means the air temperature is uniformly distributed in the room. After the air conditioning system starts, air temperature falls down, the vertical temperature difference becomes great. Temperature distribution becomes stable an hour later. Average temperature from 0.1m to 0.6m high is about 25.5°C , 1.1m about 26.5°C and 1.7m about 28°C during 11:00 to 17:00. The air near the ceiling is about 30°C . Testing points on other cords have the same variation as Cord 5.

The room air temperature goes up slowly after 17:00, because the ice stored in thermal storage AHU has been used up.

The temperature profile at 12:00 at the middle section of the room, i.e. $Y=1.8\text{m}$ is show in Fig.6-10. The average temperature at 0.1m is 25°C , 0.6m 26°C , 1.1m 26.8°C , and 1.7m about 28°C . It is clearly that the air temperature is stratified along the height.

The comparison of the measured temperature and calculated results at $Y=1.8\text{m}$ is shown in Table 6-4, which shows that the simulation of Case 3 in Chapter 5 has a correlation coefficient of 0.95 with the temperature measured (Fig.6-11).

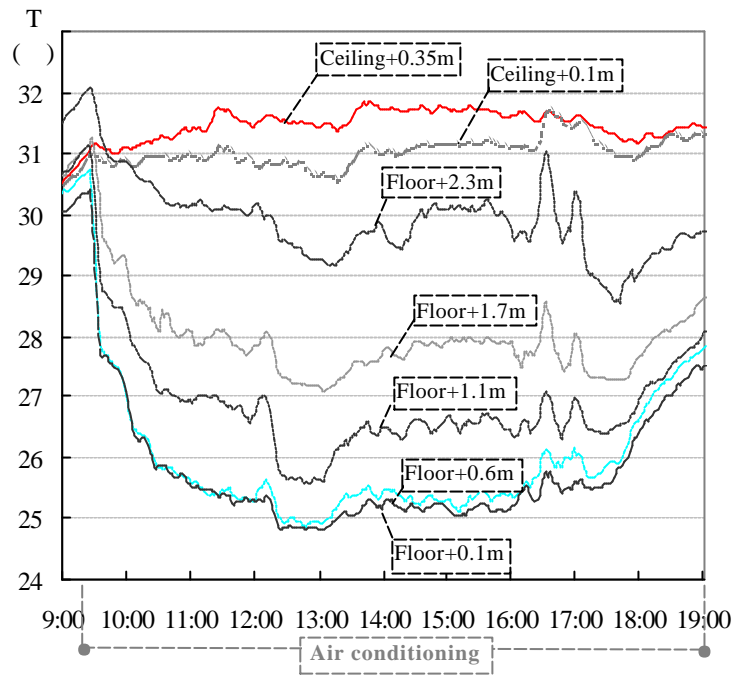


Fig. 6-9. Air temperature at different heights in the middle of the room (Cord 5 X=2.7m, Y=1.8m, Z=0m from 9:00 to 19:00)

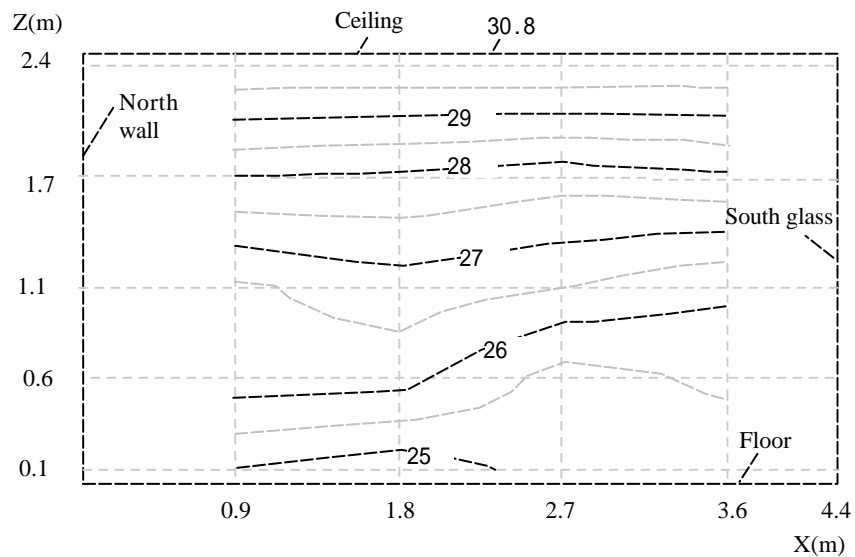


Fig. 6-10. Air temperature at different heights in the middle of the room (at the section of Y=1.8m, at 12:00)

Table 6-4. Comparison of simulation and measurement at Y=1.8m (12:00)

X (m)	Z (m)	Temperature (°C)	
		Simulation Value	Measured Data
0.9	0.1	24.7	25
0.9	0.6	25.3	26.3
0.9	1.1	26.3	26.4
0.9	1.7	28.1	28
1.8	0.1	24.3	24.7
1.8	0.6	25.1	26.2
1.8	1.1	26.2	26.8
1.8	1.7	28	27.9
2.7	0.1	24.3	25.2
2.7	0.6	24.9	25.3
2.7	1.1	26	26.5
2.7	1.7	28	27.7
3.6	0.1	24.5	25.2
3.6	0.6	24.7	25.6
3.6	1.1	25.7	26.1
3.6	1.7	28.1	27.9
2.7	2.3	30.3	30.8

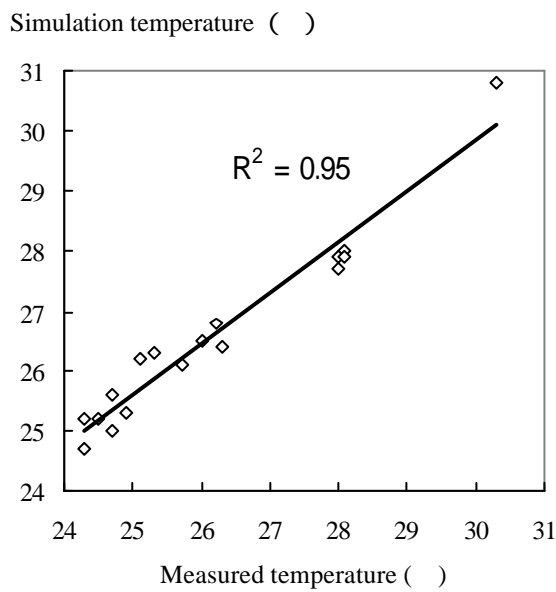


Fig. 6-11. Correlation coefficient of the simulation result and measurement

6.3.3.3. Temperature deviation

Temperature distribution at different heights at 12:00 is shown in Fig.6-12. According to Equations (5-18)-(5-19) and the supply air temperature, the calculated temperature deviation is shown in Table 6-5. With the increase of height, the temperature deviation decreases from 27% at 0.1m to 3% at 1.7m when the supply air is 22°C. As the diffuser is near the floor, it has more effect on the lower places. Because of the swinging louvers, air temperature has a great deviation in lower parts. According to the simulation in Chapter 5, the lower places have a bigger deviation of about 30%. Although it was smaller in the experiment, it shows the same trend.

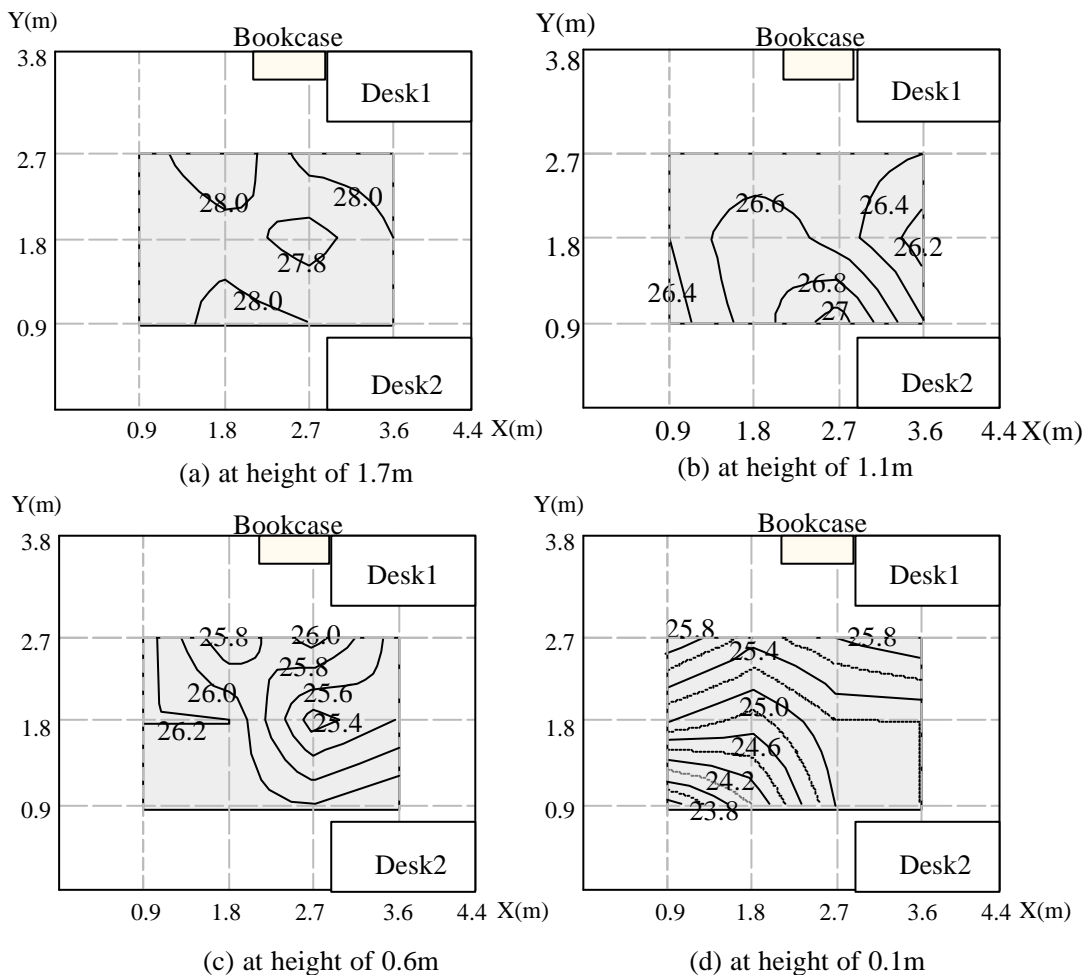


Fig. 6-12. Temperature distribution at different heights at 12:00 on August 2

6.3.3.4. Temperature gradient

The variation of temperature gradient from the floor to the ceiling is detailed in Fig.6-13. Before air conditioning system is on (at 9:00), the temperature gradient from floor to the ceiling is smaller than 0.5°C/m. After it starts, the temperature gradient increases with the time. For example, it is about 1.3°C/m at 10:00 when the system has been put into operation for one hour; and it increases to 1.7°C/m at 11:00, then it comes to a relatively steady state with a stable temperature gradient (Fig.6-13a). While the temperature gradient reaches 3°C/m near the air inlet (Fig.6-13b). After the air conditioning system is turned off, the temperature gradient becomes smaller, and two hours later, it comes back to about 0.5°C/m. The comparison of the temperature gradient between experiment and simulation is shown in Fig.6-14, and the simulation has a quite good accuracy.

Table 6-5. Temperature deviation at difference heights (12:00)

H(m) \ Temp	$T_{1.7m}-T_{sa}$	$T_{1.1m}-T_{sa}$	$T_{0.6m}-T_{sa}$	$T_{0.1m}-T_{sa}$
	(°C)	(°C)	(°C)	(°C)
Cord1	5.94	4.19	3.26	3.81
Cord2	5.79	3.86	3.36	3.01
Cord3	5.79	4.20	4.00	3.01
Cord4	5.88	4.28	3.87	3.63
Cord5	5.52	4.29	3.08	2.96
Cord6	5.83	4.82	3.85	2.82
Cord7	5.44	4.20	3.38	3.25
Cord8	5.74	4.57	3.96	2.52
Cord9	5.90	4.53	3.93	1.78
Cord10	5.71	4.29	4.07	3.80
Cord11	5.77	4.15	4.07	2.75
Cord12	5.56	4.10	3.93	1.14
Average of T_i-T_{sa}	5.74	4.29	3.73	2.87
t_{dev}	2.7%	5.8%	9.4%	27.4%

Note: The supply air is 22.2°C in calculation.

Temperature gradient in the occupant space from the ankle (0.1m high) to the face (for a sitting man is about 1.1m high) is within 2°C/m. According to the standard of ISO7730, temperature gradient is recommended within 3°C/m. The guidance of SCANVAC (Murata,

1997) states that the temperature gradient of $2^{\circ}\text{C}/\text{m}$ will cause 3% dissatisfaction degree (Fig.6-15).

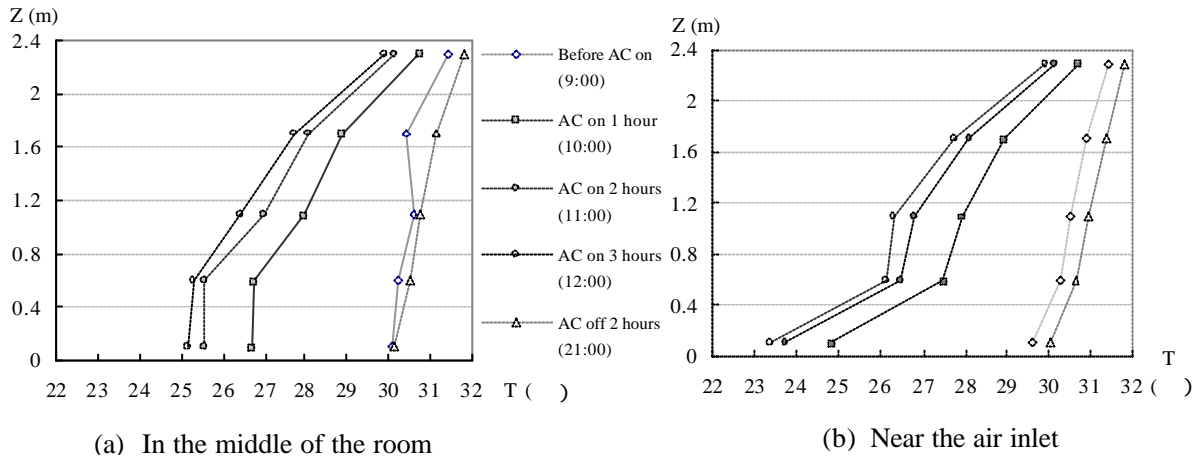


Fig. 6-13. Indoor temperature gradient

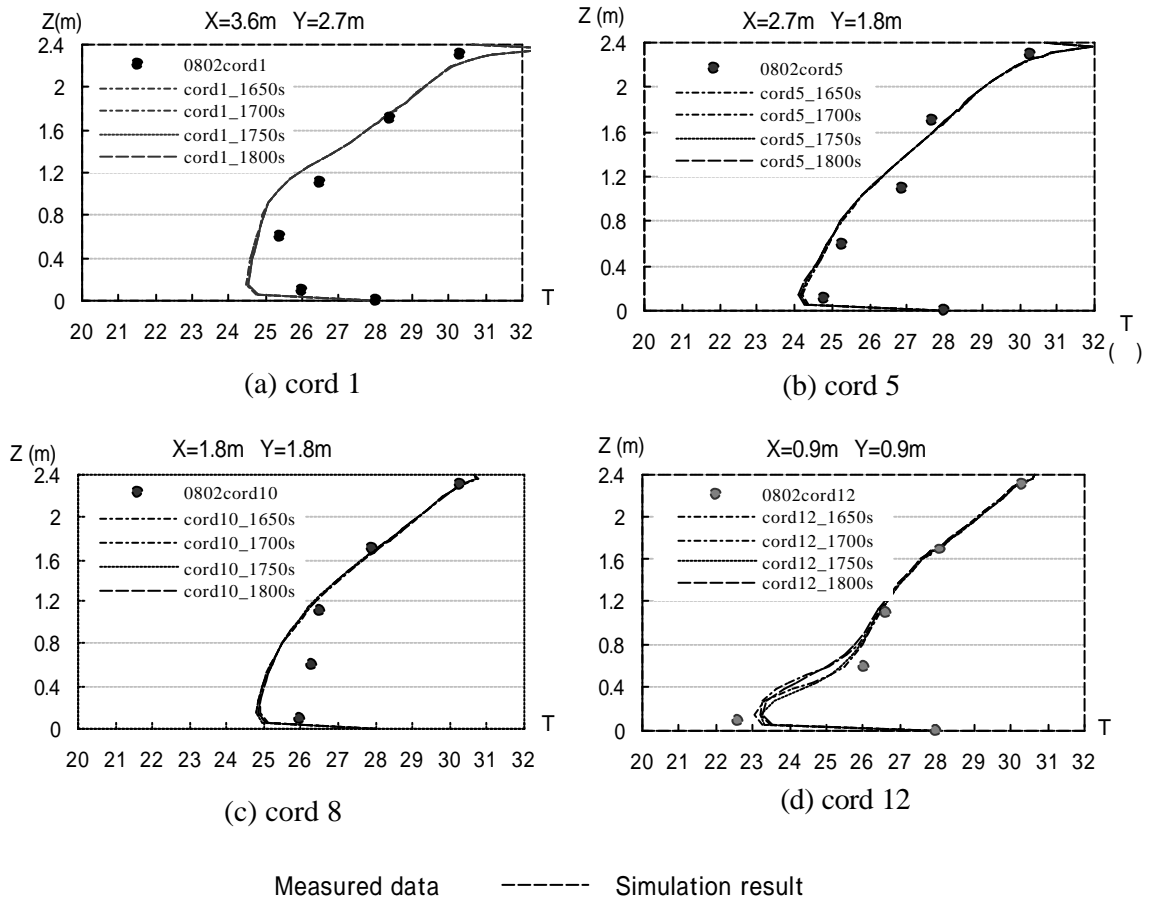


Fig. 6-14. Comparison of temperature gradient between experiment and simulation

The temperature gradient near the air inlet is about 3°C/m, which means 8% dissatisfaction, and the occupant will feel a little cool there. In the occupant space, it can be considered that the temperature gradient caused by displacement ventilation has little effect on thermal comfort.

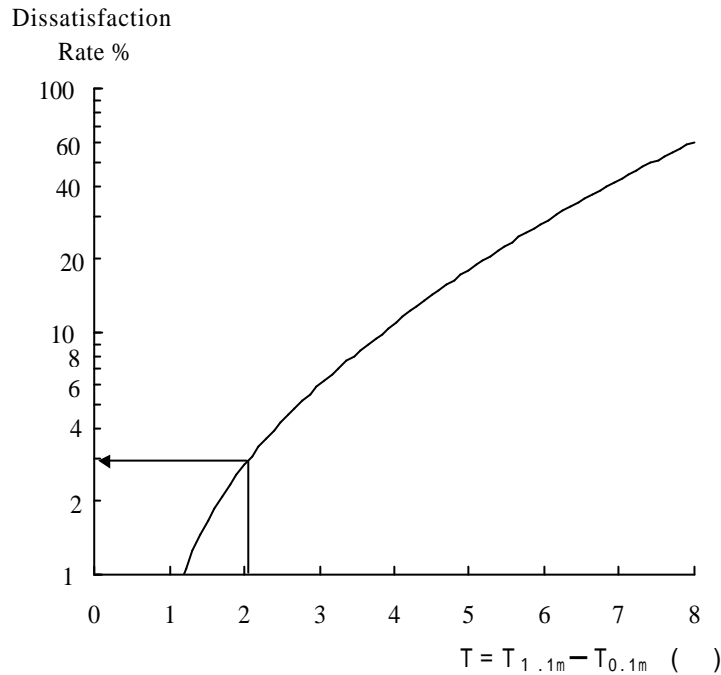


Fig. 6-15. Dissatisfaction rate caused by temperature stratification

6.3.4. Air humidity

The humidity and temperature of air are measured at the height of 1.3m on the fan unit. From 11:30 to 12:30, the average temperature is 24.5°C, and the average humidity is 65%, thus to calculate the absolute humidity to be 0.0126kg/kg.

Take absolute humidity as constant, according to temperature distribution, the humidity distribution can be calculated, which is shown in Fig.6-16. And the relative humidity of air in the occupied zone is in the range of 50-60%.

6.3.5. Velocity distribution

The air velocity of points on Cord 1, Cord 2, Cord 4 and Cord 5 at the height of 1.1m is shown in Fig.6-17, and the average velocity is below 0.25m, while the velocity above 1.8m is smaller than 0.1m/s. Because of the swinging of the air diffuser, the turbulent intensity of velocity in the occupied zone is about 20%.

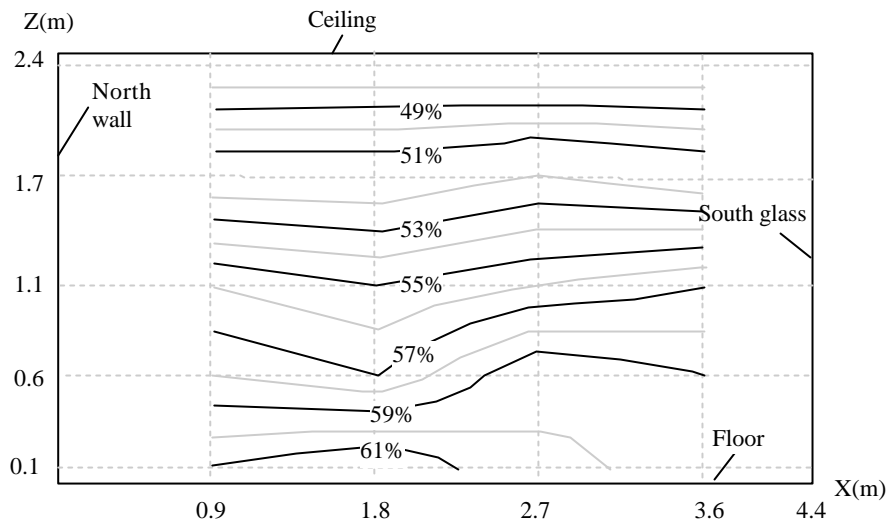


Fig. 6-16. Distribution of relative humidity in the middle of the room (at Y=1.8m)

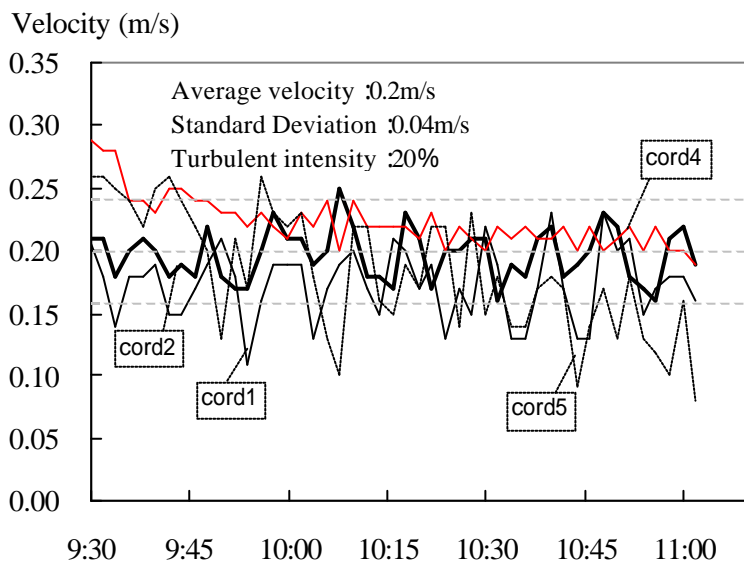


Fig. 6-17. Velocity at 1.1m in the middle of the room from 9:30 to 11:00

The flow rate of supply air from the fan unit is about 425m³/h at 12:00, with the average velocity of 0.65m/s at the air inlet surface, and the velocity distribution at the height of 0.1m is shown in Fig.6-18.

Compared with these measured velocity, the simulation has a correlation coefficient of 0.82 with experiment. Although the air velocity is faster than 0.4m/s near the air inlet, and the

flow direction changes frequently, it is below 0.3m/s in the occupied zone.

Thus the air inlet has little impact on the velocity distribution in the occupied zone.

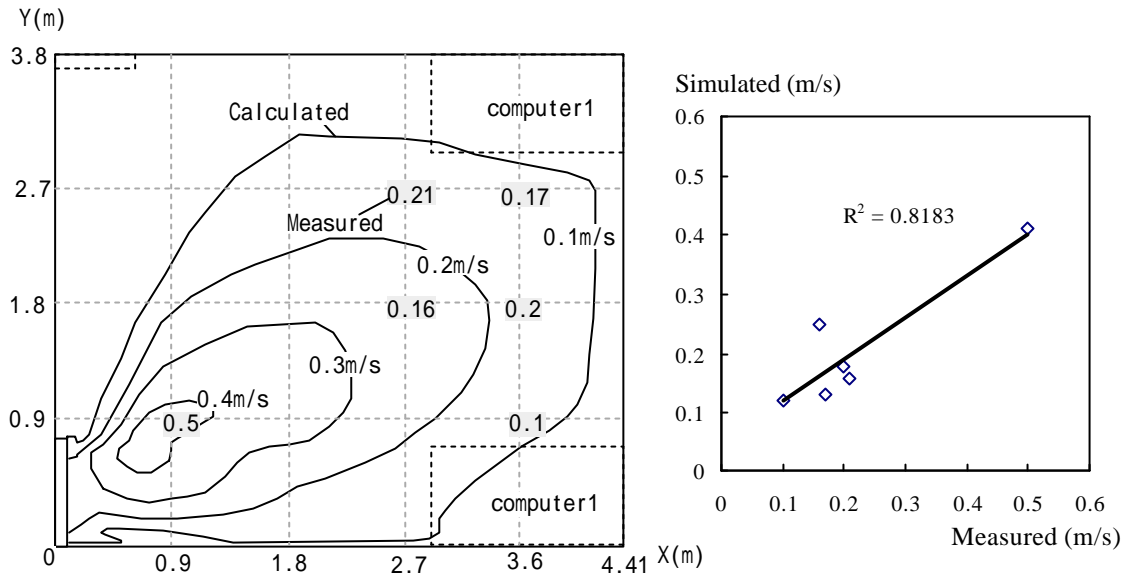


Fig. 6-18. Comparison of velocity distribution between field experiment and simulation (at the height of 0.1m at 12:00)

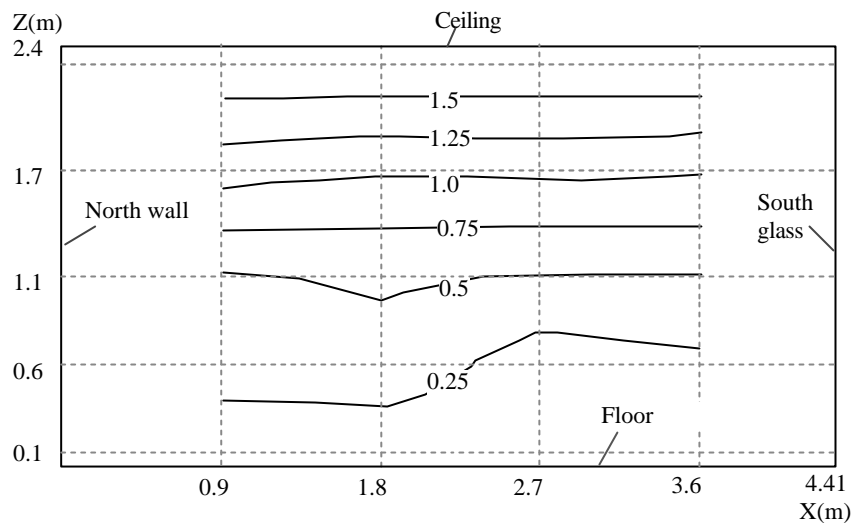
6.3.6. Draft

The variation of air velocity in the occupied zone will lead to draft sensation. According to Standard 55-1992, the percentage of people dissatisfied due to draft can be expressed by Equation (5-22).

Therefore in this field experiment the average draft in the occupied zone is about 10%, while it is 80% near the air inlet, because of great air velocity and intensity. The intensity near the air inlet is assumed to be 35%, which is detailed in Chapter 5. Occupant may feel more comfortable in the middle of the room with the dissatisfactory rate of only about 10%.

6.3.7. PMV

According to the air temperature and velocity measured, the PMV distribution at Y=1.8m in the occupied zone is shown in Fig.6-19, where the clothing value is 0.5 clo, and the metabolic rate is 1.2 met (70W/m²). The radiation temperature is assumed to be equal to the dry-bulb temperature, while the relative humidity is assumed to be 60%.



Note: the air velocities between the height of 0.6m and 1.1m are taken as 0.2m/s; at 1.7m is 0.15m/s; and it is 0.1m/s at the height of 2.3m.

Fig. 6-19. PMV distribution at Y=1.8m in the middle of the room at 12:00

Below the height of 1.1m, PMV is smaller than 0.5, while it is 1.0 at the height of 1.7m and over 1.5 at the height of 2.2m. Although it is over 1.0 above the height of 1.8m, it has little effect on a sitting occupant (at the height of 1.1m).

6.3.8. CO₂ concentration

After the temperature distribution became stable, concentration of CO₂ is measured vertically at the section of Y=0.45 (Fig.6-20). The Concentration of CO₂ is relatively low near inlet, while it is quite high near the ceiling. For example, the average concentration in the occupied zone is 600ppm, and it is 800ppm near the ceiling, while the outdoor CO₂ concentration is about 360ppm.

Carbon dioxide has been widely used as an indicator of indoor air quality. The maximum limit of 1000ppm CO₂ is recommended to satisfy comfort (odor) criteria, according to Indoor Environmental Management Standard in buildings of Japan (Inoue, U. 1996).

Although the age of air has not been measured in this test, according to those measured CO₂ concentration, it is lower in the occupied zone than that in the higher places. While the CO₂ concentration in the mixing ventilation would be uniformly distributed. Therefore it can be concluded that the air exchange efficiency of displacement ventilation is better than that of the mixing ventilation.

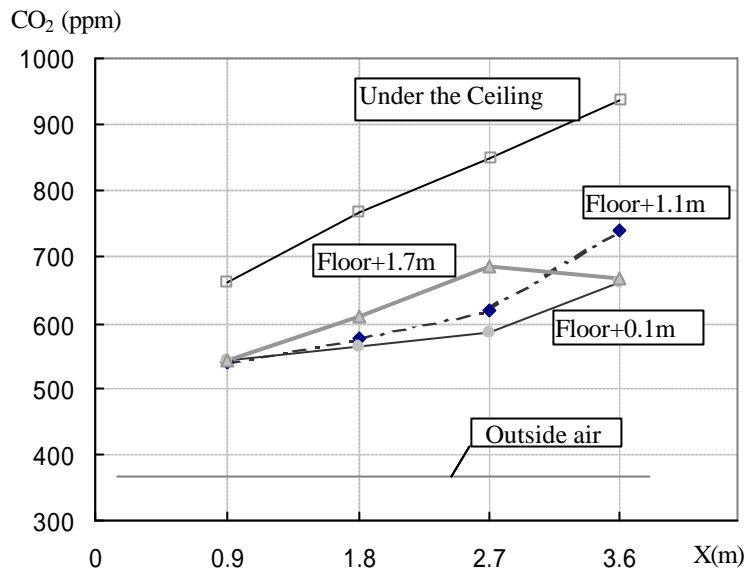


Fig. 6-20. CO₂ concentration distribution at the section

6.3.9. Energy consumption of cooling

According to Equations (5-8) to (5-12), the cooling load (sensible heat) in the room can be calculated, which is shown in Fig.6-21. Here, the convection heat transfer coefficient α is taken as 4w/m^2 , and the ratios of convection for $q_{appliance}$, q_{person} and q_{light} are all set to be 50%.

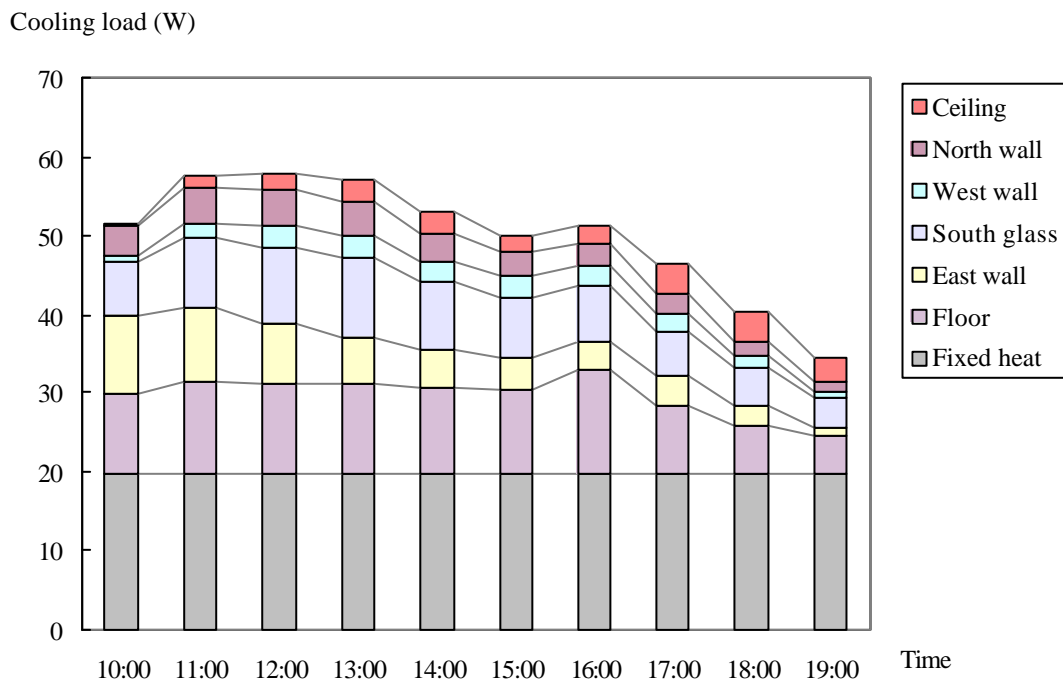


Fig. 6-21. Calculated cooling load in the experiment room

The average cooling load in this SOHO room is about $50\text{W}/\text{m}^2$, among which the fixed heat from appliance, person and lights accounts for 40%, and the other 60% is convection heat from walls, floor and ceiling.

The heat from floor accounts for 20%, which is the biggest, then the heat from south is 14%, and the heat from east 11%, while the heat from ceiling is very small, only about 5%.

The cooling load of experiment result at 12:00 is $58\text{W}/\text{m}^2$, compared with the simulation result of Case 3 in Chapter 5, which is about 10% higher. The reason is that the air temperature measured in the experiment is 0.9m from the walls, while it is 0.1m from the walls in the simulation. The smaller the distance is, the smaller temperature difference is, which could lead to small calculation results.

6.4. Summary and Conclusion

According to the field experiment in the residential house, the effectiveness of displacement ventilation system is confirmed. The conclusions are as follows.

- Thermal comfort

Air temperature is stratified along to the height by the displacement ventilation, and the average temperature in the occupied zone is about $25\text{-}28^\circ\text{C}$, while it is 23°C higher at the places near the ceiling. Temperature gradient from the ankle (0.1m high) to the face (for a sitting man is about 1.1m high) is within $2^\circ\text{C}/\text{m}$ in the occupant space. According to the standard of ISO7730, temperature gradient is recommended within $3^\circ\text{C}/\text{m}$. The guidance of SCANVAC states that the temperature gradient of $2^\circ\text{C}/\text{m}$ will cause 3% dissatisfaction degree.

The temperature gradient near the air inlet is about $3^\circ\text{C}/\text{m}$, which means an average of 8% dissatisfaction, and the occupant will feel a little cool there. From the whole temperature distribution in the occupant space, it can be considered that the displacement ventilation has little effect on thermal comfort with careful design.

From the point view of draft, there is about 10% dissatisfaction in the middle of the room, while it is about 80% near the air inlet.

Moreover, as to the PMV distribution, PMV is below 0.5 under the height of 1.1m, which means a comfortable environment. From 1.1m to 1.7m, PMV becomes greater, which corresponds to 20% dissatisfaction degree. But to a sitting person there is little effect. Above 1.7m the average PMV is 1.5, which means it is a little hot, but it has no effect on occupants.

According to distribution of temperature, humidity, temperature gradient, draft rating and PMV in occupant space, it can be concluded that comfortable indoor environment is realized in the occupied zone.

- Air exchange efficiency

As fresh air is induced directly to occupant space in displacement ventilation system, the air will be fresher in the occupant space than that under the ceiling. The Distribution of CO₂ concentration shows the CO₂ concentration below 1.8m is 30% lower than that above 1.8m. In the occupant space, CO₂ concentration is about 600ppm, which is smaller than the recommendation of Standard of Indoor Environmental Management in buildings of Japan.

Therefore displacement air conditioning system is considered to have good air change efficiency.

- Energy conservation

According to measured results, sensible heat load in summer is about 50-60W/m². In conventional air conditioning system, when the indoor air temperature is supposed as 27°C or 26.5°C uniformly, the sensible heat load increases about 22% and 38% respectively. As the return air is set at the height of 1.8m, the air in the occupied zone can be reused in the air-handling unit, while the air at those higher places keeps at a high temperature. Because heat convection from ceiling and the high part of walls decreases, only 5% of the total, which leads to 20-40% energy saving.

Therefore, displacement ventilation system is contributed to energy saving, as an effective method for the active air conditioning system.

Moreover, as the supply air temperature is higher than the conventional mixed system, some natural cooling sources can be available for this system, such as water wells. During the intermediate seasons, only the outdoor air may be available for free cooling.

As the simulation results have a good accordance with the measured values, the correlation coefficient for temperature is 0.95, and 0.82 for air velocity. This shows that the CFD simulation in Chapter 5 has a well prediction, and it can be helpful for the design of displacement ventilation system in the residential houses.

CHAPTER 7

EFFECTIVENESS OF THERMAL STORAGE SYSTEM IN A RESIDENTIAL HOUSE

The thermal storage systems have been often used in office buildings, but have few applications in residential houses. As the displacement air conditioning system is used in the experimental house, an air-handling unit is necessary. Here a special thermal system, which combines the thermal storage tank with the air-handling unit, is proposed in the residential house. Therefore it makes the thermal storage system possible for houses, which is expected to shift the peak load, save space for equipment, and reduce the running cost. Furthermore, as the fresh air will be introduced to the room, this will lead to good indoor air environment and occupant health.

7.1. Proposition of thermal storage system for residential house

In order to decrease the equipment size, the direct heat exchange method is proposed for the thermal storage system in the experimental house. The energy system is shown in Fig.7-1, the details are explained in the following part.

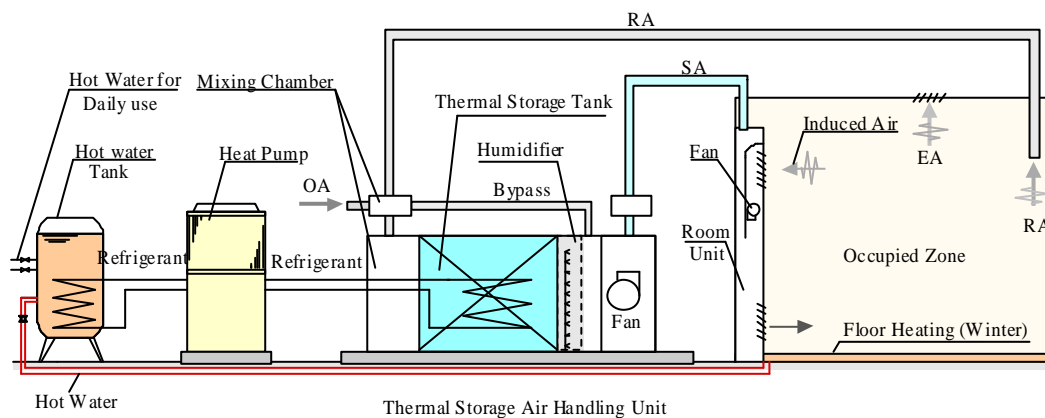


Fig.7-1. Energy system in the experimental house

7.1.1. Thermal storage air-handling unit

7.1.1.1. Direct heat exchange method

In existing ice storage systems two-phase heat exchange method is adopted as showing in

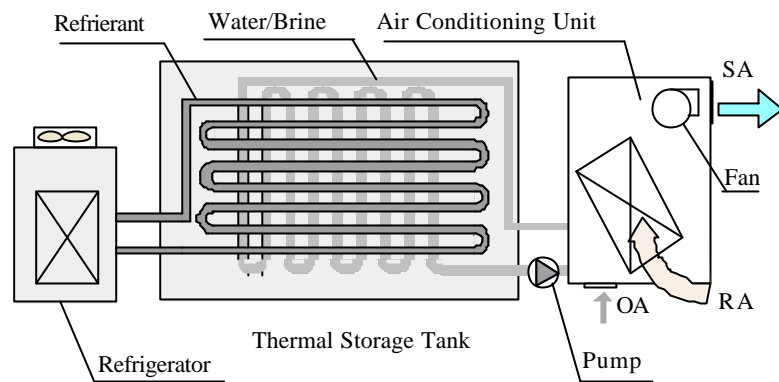


Fig.7-2. Heat exchange of the conventional system

Fig. 7-2. The one heat exchange happens between refrigerant and water or refrigeration brines, and the other happens between water and air. So one pump is necessary, which means that more space is needed. That limits the popularization of ice storage system in residential houses.

Here a simplified heat exchanger is suggested, where air exchanges heat with ice directly. Fig.7-3 shows the characteristic of this method.

The proposed storage tank is constituted of inner pipes and external copper tubes. During the summer, refrigerant circulated inside the inner refrigerant pipe, and water in the tubes becomes ice by the cold refrigerant (-20°C) from the heat pump at midnight. In the daytime, the mixed air passes through the tubes containing ice, and it directly exchanges heat with the ice inside the tube, thus the conditioned air is created.

During the winter, when the heat stored in the hot water tank becomes full, the water in the tubes can also be used for heat storage. Thus the proposed thermal storage tank acts as an auxiliary hot water tank.

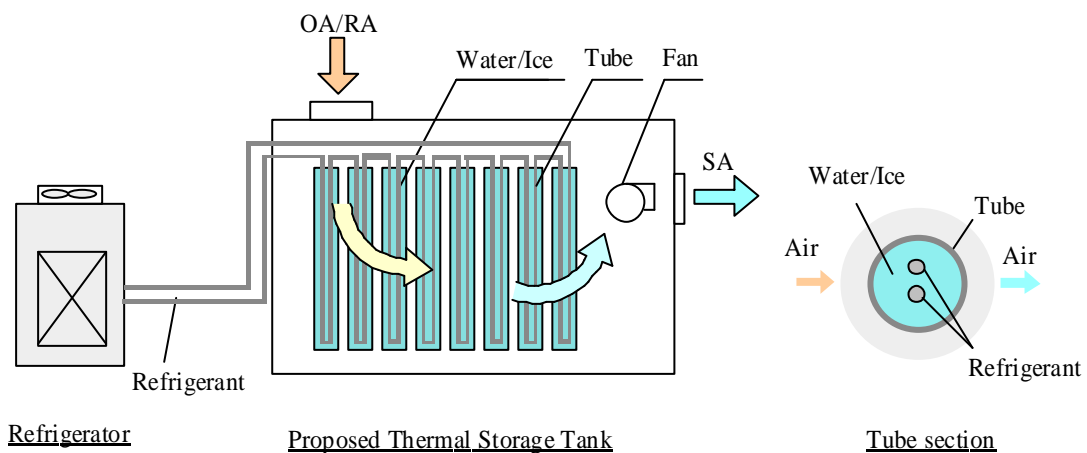


Fig.7-3. Heat exchange of the proposed system

7.1.1.2. Detail of proposed air-handling unit

The thermal storage air-handling unit consists of a mixing chamber, a thermal storage tank, a water humidifier, a flow straightener and a fan (Fig.7-4).

The hot water humidifier is only used during winter to make sure of the humidity in the rooms.

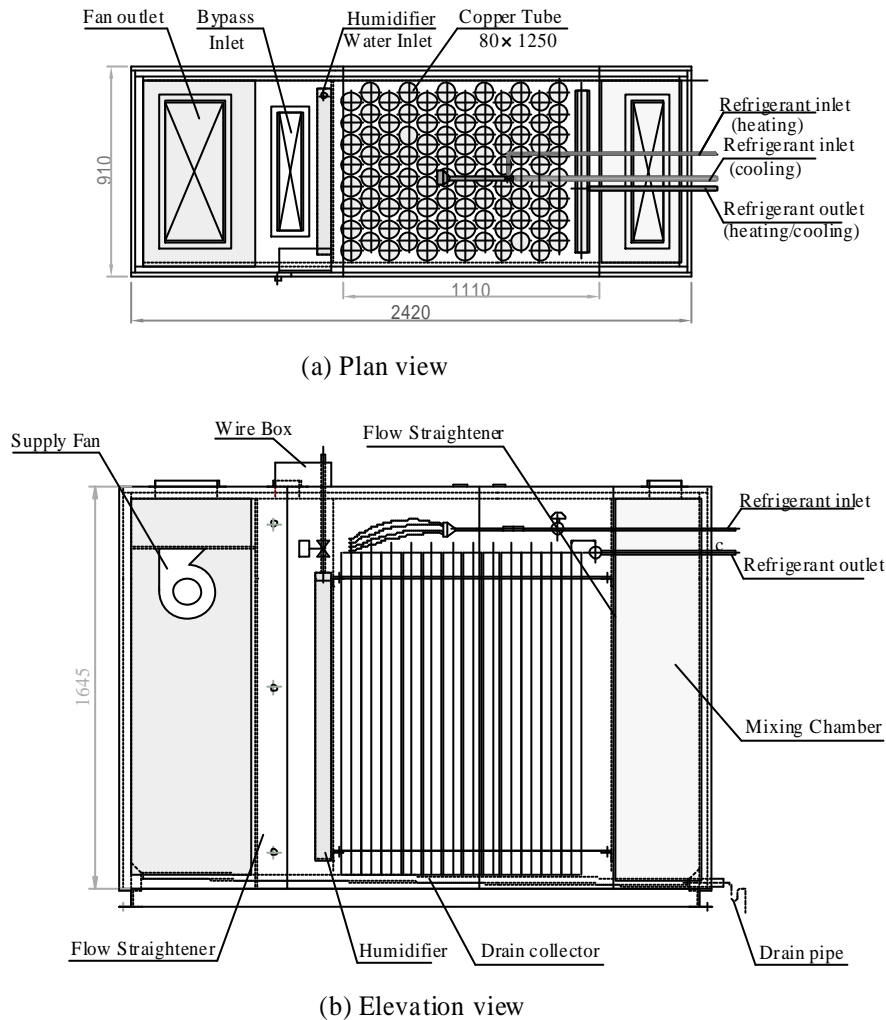


Fig.7-4. Plan view and elevation of the proposed thermal storage air handling unit

7.1.2. Hot water tank

Hot water can be guaranteed for the daily hot water supply in the whole year, and also for the floor heating system in the winter. The waste heat from the heat pump is reused by producing hot water during the summer, while in the winter the hot water is produced by heat pump. Because the COP of heat pump is larger than that of the electric water heating, as well as

heat recovery, and these will lead to better energy efficiency for the whole system.

7.1.3. Characteristics of the proposed system

Besides the benefits of common thermal storage system, such as reducing the equipment size, saving the capital cost and energy cost saving, the above system has the following merits:

- High ice packing factor (IPF)

As the refrigerant circulates in the water tubes, heat exchange between water and refrigerant is very intensive, which leads to high ice-packing factor.

- Simplified system

The air conditioning unit can be combined with the storage tank, and no pump is necessary in this process, thus the operation can be simplified due to direct heat exchange. This can lead to less space for machine and low noise for operation, which would make the thermal storage available for residential use.

- Low heat loss and transportation power

Compared with the conventional system, there is no circulation of brine, thus the simple heat change mode can lead to less heat loss. Moreover, low-temperature supply air can be available, and this will lead to low transportation power for the fan in the air-handling unit.

- High efficiency

Heat pump has higher COP than the conventional electric water heater, and waste heat is used during the summer, all these make the whole system have a good efficiency.

- Good indoor environment

The outside air will be mixed with the return air, then to be supplied to the occupant zone. Fresh air can be ensured, thus to meet the healthy requirement of occupant. While no outside air is introduced in the conventional room air conditioner.

- Mechanical ventilation and free cooling

The another function of the thermal storage air conditioning unit is that the supply fan can also be used for mechanical ventilation during the spring and autumn, or when the outside air is available for free cooling. When the natural ventilation caused by wind or thermal effect is small, this would be a backup for the mechanical ventilation, which is a key aspect of the hybrid ventilation system.

7.2. Case study

The above thermal storage system is proposed for the experimental house in Kitakyushu. The two-story residential house with floor area of 174.6m² is designed for a two-person family. The first floor is designed for future residential houses, including a SOHO room, a reception room and a machine room, etc. And the second floor is conventional living space, including a living room, a bedroom, a bathroom, etc. Basing on the SOHO function, life schedule changes correspondently, as people can work at their homes during the daytime (Fig.7-5), which leads to a different air conditioning load characteristic.

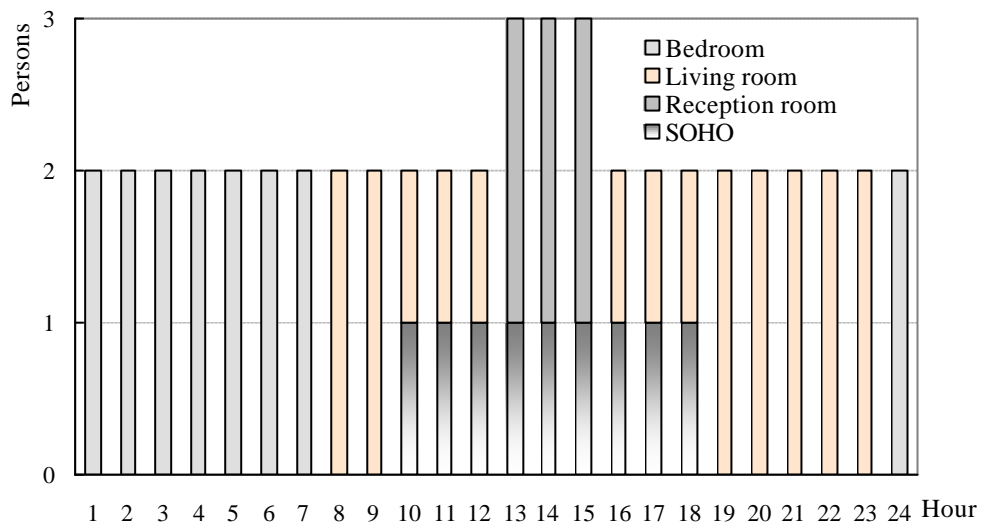


Fig.7-5. Daily schedule in the experimental house

7.2.1. Air conditioning load

The set value and calculation value of air conditioning load is listed in Table 7-1, according to different the time-dependent schedule, the total peak load of cooling and heating are 12.4kW and 14.7kW respectively, while the calculation is based on SMASH 2.0 of IBEC (1997). The annual heating load is 14777MJ while the annual cooling load is 33441MJ, which is much greater than heating load.

The comparison of the air conditioning load between this experimental house and other residential houses (Ojima, T. 1995) is shown in Fig.7-6. It can be seen that cooling load of this house is higher than the others because of SOHO applications with more heat generation.

Fig.7-7 details the hourly cooling load on August 4 in the summer, which shows that the difference between peak and off-peak is very big. The load in the daytime (8:00-22:00) is

359.7MJ, while it is only 44.8MJ in the nighttime, and the unbalanced load distribution tells that the thermal storage system is suitable for this house.

Table 7-1. Set values and calculation of air conditioning load in the experimental house

Setting Values		SOHO	Reception	Living Room	Bedroom
Indoor temperature (C/H) (°C)		26/20	26/20	26/20	26/20
Indoor humidity (%)		50	50	50	50
Heat release of equipment (kW)		1	0.12	0.12	0.12
Lighting heat (kW)		0.12	0.12	0.12	0.12
Heat release rate at night* (%)		30	0	0	0
Human heat release (kW)		0.1	0.2	0.2	0.2
Shielding rate		0.27	0.27	0.27	0.9
Room volume (m ³)		38.9	38.9	70	31.1
Cooling load (kW)		4.2	6.0	6.4	2.6
Heating load (kW)		3.8	5.6	14.7	8.6

Note: C/H, Heating/cooling; Heat release of machine at night is assumed to be part of the peak value. Here assumes that there are two computers, one duplicating machine and others in SOHO.

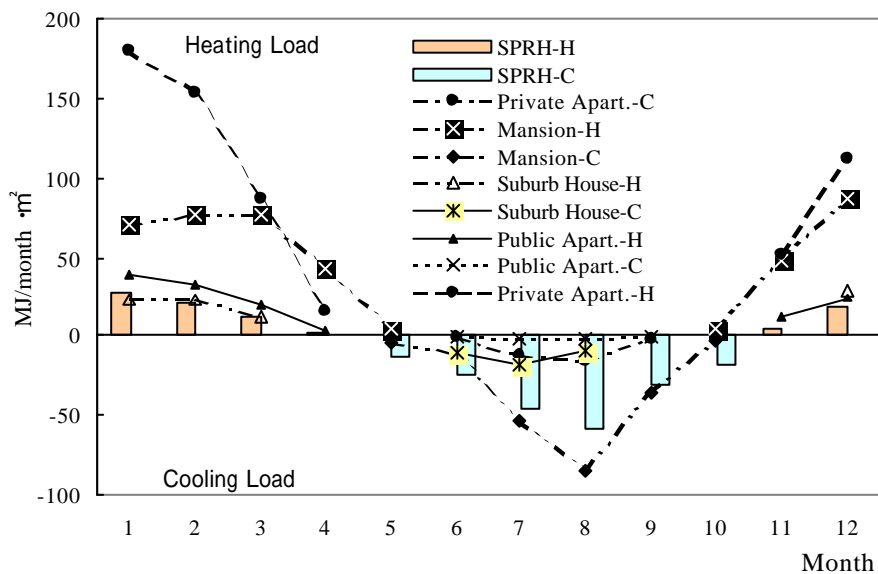


Fig.7-6. Comparison of air conditioning load between the experimental house and other houses

On the other hand, the peak-heating load in winter is 278MJ/d, which is 31% lower than the peak cooling load because of the double skin space in the south façade of the experimental house.

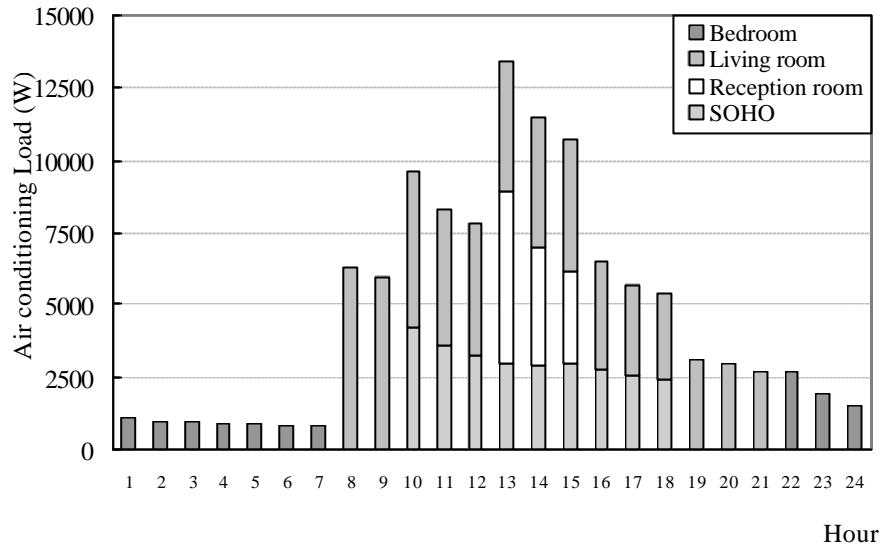


Fig.7-7. Hourly cooling load on August 4 in the experimental house

7.2.2. Hot water load

According to the number of persons living in the experimental house, hot water demand can be decided by Equation (7-1). Suppose the temperature difference is 45°C, supply hot water volume is 150kg/d per person, hot water load can be calculated as following:

$$Q_{wt} = r_{wt} V_{wt} C_{p_{wt}} \Delta t \quad (7-1)$$

where Δt is the temperature difference between city water and hot water, which is supposed to be 45°C; V_{wt} is the volume of hot water supply, which is 150kg/d for one person (JBMEEA, 1992a). Because there are two persons in this house, the hot water load is 56.5MJ/d calculated by Equation (7-1), and the peak load rate reaches 2.3kW when supply water volume is 45kg.

7.2.3. Setting of thermal storage air conditioning system

7.2.3.1. Capacity of thermal storage tank

The effective volume of the ice storage tank (V_{ist}) can be calculated by Equation (7-2).

$$V_{ist} = \frac{Q_{isc} \times (1 + k_{st})}{C_{p_{wt}} \times r_{wt} \times \Delta t_{cwt} + Q_{l_{ice}} \times r_{ice} \times IPF} \quad (7-2)$$

where Q_{isc} is ice storage capacity, which is supposed to be 50% of the peak day cooling load, i.e. 180MJ; k_{st} is heat loss of ice storage, which is supposed to be 5%, Δt_{cwt} is the sensible heat

temperature difference of water, which is supposed to be 7°C, and IPF is supposed to be 0.95.

Thus the effective volume of ice V_{ist} is calculated to be 0.59m³. As the length of the copper tube is 1.25m with the outside diameter of 80mm and the diameter of refrigerant pipe is 10mm, the net volume in one tube is 0.0062m², and the total number of the tubes should be larger than 95. Therefore, the tubes in the tank are arranged in 12 columns and 8 rows, altogether there are 96 tubes.

The output of heat pump is calculated by Equation (7-3),

$$W_{HP\ output} = \frac{Q_{isc} \times (1 + k_{st}) + Q_{night}}{t_{ts} \times 3600} \quad (7-3)$$

where Q_{night} is the air conditioning load from 22:00 to 8:00 of the next morning, i.e. 44.8MJ, and the time t_{ts} for thermal storage is 10 hours.

Therefore the output of heat pump is 6.2kW.

7.2.3.2. Capacity of hot water tank

In winter ice storage tank acts as an auxiliary hot water tank, the volume of hot water tank can be calculated by Equation (7-4),

$$V_{hwt} = \frac{Q_{hwt} \times (1 + k_{st})}{Cp_{wt} \times r_{wt} \times \Delta t_{hwt}} - V_{ist} \quad (7-4)$$

where Q_{hwt} is 50% of peak daytime hot water load for heating and daily use, i.e. 155.2MJ; heat loss k_{st} is 5%, sensible heat temperature difference Δt_{hwt} is 25°C.

Therefore, the volume of the hot water tank is 0.96m³, and the water tank is designed to be 1.7m in height with the diameter of 0.8m.

Detail constitution and capacity of the proposed thermal storage system are shown in Table 7-2.

Table 7-2. Thermal storage capacity and electricity consumption of the proposed system

Item \ Data	Volume (m ³)	Storage capability (MJ)	Effective output (MJ)
Thermal storage tank	0.08 × H1.25 × 8(R) × 12(C)=0.6	193.2	190.7
		62.8*	59.7*
Hot water storage tank	0.8 × H1.7=0.96	100.5	95.5
		Input (kW)	Output (kW)
Heat pump	-	3.2 (c)	6.2 (c)
		3.0 (h)	9.0 (h)
Auxiliary	-	1.1	
Fan	1000m ³ /h	0.2kW	
Total contract electricity capacity		4.3kW	

Note: * refers to the heat storage in the thermal storage tank in winter

7.2.4. Setting of conventional system

The conventional system for the experimental house is supposed to be composed of room air conditioner and electric water heater. Heating and cooling are realized by air conditioner and water heater uses midnight electricity to supply hot water.

Table 7-3 shows the detail composition of the conventional system, where the total contract electricity capacity is twice more than that of the proposed system.

Table 7-3. Composition of the conventional system

Type of room air conditioner	Quantity	Heating		Cooling	
		Input (kW)	Output (kW)	Input (kW)	Output (kW)
S40	1	1.8	6	1.1	4
S28	4	1.1 × 4	3.8 × 4	1.0 × 4	2.8 × 4
S25	1	1.0	3.4	0.9	2.5
Electric water heater	1	2.4	200kg	-	-
Total contract electricity capacity		9.8			

Note: The data of room air conditioner is from the specification of DAIKIN Co., and the data of water heater from TOTO; and two of the four S28-air conditioners are for the living room, while the other two are for the reception room.

7.3.Evaluation by simulation

In order to know the characteristic of thermal transfer for the proposed direct heat exchange air conditioning unit, the air temperature and airflow can be predicted, according to temperature variation of the water/ice in the tubes of the thermal storage tank and the conditions at the air inlet.

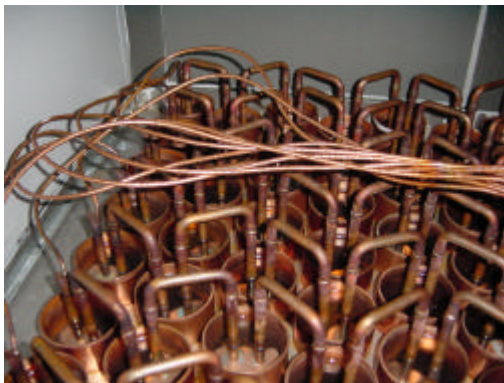
7.3.1. Simulation model

7.3.1.1. Standard *k-e* model

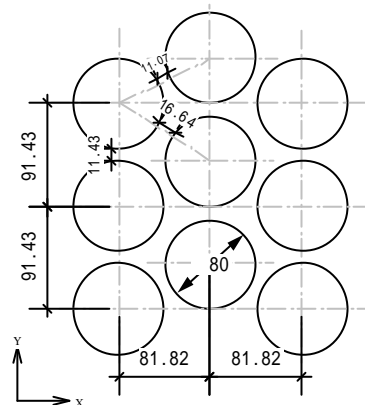
The simulation model used here is the same as in Chapter 5, i.e. the standard *k-e* turbulence model. But the turbulence intensity and turbulence length scale at the air inlet are not the same, here the default values of *Airpak* are used, i.e. 10% of the air inlet.

7.3.1.2. Sketch of the direct heat exchange tubes

The tubes for direct heat exchange in the thermal storage air conditioning unit are arranged in 8 columns and 12 rows, and the detail layout is illustrated in Fig.7-8. The space between the rows and columns is 81.82mm and 91.43mm respectively.



(a) Photo of the tubes



(b) Detail layout of tubes (mm)

Fig.7-8. Layout of proposed direct heat exchange tubes in the air conditioning unit

Both the inlet and outlet are 0.4m in width and 0.6m in height, with an area of 0.24m². Each tube is 1.2m long with the diameter of 0.8m, and the space between the tubes is about 0.11m to 0.16m. Because of the symmetry in the Z direction, half of simulation model is illustrated in Fig.7-9.

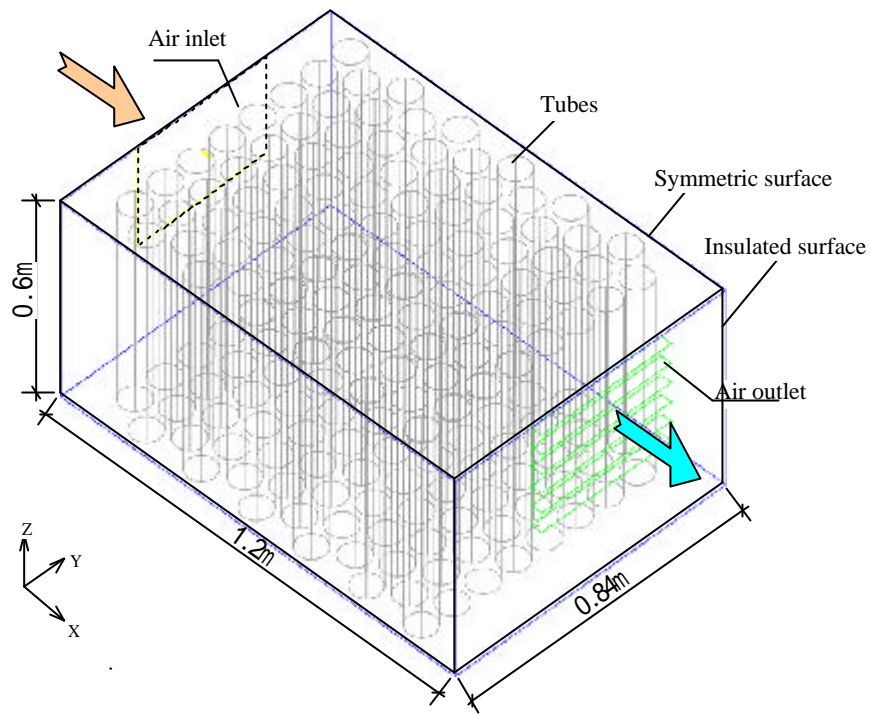


Fig.7-9. Illustration of the coil layout in the thermal tank

7.3.1.3. Boundary conditions

The fixed velocity, temperature and static pressure are set at the air inlet, while the four interior surfaces are supposed to have enough good insulation, and have no heat loss. Radiation between the tubes is neglected during computation.

And the air velocities of inlet and outlet for different cases are shown in Table 7-4.

Table 7-4. Cases of direct heat exchange

Case No.	Tube Temperature	Air inlet	
		Temperature	Velocity
Case 7-1	0 °C	28°C	1 m/s
Case 7-2	0 °C	28°C	2 m/s
Case 7-3	0 °C	28°C	3 m/s
Case 7-4	0 °C	28°C	4 m/s
Case 7-5	7 °C	28°C	1 m/s
Case 7-6	7 °C	28°C	2 m/s
Case 7-7	7 °C	28°C	3 m/s
Case 7-8	7 °C	28°C	4 m/s

7.3.1.4. Initial conditions

It is assumed that the air temperature is uniformly distributed before heat exchange, and

the initial temperature of air is set to be the same as the ambient air (28°C).

7.3.1.5. Case setting

The cases are set according to the conditions of air inlet and tubes, listed in Table 7-4 are studied.

Case 7-1 to Case 7-4 represent the thermal storage tank is fully charged, and the temperature of tubes at 0°C, while Case 7-5 to Case 7-8 represent the stored heat is emptied, according to the setting of operation for heat pump.

7.3.1.6. Computational mesh

Hexahedral mesh is also used here, with the maximum size of mesh is 0.04m×0.04m×0.04m, and the maximum size ratio is 2, while the meshes near the tubes are refined. The total number of meshes in the room reaches 315000, and the plan cut of the mesh, at Y=0.5 is shown in Fig.7-10.

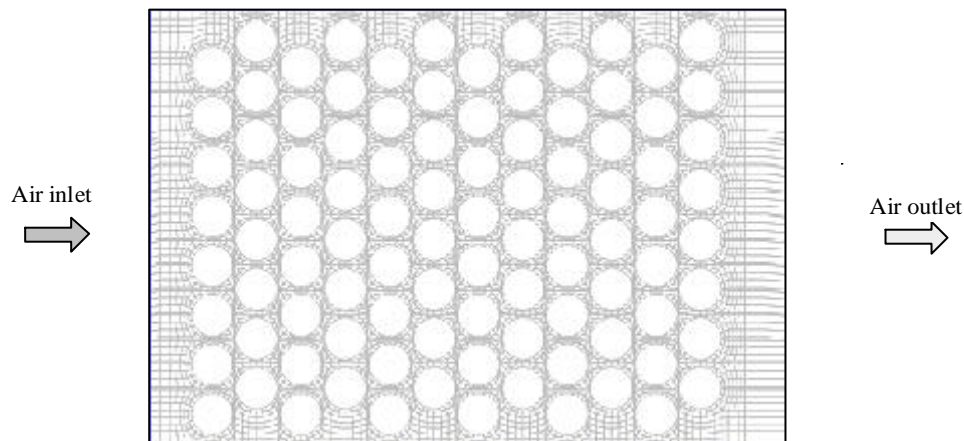


Fig.7-10. Profile of mesh around the tubes

7.3.1.7. Transient simulation

Transient simulation is carried out for different cases.

Time starts at 0s and ends at 10s, with the time increment of 0.05s for each step.

7.3.1.8. Under-relaxation factors

The iterations for each time step is 20, and the values of the under-relaxation factor for the Equations (5-1)-(5-7) are detailed in Table 7-5.

Table 7-5. Under-relaxation factors for equations

Under-relaxation factor	Values
Pressure	0.3
Momentum	0.7
Temperature	1
Viscosity	1
Body forces	0.1
Turbulent kinetic energy	0.5
Turbulent dissipation rate	0.5

7.3.2. Simulation results

7.3.2.1. Heat transfer characteristic

When all the tubes are filled with ice, i.e. temperatures of the tubes are 0°C, which means the capacity of the thermal storage is full. When all the ice is turn to be water, and then the temperature of water increases gradually. When the water temperature is 7°C, the capacity of the thermal storage is assumed to be empty. These two situations are the two extreme conditions, and the heat exchange speed with air velocity of the proposed thermal storage tank is detailed in Fig.7-11, and the initial air temperature is 28°C. Fig.7-11(a) shows that the temperature variation in 10 seconds for different air velocity when the tubes are at 0°C for Case 7-1 to Case 7-4, while Fig.7-11(b) shows the temperature variation when the tubes are at 7°C for Cases 7-5 to 7-8.

From the air temperature at the outlet, it can be seen that, when the air velocity at the air inlet is 1m/s, and the tubes are at 0°C (Case 7-1), the outlet air temperature is about 6°C and it is the lowest, but when the air velocity is 4m/s (Case 7-4), the outlet temperature is about 13°C. The greater the air velocity is, the higher the air temperature is, which means that the heat exchange between air and tube is more completely at the lower velocity.

When the tubes are kept at 0°C (Cases 7-1 to 7-4), and the temperature distribution in the thermal tank at different air velocity is shown in Fig.7-12. With the increase of air velocity, the average temperature at the outlet increases. This means heat exchange between air and tubes is not enough when the velocity is big. For Cases 7-5 to 7-8, they have similar temperature distributions as in Fig.7-12. In this study, velocity at 1m/s, i.e. the equivalent average velocity at the section is about 0.4m/s, can lead to the lowest temperature at the outlet.

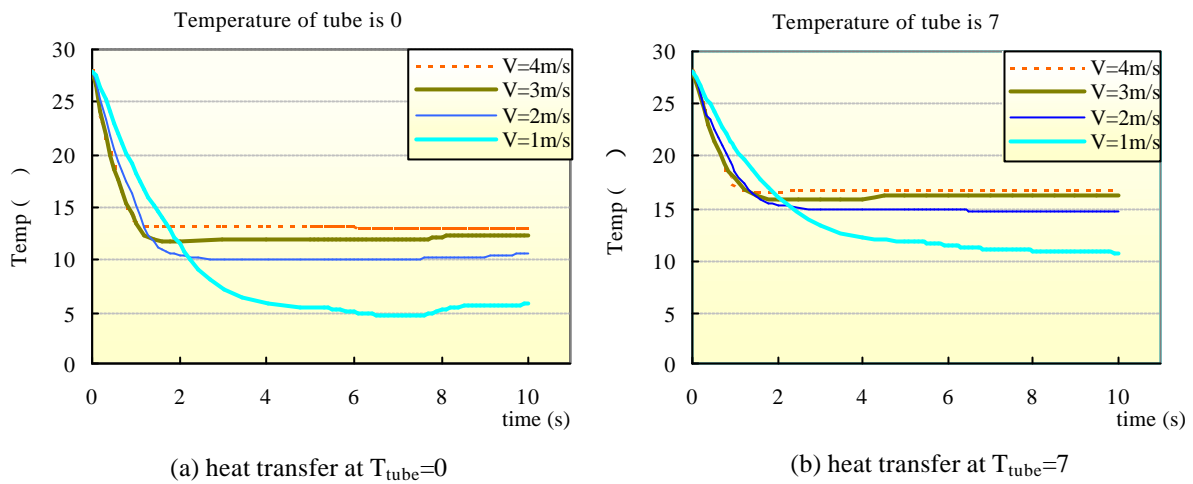


Fig.7-11. Temperature variation at different air velocity when the tubes are at 0°C and 7°C

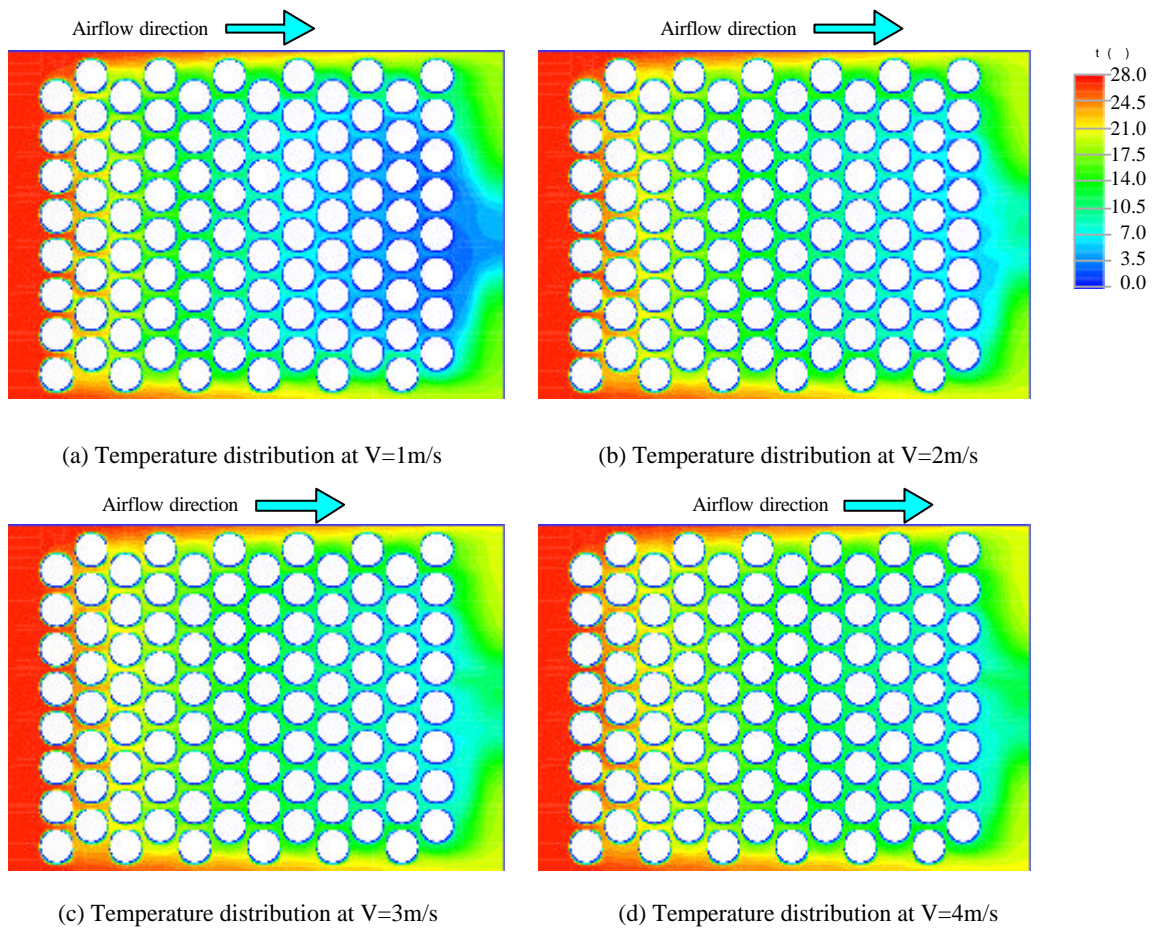


Fig.7-12. Temperature distribution at different air velocity when the direct heat exchange tubes are at 0°C

Therefore, for the sake of adequate heat exchange, the velocity should be smaller. But this will lead to bigger area for heat exchange.

7.3.2.2. Airflow

- Velocity distribution

When the velocity at air inlet is 2m/s (Case 7-2 and Case 7-6) and the heat exchange between the air and the tubes reaches balance, the air velocity distribution around the tubes is shown in Fig.7-13. The maximum velocity occurs at the distance between the tubes and the first column, and the bigger values also occur near the wall of the air-handling unit.

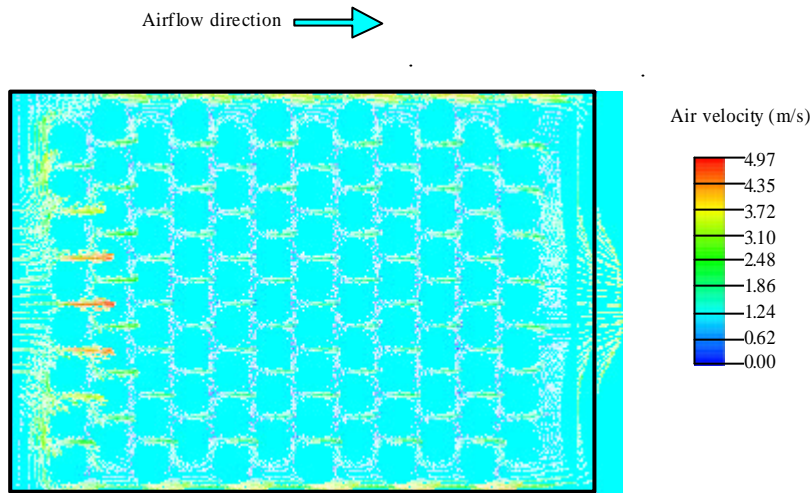


Fig.7-13. Distribution of air velocity around tubes in the heat exchanger when the velocity at air inlet is 2m/s

For the other cases with different air velocities, the similar distribution can be obtained, just as shown in Fig.7-13. As the section area of the thermal storage tank is about 1m^2 , and the inlet area is about 0.24m^2 , the maximum velocities and average velocities in the cross section of different cases are shown in Fig.7-14, which have a linear relationship with the inlet velocity.

The bigger velocities occur in the space between columns, while they are smaller around the front and back surfaces. The maximum velocities occur between the middle 3 rows in the first column. For example, when the average velocity on the section is 1m/s, the biggest velocity reaches 5m/s for Case 7-2 and Case 7-6. Therefore, these places should be strengthened from erosion. In addition, the bigger velocities occurs near the vertical surfaces of the tank.

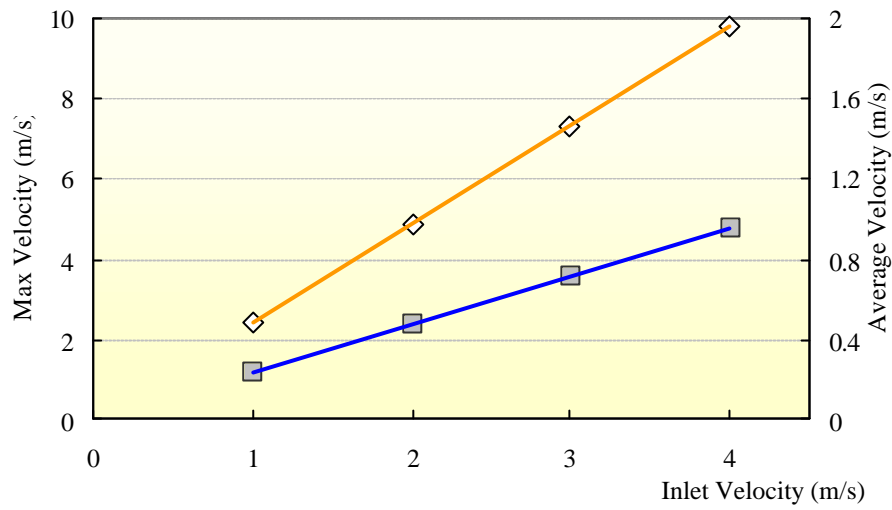


Fig.7-14. Relationship of maximum velocity and average velocity with inlet velocity

- Pressure drop

The pressure distribution of Case 7-2 and Case 7-6 is shown in Fig.7-15, the average pressure at the inlet is about 40Pa to 50Pa, and it turns to near 0 at the outlet. The total pressure drop from the inlet to the outlet is about 50Pa when the inlet velocity is 2m/s.

While the pressure drop between columns is shown Fig.7-16.

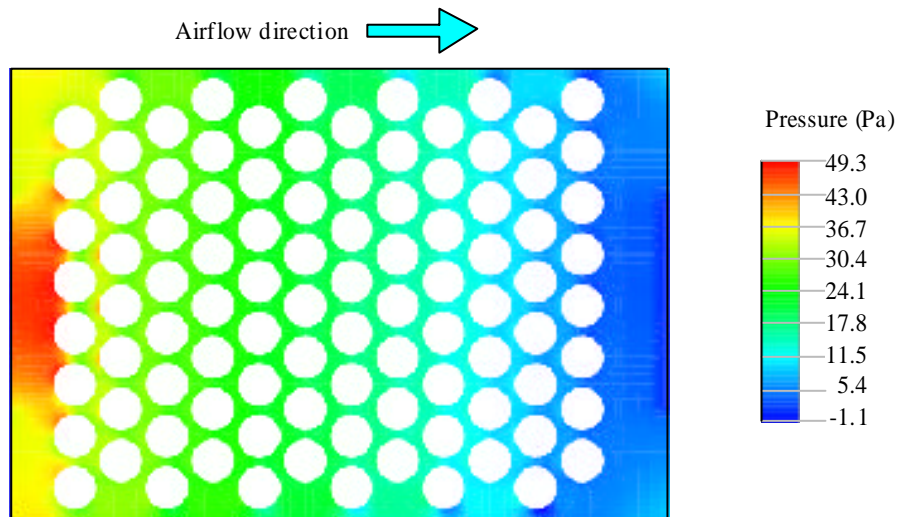


Fig.7-15. Pressure distribution around the tubes when the air velocity at the inlet is 2m/s

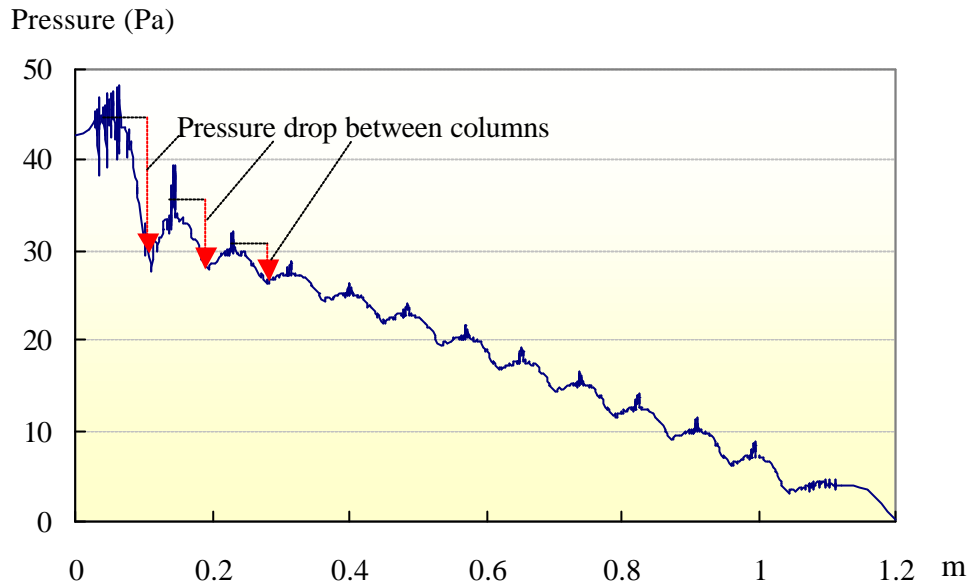


Fig.7-16. Pressure drop between columns in Case 7-2 and Case 7-6

Pressure drop in the first column is the biggest, about 15Pa, and the second column is about 7Pa, while it is about the same from the third column about 4Pa. This confirms that the tube in the first column should be strengthened.

Although the airflow rate does not affect the heat exchange rate greatly, especially when the inlet velocity is in the range of 2 to 4m/s, the pressure drop is astonishingly drops from 10Pa in Case 7-1 (inlet velocity is 1m/s) to 250Pa in Case 7-4 (inlet velocity is 4m/s). It has a great effect on the pressure drop from the inlet to the outlet, as is shown in Fig.7-17

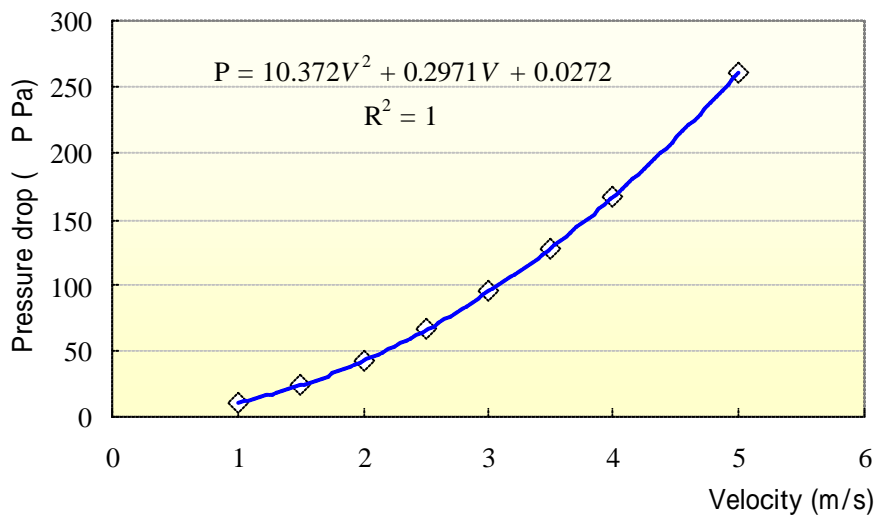


Fig.7-17. Pressure drop at different velocity through direct heat exchange tubes

7.3.2.3. Coefficient of convection transfer

The heat transfer coefficient is a derived scalar quantity, which is calculated by Equation (7-5)

$$h = \frac{q}{T - T_{ref}} \quad (7-5)$$

where q is the heat flux for the surface, T_{ref} is a reference temperature, T is the temperature of the tube surface.

If the reference temperature is taken as 28°C, the average heat transfer coefficients around the tubes are shown in Fig.7-18. As it is a scalar quantity, it is independent on the surface temperature, i.e. the heat transfer coefficient is the same when tubes are at different surface temperatures. With the increase of air velocity, the coefficient is increased. And the tubes in the first two columns have bigger value, while the last two columns have the smaller. Generally, it is in the range of 8-40W/m².°C.

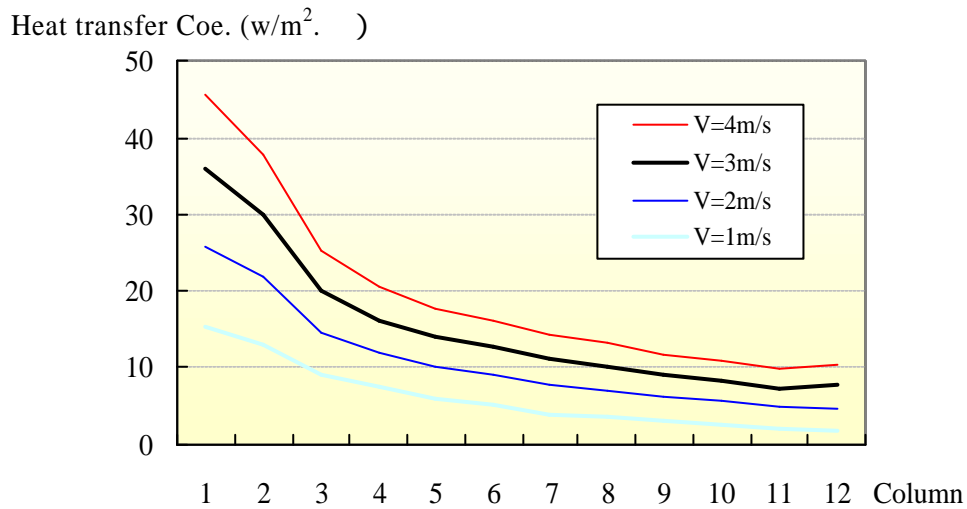


Fig.7-18. Heat transfer coefficient on the surface of tubes

7.3.2.4. Recommended speed

From the points of characteristic of heat exchange and the simulation results of the pressure drop, the smaller section velocity is recommended because of the completely heat exchange and low flow resistance. On the other hand, the smaller section velocity will lead to more area for heat exchange, for example, if the airflow rate is 2000m³/h, when the average

velocity at cross section is 0.4m/s, the section area is 1.4m², while it is 0.8 m² when the average velocity is 0.7m/s. As for the residential house, the machine size is required to be small, thus a large velocity is necessary.

In this study, the recommend speed at the inlet should be smaller than 3m/s, i.e. the average velocity at the cross section of the tubes should be smaller than 0.7m/s. Thus the pressure loss can be smaller than 100Pa, and the heat transfer coefficient is about 8-35 W/m².°C.

7.4.Prospect evaluation for thermal storage system in residential house

According to the air conditioning load and hot water load, the proposed system and the conventional system are compared in terms of energy consumption, annual cost and impact on environment.

7.4.1. Comparison of electricity consumption

According to equivalent operation time under full load conditions, annual electricity consumption can be calculated. Fig.7-19 shows the annual electricity consumption of the proposed system and conventional system, in which the annual electricity consumption of the proposed system is 23% lower than that of conventional system. And it also demonstrates midnight electricity utilization ratio (including air conditioning and hot water supply) of two systems, the midnight electricity of proposed system accounts for 73.8% of the total, while the conventional system only 47.9%.

7.4.2. Electricity cost

Electricity cost relates greatly to the electricity contract plan. Regarding to the proposed system, 78% of the daytime electricity consumption has been transferred to midnight (22:00 to next 8:00). According to the *night 10 plan* of KYUSHU Electricity Corporation, the time-dependent energy cost is a major economic incentive for the use of thermal storage.

Energy cost for the conventional system depends on the consumption amount based on *plan C*, while the difference of electricity charge among the three contract plans is listed in Table 7-6 (Kyuden, 2002). The comparison of energy cost is detailed in Table 7-7. Because most of the electricity is used during the nighttime, when the electricity charge is only 30% of the Plan C, and this can lead to about 42% reduction in energy cost.

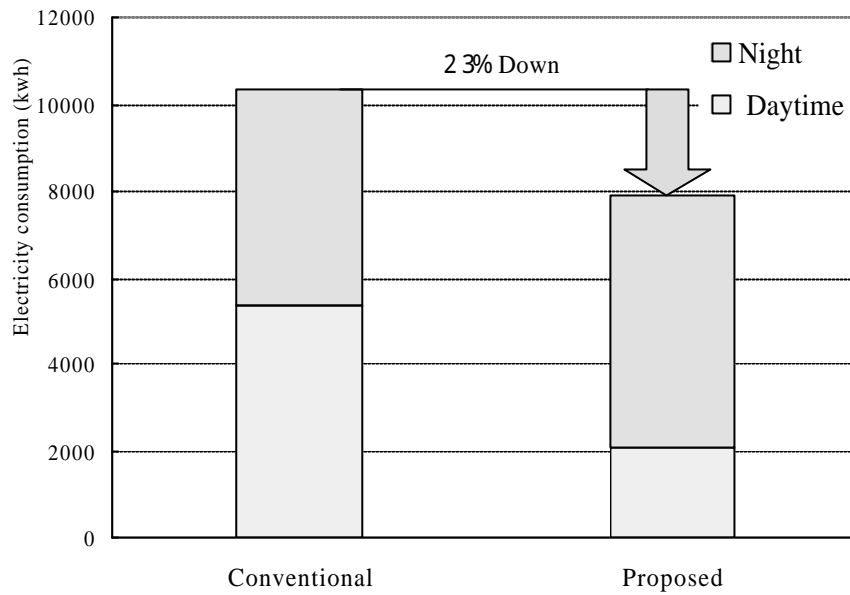


Fig.7-19. Comparison of electricity consumption between the proposed system and the conventional system

Table 7-6. Electricity charge with different contract plans

Contract plan		Night 10 plan	Plan C	Midnight plan
		¥	¥	¥
Basic charge		1100 (<6kVA)	270/1kVA	230/1kW
Daytime	<120kWh	21.00/kWh	15.45/kWh	-
	120~300kWh	27.18/kWh	20.00/kWh	
	>300kWh	29.42/kWh	21.65/kWh	
Night		6.55/kWh		6.25/kWh

Source: http://www.kyuden.co.jp/elec/denki/ryokin/ryokin/4_index.htm, Sept. 2002

It should be pointed out that according to the *Night 10 Plan*, the electricity in the daytime is higher than *Plan C*. If they are the same during the daytime, the proposed thermal storage system will have a greater running cost saving.

Table 7-7. Electricity cost for two systems

	Proposed System	Conventional System	
Contract capacity	6kVA	9kVA	4kW
Average daytime electricity consumption	172.7kWh	448.8 kWh	-
Average nighttime electricity consumption	487.4 kWh	-	412.6 kWh
Basic charge	1100¥	2430¥	920¥
Daytime electricity charge	4694¥	9717¥	
Nighttime electricity charge	3192¥		2579¥
Total cost	8986¥	15646¥	

Note: 100 ¥(Japanese Yen) =0.8333 US\$

7.4.3. Comparison of annual cost

The annual cost consists of initial cost, maintenance cost, energy cost depreciation fee, interest, insurance and taxation of the whole project, the later 4 costs can be decided by Equations (7-8)-(7-11), according to the given interest rate, project life, insurance rate and tax rate (JBMEEA, 1992b)

$$\text{Depreciation Cost} = \text{Initial Cost} \times (1 - \text{Redundancy}) \times \frac{1}{\text{Project Life}} \quad (7-8)$$

$$\text{Interest} = \text{Initial Cost} \times \frac{(\text{Project Life} + 1) \times \text{Interest Rate}}{2 \times \text{Project Life}} \quad (7-9)$$

$$\text{Insurance cost} = \text{Initial Cost} \times \text{Insurance rate} \quad (7-10)$$

$$\text{Taxation} = \text{Initial Cost} \times \text{Interest Rate} \times \left\{ \left(\frac{6}{1000} + \frac{30}{1000} \right) \times \frac{1}{\text{Project Life}} + \frac{(\text{Project Life} + 1) \times \text{Interest Rate}}{2 \times \text{Project Life}} + \frac{14}{1000} + \frac{2}{1000} \right\} \quad (7-11)$$

Detail comparison of the two systems is listed in Table 7-8. Lifetime of the proposed system is supposed as 15 years and the conventional system as 10 years, because of simple structure of the proposed heat exchange method.

Table 7-8. Comparison of cost effectiveness between the proposed system and the conventional system

Items	Proposed plan	Conventional Plan
Project life	15 Year	10 Year
Redundancy	0.1	0.1
Interest rate	0.1	0.1
Insurance rate	0.01	0.01
Assessable tax rate	0.7	0.7
Initial Cost (×10,000Yen)	250	164
Depreciation cost (×10,000Yen)	15.00	14.76
Interest (×10,000Yen)	13.30	9.02
Insurance cost (×10,000Yen)	2.50	1.64
Taxation (×10,000Yen)	3.56	2.48
Electricity cost (×10,000Yen)	10.98	18.23
Maintenance cost (×10,000Yen)	3.75	2.46
Total Annual Cost (×10,000Yen)	49.09	48.59

From Table 7-8, it can be seen that the total annual cost of the two systems is almost the same. If the lifetime of the proposed thermal storage air conditioning system is assumed to be 20 years, because of its simple structure and low maintenance, its annual cost will be 8% lower than that of the conventional system. With the popularization of this system, the initial cost will be reduced, which shows great promise for the proposed system.

7.4.4. Impact on environment

As we know, CO₂ will be emitted accompanying with electricity consumption. Here we consider CO₂ emission caused by electricity consumption is 0.131kg-C/kWh from 22:00 to 8:00 of next day, which is 10% lower than that caused in the daytime (Hashimoto, et al. 1996). From Fig.7-20, it can be seen that the CO₂ emission of proposed system is 25% lower than that of conventional system.

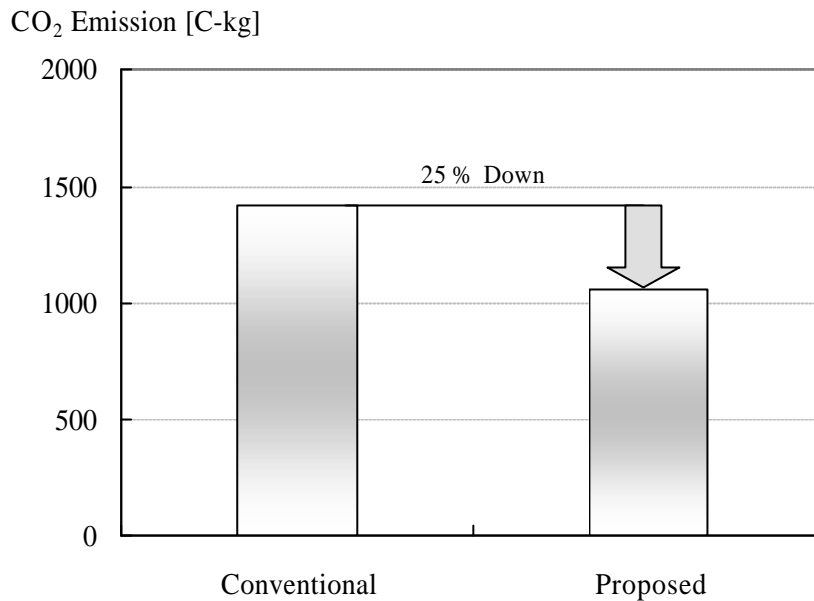


Fig.7-20. Comparison of Annual CO₂ Emission between the proposed system and the conventional system

7.5. Field experiment

7.5.1. Test points

In the field experiment in the summer of 2001, the air temperature in the thermal storage tank, water/ice temperature in the copper tubes, airflow rate, and the electricity consumption, etc. were measured, and the list of test points are shown in Table 7-9.

Table 7-9. Test points of thermal storage air conditioning unit

No.	Point name	Quantity	Apparatus	Memo
1	Surface temperature of AHU	10	Thermo Couple	Data collector
2	Air temperature in AHU	6	Thermo Couple	Computer
3	Water/ice temperature in Tubes	3	Thermo Couple	Data collector
4	Supply air temperature/humidity	1	Thermal record	
5	Return air temperature/humidity	1	Thermal record	
6	Outside air temperature/humidity	1	Thermal record	
7	Airflow rate	6		Computer
8	Heat loss	1	Shotherm HFM	Data collector
9	Room air temperature/humidity	6	Thermal record	
10	Electricity consumption	1	Electric meter	

And the distribution of test points is illustrated in Fig.7-21.

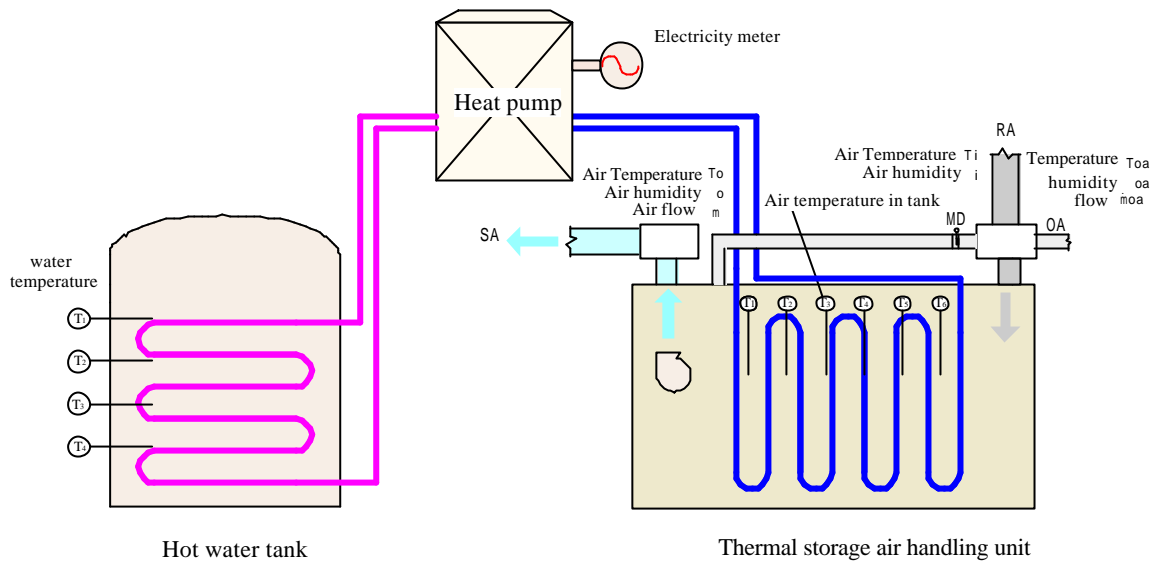


Fig.7-21. Illustration of test points in thermal storage system

7.5.2. Test results

7.5.2.1. Ice charging and discharging

The experiments show that the ice charging and discharging are realized by the proposed direct heat exchange method. The situations of the tubes after being charged and during discharging are shown below. Fig.7-22 (a) shows that the thermal tank is charged with ice after heat pump runs for about 10 hours when the initial temperature of water is 28°C , while Fig.7-22 (b) shows the situation when it is in discharging.



(a) After charged

(b) In discharging

Fig.7-22. Scene after charge and in discharging in the thermal storage tank

7.5.2.2. Temperature distribution

- Charging process

In the charging process (22:00 to next 8:00), temperature of water in the tubes drops from 20°C to the lowest nearly -20°C (Fig.7-23), which shows that it takes about 2 hours for water decreasing from 20°C to 0°C, i.e. the phase-change point, and then about 4-5 hours later water will turn to be ice, finally about 1 to 2 hours later the ice can be dropped to nearly -20°C, until the heat pump is stopped, according to the setting of operation.

Because the latent heat of water/ice is much larger than the sensible heat, it takes more time in the phase-change.

While the air in the tank decreases from about 25°C to the lowest of about -3°C. The temperature in the hot water tank reaches 55°C. This makes sure that the waste heat of heat pump can be effectively used.

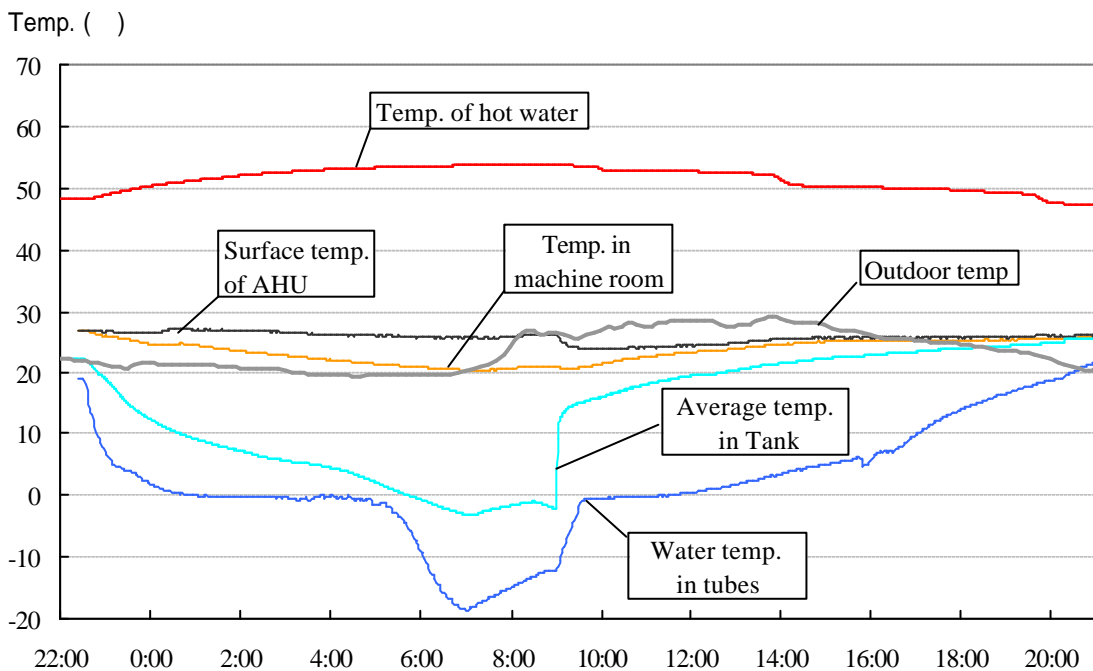


Fig.7-23. Temperature variation in a charge-discharge process

- Discharging process

In the discharging process (8:00 to 22:00), temperature of water in the tubes increases from -10°C to about 22°C, when the stored heat is emptied. Fig. 7-23 shows that it takes about 1 hour for ice going from -10°C to the phase-change point 0°C, and then about 4 hours later ice will turn to water, finally about 3 to 4 hours later the water temperature increases to 10°C. If

heat pump is not put into operation, the water temperature continues to increase.

The average air temperature in the tank increases to about 22°C, after the ice in the tubes is completely melted. And this process takes about 6 hours before the storage is emptied when the airflow rate is 400-600m³/h.

The discharging speed depends on the air velocity in the tank. As the speed is controlled by the inverter of the fan, when the frequency decreases from 60Hz to 30Hz, the average velocity on the cross section of the tank decreases from 0.2m/s to 0.1m/s, the variation speed of air temperature in the tank is shown in Fig.7-24.

It can be seen that with the increase of air velocity, air temperature increases quickly. For example, when it is about 0.2m/s, i.e. airflow rate of about 750m³/h, the discharging time lasts about 4 hours till the air temperature turns to be 22°C. While the air rate decreases to half, i.e. about 370m³/h, the discharging rate lasts over 14 hours.

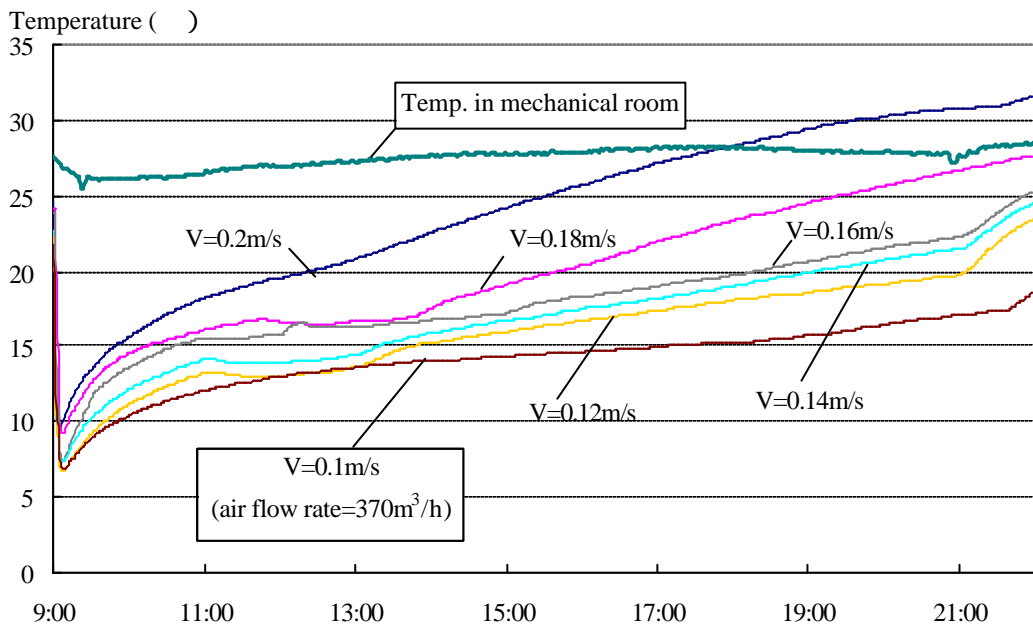


Fig.7-24. Temperature variation at different airflow rates

7.5.2.3. Performance of the thermal storage system

According to the electricity consumption of heat pump, air conditioning load, and the temperature variation, the energy utility of the whole thermal storage system can be analyzed.

The energy consumption by heat pump can be calculated by Equation (7-12)

$$Q_{hp} = 3600E_{hp} \tag{7-12}$$

where E_{hp} is electricity consumption of heat pump (kWh)

The cooling load used by air conditioning system can be calculated by Equation (7-13)

$$Q_{hp} = r_a (\dot{V}_{sa} - \dot{V}_{oa})(h_{ra} - h_{sa}) + r_a \dot{V}_{oa} (h_{oa} - h_{sa}) \quad (7-13)$$

where \dot{V}_{sa} is airflow rate of supply air (m^3/s); \dot{V}_{oa} is airflow rate of outside air (m^3/s); ρ_a is the density of air; h_{sa} is enthalpy of supply air (kJ/kg); h_{oa} is enthalpy of outside air (kJ/kg).

The energy absorbed by hot water can be calculated by Equation (7-14)

$$Q_{hw} = C_{hw} m_{hw} \Delta t \quad (7-14)$$

where C_{hw} is specific heat of water (kJ/kg.°C); m_{hw} is hot water mass in the tank (kg); Δt is the temperature increase in hot water tank (°C).

The energy utilization on August 1 is shown in Fig.7-25. As heat pump works at the 100% load in the nighttime from 22:00 to next 8:00 to charge the thermal storage unit. From 10:00 to 15:00, it continued to work for both thermal storage and cooling load.

While air conditioning uses the storage ice from 9:00 to 22:00, hot water is used from 7:00 to 9:00, and in the afternoon from 13:00 to 20:00.

It should be pointed out that because the heat pump continues to work from 10:00 to 15:00, the charged heat provides air conditioning till 22:00. Otherwise, the stored heat will be emptied before 18:00.

Besides, there is about 30% heat loss in the system, which accounts for a large part of the energy consumption.

From the above data, the effective utility for air conditioning and for the whole system can be defined as

$$h_{ac} = \frac{Q_{ac}}{Q_{hp}} \times 100\% \quad (7-15)$$

and

$$h = \frac{Q_{ac} + Q_{hw}}{Q_{hp}} \times 100\% \quad (7-16)$$

where h_{ac} refers to the energy used by air conditioning, and h refers to the total energy utility.

And the performance of the whole system is shown in Fig.7-26. As the maximum COP for air conditioning is 0.6, about 0.3 for hot water, and the total COP of 0.85, and they have the same decreasing trend with the time going.

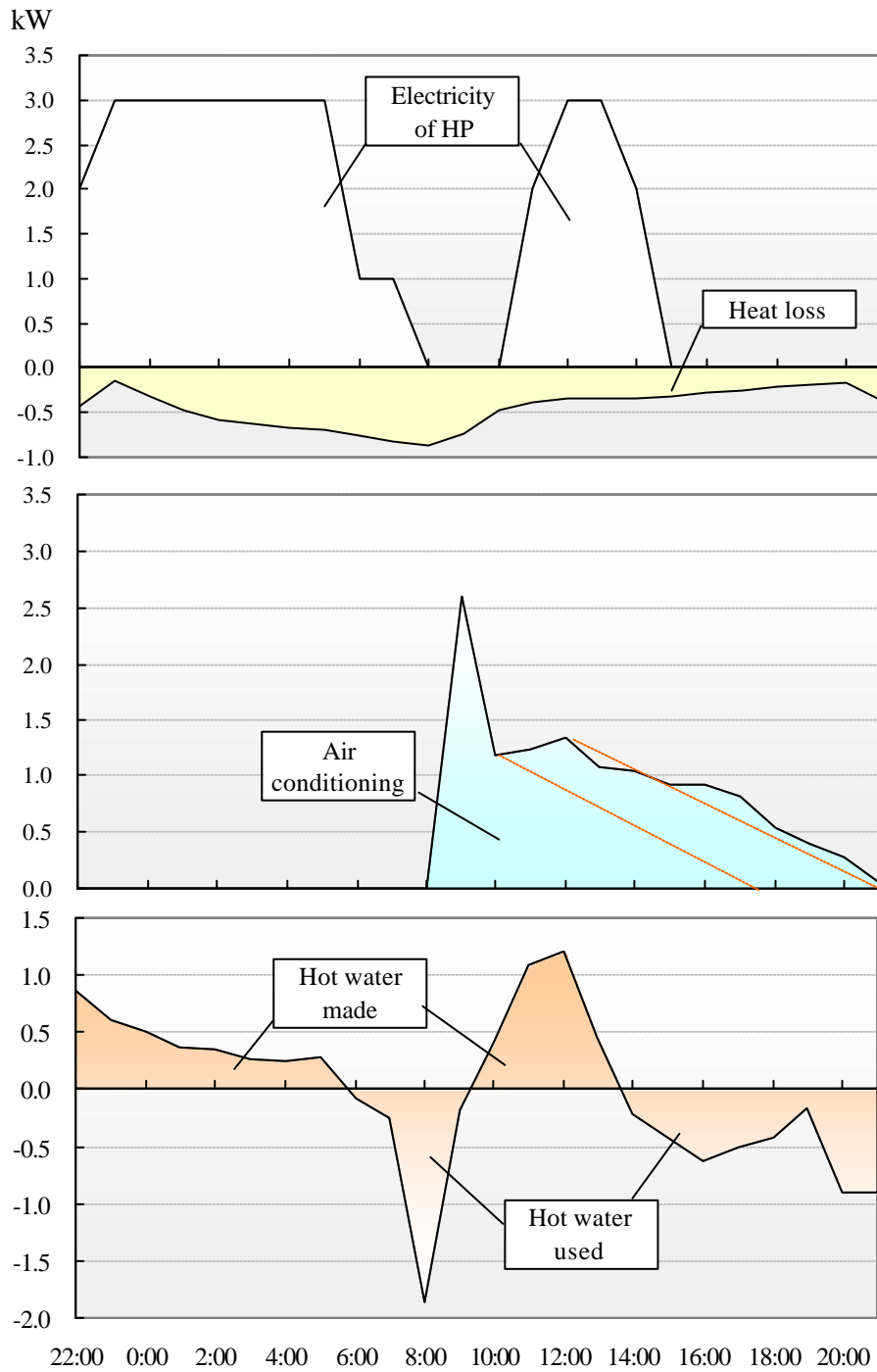


Fig.7-25. Energy utility analysis on August 1,2001

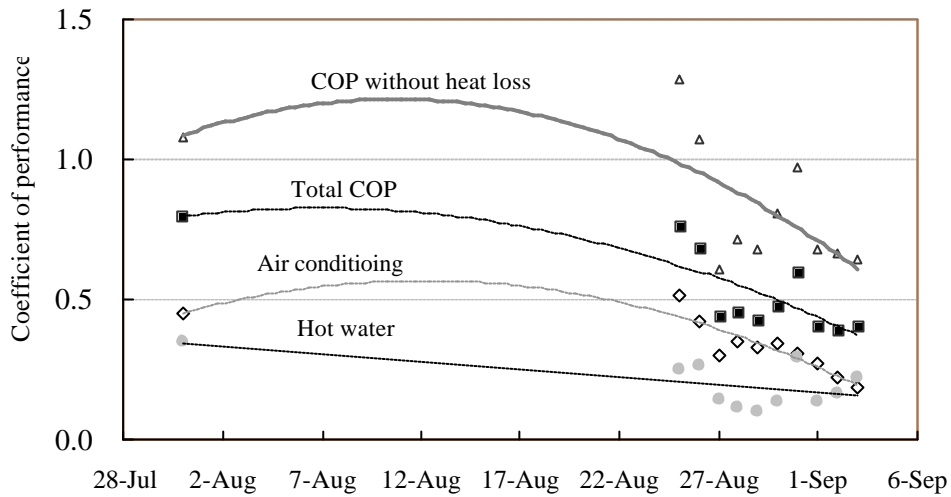


Fig.7-26. Coefficient of performance of the whole system

7.5.3. Existing problems and prospect analysis

- Existing problems

The reasons for low COP can be analyzed as follows:

The one main reason is the heat loss of the thermal storage tank because of inadequate insulation. As dewdrops occur on the exterior surfaces when the temperature becomes low in the tank. This leads to very large amount of heat loss. According to measurements, the heat loss reaches 25-30% of the total.

The other reason is that hot water has been used every day because of less demand in the summer for only one resident. As the temperature of hot water keeps over 50°C, it is quite high comparing with the temperature of waste heat. Therefore the waste heat can be effectively used, and this lead to the low COP for hot water producing.

And the leakage of tubes is also found during the experiment because of manufacture. With the time going, the number of leaked tubes increases, which leads to the decrease of COP.

- Prospect analysis

If all these problems are settled, the COP for air conditioning will be increases to 0.7-1.0, and the COP for hot water producing will be up to 0.6-1.0, therefore the total COP of this system will be increased to 1.3-2.0. Under this expectation, the energy flow in Fig.7-25 for August 1 can be recalculated as in Table 7-10.

Table 7-10. Energy flow on August 1

Load	Quantity	Electricity Consumption (kWh)		
		Proposed storage plan		Conventional plan (kWh)
	kW	Nighttime	Daytime	Daytime
AC load	12.4	12	7	5
Hot water load	13.1			16.4

Note: COP for air conditioning of the conventional plan is 2.5 considering of the part load rate, and the COP for hot water supply is 0.8.

The energy conservation and decrease of energy cost are shown in Fig. 7-27 and Fig.7-28.

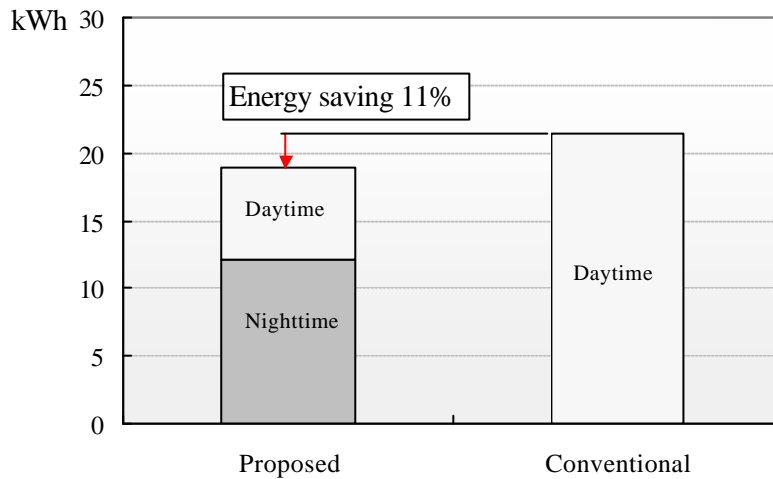


Fig.7-27. Energy conservation of the proposed system (in one day)

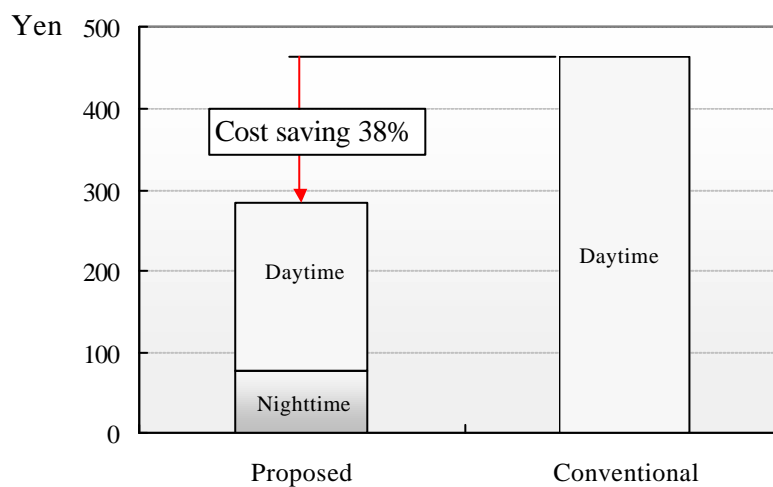


Fig.7-28. Energy cost saving of the proposed system (in one day)

Although there is only about 10% energy saving, the energy cost reaches 38%, and the electricity price is the same as in Table 7-6. Furthermore, the 10% energy saving will lead to the same part of decrease of emissions.

7.6. Summary and Conclusion

In this chapter the thermal storage air conditioning system with direct heat exchange method is proposed for future residential house. With the increase of cooling load because of the SOHO applications, it is necessary to use the thermal storage system in residential houses.

According to the simulation and experimental results, the proposed thermal storage system is confirmed to be effective for residential house.

The direct heat exchange method for thermal storage is available for ice freezing and melting in the tubes, and the conventional air handling unit and thermal storage tank can be combined into a thermal storage air conditioning unit. This method for direct heat exchange works successfully in the summer.

According to the experiment, it takes about 10 hours for the proposed thermal storage tank to be fully charged, and the discharging time depends on the airflow rate. When the storage is full, the lowest temperature of supply air reaches 6-10°C.

Heat pump can meet both of the air conditioning load and hot water load in the summer, as the waste heat is recycled for hot water supply. Therefore the performance of the proposed system is high theoretically. Although there are some accidents in the field experiments, such as the large amount of heat loss, and the leakage of the tubes because of manufacture process, accounting for all these unexpected points, the whole system has a coefficient of performance of about 1.3-2.0.

Compared with the conventional system of room air conditioner and electrical hot water heater, the proposed plan has about 10% energy saving. As the proposed system uses about 60-70% electricity in the nighttime, and this will lead to 38% energy cost because of the low electricity price in the nighttime.

The proposed system will also cut down the emission of CO₂, SO_x, NO_x because of the energy saving.

The energy system as an auxiliary for the whole hybrid air conditioning system provides an active method for air conditioning when the outdoor conditioning is unavailable for direct

use through the passive system. This, on the other hand, increases the reliability and safety of the hybrid air conditioning system.

CHAPTER 8 CONCLUSIONS

With the information technology (IT) revolution and the improving requirement for indoor air environment, the energy consumption for household air conditioning has increased. In order to realize the thermal comfort and energy conservation of air conditioning in residential houses, a hybrid air conditioning system, which is an integration of passive air conditioning and active air conditioning system, has been proposed for an experimental house and its effectiveness has been verified. The double skin system derived from the corridor space in the traditional Japanese Folk Dwelling is studied as an example of passive air conditioning method, and its effectiveness of natural energy utilization is analyzed. The displacement ventilation system, which supplies cold air only to the occupied zone, is studied as one means of energy saving of active air conditioning. In addition, the thermal storage system, which aims to use the cheap night electricity, is proposed as an available method for the heating/cooling sources. The effectiveness of this hybrid system is assessed by CFD simulation and field measurements.

In Chapter 1 *Introduction*, according to the investigation on the energy consumption in residential houses, the reasons for the increase of energy consumption, especially for air conditioning are explained. And the conventional research on energy conservation and indoor environment is overviewed. For the sake of energy conservation, occupancy health and easy operation, the importance of the proposition of a new air conditioning system for residential houses is emphasized. At last, it points out that the passive system, such as the double skin system and efficient air conditioning system, such as displacement system and thermal storage will be good solutions for residential houses.

In Chapter 2 *Concept of Hybrid Air Conditioning System and its Plan for Residential House*, definition and targets of hybrid air conditioning system are presented. It points out that the hybrid air conditioning system aims at energy conservation, occupant healthy and convenience for operation, with the integration of passive air conditioning system and efficient active air conditioning system. According to the current technology, the double skin system, which is one example of passive system, displacement ventilation system, together with ice thermal storage system, which is the improvement of active air conditioning system, are adopted successfully in an experimental house in Kitakyushu. The details of the experimental house and

its hybrid air conditioning system are also introduced.

In Chapter 3 *Simulation on Natural Energy Utilization in a Residential House with Double Skin System*, compared with the conventional house without double skin system, the effectiveness of double skin system in residential house is verified according to the simulation in summer and winter. Considering the weather conditions of Kitakyushu, because of the interior shading effect and stack effect, natural ventilation is promoted in the double skin system, the temperature stratification in the vertical direction is verified, with the temperature gradient of about $0.5-1^{\circ}\text{C}/\text{m}$, and about 10% solar radiation in the south direction can be exhausted directly. Compared with the conventional type, the cooling load in 1F room has a cut of 16%, while the cooling load in 2F room has a cut of 15%. During the winter, as the solar radiation from the south direction can be introduced into the rooms, the peak of natural temperature can be about 10°C higher than the outside air, while the temperature in the double skin is more higher, which exceeds 30°C . The heating load in the 1F room has a cut of 23%, while the cut of heating load in the 2F room is greater, of about 30%. Therefore, the energy conservation of double skin system is appraised by simulation.

In Chapter 4 *Field Experiment of Double Skin System in the Experimental House*, the effectiveness of the double skin system is further verified according to the field experiments in the experimental house in Kitakyushu. In summer, the stack effect is observed in the double skin space with the temperature gradient of $0.5-1^{\circ}\text{C}/\text{m}$ in the vertical direction. About 10-25% solar radiation is exhausted by natural ventilation, and this leads to 15-20% energy saving in cooling in the 1F room, while it is a little smaller in the 2F room of about 10%. In winter, with introducing more solar radiation, room air temperature becomes $5-10^{\circ}\text{C}$ higher than outside air temperature, while the air temperature in the double skin space is much higher, of about 20°C higher than the outside air. Therefore the heating load in room has a cut of 20-30%, comparing with the conventional house, because of the green house effect in the double skin system. The results of experimental measurement accord with the simulation results in Chapter 3 quite well. In the intermediate seasons, the indoor environment can be greatly improved by ventilation or adjusting the opening area (including windows) without active air conditioning, and the subjective experiment shows that the occupants are willing to use this system because of the convenience for operation.

In Chapter 5 *Evaluation of Displacement Ventilation System in a Residential Room by CFD Simulation*, the improvement on active air conditioning is proposed, and the effectiveness of displacement system is verified by simulation. Cases of different air change rate, different inlet/outlet positions and diffuser character are carried out in a residential room, and the energy consumption for cooling and the thermal comfort in the occupied zone are analyzed. According to the simulation results, although the air temperature is stratified in the vertical direction, this may not have an effect on thermal comfort in the occupied zone with suitable air supply. Compared with the mixing system, the displacement ventilation may cut down 12-26% of the cooling load, and the outlet of return air set at a lower position may lead to more energy saving. Moreover the displacement ventilation system has a better air change efficiency, which is 30% higher than the mixing system. In addition, the swinging diffusers will be helpful for air distribution, especially when there are some partitions in rooms. Therefore the availability of the displacement ventilation system is predicted.

In Chapter 6 *Field Experiment of Displacement Ventilation in a Residential Room*, the availability of displacement air conditioning system is further verified. The experimental results show that air temperature is stratified in the vertical direction. It is 26-28°C in the occupied zone (below 1.8m), and about 2°C greater above 1.8m. The temperature gradient is about 2-2.5°C/m, which is smaller than the recommendation of ISO7730. PMV is in the range of -0.5 to 0.5 under 1.4m, which means comfortable environment is realized. The average CO₂ concentration is 600ppm in the occupied zone, while it is 200ppm greater near the ceiling, and this shows the air change efficiency of the displacement system is better. When return outlet is set at 1.8m high, heat is exhausted from ceiling and the cooling load is about 50-60W/m², which is 20-30% smaller than that of conventional mixing system. In addition, the simulation results in Chapter 5 have a good accordance with the measured values, as the correlation coefficient for temperature is 0.95, and 0.82 for air velocity. Therefore the effectiveness of displacement ventilation is verified. As to improvement on the active air conditioning system, the introduction of displacement ventilation will lead to energy conservation, good environment and better air change efficiency.

In Chapter 7 *Effectiveness of Thermal Storage System in a Residential House*, the improvement on heating and cooling system is studied. In order to make use of midnight electricity, the proposed thermal storage system uses heat pump uses to produce ice, and store

the ice for air conditioning in the next day. Furthermore, the waste heat is used for hot water supply, and all these lead to a higher coefficient of performance. As the direct heat exchange between air and ice is adopted in the thermal storage system in the experimental house, the performance of this system is analyzed by simulation. From the results, electricity consumption of suggested system is 23% lower than that of conventional system. About 40% energy cost can be saved and 25% CO₂ emission can be cut down because of the nighttime operation and heat recovery. Suppose the life of the equipment as 20 years, the sum of initial cost and running cost of these two systems is almost the same. The experimental results in summer show that the direct heat exchange is available, and the performance of the thermal storage system will go up with the predictions if the heat loss is small. Therefore, the thermal storage system, as improvement on the heating and cooling devices in active air conditioning system, is verified to be available for energy conservation, and it will make contribution for the improvement on the global environment.

In Chapter 8 *Conclusions*, the whole summary of this thesis is presented. With the simulation and experiment, the proposed hybrid air conditioning system makes the best use of natural energy by the means of double skin system, and it further cuts the energy consumption of air conditioning system by the way of displacement ventilation and thermal storage technology. This hybrid system is verified to be effective in the residential house.

Further study will go on, considering the specific geography and climate conditions for different projects, the detail composition of the hybrid air conditioning system will be different, especially the passive air conditioning system. To make the best use of the renewable energy, such as solar radiation, light, and winds, is the key point of the passive system.

As to the improvement of active air conditioning system, the task ambient air conditioning system will be another good solution, but its implication and its impact on thermal comfort should be paid enough attention. As to the thermal storage in residential house, the size of the storage tank and the efficiency of the whole system in operation should be emphasized.

The most important point of the hybrid air conditioning system is to make the best use of natural resources and cut down the most nonrenewable energy consumption. In order to fulfill this goal, the occupants in the rooms should not be neglected. On the contrary, a successful

hybrid air conditioning system should consider the participation of the occupants, let them control the environment, and adjust the environment to meet their own requirements.

REFERENCE

- AIJ. 1980. *Handbook of Architecture-I Urban planning*. Architectural Institute of Japan. Maruzen Co. Ltd., Tokyo. pp.925
- ASHRAE. 1995. ASHRAE Handbook-HVAC Applications (SI Edition). American society of heating, refrigerating and air conditioning engineers, Inc., Atlanta. pp. 3.20-21
- ASHRAE. 1996. ASHRAE Handbook-HVAC Systems and Equipment (SI Edition). American Society of Heating, Refrigerating and Air-Conditioning Engineers, Inc., Atlanta. pp. 8.14-15
- ASHRAE. 1997. ASHRAE Handbook-HVAC Applications (I-P Edition). American Society of Heating, Refrigerating and Air-Conditioning Engineers, Inc., Atlanta. pp. 3.22
- ASHRAE. 2001. ASHRAE Handbook-Fundamental(SI Edition). American Society of Heating, Refrigerating and Air-Conditioning Engineers, Inc., Atlanta. pp. 3.8, 8.22, 29.15-29.20, 29.38
- ASHRAE. 2001. ASHRAE Handbook. American Society of Heating, Refrigerating and Air-Conditioning Engineers, Inc., Atlanta. pp.26.10-26.11
- Akasaka, H. 1998. Weather data for Energy Analysis and Design of Air conditioning system (WEADAC) Program, <http://the.aae.kagoshima-u.ac.jp/weadac.html>
- Akasaka, H. et al. 2000. Extensive AMeDAS Climate Data. (CD-ROM) Architecture Institute of Japan, Tokyo.
- Brager, G. S. and de Dear, R. 2000. A standard for natural ventilation, ASHRAE Journal 42(10): 21-28
- CIBSE. 1997. Natural ventilation in non-domestic buildings-applications manual AM10:1097, The Chartered Institution of Building Services Engineers, London.
- Chen, Q. and Xu, W. 1998. A zero-equation turbulence model for indoor airflow simulation, Energy and Buildings 28 (2): 137-144
- Committee of Speciation on New Standard for Residential Houses. 1998. New Standard and Guidance for Energy Conservation in Residential Houses, Institute for Building Environment and Energy Conservation, Tokyo. pp.109-111
- Crawley, B. D., Lawrie, K. L. et al. 2001. Energy Plus: creating a new-generation building energy simulation program, Energy and Buildings 33 (4): 319-331
- ECCJ. 2002. Catalog of air conditioner for houses (Summer of 2002). The Energy Conservation Center of Japan. <http://www.eccj.or.jp/catalog/2002s-h/air-con/index.html>
- Fiorino, D.P. 1994. Energy conservation with thermally stratified chilled-water storage. ASHARE Transactions 100(1): 1754-1766

- Fluent Inc. 2001. Airpak 2.0 User's Guide. pp. 1.2-1.9, pp. 18.1-18.13
- Furubayashi, T. et al. 2001. Sendai Mediatheque, The Magazine of Building Equipment 52(5): 29-37
- Hashimoto, T., Sato, M. and Nohara, F. 1996. Environmental assessment of building systems. Journal of the Society of Heating, Air Conditioning and Sanitary Engineers of Japan 70 (2): 23-36
- Hensen, J. 2002. Modeling and simulation of a double-skin façade system, http://www.bwk.tue.nl/fago/hensen/publications/02_ashrae_dskin.pdf
- IBEC. 1985. The Design of Passive System for Residential House. Institute of Building Environment and Energy Conservation. Maruzen Co., Ltd., Tokyo. pp.8, pp.11
- IBEC. 1997. Manual of SMASH for windows Ver.2. Institute of Building Environment and Energy Conservation. Tokyo.
- IEEJ. 2002. EDMC Handbook of Energy & Economics Statistics in Japan. The Energy Conservation Center, The Institute of Energy Economics, Japan, Tokyo. pp. 75-77, 83, 85
- Ikeda, K. 1996. Results of research on comfortable and healthy indoor environment. <http://www1.mhlw.go.jp/houdou/0807/0716-1.html>
- Inoue, U. 1996. Handbook of air conditioning. Maruzen Co., Ltd., Tokyo. pp. 5
- JBMEEA. (Japan Building Mechanical and Electrical Engineers Association) 1992a. Building Equipment Design Manual 2-Water Supply and Drainage Technical Publishing Press, Tokyo. pp.52-54
- JBMEEA. (Japan Building Mechanical and Electrical Engineers Association) 1992b. Building Equipment Design Manual 1-Air conditioning, Technical Publishing Press, Tokyo. pp. 356-357
- JBMEEA. (Japan Building Mechanical and Electrical Engineers Association) 2000. Building Equipment Design Manual for Apartment. Ohmasha Co., Tokyo. pp.377
- Jackman, P. J. 1991. Displacement Ventilation. CIBSE National Conference, Chartered Institution of Building Services Engineers, London.
- Kanemori, Y. 2002. Reuse and recycling rate of a case study house. J. Archit. Plann. Environ. Eng., AIJ. No. 555, pp. 123-129
- Kimura, K. 1997. Fundamental Theories of Building Services. Gakkensha Co. Tokyo. pp. 98-100
- Kyuden, Co. 2002. http://www.kyuden.co.jp/elec/denki/ryokin/ryokin/4_index.htm, Sept. 2002
- Matsumoto, H. et al. 2002. Field measurements method for ventilation effectiveness in rooms. Journal of the Society of Heating, Air Conditioning and Sanitary Engineers of Japan 76 (1):

84-93

Mundt, E. 1994. Contamination distribution in displacement ventilation – Influence of disturbances. *Building and Environment*, 29(3)

Murata, T. 1997. Displacement ventilation system design. *Journal of the Society of Heating, Air Conditioning and Sanitary Engineers of Japan* 70 (8): 597-602

NCAC. 1998. Investigation on Healthy House-according to the Questionnaire on Indoor Environment in Public Houses from House Makers. National Consumer Affairs Center of Japan, Tokyo.

Nakajima, Y. 2000. Residential system for low environment and resources circulation. Doctoral thesis, Waseda University, Tokyo

Ohga, H. 2001. Performance of windows (part 5)-Towards an almost transparent building. *Journal of the Society of Heating, Air Conditioning and Sanitary Engineers of Japan* 75 (10): 887-892

Ohnaka, T. and Ikeda, K. et al. 1996. An experimental study on thermal comfort under the stratified air conditioning system. *Proceeding of Research Meetings of Society of Heating, Air Conditioning and Sanitary Engineers* 1996: 593-596

Ojima, T. 1995. Units of Energy Consumption for Buildings in Tokyo. Waseda University Press, Tokyo. pp. 49, 152, 154,168,174, 175

Oka, T. 1984. Passive systems for solar heating and cooling, Part 2 Evaluation of Performance of the Double skin. *Journal of the Society of Heating, Air Conditioning and Sanitary Engineers of Japan* 24 (2): 59-65

Olesen, W. B. 2000. Guidelines For Comfort. *ASHRAE Journal* 42 (8): 41-46

SOHO Think Tank. 2001. SOHO White Book. Doyukan Co., Tokyo. pp. 77

Samet, J. M. et al. 1988. Health effects and sources of indoor air pollution, part 2. *American Review of Respiratory Disease* 137: 915-939

Schlichting, H., (Translated by Kestin, J.) 1979. *Boundary-Layer Theory* (Seventh Edition). McGraw-Hill, Inc. pp.475, 605

Schoenwetter, W. F. 1997. Building a healthy house. *Annals of Allergy, Asthma & Immunology* 79 (1): 1-4

Skistad, H. et al. 2002. Displacement ventilation in non-industrial premises. *Rehva*, Federation of European Heating and Air-conditioning Associations, Brussels, Belgium. pp.47

Statistics Bureau, Ministry of Public Management, Home Affairs, Posts and Telecommunications, Statistical Information Institute for Consulting and Analysis. 2002.

Population Census of Japan in 2000. Volume 1, Sex, Age and Marital Status of Population, Structure and Housing Conditions of Households (CD-ROM). Japan Statistical Association, Tokyo.

Svenson, A. G L. 1989. Nordic experience of displacement ventilation systems, ASHRAE Transactions 89 (1): 1013-1017

Tanabe, S. and Kimura K. 1996. Comparisons of ventilation performance and thermal comfort among underfloor, displacement ventilation, and ceiling diffuser systems by experiments in a real sized office chamber. ROOMVENT 96: 299-306

Yan, Q. et al. 1986. The Process of Thermal Transfer in Buildings, Chinese Construction Publish House, Beijing. pp.134

Zhang, Q., Ishihara, O. and Hayashi, T. 1997. Development of residence with solar heating, earth cooling and air circulation, ASHRAE Transactions 1997 Part 1. pp. 333-341

APPENDIX 1. ABSTRACT (IN JAPANESE)

日本の民生部門でのエネルギー消費量は最終エネルギー消費の 1/4 を超え、ライフスタイルの変化等により、生活の利便性、快適性、豊かさを追求するため、エネルギー消費量は増加している。IT 情報化により在室ワーク (SOHO) 機能具備が進むため、住宅におけるエネルギー消費量、特に冷暖房のエネルギー消費量は伸び続けると予測される。一方で、居住者の健康志向が高まり、室内空気質に対する要求も高くなる。建築設備の空調システムは省エネルギーと高度な室内環境を実現するために、更なる高性能化・高機能化が図られ、複雑なシステムが多くなっている。しかし、実際の建物は、自動制御の未調整や設定値の不具合によって多くの無駄なエネルギーが消費されていることが多い。京都議定書の目標達成は決して容易ではない。

本研究は、住宅における空調システムの省エネルギー性と室内の快適性を実現することを目指し、ハイブリッド空調システムを提案する。具体的には、パッシブ手法に関する研究として、日本の民家の縁側空間をダブルスキンとして活用した自然エネルギーの利用効果に関する研究、また、アクティブ空調手法に関する研究として、居住域のみを空調する温度成層型空調システムの快適性と省エネルギーに関する研究、さらに、空調熱源として、氷蓄熱空調システムの導入に関する研究を行っている。研究手法としては、シミュレーションと実測を行い、住宅におけるハイブリッド空調システムの有効性に関して実証する。

第 1 章は『従来研究及び本研究の位置づけ』と題して、ライフスタイルの変化によりエネルギー負荷が増加することから本研究に至った背景を調査した。まず、建物における空調設備の省エネルギー手法に関する取り組みの現状を記し、特に住宅に関する省エネルギー手法の特性を詳述した。建築外皮の改善により、パッシブ空調とアクティブ空調を併用した本研究における「ハイブリッド空調システム」の必要性とその研究課題を明らかにした。本研究では、自然換気量、内表面の温度及び内部の発熱、空調機の給気風量、温度などを初期条件として、連続方程式、運動方程式、エネルギー方程式等により、室内のシミュレーションツールを解析する。空気温度、気流、空気質などの分布を求め、室内の熱、空気流動の性状を分析した。以上の結果により、再びマクロモデルを利用してシステムのエネルギー消費、室内の快適性の評価を行った。

第 2 章は『ハイブリッド空調システムの基本コンセプトと提案』と題して、住宅に向けハイブリッド空調システムの基本的な考え方を考察した。ハイブリッド空調システムの目標としては、居住の快適性、エネルギー消費の削減、操作利便性と維持管理の容易性である。また、自然エネルギー利用の可能性を分析した上で、パッシブ空調システムの一例として、住宅でのダブルスキンシステム導入の可能性を分析した。又、アクティ

ブ空調方式を改善する一例として、住宅での成層空調システム導入及び氷蓄熱システム導入の可能性を分析した。そして、住居の快適性、システムの省エネルギー性及び操作、管理の利便性を考慮し、北九州における実験住宅でハイブリッド空調システムを提案した。民家の縁側空間を活用したダブルスキンシステムを研究し、夏には煙突効果を利用する工夫、冬には温室効果を利用する工夫等自然換気を導入するポイントを研究した。また、ハイブリッド空調の一環であるアクティブ空調の改善として成層空調システムを提案し、給気口及びリターン口の位置を研究した。さらに、成層空調システムの熱源の改善策として、氷と空気を直接熱交換する氷蓄熱空調システムを考案した。

第3章は『ダブルスキンによる室内環境への影響に関するシミュレーション』と題して、ダブルスキン無しとダブルスキンありの場合のシミュレーションモデルを比較した。まず、北九州の気象条件に基づいて、熱バランスと仮定する開口部の流量係数より、マクロモデルを利用して、ダブルスキン内における自然換気量、平均気温及び各表面の温度を解析した。また、連続方程式、運動方程式、エネルギー方程式等により、空気温度と気流分布を解析する。ダブルスキンシステムの省エネルギー性、室内の快適性のシミュレーションを行った。その結果、夏季の自然換気時では、内側ブラインドの高度遮蔽効果や空気温度差からの煙突効果等により、ピーク時では従来式より約10～30%排熱率が確認できた。二階の部屋よりも一階の負荷削減率は約2%大であり、冷房季には、ダブルスキンにより約15%の負荷削減ができる。冬季にはダブルスキンの密閉モードで、内側のブラインドを上げる場合、日射が直接部屋の奥まで入り込み、室内の温度が外気より10～15℃高く、暖房季には、約20～30%の削減できる。中間期では、ダブルスキン空間の開口面積が自由に調整することができるため、非常に幅広い範囲で室内温度を調整でき、空調に頼らず快適な環境も実現することができた。

第4章は『ダブルスキンによる室内環境への影響に関する実測研究』と題して、北九州にある実験室でダブルスキンシステムの実測概要を紹介し、計測内容、計測ポイントの分布を示した上で、夏季、冬季、中間期の、実測研究を行った。その結果、夏季ピーク時(昼間)には、ダブルスキンの内ブラインドを閉め、自然換気時には、高さ方向の空気温度が0.5～1℃/m上昇し、南面の日射では、約10%が自然換気により排熱されて、室内の空調負荷は約12%を削減した。冬季では、ダブルスキンの内ブラインドを上げ、換気口を密閉した場合、ダブルスキン内の温度が外気より5～10℃高く、室内の暖房負荷が約30%を削減した。実測結果とシミュレーションはほぼ一致している。また、中間期では、ダブルスキンの運転モードを調整することができる。外気が23℃で、窓を開放する換気の場合、室内の気温は24℃で、外気とほぼ一致する。密閉モードでは、外気は20℃で、二階部屋における気温が約5～10℃高くなり、空調に頼らず快適な環境を操作ができる。自然気候が変動している時、室内の快適性を確保するためには、アクティブ空調も必要であり、次章では空調方式から、アクティブ空調を改善する成層空

調システムの快適性と省エネルギーを研究する。

第5章は『成層空調に関するシミュレーション研究』と題して、ハイブリッド空調システムの一環としてのアクティブ空調の改善策として、住宅では成層空調を提案し、換気量を代表する換気回数、給排気口の位置及び給気口の特性による室内の快適性及び省エネルギー性への影響を把握するため、シミュレーションによるケースケーススタディーを行った。また、従来の混合式換気システムとの比較研究を行い、夏季住宅における成層空調の室内快適性とエネルギー消費を比較した。結果は、換気回数は室内の快適性及び空調の省エネルギー性への影響が大きい。換気回数が多いほど、快適性の範囲は広がるが、換気回数が1回/時増えれば、冷房負荷は約 $2.6\text{W}/\text{m}^2$ 増加する。換気回数を10~12回/時に設定すれば、居住空間では快適な温熱環境が実現でき、活動度は1.0metで、着衣量は0.5cloと仮定すると、1.4m以下の空間ではPMVは0.5以下であり、それに伴う冷房負荷はやや少なく、約 $50\sim 60\text{W}/\text{m}^2$ である。また、給気口がスウィングした場合には、気流に影響する障害物があっても、室内気温の分布への影響は少ない。リターン口の位置は居住区域の快適性の影響が小さい反面、冷房負荷への影響が大きい。同様の成層空調において、リターン口が2.4m高さの位置から、1.8m高さの位置に移動すると、冷房負荷を約14%削減できる。さらに、従来の完全混合式システムと比べて、成層空調システムは、約12%~26%の冷房負荷の削減効果が認められる。その原因は、主に天井と上部壁面からの熱損失が削減されるためと考えられる。換気効果からみると、成層空調システムにより、居住域において、空気齢の平均値が1.25であり、従来式は1しかないことを考えれば、成層空調システムの換気効率は優れていると確認した。

第6章は『成層空調に関する実測研究』と題して、夏季のピーク時、北九州における実験室で成層空調システムの実測結果とシミュレーションの比較をした。まず、実測の概要と計測ポイントの分布を示し、室内の温度、風速、室内のCO₂濃度及び内表面の温度などを実測した。その結果、高さ方向の温度分布から、成層空調の形成が確認できた。居住空間(1.8m以下)は26~28℃で、1.8m以上の空間は約2℃高くなっており、上下温度勾配は2~2.5℃/mであり、ISO7730の推奨値3℃/mより小さく、シミュレーション結果との相関係数は0.95であった。また、室内の気流速度が0.25m/s以下であり、乱流強度は20%で、シミュレーション結果との相関係数は0.85であった。活動度は1.0Metで、着衣量は0.5cloと設定して、居住域におけるPMVの分布が-0.5~0.5であり、快適な環境を実現することができた。CO₂濃度の分布からみると、居住域の平均値は600ppmで、天井は800ppm、屋外のCO₂濃度は約350ppmであった。完全混合式より、成層空調システムはより効果的に換気することができる。リターン口の位置を1.8m高さに設置した場合、天井からの排熱のため、ピーク時では、空調負荷は約 $60\text{W}/\text{m}^2$ で、従来の完全混合システムより20~30%低くなった。空調負荷の実測結果はシミュレーションと比べて、約10~15%高いのは、引き違いドアの隙間からの熱損失と考えられ

る。快適性、省エネルギー性などから、成層空調方式が効果的であり、次章では、住宅向け氷蓄熱空調システムの有効性を検討する。

第7章は『氷蓄熱空調システムの有効性に関する研究』と題して、成層空調システムの導入に伴い、ハイブリッド空調システムの熱源エネルギーを削減するために、深夜電力及び大温度差送風を利用する直接氷蓄熱システムの有効性を研究した。まず、実験住宅における年間空調負荷及び給湯負荷を計算し、氷蓄熱システムのヒートポンプ、貯湯槽容量、従来型システムのルームエアコンと電気温水器の容量を決め、氷蓄熱システムを設計した。また、シミュレーションモデルを構築し、直接熱交換式氷蓄熱空調システムの熱交換特性を明らかにし、システムのエネルギー消費、及び環境への影響、及び経済性を比較した。さらに実測により提案システムの評価を行った。シミュレーション結果からみると、熱交換器の面風速が 0.5 m/s 時には、直接熱交換器の圧力損失が 50 Pa で、熱伝達係数 $8\sim 40\text{ W/m}^2$ である。ルームエアコンと電気温水器という従来型システムに比べて、提案型システムの電力利用量を 23% 削減することができ、エネルギーコストは約 40% 節約、 CO_2 排出量は約 25% 削減できる。設備更新時期を 20 年とした場合、提案システムと従来方式の経済性はほぼ一致している。夏の実測結果により、氷と空気を直接熱交換する方式が実現したが、エネルギー消費の削減率がシミュレーションにより低い。その原因は熱損失が大きいためと考えられる。十分に保温すればエネルギー消費とランニングコストの削減も可能であると明らかにしている。

第8章『総括結論』では、各章における結論を総括した。以上を要するに本研究は、パッシブ空調とアクティブ空調システムを統合して、住宅における新しいハイブリッド空調システムを構築した。シミュレーションと実測の上で、快適な室内環境の実現の上で、システムの省エネルギー性及び有効性の検証をおこなったものである。

APPENDIX 2. RESUME (IN JAPANESE)

履 歴 書

本 籍 中国江蘇無錫市惠銭路紅光村許巷 51 号

現 住 所 〒162-0041 東京都新宿区早稲田鶴巻町 564-305

TEL . (03) 3203-6817

ふりがな きよ らい

氏 名 許 雷 (Lei XU)

生年月日 1970 年 10 月 15 日 (32 歳)

学 歴

1985 年 9 月 中国江蘇省無錫市第一高等学校入学
1988 年 7 月 同上卒業
1988 年 9 月 南京理工大学工程熱物理学部エネルギー学科入学
1992 年 7 月 同上卒業、学士
1995 年 4 月 上海同済大学大学院修士課程、エネルギー工学専攻研究入学
1998 年 3 月 同上修了、修士
2000 年 4 月 早稲田大学大学院理工学研究科博士後期課程
建設工学専攻都市環境研究入学
現在に至る

職 歴

1992 年 8 月 中国江蘇省無錫市熱電力会社入社、助技師
1995 年 8 月 同上退社 (進学)
1998 年 4 月 上海同升技術工程会社入社、助技師
2000 年 1 月 同上退社 (進学)

賞 罰

1989 年 12 月 中国江蘇省大学生物理競争二等賞
1996 年 10 月 倪李氏奨学金、同済大学
2000 年 4 月 吉田育英会アジア 100 奨学金
2001 年 1 月 日本建築学会設計競技最優勝賞
(ヘルシーハウスコンペ)
2002 年 8 月 日本建築学会設計競技優勝賞
(ゼロエミッション化住宅)

APPENDIX 3. RESEARCH EXPERIENCE (IN JAPANESE)

種類別	題目・発行箇所・掲載誌名・発行年月・連名者（申請者含む）
論文 (報文)	Simulation on Thermal Comfort and Energy Conservation for displacement ventilation in a Residential Room-Effect of air change rate and position of air inlet/outlet, 日本建築学会計画系論文集, No.565, 2003年3月 掲載予定 <u>Lei Xu</u> , Weijun Gao, and Toshio Ojima
論文 (報文)	Validation of Displacement Ventilation System in a Residential Room, Journal of Asian Architecture and Building Engineering, 日本建築学会, Vol.1 No.2 pp.87-92 (2002), <u>Lei Xu</u> , Weijun Gao, and Toshio Ojima
論文 (報文)	Study on the Installation of Thermal Storage System in Residential Houses, Journal of Asian Architecture and Building Engineering, 日本建築学会, Vol.1 No.1, pp. 113-118 (2002) <u>Lei Xu</u> , Takashi Yagi, Weijun Gao, and Toshio Ojima
論文 (報文)	Effect Of Air Outlet Position For Displacement Ventilation In A Residential Room, Proceedings of 4th International Symposium on Architecture Interchange In Asia, Chongqing, China, pp.629-632 (2002), <u>Lei Xu</u> , Weijun Gao, and Toshio Ojima
論文 (報文)	Study on Thermal Environment Evaluation in the Central Business District of Shanghai, Proceedings of International Symposium Air Conditioning In High Rise Buildings' 2000, Shanghai, China, pp.551-554 (2000), <u>Lei Xu</u> , Weijun Gao, Penglin Zhao, and Toshio Ojima
論文 (報文)	上海における建築のエネルギー消費現状と省エネルギー可能性に関する研究、暖通空調（中国）、1998年6月, pp.81-87, 龍惟定、範存養、 <u>許雷</u> 等

Research Experience (Continued)

種類別	題目・発行箇所・掲載誌名・発行年月・連名者（申請者含む）
論文 (報文)	空調システムの熱源設備のエネルギー消費とその環境への影響、上海制冷技術（中国） 1997年第3期、pp.1-5 許雷、範存養、吳味隆
論文 (報文)	上海における空調システムの調査とエネルギー消費、上海制冷技術（中国）、1998年、第1期、pp.25-30 許雷、範存養
講演	シミュレーションにより住宅における成層空調システムに関する研究、日本建築学会学術講演会・北陸、D-2 環境工学、pp.1043-1044（2002）許雷、高偉俊、尾島俊雄、
講演	成層空調システムの性能評価のための温熱環境実測調査、空気調和・衛生工学会 九州支部研究報告 第9号、pp.7 - 10（2002）依田浩敏、高偉俊、許雷、尾島俊雄
講演	成層空調システムの性能評価のための温熱環境実測調査、空気調和・衛生工学会 九州支部研究報告 第9号、pp.11 - 14（2002）高偉俊、依田浩敏、許雷、尾島俊雄
講演	住宅における成層空調システムの導入とその効果に関する実測研究、日本建築学会関東支部研究発表会 2001年度、pp.473 - 476（2002）許雷、高偉俊、尾島俊雄
講演	住宅における氷蓄熱空調機の性能評価のための実測調査、日本建築学会九州支部研究発表会 2001年度、pp.469 - 472（2002）後藤雄二、依田浩敏、許雷、高偉俊、尾島俊雄

Research Experience (Continued)

種類別	題目・発行箇所・掲載誌名・発行年月・連名者（申請者含む）
講演	ダブルスキン空間における中間季の温熱環境に関する実測調査、日本建築学会九州支部研究発表会 2001 年度、pp.409 - 412 (2002) 手島敬介、依田浩敏、 <u>許雷</u> 、高偉俊、尾島俊雄、
講演	成層空調システムの性能評価のための実測調査、日本建築学会九州支部研究発表会 2001 年度、pp.181 - 184 (2002) 永末剛、依田浩敏、 <u>許雷</u> 、高偉俊、尾島俊雄、
講演	住宅における氷蓄熱式空調システムの有効性に関する研究 - その 1 住宅用氷蓄熱式空調システムの提案、日本建築学会学術講演会・関東、D-2 環境工学 、 pp.1113 - 1114 (2001) <u>許雷</u> 、八木崇、高偉俊、尾島俊雄、
講演	住宅における氷蓄熱式空調システムの有効性に関する研究 - その 1 住宅用氷蓄熱式空調システムの提案、日本建築学会学術講演会・関東、D-2 環境工学 、 pp.1113 - 1114 (2001) <u>許雷</u> 、八木崇、高偉俊、尾島俊雄
講演	住宅における氷蓄熱式空調システムの有効性に関する研究 - その 2 エネルギー面における予測評価、日本建築学会学術講演会・関東、D-2 環境工学 、 pp.1115 - 1116 (2001) 八木崇、 <u>許雷</u> 、高偉俊、尾島俊雄
講演	住宅における設備制御のデジタル化 - その 1 デジタル設備制御への転換、日本建築学会関東支部研究発表会 2000 年度 (2001) pp.369 - 372、 <u>許雷</u> 、高偉俊、尾島俊雄、
講演	上海の高層ビルにおける空調設備の実態調査、日本建築学会学術講演会・東北、D-1 環境工学 、 pp.685 - 686 (2000) <u>許雷</u> 、高偉俊、尾島俊雄

APPENDIX 4. COMMITTEE REPORT ON EXAMINATION OF CANDIDATE
FOR THE DEGREE OF DOCTOR OF ENGINEERING (IN JAPANESE)

早稲田大学大学院理工学研究科

博士論文審査報告書

論 文 題 目

Effectiveness of Hybrid Air Conditioning
System in a Residential House

住宅におけるハイブリッド空調システムの
有効性に関する評価研究

申 請 者

氏 名

許 雷
Lei XU

専攻・研究指導
(課程内のみ)

建設工学専攻・都市環境

2003 年 3 月

近年のライフスタイルの変化等により、生活の利便性、快適性、豊かさが追求されるようになり、日本における民生部門でのエネルギー消費量は最終エネルギー消費の 1/4 を超えている。在室ワーク(SOHO)機能が進み、住宅におけるエネルギー消費量、特に冷暖房のエネルギー消費量が伸び続けている。一方で、居住者の健康や快適性に対する志向が高まり、室内環境に対する要求も高くなっている。そのため空調システムは省エネルギーと高度な室内環境を実現するために、更なる高性能化・高機能化が図られ、複雑なシステムが多くなっている。しかし、実際の建物は、自動制御の未調整や設定値の不具合によって多くの無駄なエネルギーが消費されている。

本論文は、住宅における空調システムの省エネルギー性と室内の快適性を実現することを目指し、ハイブリッド型空調システムに関する実証的研究をしたものである。具体的には、パッシブ手法としては、縁側空間をダブルスキンとして活用した自然エネルギー利用の効果に関する研究であり、アクティブ空調手法として、居住域のみを空調する温度成層型空調システムの快適性と氷蓄熱空調システムの導入に関する研究を行っている。住宅におけるハイブリッド空調システムに関するシミュレーションと実測から、本システムの有効性を実証している。この研究成果は、パッシブ手法とアクティブ手法の両面から住宅の空調システムの新たな方向性を提示した研究として意義あるものと考えられる。

第1章は『従来研究及び本研究の位置づけ』と題して、近年のライフスタイルの変化よりエネルギー負荷が増加していることから本研究に至った背景を調査した上で、建物における空調設備の省エネルギー手法に関する取り組みの現状を記し、特に住宅に関する省エネルギー手法の特性について研究している。その結果として、建築外皮の改善により、冷暖房負荷を少なくするパッシブ空調と省エネルギー機器を利用するアクティブ空調を併用した「ハイブリッド空調システム」の可能性を示している。これにより、シミュレーションと実測でその有効性を確認する研究が必要であることを指摘している。

第2章は『ハイブリッド空調システムの基本コンセプトと提案』と題して、住宅におけるハイブリッド空調システムの基本的な考え方を示している。この空調システムの目的は、居住の快適性、エネルギー消費の削減、操作の利便性と維持管理の容易性である。また、自然エネルギー利用の可能性を分析した上で、パッシブ空調システムとして、住宅でのダブルスキンシステムを導入している。アクティブ空調方式を改善するために、日本の住宅で使われることのなかった成層空調システムと氷蓄熱システムを導入している。住居の快適性とシステムの省エネルギー性や操作管理の利便性を考慮し、北九州における実験住宅でこのシステムを試作し運転した結果は、良好であったとしている。

第3章は『ダブルスキンによる室内環境への影響に関するシミュレーション』と題して、ダブルスキン無しとありの住宅モデルを作成し、シミュレーションにより室内の空調負荷への影響を検討している。夏季自然換気時では、ダブルスキン内のブラインドの遮蔽効果と温度差換気効果により、ピーク時ではダブルスキンなしの場合より一階の空

調負荷削減率は 16%であり、二階は 15%となっている。冬季ダブルスキン内の上下開口部を密閉し、ダブルスキン内のブラインドを上げた場合には、日射が直接部屋奥まで入り込み、室内の温度が外気より 10~15 高く、暖房負荷は 20~30%削減できるとしている。縁側空間を活用したダブルスキンは外部との緩衝空間となるため、夏季の煙突効果と冬季の温室効果により、空調負荷の削減状況は明らかにしている。これより、ハイブリッド空調の一環として、ダブルスキンによるパッシブシステムの有効性をシミュレーションにより明らかにした成果は大である。

第 4 章は『ダブルスキンによる室内環境への影響に関する実測研究』と題して、ダブルスキンシステムの実測研究を行っている。その結果、夏季自然換気の場合には、ダブルスキン内の高さ方向の煙突効果を確認した上で、約 10%が自然換気により排熱され、室内の空調負荷は約 15%削減できるとしている。また、冬季密閉する場合には、ダブルスキンの温室効果により、暖房負荷が 31%削減できるとしている。この結果は 3 章のシミュレーション結果と良く一致している。冬季の自然室温は外気より 15 上昇し、中間期では、ダブルスキンの開口面積を自由に調整することによって空調に頼らずとも快適な環境が確保できるとしている。更に、被験者の申告調査からダブルスキンシステムの実用性を評価している。以上の成果により、ダブルスキンシステムの実用性を評価することができ、夏、秋と冬の実測からもダブルスキンの有効性を立証している。

第 5 章は『成層空調に関するシミュレーション研究』と題して、これまで住宅で実現されていない成層空調システムを提案し、給気風量、給排気口の位置及び給気口の特性による室内の快適性及び省エネルギー性のシミュレーション研究を行っている。その結果、給気風量は室内の快適性や空調の省エネルギー性への影響が大きく、給気風量が大きいほど清浄空気域は広がる。リターン口の位置は居住区域の快適性に与える影響が小さい反面、冷房負荷への影響が大きいとしている。同様の成層空調において、リターン口が 2.4m高さから 1.8m高さの位置に移動すると、冷房負荷が約 14%削減でき、さらに給気口がスウィングした場合には、気流に影響する障害物があっても室内気温の分布への影響は少ないとしている。従来の完全混合式システムと比べて、約 12~26%の冷房負荷の削減効果がみとめられる。その原因は、主に天井と上部壁面からの熱損失が削減するためと考えられる。換気効果からみると、成層空調システムによる居住域の換気効率の平均値は 1.25 で、完全混合式でも 1 しかないことを考えれば、成層空調システムの換気効率は優れていると評価される。以上のように、日本の住宅では実現困難と考えられていた成層空調システムの有効性を提示したユニークな研究として評価に値する。

第 6 章は『成層空調に関する実測研究』と題して、成層空調システムの実測研究を行

っている。高さ方向に空気の温度成層が確認でき、1.8m以下の居住空間では26~28で、1.8m以上の空間では約2 高くなり、上下温度勾配は2~2.5 /mとなっている。また、室内の気流速度は0.25m/s以下、乱れの強さは20%、活動量は1met、着衣量は0.5cloの場合、居住域におけるPMVの分布が-0.5~0.5であり、居住域CO₂濃度は天井より低く、より効果的に換気することができることを明らかにしている。リターン口の位置を1.8m高さに設置して天井から排熱したため、ピーク時では従来の完全混合システムより20~30%低くなっているが、空調負荷は約60~70W/m²でシミュレーション結果と比べて約10~15%高くなっている。その原因は引き違いドアの隙間からの熱損失と考えられる。以上から、成層空調方式の快適性と省エネルギー性を実測し、住宅での成層空調システムが有効に運転されていることを実証している。

第7章は『氷蓄熱空調システムの有効性に関する研究』と題して、氷蓄熱システムの有効性に関する研究を行っている。住宅における冷房負荷の増加による蓄熱空調システムの必要性から、蓄熱空調システムの省エネルギー性、経済性を予測している。直接熱交換式氷蓄熱空調システムを提案し、シミュレーションにより直接熱交換式蓄熱コイル部分の熱交換特性を解析し、実測により提案システムの評価を行っている。シミュレーション結果からみると、直接熱交換器を用いた提案システムは従来型のルームエアコンと電気温水器併用型と比較し、電力利用量を23%削減することができ、エネルギーコストは約40%節約、CO₂排出量は約25%削減できることを示している。設備更新時期を20年とした場合、提案システムの経済性と従来方式はほぼ一致している。夏の実測結果では、氷と空気を直接熱交換することに成功しているが、エネルギー消費の削減率がシミュレーション結果より低いのは熱損失が大きいためと考えられる。十分に保温すればエネルギー消費とランニングコストの削減も可能であるとしている。以上のように、ハイブリッド空調システムとして氷蓄熱システムを利用する有効性を提示している。

第8章『総括結論』では、各章における結論を総括している。

以上を要するに、日本の住宅で最も数多い戸建住宅に自然エネルギーを活用したパッシブ空調と改良したアクティブ空調を統合した「ハイブリッド空調システム」を適用することによる有効性を、シミュレーションと実測により定量的に実証したユニークな研究成果である。本論文は今後の都市環境工学の発展に大きく寄与するものであり、博士(工学)の学位授与に値するものと認められる。

2003年3月

審査員(主査)	早稲田大学理工学部教授	工学博士(早大)	尾島 俊雄
	早稲田大学理工学部教授	工学博士(早大)	長谷見雄二
	早稲田大学理工学部教授	工学博士(早大)	田辺 新一
	早稲田大学理工学部総合研究センター客員教授	工学博士(早大)	中島 康孝